pennsylvania
DEPARTMENT OF TRANSPORTATION

District 3-0 Investigation of Fiber Wrap Technology for Bridge Repair and Rehabilitation (Phase III)

FINAL REPORT

January 14, 2010

By Julio F. Davalos, An Chen,
Indrajit Ray, Adam Justice
and Matthew Anderson
West Virginia University

PENNSTATE

COMMONWEALTH OF PENNSYLVANIA
DEPARTMENT OF TRANSPORTATION

Contract No. 510401
Work Order No. MAUTC 014

DEPARTMENT OF TRANSPORTATION
UNITED STATES OF AMERICA

Technical Report Documentation Page

1. Report No.	2. Government Accession No.	3. Recipient's Catalog No.
FHWA-PA-2010-002-510401-014		

4. Title and Subtitle	5. Report Date
District 3-0 Investigation of Fiber Wrap Technology for Bridge Repair and Rehabilitation – Phase III	January 14, 2010
	6. Performing Organization Code

7. Author(s)	8. Performing Organization Report No.
Julio F. Davalos, An Chen, Indrajit Ray, Adam Justice, and Matthew Anderson	WVU-2007-01

9. Performing Organization Name and Address	10. Work Unit No. (TRAIS)
West Virginia University P.O. Box 6103 Morgantown, WV 26506-6103	**11. Contract or Grant No.** 510401 and DTRT07-G-0003 MAUTC WO 14

12. Sponsoring Agency Name and Address	13. Type of Report and Period Covered
The Pennsylvania Department of Transportation Bureau of Planning and Research Commonwealth Keystone Building 400 North Street, 6th Floor Harrisburg, PA 17120-0064 U.S. Department of Transportation Research and Innovative Technology Administration 3rd Fl, East Bldg E33-461 1200 New Jersey Ave, SE Washington, DC 20590	Final Report: January 15, 2008 – January 14, 2010
	14. Sponsoring Agency Code

15. Supplementary Notes
COTR: Jeff Levan, 570-368-4304, jelevan@state.pa.us

16. Abstract

Based on guidelines for project selection, a candidate bridge was selected for a contract repair project. Pre-repair testing of bridge materials is described. The FRP design was based on strengthening the bridge to sustain an HS-20 AASHTO truck loading. The FRP repair system was designed based on current ACI 440.2R-08 design guidelines. Repair work and post-construction load testing were completed. Finite Element (FE) modeling was performed to determine capacity of the repaired bridge and the FE model was calibrated against load testing results. Supporting full-scale lab studies were conducted to evaluate the most effective concrete substrate repair method and FRP strengthening scheme. An exploratory study on an electrochemical chloride extraction technique was completed. Systematic documents, including draft guidelines on project selection and management, design guidelines, and construction specifications, were developed for use on future T-beam rehabilitation projects.

17. Key Words	18. Distribution Statement
Concrete T-beam bridge, rehabilitation, FRP composites, bridge testing, finite element analysis, lab-scale testing, guidelines for project selection and management, design guidelines, construction specifications	No restrictions. This document is available from the National Technical Information Service, Springfield, VA 22161

19. Security Classif. (of this report)	20. Security Classif. (of this page)	21. No. of Pages	22. Price
Unclassified	Unclassified	260	**N/A**

This work was sponsored by the Pennsylvania Department of Transportation, the Mid-Atlantic Universities Transportation Center, and the U.S. Department of Transportation, Federal Highway Administration. The contents of this report reflect the views of the authors, who are responsible for the facts and the accuracy of the data presented herein. The contents do not necessarily reflect the official views or policies of the Federal Highway Administration, U.S. Department of Transportation, the Mid-Atlantic Universities Transportation Center, or the Commonwealth of Pennsylvania at the time of publication. This report does not constitute a standard, specification, or regulation.

DISTRICT 3-0 INVESTIGATION OF FIBER-WRAP TECHNOLOGY FOR BRIDGE REPAIR AND REHABILITATION (Phase lll)

Final Report

Submitted to:

Pennsylvania Department of Transportation
Bureau of Planning and Research
400 North Street
6th Floor East
Harrisburg, PA 17120

Submitted by:

Dr. Julio F. Davalos, Benedum Distinguished Teaching Professor
Dr. An Chen, Research Assistant Professor
Dr. Indrajit Ray, Research Assistant Professor
Adam Justice, Graduate Research Assistant
Matthew Anderson, Graduate Research Assistant

Department of Civil and Environmental Engineering
West Virginia University
Morgantown, WV 26506-6103

January 14, 2010

ACKNOWLEDGMENTS

The authors would like to acknowledge the financial support received from the Bureau of Planning and Research, Pennsylvania Department of Transportation, and the invaluable suggestions from the officials and engineers of PennDOT, District 3-0. In addition, special thanks go to Mr. Jeffrey Levan, P.E., Project Technical Advisor, PennDOT, District 3-0, for his assistance in field evaluations, and testing of the selected bridge, without whom this project could not have been successfully completed.

Table of Contents

Introduction

In Phase I, both the technical and economical feasibility of externally bonded FRP for concrete bridge repair or retrofit was extensively evaluated. Through a comprehensive literature review and an effective survey of state DOTs, it was concluded that FRP technology showed favorable attributes and advantages over conventional repair methods. A criterion was developed for ranking the District 3 concrete T-beam bridges into three categories as candidates for possible repair with FRP: Level 1, having extensive damage and all work to be done by contract; Level 2, having moderate damage and the repair work to be implemented by a combination of contract and District forces; and finally Level 3, with minor damage and all repair work to be performed by District forces.

It was recommended in Phase I that the field implementation phase should follow sequentially bridge projects beginning with Level 1, followed by Levels 2 to 3. This proposed approach will serve effectively to transfer knowledge to District personnel and permit them to participate in hands-on training. A cost analysis was performed for actual representative District 3 bridges for the three levels of proposed repair indicated above. In relation to conventional repair methods, the FRP technology was shown to be significantly more cost effective for Level 1, particularly in relation to total bridge replacement, and either less or equally costly for Levels 2 and 3, depending on the scenarios considered. Thus, it was concluded in Phase I that District 3 would significantly benefit from implementation of FRP technology for the repair of concrete T-beam bridges, with potential application to a large majority of the 300 District 3 bridges considered in this study. Moreover, the guidelines developed through a District 3 field demonstration project can serve PennDOT statewide for T-beam repair/retrofit and in general for future applications to various types of concrete bridges.

With the completion of Phase II, the technical and cost-effective application of externally bonded FRP for Level-1 retrofit of a concrete T-beam bridge had been demonstrated. A forum for technology transfer had been created by close involvement of District 3 personnel throughout all aspect of the demonstration project. The candidate bridge was

selected, field assessments and structural evaluations were implemented, a design approach for the FRP was proposed, and assistance with bid documents and requirements was provided. This phase led to future field implementation work and research support including: assisting with QC procedures for materials and workmanship, implementing supporting small- and large-scale laboratory tests, performing structural and cost analyses of the completed work, and finally developing guidelines for PennDOT.

The Phase III project was organized into 7 tasks; namely, Task 1: Planning Activities for Field Work and Research, Task 2: Assisting with QC and Field Performance Tests of Repairs, Task 3: Evaluating Concrete, FRP, and FRP-Concrete In-situ Materials, Task 4: Testing of Repaired Structure, Task 5: Conducting Supporting Lab-scale Studies, Task 6: Developing Guidelines for Project Selection and Management, and Task 7: Developing Guidelines for Concrete T-beam Bridge Design and Construction. The present report summarizes the work performed in all seven tasks. In Task 1, planning activities were conducted in preparation for field and research work. Contract documents were reviewed, field activities and laboratory-scale testing activities were planned, and PennDOT specifications were reviewed. In Task 2, the research team assisted the District in overseeing the contractor to enhance quality control of workmanship and field performance tests to evaluate the acceptability and adequate performance of the application. Activities monitored included: concrete repair; surface preparation; corrosion of rebar and necessity for replacement; FRP installation; acceptance tests and inspections; and any repairs and rework that may have been necessary. This task led to various aspects of Task 3, which relates to research team participation in evaluating the quality of repair material and by-layer FRP-concrete systems through field evaluations of the structure. Also, witness coupon samples, produced by the contractor under guidance from the research team, were tested. In general, repair materials, FRP materials, and combined FRP-concrete samples were produced and tested in the field and in the laboratories at WVU. Performance of the FRP system and capacity increases due to the retrofit were determined through Task 4 via load testing of the retrofitted structure. A Finite Element model of the system was analyzed for FRP system performance as well. Task 5 includes comprehensive testing and evaluation protocols at the component level.

The purpose of Task 5 was to simulate the aging process by accelerated corrosion of the rebar using induced electric current. Retrofit and testing of these corroded specimens was carried out accordingly. The culmination of the previous tasks led to the development of practical guidelines and recommendations for the effective implementation of surface-bonded FRP on concrete T-beam bridges in Pennsylvania, Task 6. Complimenting Task 6, guidelines were developed to be more directed to technical issues for T-beam bridges. These more technically directed guidelines formulate Task 7. Task 7 can be further described as three separate sub-tasks: (1) Design Guidelines for Concrete T-beam Bridges; (2) Construction Specifications for Repair and Rehabilitation Procedures with FRP; and (3) Guidelines for Bridge Testing and Long-term Inspections and Monitoring of Repair and Rehabilitation Work. All guidelines developed in Task 7 followed established procedures and other specific recommendations developed and/or suggested by the researchers. Guideline formatting was specified by PennDOT. Following the tasks of Phase III, summary and conclusions are given.

Task 1 Planning Activities for Field Work and Research

Task 1 concerned the project's planning activities for field work and research. This task was completed within 3 months from the project initiation date. The activities under this planning task included four sub-tasks: (1) reviewing contract documents; (2) planning of all field activities; (3) planning of lab-scale concrete beam testing; and (4) reviewing PennDOT construction and design specifications.

1.1 Reviewing Contract Documents

The authors reviewed the technical sections of the contract documents and provided input and comments as requested. We submitted both a summary report and a detailed commentary on BASF's design of a fiber reinforced polymer strengthening system for application to PennDOT's bridge project. The report included: Section 2 comments on flexural design; Section 3 comments on shear design; Section 4 discussion on FRP installation procedure; Section 5 discussion on procedures used to repair defects in FRP systems; Section 6 comparison of materials used for repair; and Section 7 summary and reference figures illustrating the original FRP strengthening design submitted by WVU specifying Fyfe Co. materials and the design submitted by BASF specifying MBrace materials.

1.2 Planning of Field Activities

The following table provides information on field activities by WVU based on the proposal activities and contract milestones and the contractor's work schedule. Any change in the schedule by the contractor would accordingly be adjusted. The date for load testing would be decided after the construction work was completed, but it would be conducted before the winter season.

Date	Activities	Equipment/Materials supplied/carried by WVU	Comments
21-Apr-08	We will deliver five prismatic substrate molds to the contractor for casting over patching materials, using the same products applied to the actual beams. We will also supply 12 cylinder molds (4 in. diameter x 8 in. long) for test samples on compressive and splitting tensile strengths of patching materials. We will meet with the contractor to explain how to place and field-cure the bi-layer molds and cylinders. During this time we can also oversee the on-going work and discuss activities as necessary.	Five prismatic molds with substrate materials and 12 cylinder molds.	Repairing materials will be applied to all five prismatic molds and the samples will be site-cured. Also, all 12 cylindrical samples will be cured at the bridge location. Two of the prismatic samples and 12 cylindrical samples will be brought back to WVU on May 21st for testing. The remaining 3 prismatic samples will be left on site for FRP bonding, at the time when the FRP is applied to the bridge in June, 2008.

Date	Activities	Equipment/Materials supplied/carried by WVU	Comments
21-May-08	An on-site field coordination meeting will take place among PENNDOT, WVU, and the contractor. The FRP materials list and FRP design will be reviewed. We will bring back two prismatic molds for pull-out bond strength (ASTM C 1583) and 12 cylindrical specimens for compressive strength (ASTM C 39) and splitting tensile strength (ASTM C 496) tests, respectively.	We will conduct tests for pull-out strength, compressive strength, and splitting tensile strength tests at the WVU lab.	This is a proposed date. An revised date can be defined depending on availability of participants, but preferably at a date close to May 21st.

Date	Activities	Equipment/Materials supplied/carried by WVU	Comments
June 3-15	Witness FRP laminates will be produced in the field as described in ACI 440-2R-section 3.6, and according to Task 3 of the proposal. Cured FRP laminates and other necessary samples will be brought back to the WVU laboratory for testing. After FRP wrapping, pull-off strength of FRP will be evaluated per ASTM D 4541 at pre-defined test locations on actual beams. Tap tests will be conducted on the entire repair work. The three concrete prismatic specimens previously cast will also be bonded and cured with FRP under field conditions. Then pull-off tests will be conducted at different ages. The locations for bonding the strain gages on girders will be selected, and surface preparation will be accomplished by sanding and epoxy coating. The strain gages will be installed prior to load testing, but after the retrofitting.	A waxed wood surface of about 8-inch x 24 inch for witness samples. Concrete hammer ("Q" value or physical rebound coefficient) and ultrasonic pulse velocity testing apparatus. Pull-off tester with dollies. Hand held core cutting machine.	Members of the WVU team will visit and stay on-site rotationally to carry out the necessary field evaluations and tests, as per Task 3 of the proposal.

Date	Activities	Equipment/Materials supplied/carried by WVU	Comments
To be decided after retrofitting work is completed (before winter season.)	Load testing will be conducted on the retrofitted structures to determine the performance of the FRP system and capacity increase.	Strain gages, LVDTs, data acquisition system, and accelerometers for static and dynamic load tests.	Strain gages will be attached to the previously prepared surfaces on girders. Displacement transducers and accelerometers will be installed during this time. All these installations will be completed prior to the load testing.

1.3 Planning of Lab-scale Concrete Beam Testing

When designing this experiment, it was desired to create a corroded beam specimen that simulated the common conditions found in an actual aged, chloride-contaminated, reinforced concrete bridge girder. The primary step, therefore, was to determine the most destructive sources of deterioration that are common in most deteriorated bridges. To obtain direct insight, the material samples from PennDOT Bridge #49-4012-0250-1032 were analyzed. Scanning electron microscope (SEM) images revealed that the deck and girders consisted of a very porous concrete that was saturated with deicing salts and other contaminants. Chloride content analysis results supported these findings. Chloride-induced pitting corrosion appeared to be the cause of the deterioration of tension steel samples extracted from one of the bridge girders. In addition to Bridge #49-4012-0250-1032, several other similar bridges from the PennDOT District-3 inventory were visually observed. Concrete cracking, spalling and delamination in the cover layer were common in every deteriorating bridge that was visited. It was also observed that the girders seemed to have a significant moisture content, as was evidenced by the active seeping of water, steel corrosion products, and ettringite formation, even though the visits were made during the relatively dry summer months.

Based on visual observations and the study of corrosion in reinforced concrete, it was determined that the test specimens should have the following deteriorated properties common to an aged concrete beam before repair:

- The concrete should be low-strength and porous.
- The concrete should be contaminated with embedded chloride salts.
- The reinforcing steel should be corroded, preferably by pitting.
- The concrete cover layer should be cracked and preferably delaminated due to expansive corrosion of the reinforcing steel.
- The specimen should be kept wet.

Basic fundamentals of concrete mix technology were applied to produce a concrete that is low strength, porous, and contaminated in order to provide a favorable environment for corrosion of reinforcement within concrete.

The lab testing plan was organized into two parts. For Part I, two unique substrate repair methods were incorporated and compared while the FRP wrapping scheme was the same for all beams. This approach was intended to determine performance differences for FRP repair for two substrate repairing conditions, one with minimal substrate repair and one with complete substrate replacement.

Then, in Part II, the effectiveness of three unique wrapping schemes was studied. The variable between the three repair schemes was the extent of U-wrap anchorage provided. Wrapping Scheme 1 consisted of flexural FRP with no U-wrap anchors. Wrapping Scheme 2 consisted of flexural FRP with only one strategically placed U-wrap anchor on each side of the beam's profile centerline. Wrapping Scheme 3 consisted of flexural reinforcement with evenly spaced FRP U-wrap anchors. The main objective of Part II of this study was to determine the differences in load capacity, stiffness, ductility, and failure mechanism based on the extent and scheme of anchorage used. The following figure shows the schematic plan of the laboratory testing program.

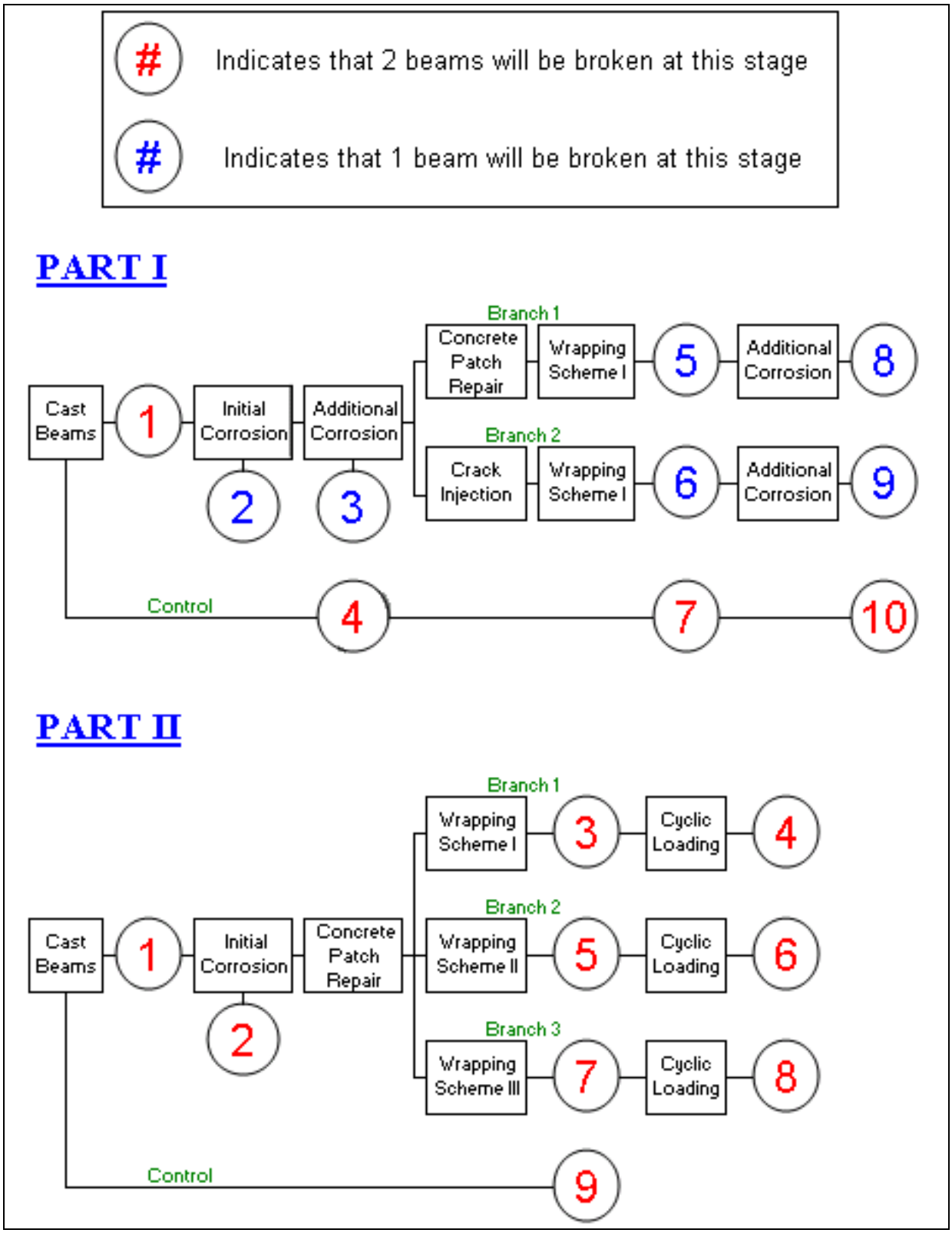
# Indicates that 2 beams will be broken at this stage
# Indicates that 1 beam will be broken at this stage
PART I
Cast Beams
1
Initial Corrosion
2
Additional Corrosion
3
Branch 1
Concrete Patch Repair
Wrapping Scheme I
5
Additional Corrosion
8
Branch 2
Crack Injection
Wrapping Scheme I
6
Additional Corrosion
9
Control
4
7
10
PART II
Cast Beams
1
Initial Corrosion
2
Concrete Patch Repair
Branch 1
Wrapping Scheme I
3
Cyclic Loading
4
Branch 2
Wrapping Scheme II
5
Cyclic Loading
6
Branch 3
Wrapping Scheme III
7
Cyclic Loading
8
Control
9

1.4 Reviewing PennDOT Construction and Design Specifications

The authors have initiated the review of DM-4 and Publication 408 for addition of FRP Strengthening Systems for Concrete Structures.

The prescriptions given in the "Guide for the Design and Construction of Externally Bonded FRP Systems for Strengthening Concrete Structures" (ACI 440.2R-02) will have to be integrated into sections of PennDOT's DM-4 and Publication 408. Fiber reinforced polymer (FRP) systems have emerged as an alternative to traditional materials and techniques for the strengthening of existing concrete structures to resist higher design loads, correct deterioration-related damage, correct design or construction error, or increase ductility. Structural elements strengthened with externally bonded FRP systems include beams, slabs, columns, walls, joints/connections, chimneys and smokestacks, vaults, domes, tunnels, silos, pipes, trusses, and other structures.

Several sections of PennDOT's design manual will be updated to allow for the use of fiber reinforced polymer strengthening systems. Some of the possible sections for review include:

Design Manual Part 4 - Volume 1

Part A: Policies and Procedure
Chapter 1 - Administrative Considerations
Chapter 3 - Design Considerations
Chapter 4 - Bridge Economics
Chapter 5 - Rehabilitation Strategies

Part B: Design Specifications
Section 4 - Structural Analysis and Evaluation
Section 5 - Concrete Structures
Section 10 - Foundations
Section 11 - Abutments, Piers and Walls

It may also be advisable to add a new section specifically for fiber reinforced polymer strengthening systems and the design and construction of such systems. Design

guidelines may be more acceptably added to DM-4, whereas construction guidelines should be added to Publication 408. Also, Appendices may have to be updated.

The discussion of Task 7 includes a detailed report of modifications, including possibly a specific section for FRP wrap technology.

1.5 Closing Statements

In summary, the proposed work for Task 1 described in this report was successfully completed according to the sub-task outlined in the proposal.

Task 2 Assisting with QC and Field Performance Tests of Repairs

In this task, the research team primarily assisted PennDOT District 3-0 in overseeing the quality control of the repairing and rehabilitation process, to evaluate the acceptability and adequate performance of the application. They monitored demolition of deteriorated concrete, concrete repair, FRP design, FRP installation, and acceptance testing and inspection. The FRP design criteria for rehabilitation of the bridge were clearly defined. There was no necessity for rework or repair of the FRP applications and no problem areas were found. The following sections highlight the steps of the work followed:

The authors made four field trips during this period: April 21, 2008; May 14, 2008; June 12, 2008; and July 18, 2008.

2.1 First Field Visit on April 21, 2008—Concrete Demolition and Sample Collections

On April 21, 2008 the researchers made a field visit to interact with the contractor and PennDOT District 3-0 personnel, and also to deliver concrete molds. During this period we observed the following:

1. The contractors completed most of the demolition work of deteriorated and damaged concrete, as can be seen in Figures 1 and 2 below.

Figure 1: Complete Removal of Concrete from Beam 6, Exposing the Reinforcement

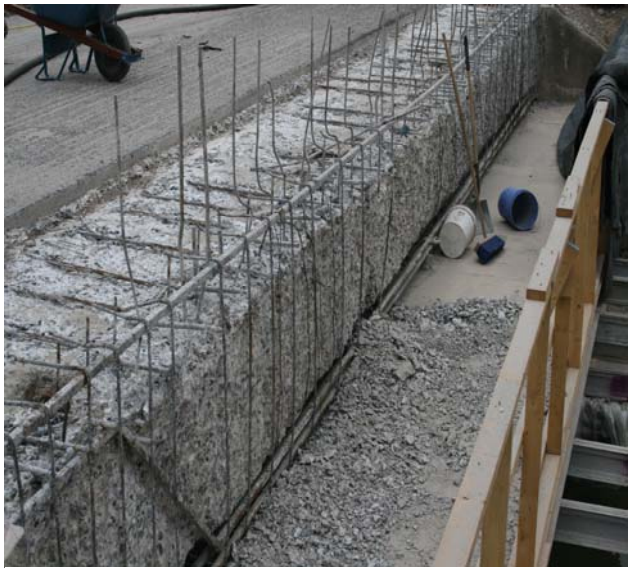

Figure 2: Partial Removal of Concrete from Beam 1, Exposing the Reinforcement

2. When the contractors removed the concrete from edge beams, they found tensile reinforcement missing of about 20% less than reported in the drawings. The rest of the beams not exposed were thought to have missing reinforcement as well. Also, some of the diagonal shear bars were missing. Moreover, the vertical stirrups within the central 15 feet were also missing. Figure 3 displays the central portion of Beam 6, where the two middle bars of the top layer of tension steel are missing, in contrast to what was specified in the original design plans. Also, complete absence of stirrups for the mid-section of the beam can be seen in this figure. Resulting discussions concerning this missing reinforcement are presented in Section 2.3.
3. One issue of concern was the need to possibly reevaluate the capacity of the bridge girders due to finding of less steel than in the original plan. It was decided that the FRP design would account for the missing steels (both in tension and shear).

Figure 3: Central Portion of Beam 6 with Two Missing Bars in the Top Layer of Tension Steel

4. We delivered five prism molds of size 6 in. W x 6 in. H x 36 in. L with a 4 in. thick simulated field concrete comparable to quality of existing beams for conducting bond pull-off tests between simulated old concrete and new repair material as well as between repair material and FRP. We also supplied twelve 4 in. diameter x 8 in. long cylinders and six 6 in. diameter x 12 in. long plastic cylinder molds for casting samples with bag repairing materials and triple A mix, respectively.
5. Beam 6 was to be fully poured by triple A mix, Beam 5 poured up to 10 in. with triple A mix, and Beam 1 encased by triple A mix. Beams 2,3, and 4 would be patched with bag repairing material. The top 10 in. of Beam 5 would also be filled up with bag repairing material.

2.2 Second Field Visit on May 14, 2008 -- Repairing of Concrete and Sample Preparations

In our second field visit on May 14, 2008 we gathered information and made observations as follows:

1. Beams 6, 5 and 1 were repaired with triple A mix by using pumps, in which Beam 6 was fully poured, Beam 5 was poured up to the top 10 in. and Beam 1 was encased. The top 10 in. of Beam 5 was poured using bag repairing material. Triple A was used for these larger pours, as it can be delivered via trucks and easily pumped into place.
2. Beams 2, 3, and 4 were patched using bag repairing materials.
3. The repairing was done following ACI 546R and ICRI no. 03730 guidelines. Form-and-pour techniques were used for bag repairing materials. The bag material is a BASF product, Emaco S66 CI "Flowable Structural-Repair Concrete with Integral Corrosion Inhibitors." It's a cement-based silica fume modified repair concrete with high durability and strength. It was mixed at the site and poured within forms using chutes attached to forms; the materials were properly compacted using rods and mallets only, as the patching method and form

construction did not provide vibrator access. Figures 4, 5, and 6 show the formwork for patch repairing and triple A mix application.

4. For the top of the deck the contractors removed a deck section of concrete from each side up to a thickness of 4 to 5 in. and poured triple A mix monolithically with the beam.
5. They also molded twelve 4 in. diameter x 8 in. long cylinders with bag repairing materials for our testing. They cured the samples for 7 days under similar curing conditions they followed for field bag materials. We picked up the samples for testing in our laboratory.
6. We collected six cylinder specimens made with triple A mix for testing in our lab. The concrete specimens were cured under similar to field conditions. The 28-day tests were scheduled on May 21, 2008.
7. They filled up the top 2 in. of two prism molds with triple A mix, and similarly three molds with bag repairing material and cured them in the field. Out of five, we collected one prism mold topped with triple A for pull-off test per ASTM C 1583 and ACI 503R-Appendix A.
8. We observed the following and reported in an email on May 16, 2008:
   The concrete at the bottom of the deck (only in the location of the central strip) deteriorated badly. Due to severe spalling and cracking of concrete the reinforcements are exposed in places. This needs to be repaired immediately.

Figure 4: Formwork for Patch Repairs along Beams 3 and 4

Figure 5: Formwork along Beam 5

Figure 6: Extensive Formwork along Beam 1

2.3 Design Aspects of FRP under New Circumstances

1. PennDOT District 3-0 sent the BASF re-design (Beam 5 only) based on actual as-built steel found after demolition of Beams 5 and 6. BASF is a chemical company and its construction chemical division provides materials for construction projects. BASF provided the strengthening design and the materials. It also sent the re-

submittal of Beams 1 through 6 on May 23, 2008. WVU submitted the review for BASF's FRP design of Beam 5 on May 28, 2008. However, WVU initiated discussions on the extremely important issues of what design load should be used for FRP design calculations.

2. A conference call was held with District 3 on WVU's recommendations of designing the FRP not to "restore the bridge to the assumed initial capacity design," but to use existing conditions as bases for FRP design and AASHTO HS 20 loading, as currently being used by bridge standard practices.
3. Rather than being concerned with any discrepancies between original design plans/specs and as-built conditions, WVU proposed to use FRP strengthening to sustain a current AASHTO load, based on best evaluations of current conditions of the bridge, including details on material properties (concrete strength as per recommendations, steel section loss due to corrosion, etc.) Specifically, WVU proposed to design the FRP for an HS-20 loading.
4. Then, BASF could check the AASHTO live load moment and dead-load moment, and then proceed to check or redesign the suggested FRP lay-up given by WVU.
5. The benefits of doing this are: (1) A rational basis for design, to serve as an example for future projects, while optimizing materials and detailing, as well as providing load capacities in conformance to modern codes and standards; (2) to place the FRP better, to allow for "concrete breathing sections" to avoid trapping humidity and contaminants as much as possible.
6. PennDOT District-3 agreed with the WVU recommendations as the best option both for completing this construction project on time and providing a solid baseline for any future FRP rehabilitation projects. PennDOT District 3-0 asked WVU to provide designs for the FRP strengthening of all six beams.
7. Based on the above discussions WVU submitted the design entitled "WVU Design Suggestions for FRP Strengthening Design of PennDOT Bridge #49-4012-0250-1032 on State Route 4012 in Northumberland County, PennDOT-District 3-0," on June 9, 2008.

8. Finally, on June 26, 2008 (Rev-3), BASF submitted the working drawing details and recommendations for FRP design based on standards of existing construction practice, the latest bridge inspection report provided by PennDOT, and the above-mentioned West Virginia University report.

2.4 Third Field Visit on June 12, 2008 − Pull-off Test and Sample Collections

1. On June 5, 2008 the contractors conducted pull-off tests on triple A mix and bag repair materials. But due to insufficient epoxy curing and hardening, the test failed in all but two cases. As a result, PennDOT District 3-0 decided to repeat the test again on June 12, 2008.
2. On June 12, 2008 the WVU team visited the site and noticed the pull-off tests conducted by the contractors. All the tests were successful and done according to standards. The results will be shown under Task 3. Figure 7 shows the patched surface and Figure 8 displays the portable adhesion tester attached to a dolly.
3. WVU collected twelve 4 in. diameter x 8 in. long cylinders cast with bag repaired materials and one prism mold topped with bag repairing materials. The test results of these cylinders and prism mold will be provided under Task 3.

Figure 7: Beam 4 after Patch Repair

Figure 8: Tension Test of Portion of Patch Material using the Portable Adhesion Tester

2.5 Fourth Field Visit on July 18, 2008 – FRP Installation Inspection and FRP-Concrete Sample Preparations

1. PennDOT District 3-0 reported about the FRP pre-placement meeting on July 14, 2008, in which they discussed issues related to weather, material considerations, installation procedures, test samples, construction timeline, and strain gage installations.
2. WVU's visit on July 18, 2008 included the activities and observations given below, which were summarized and sent to Jeff Levan on July 24, 2008.

- During our visit to the PennDOT bridge site on Friday, July 18, 2008, the FRP application had just been completed. The FRP installation was done according to WVU design as approved by PennDOT and modified by BASF. The workers were applying the UV protective coating to the entire surface of beam.

- The wrapping schemes were as presented in Table 1:

Table 1: FRP Wrapping Schemes

Beam No.	# of Flexural Plies	# of Side Plies	# of Shear anchors
6	1	-	2 (@ the ends)
5	1	2	14
4	1	-	14
3	1	-	14
2	1	-	14
1	2	-	2 (@ the ends)

- The FRP was applied using a dry application process as opposed to a wet lay-up process. In this dry application process, a primer was applied to the concrete surface that was to receive the FRP. After the primer, the saturant was applied and then the FRP was rolled tightly onto the concrete surface. The FRP was pressed down onto the surface with a squeegee, allowing the saturant to rise up through the FRP. Another layer of saturant was applied to the top of the FRP as the final step.

For 2-plies, the process was simply repeated. Figures 9, 10, and 11 show different FRP layouts.

- There was a 1-in. chamfer along each longitudinal edge of all the beams.

Figure 9: Flexural FRP Reinforcement along the Bottom of Beam 1

Figure 10: FRP U-Wrap along Beam 5

Figure 11: FRP Shear Reinforcement on Beam 2

- Each beam had a small rectangular patch of FRP near the north abutment that was used for pull-off testing. The Beam 6 patch had 2 layers and all other beams had 1 layer. The pull-off tests were conducted on Monday, July 21, 2008.

- Each beam was marked for strain gage placement. The contractor covered these marks with an adequately sized piece of duck tape prior to coating these areas with the protective coating. Three concrete strain gages were placed at the centerline of each beam. Also, three FRP strain gages were placed on adjacent shear strengthening FRP. These gages were placed at quarter points throughout the depth of the web.

- FRP was applied to three concrete test prisms. The procedures used as for dry lay-up in the real structure were followed for FRP bonding. Both one layer and two layers of FRP were bonded. These prisms would be used for pull-off testing per ASTM D 4541. Figures 12, 13, and 14 describe the procedures followed.

Figure 12: Test Prism Coated with Primer Prior to FRP Installation

Figure 13: Resin Applied to Test Prism Prior to FRP Installation

Figure 14: Installation of FRP using to Roller to Fully Impregnate the FRP with the Resin

- FRP laminates were produced using a plywood base (backed by plastic sheet) with the same fabric, primer, saturant, and application technique as in the bridge. Both one layer and two layer laminates were produced. Figure 15 displays the procedure of production of laminates.

Figure 15: Fabrication of FRP Laminate to be used for Direct Tension Testing

- We left both bonded concrete-FRP and FRP laminate samples on the site for curing, and later we picked them up for testing in our laboratory.

- On the same day we noticed some hair cracking on the triple A concrete surface of Beam 6. The hairline cracking occurred for about a length of 1/5 the span length and was located at the midspan. The time of occurrence for this cracking is not known since it was already there upon inspection.

Task 3 Evaluating Concrete, FRP, and FRP-Concrete In-situ Materials

In this task, the WVU team participated in evaluating the quality of concrete repair materials (both triple A and bag repairing materials), Concrete-FRP, and also FRP laminates. The test results are being provided in tables and figures with comments. The test results collected from PennDOT District 3-0 will also be furnished.

3.1 Strength and Modulus of Elasticity of Triple A Mix

This triple A mix was used for Beam 6, most of Beam 5, and the encasement of Beam 1. The following mix properties are reported below:

1. The 28-day mean (three specimens) compressive strength (ASTM C 39) = 5550 psi (COV=0.03);
2. The 28-day mean (three specimens) static modulus of elasticity (ASTM C 469) = 4615 ksi (COV=0.032);
3. The 28-day mean (three specimens) dynamic modulus of elasticity (ASTM C 215) = 5920 ksi (COV=0.025);
4. The mean (six specimens) unit weight (ASTM C 642) = 2260 kg/m^3
5. The 90-day mean (three specimens) compressive strength which is close to FRP installation day = 6530 psi. The curing of these specimens was done in laboratory air after 28 days to simulate field air curing.

The above values show that triple A mix gained strength over time and attained standard strength and modulus of elasticity during FRP installation. The concrete strength and modulus of triple A was also close to the old concrete existing in the other beams. Though the unit weight of the triple A mix was slightly lower than typical normal weight concrete, the values were within expected limits.

PennDOT conducted the compressive strength tests of triple A mix and sent the results to the authors; the results are furnished below. The mean strength mentioned below is based on test results of two specimens.

For Beam 6:

1. The mean 7-day compressive strength (QC)= 2545 psi
2. The mean 14-day compressive strength (QC)= 5165 psi
3. The mean 28-day compressive strength (QC)= 6395 psi
4. The mean 28-day compressive strength (AT)= 6260 psi

For Beam 1 (repair) and Beam 5 (bottom part):

1. The mean 13-day compressive strength (QC)= 4435 psi
2. The mean 28-day compressive strength (QC)= 5555 psi
3. The mean 28-day compressive strength (AT)= 6400 psi

3.2 Compressive and Splitting Tensile Strength of Bag Repairing Materials

The bag repairing materials were used for Beams 2, 3, 4, and also for the top 10 in. of Beam 5. The strength values are reported below:

1. The 56-day mean (three specimens) compressive strength (close to FRP installation day) = 9250 psi (COV=0.08)
2. The 90-day mean (three specimens) compressive strength (long-term) = 9500 psi (COV=0.04)

The compressive strength of bag material did not change much between 56-day and 90-day as it is of the high-early strength variety, which is common for most repairing or

patching materials. PennDOT specified the use of this repairing material. It is easily flowable, pourable, and durable cement-based concrete repair material having good bond with the old concrete surfaces. It has high freeze-thaw durability, sulfate and chloride resistance and corrosion resistance due to the corrosion inhibitor added. The compressive strength of bag material was about 46% higher than triple A mix at 90 days. Therefore, it is expected to be much higher than the strength of existing beams with old concrete. The 56-day mean (three specimens) splitting tensile strength (ASTM C 496) of bag material close to FRP installation day, was 595 psi (COV=0.05). Figures 16 and 17 display the compressive strength and splitting tensile strength of bag material.

Figure 16: Cylinder after Compressive Strength test

Figure 17: Cylinder after Splitting-Tension test

3.3 Bond Strength between Old and New Concrete by Pull-off Method

Core cutting tools with 2 in. diameter were used to cut cores of depths slightly more than 2 in. from the surface of both triple A and bag material, in order to reach barely within the substrate old concrete (Figure 18). After cutting the cores, aluminum discs of diameter 2 in. were bonded with epoxy, and the epoxy was cured for 48 hours. The pull-off test was conducted by pulling an attached disc until the concrete ruptured. The equipment used was a hydraulic type pull-off tester with digital recorder. For each concrete type about 8 locations were tested and the ultimate strength, location, and nature of failure were

recorded (Figure 19). The purpose of the test was to obtain the bond strength between old concrete and both triple A mix and bag material, according to ASTM C 1583 and ACI 503R Appendix A.

Figure 18: Core Drill Set-up used for Concrete

Figure 19: Cores Drilled for Pull-Off

For triple A mix, the first test was conducted after 14 days of casting (7-day field curing and 7-day lab curing) to obtain the early bond strength. The bond strength range was found to be between 45 psi and 110 psi. However, four more tests were conducted close to FRP installation day and the values obtained were between 315 to 480 psi. Except for one case (where the failure was in the overlay), for all cases the failure was within substrate or through interface and substrate combination. This indicates that the bond between old concrete and new triple A concrete was adequate.

For bag materials, out of seven tests, two of them failed in overlays (within bag material); however, the rest of them failed in the substrate and substrate/interface combination. The values were within the range of 120 to 395 psi. This indicates that the bond strength between old and bag repairing material was also adequate.

The field pull-off tests were conducted by the contractor, using adhesion pull-off tester with dolly attached to the surface and pulled off by a portable tester. This test indicates

the quality of surface through measuring the tensile strength of surface concrete. Though their first test failed on June 5, 2008 due to inadequate bond of epoxy, their later tests conducted on June 12, 2008 were successful with values that ranged between 294 and 529 psi. The adhesion pull-off test conducted by PennDOT on our samples yielded similar results. All the results show a sound and good concrete surface. The test results are furnished in Table 2.

The surface quality of both triple A concrete and bag material was assessed by conducting a rebound hammer test (ASTM C 805) in our lab, and results were compared. A total of 97 hammer readings were taken for each prism (triple A and bag material). The comparative data show the following:

- For triple A mix: Mean = 32, Median = 34, and COV = 0.12
- For bag mix: Mean = 36, Median = 38, and COV = 0.10
- By statistical analysis using ANOVA (with 95% probability), it can be said that the surface hardness of each material is distinct and that bag material had better surface hardness compared to triple A, though both of them have adequate, sound surfaces suitable for FRP lay-up.

3.4 Bond Strength between FRP and Concrete

The bond strength between FRP attached to both triple A and bag mixes were determined per ASTM D 4541. The FRP was attached both as single layer and double layer on the prism with bag material. The FRP disc was cut by drilling a 2 in. diameter core cutter that barely penetrated into the repaired material substrate (Figure 20). The aluminum discs were attached to the top surface using epoxy as before (Figure 21). The epoxy was allowed to cure for 48 hours in a curing room.

Figure 20: Field Prepared Prism Prepped for FRP Pull-Off Tests

Figure 21: Discs Attached for the Pull-Off Test

Table 2: Field Performed Pull-Off Testing (Reported by PennDOT-District 3

Date tested: 6/5/2008

Beam #	Reading	Pass/Fail	Location	Comment
1	194	FAIL	Right face @ mid-span	Re-mount
2	71	FAIL	Bottom face @ 8' from near abutment	Epoxy failed, re-mount
2	0	FAIL	Left face just past mid-span	Pulled off, no reading, re-mount
3	116	FAIL	Bottom face at far abutment patch	Re-mount
3	529	PASS	Left face at 3/4 point	Okay
4	343	PASS	Right face @ mid-span patch	Okay
4	0	FAIL	Bottom face @ 2/3 point	Epoxy failed, re-mount
5	17	FAIL	Bottom face @ 1/3 point	Re-mount
6	0	FAIL	Inside face at 1/3 point	Pulled off, no reading, re-mount

Date tested: 6/12/2008

Beam #	Reading	Pass/Fail	Location	Comment
1	442	PASS	Right face @ mid-span	Okay
2	294	PASS	Bottom face @ 8' from near abutment	Okay
3	529	PASS	Left face at 3/4 point	Okay
3	430	PASS	Bottom face at far abutment patch	Okay
4	325	PASS	Bottom face @ 2/3 point	Okay
6	529	PASS	Left face @ mid-span	Okay

Date tested: 7/21/2008
*

Beam #	Reading	Pass/Fail	Location	Comment
1	319	PASS	Right vertical face, 65" from NAB, 5" up from bottom	Okay
2	401	PASS	Right vertical face, 54" from NAB, 5" up from bottom	Okay
3	421	PASS	Left vertical face, 52-1/2" from NAB, 5-1/2" up from bottom	Okay
4	544	PASS	Left vertical face, 50-1/2" from NAB, 5" up from bottom	Okay
5	441	PASS	Right vertical face, 49" from NAB, 20" up from bottom	Okay
6	0	FAIL	Right vertical face, 67-3/4" from NAB, 5-1/2" up from bottom	Gauge malfunction

* Pull-off tests performed on single layer of FRP wrap, beam #6 had two layers but test was invalid due to gauge malfunction.

Performed pull-off test on 3 samples to be sent to WVU on concrete surfaces: #1 = 491 psi (on 1st layer of concrete); #2 = 376 psi on 1st and 2nd layer of concrete. Dolly on 1/2 of each layer; #3 = 484 psi on 1st layer.

Testing on 6/5 and 6/12 witnessed by J.R. Levan and J.A. Stabinski; Testing on 7/21 witnessed by J.A. Stabinski.

The discs were pulled off using the hydraulic type pull-off tester with digital display (Figure 22). The ultimate loads were recorded and divided by the area of discs detached to obtain the pull-off strength. The ultimate load and type of failure were recorded for each case. The test results are summarized as follows:

(a) For bond between FRP and triple A:

Mean values of six successful tests = 600 psi with COV = 0.12

Out of seven tests one failed in epoxy/FRP interface and six failed through concrete substrate as cohesive failure near FRP, indicating a strong bond between FRP and concrete substrate.

(b) For bond between single layer FRP and bag material:

Mean value of six successful tests = 740 psi with COV = 0.10

All the tests except one were successful with failure planes through concrete substrate in a cohesive fashion indicating a strong bond between FRP and concrete substrate (Figure 23).

(c) For bond between double layer FRP and bag material:
Mean value of seven successful tests = 810 psi with COV=0.05
All the tests were successful and failure occurred through the concrete substrate layer for five of the samples. Since there were two layers of FRP, in two cases about 10% areas failed through the laminates and 90% through the concrete.

A comparison shows that concrete with bag material offered a better bond to FRP laminate, and double layer FRP interface was stronger than single layer in pull-off tests. The double layer test results were also more consistent as evident from lower COV.

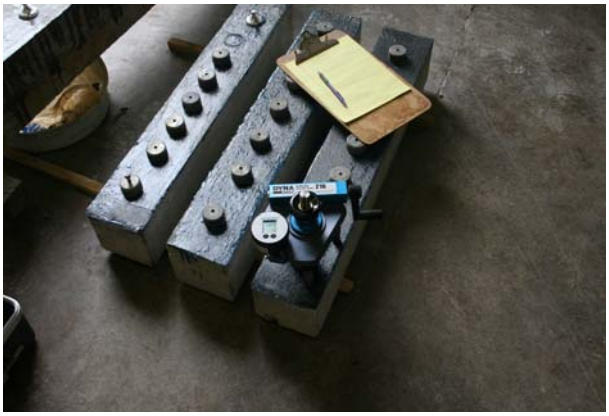

Figure 22: Testing of One Disc is in Progress

Figure 23: Pull-Off Test Showing Cohesive Failure

Table 2 in section 3.4 shows the pull-off results of single layer FRP-concrete bond in the field. All the results except one "passed." The failure occurred due to gage malfunction. The values were in the range of 319 to 544 psi. It is probable that the field tests were conducted on FRP bonded on either old concrete or triple A mix, not on bag repair materials.

3.5 Testing of FRP Tension Coupon Samples

The field prepared and cured FRP laminates were tested in an MTS machine per ASTM D3039/D3039M-00. Two FRP laminates were used consisting each of 1-ply and 2-ply.

The coupons were cut into strips 1 in. wide and 12 in. long. Two aluminum end tabs, each 1 in. by 4 in., were bonded with epoxy to each end of the sample. The tabs were externally serrated and pressure bonded to the FRP for 48 hours.

The gage length of each tension specimen was 4 in. Each specimen was tested in tension to failure at a constant load rate of 1,000 lbs/min using MTS 810 Material Testing System equipped with hydraulic wedge grips (Figure 24).

Figure 24: FRP Coupon Tension Test Setup

For each case five coupons were tested. The results are provided below:

For 1-ply:

The mean tensile strength = 115 ksi with COV = 0.10. The average thickness measured by caliper was: 0.03 in.

For 2-ply:

The mean tensile strength = 142 ksi with COV = 0.07. The average thickness measured by caliber was: 0.051 in.

As could be expected, the ultimate tensile strength of 2-ply was much higher than 1-ply. The stress vs. elongation curves (Figures 25 and 26) for FRP direct tension tests show the nearly linear-elastic behavior and brittle failure for both cases. As a result of high ultimate tensile strength for the 2-ply system, the ultimate elongation is also higher, indicating no change in stiffness due to increase in thickness for up to 2-ply.

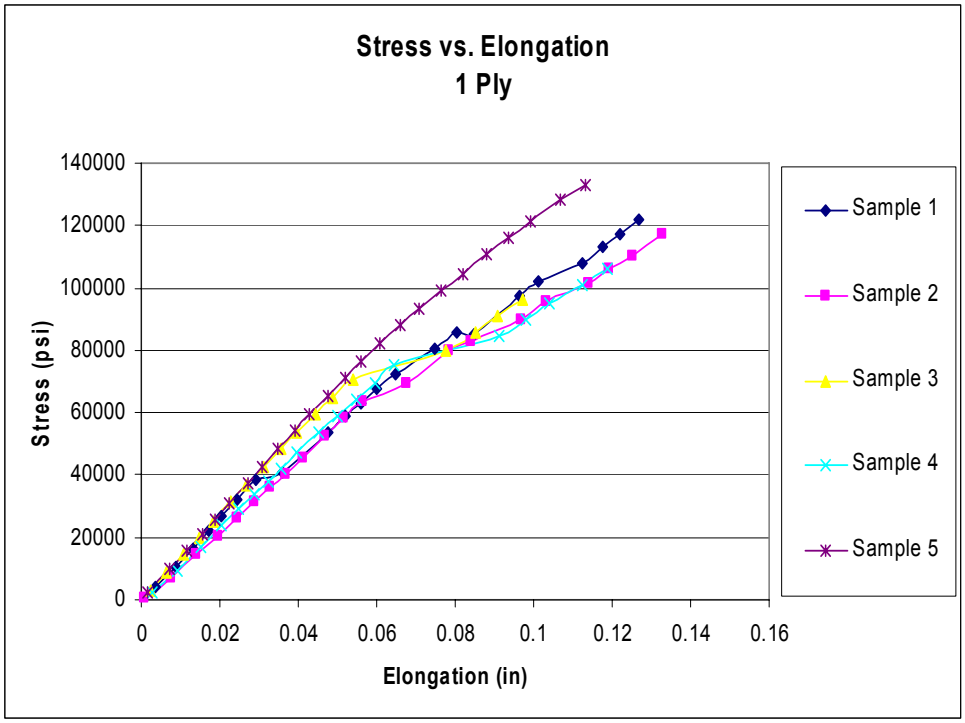

Figure 25: Five 1-Ply Samples

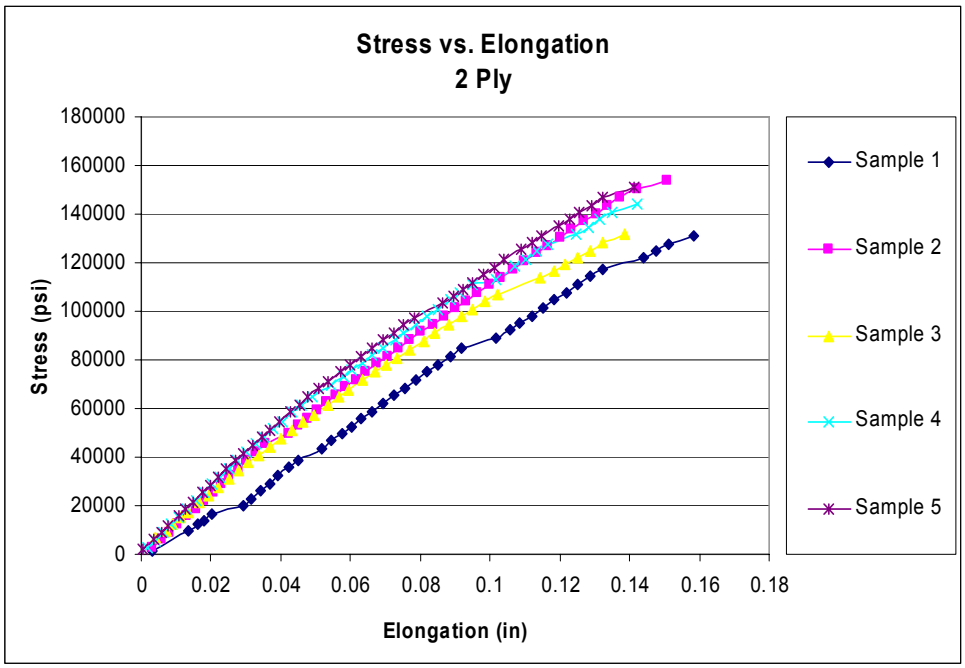

Figure 26: Five 2-Ply samples

Task 4 Testing of Repaired Structure

On April 15, 2008 the authors submitted an interim report on Task 1 covering Planning Activities Report for Field Work and Research. On September 15, 2008, a second interim report was submitted covering both Task 2, Assisting with QC and Field Performance Tests of Repairs; and Task 3, Evaluating Concrete, FRP and FRP-Concrete In-situ Materials. This section of the final report is focused on Task 4, Testing of Repaired Structure, presented in two major sections: Finite Element (FE) analysis, and field testing of the repaired bridge.

4.1 Finite Element Analysis of Repaired Bridge

The information for the FE analysis was obtained from a combination of available design documents provided by PennDOT District 3 and field information obtained from previous tasks. The model was developed in order to: (1) determine current capacities of the repaired bridge, (2) identify critical load conditions for field testing of the structure, and (3) compare predictions with field responses when actual test truck-loads are used. Subsequently, this model was calibrated using the field test results and modified to increase its accuracy. The calibrated model will permit its confident use in evaluating more thoroughly the performance of the strengthened system.

4.1.1 FE Modeling and Results

The 8-node linear brick element C3D8R, with reduced integration and hourglass control, was chosen to model the concrete. C3D8R was used for the three-dimensional modeling of concrete with or without reinforcing bars. Three-dimensional linear truss element T3D2 was chosen to model flexural and shear reinforcement in girders, deck, parapets, and curbs. T3D2 was embedded into solid element C3D8R (truss-in-solid) to provide a realistic representation for the reinforcement and the displacements of the reinforcing bar coinciding with those of the concrete (perfect bond between the reinforcing bar and the concrete was assumed). This refined approach to 3D geometric-replica analytical modeling is now practical and enables explicitly simulating every material point of the bridge for an accurate representation of the geometry, the actual behavior mechanisms

and existing repair condition. The 2.5" overlay was also modeled using C3D8R elements and tied to the composite deck. To simplify the modeling, the cross-section of the parapets was assumed to be rectangular with the same height as of the actual structure. The FRP strip was modeled using "Element-Based Surface," and the surface based "TIE" constraint was used to couple the FRP strips and concrete surfaces. The details of the reinforcing rebar and FRP system in the model are shown in Figure 27 and Figure 18. Figure 29 shows the meshed finite element model.

Several assumptions were made in modeling. All elements represented linear-elastic and isotropic material since the applied load was relatively low with respect to the ultimate load condition. Different concrete compressive strengths were used at different locations. The strength used for deck was 5,000 psi measured from deck core samples, 6,530 psi for bagging/patching materials based on WVU testing results and results provided by PennDOT. Although AASHTO Manuals for Condition Evaluation of Bridges suggests a value of 2,500 psi for bridges built prior to 1954, a value of 4,000 psi was used for all existing girders based on inspection and considering the repair/patching effect. Subsequently, this model was calibrated using the field test results and modified to increase its accuracy as detailed in Section 4.1. The calibrated model can be further used to evaluate other bridges. Therefore, with no like design, the FE model needs to simulate field conditions as closely as possible, and this is why 4,000 psi instead of 2,500 psi was used. Also, in an effort to simulate field conditions as closely as possible, the stiffness of the barriers was considered in the FE analysis. The modulus of elasticity of the concrete was based on compressive strength, according to the standard equation ACI 318-02, Section 8.5.1: $E_c = 57000\sqrt{f_c'}$. The cross-sectional area of rebar was reduced by 20 percent based on the measured dimension of the corroded rebar sample. The concrete Poisson's ratio was set to 0.15. Different element sizes were used to optimize the model and decrease the computation time. The size chosen for the longitudinal and transverse cross sections allowed for easier and more accurate location of the steel rebar and reduced the number of the elements in the "secondary" parts of the model, such as the parapets and the diaphragm beams. Based on the test results of the

rebar sample, the modulus of elasticity and the Poisson's ratio for the steel reinforcement were assumed to be 29000 ksi and 0.3, respectively. The orthotropic properties of FRP strip were based on a datasheet provided by the manufacturer as shown in Table 3. The structure was modeled using 126,419 elements and 155,001 nodes.

Since the superstructure is sitting on and connected to the abutments by 18 anchors at one end and 18 dowels at the other end through the stiff diaphragm beams, pin-pin boundary conditions were chosen to accurately represent the actual restrains at the boundaries. The bridge was vertically, longitudinally, and transversely restrained at 18 nodes corresponding, respectively, to anchor and dowel positions at each end. Besides the dead load, two lanes were loaded with an HS20 AASHTO truck loading placed on top of the overlay. The load was positioned at the center span and also near the support; these were determined to be the critical locations for bending and shear, respectively. The wheel loads were assumed as uniformly distributed over an area of 20x10 in^2, as per AASHTO specifications. The uniform loads were discretized as concentrated forces at the nodes corresponding to the truck wheel foot print, and each force was determined by dividing the total distributed load by the number of nodes. The wheel loads are listed in Table 4. The wheel spacing is shown in Figure 30. As an example, the position of the tandem truck loads used for testing the bridge (see Figure 30) is shown in Figure 31.

Table 3: Properties of MBrace CF 130

Physical Properties	Fiber Tensile Strength	720 ksi
	Areal Weight	0.062 lb/ft^2
	Nominal Thickness	0.065 in/ply
0° Tensile Properties	Ultimate Tensile Strength	550 ksi
	Tensile Modulus	33000 ksi
	Ultimate Rupture Strain	1.67%
90° Tensile Properties	Ultimate Tensile Strength	0
	Tensile Modulus	0
	Ultimate Rupture Strain	n/a

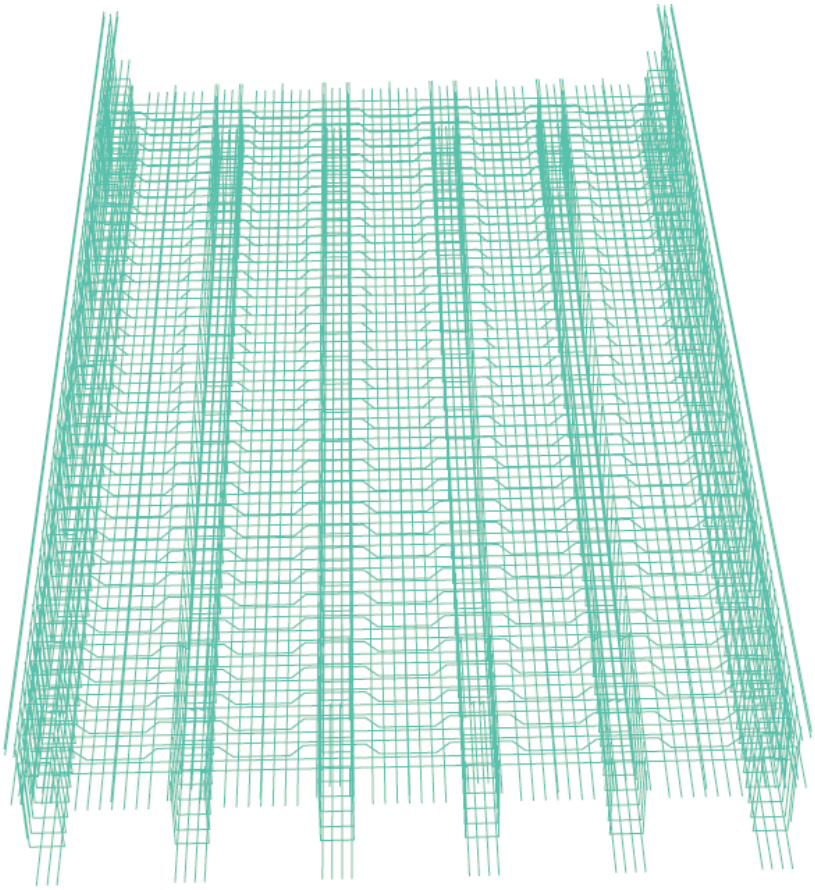

(a) 3D

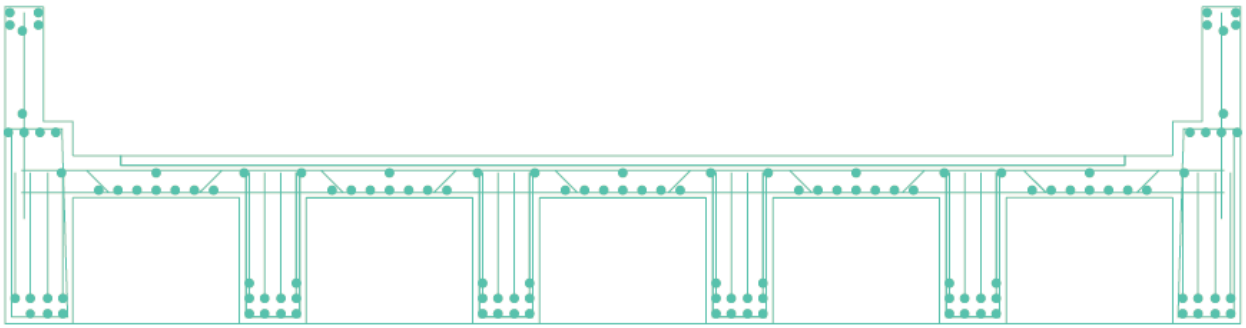

(b) Cross-section

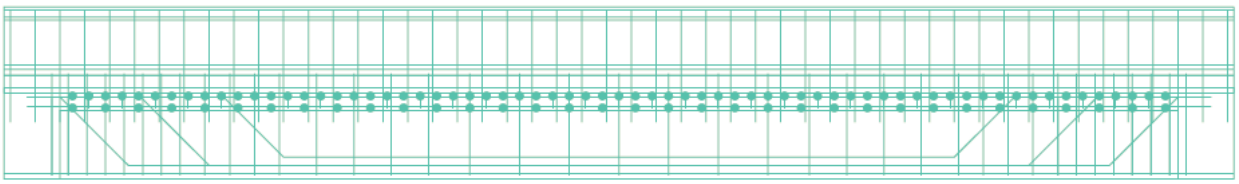

(c) Side View

Figure 27: Rebar System of the Model

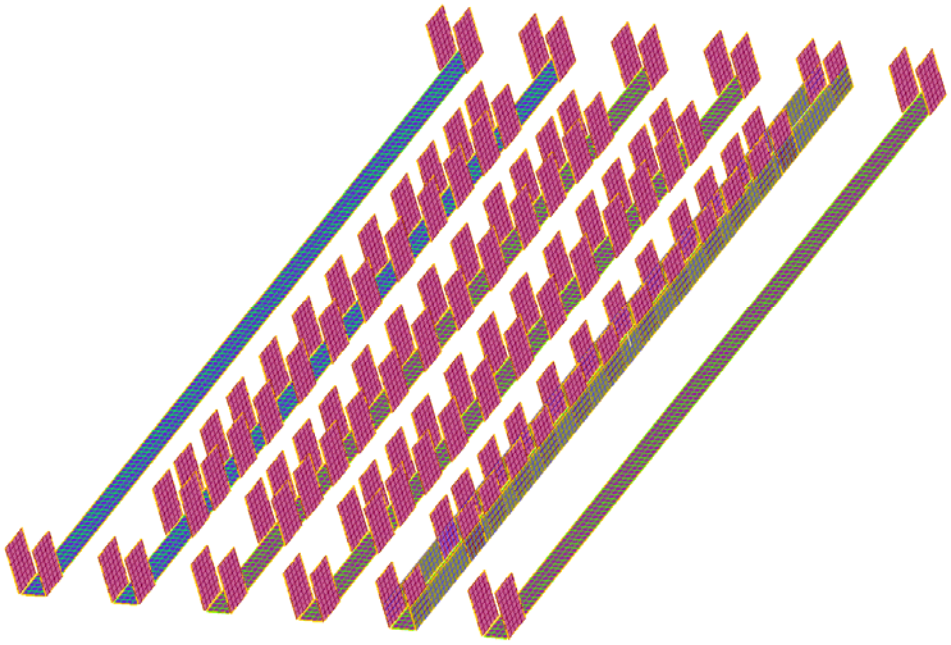

Figure 18: Reinforcing FRP System of the Model

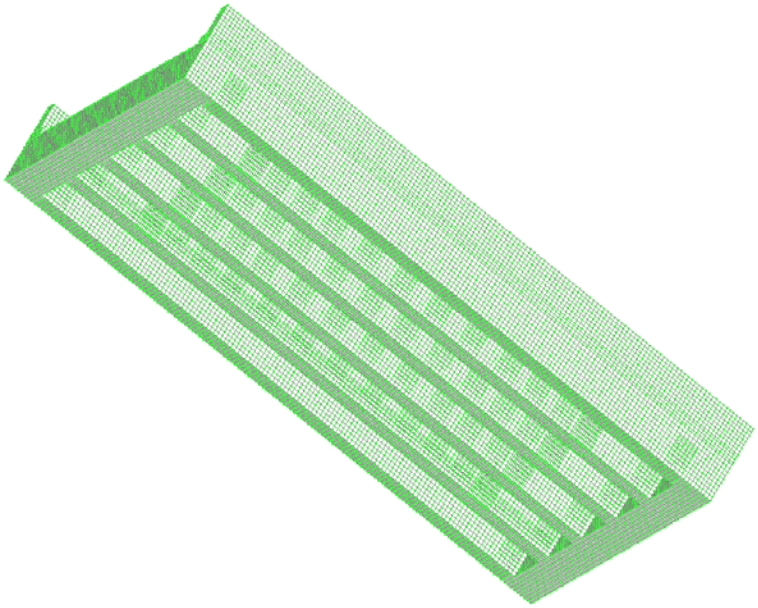

Figure 29: Meshed FE Model

Table 4: Wheel Loading (lbs) for AASHTO and Tandem Trucks

	AASHTO Truck-HS20			PennDOT Tandem Truck #1/#2		
	Left	Right	Total	Left	Right	Total
Front	4,000	4,000	8,000	7,450/7,650	8,000/8,000	15,450/15,650
Rear 1	16,000	16,000	32,000	10,300/11,150	10,300/10,800	20,600/21,950
Rear 2	16,000	16,000	32,000	10,000/11,200	10,400/10,500	20,400/21,700
Total			**72,000**			**56,450/59,300**

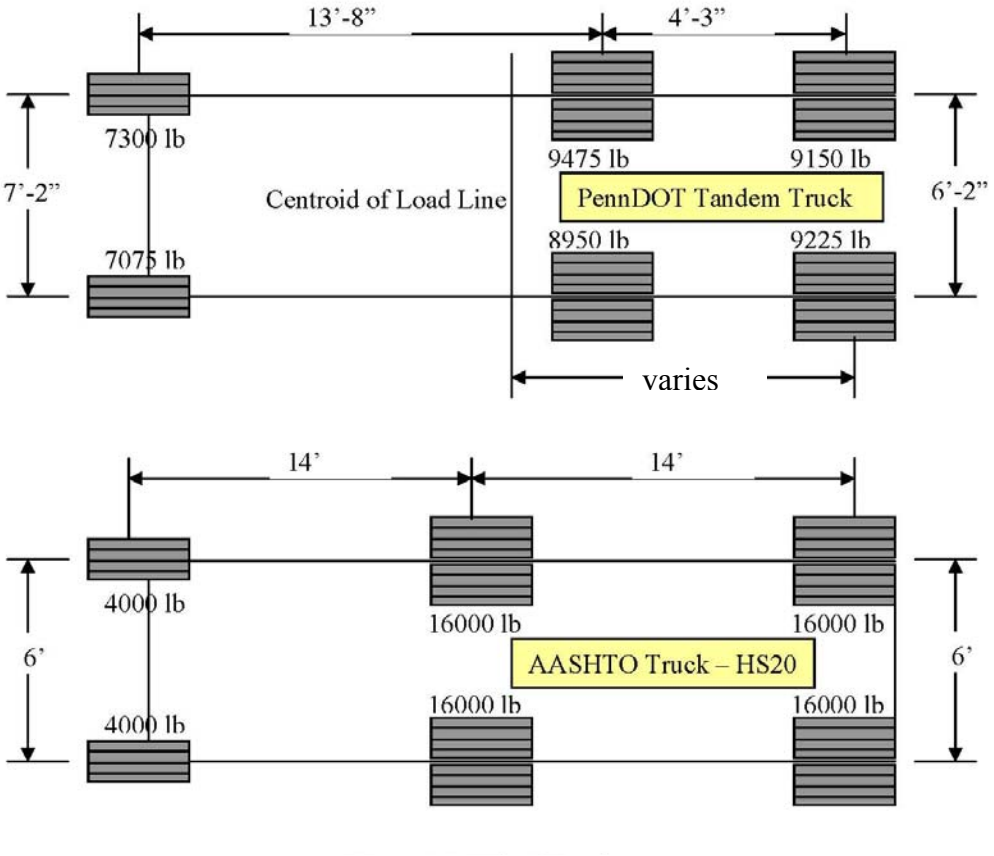

Figure 30: Wheel Spacing

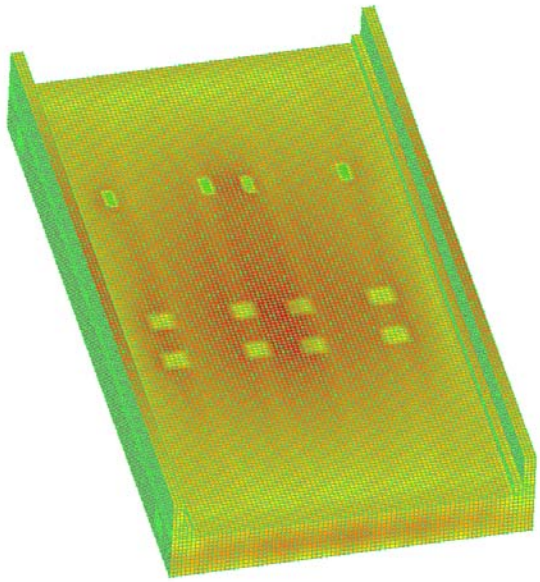

Figure 31: Tandem Truck Load Position

The loading conditions were based on AASHTO specifications. Four load cases were considered in the analysis, as shown in Figure 32. The most critical load condition was determined as Case 3 (Case 1 is almost the same as Case 3). Figure 33 shows a vertical deformation contour plot, and Figure 34 shows the in-plane stress view-cut. Figure 35 and Figure 36 report, respectively, the analytical mid-span displacements and bottom strains for load Case 6, when the center of gravity of the PennDOT tandem truck is at the mid-span. The testing results are also shown in these figures. The FE model predictions correlate well with the testing results. It is noted from Figure 36 that there is some localized effect for the strain on the girder which is directly under the wheel load, which cannot be represented by the FE model. Also, the large discrepancy for girder 3 in Figure 36 could be a result of poor strain gage mounting or simply a malfunction. Strain measurements from externally bonded strain gages on concrete surfaces can be inaccurate at times. This is due to the nature of concrete surfaces, especially for large structures in which surface irregularities occur more often and have greater magnitude.

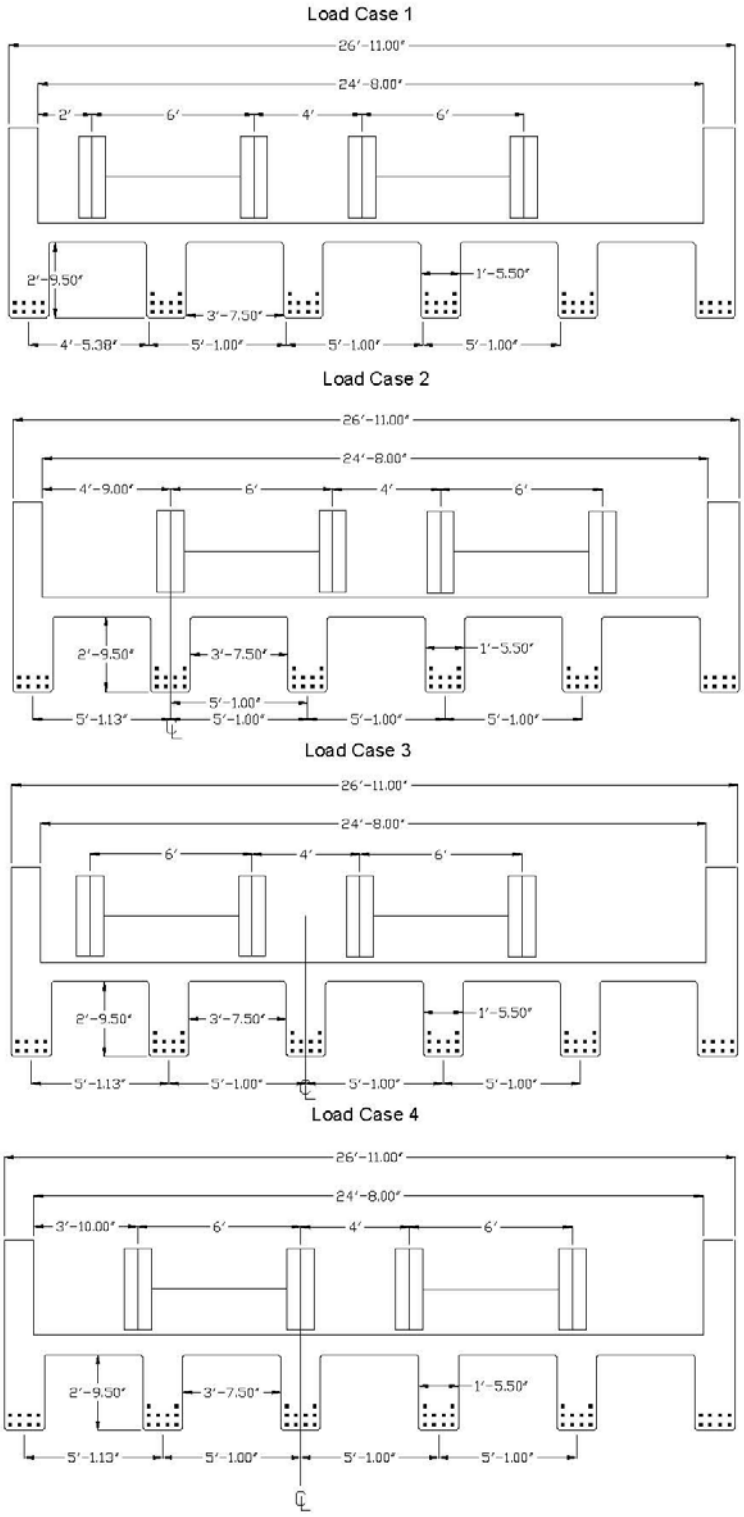

Figure 32: Loading Cases

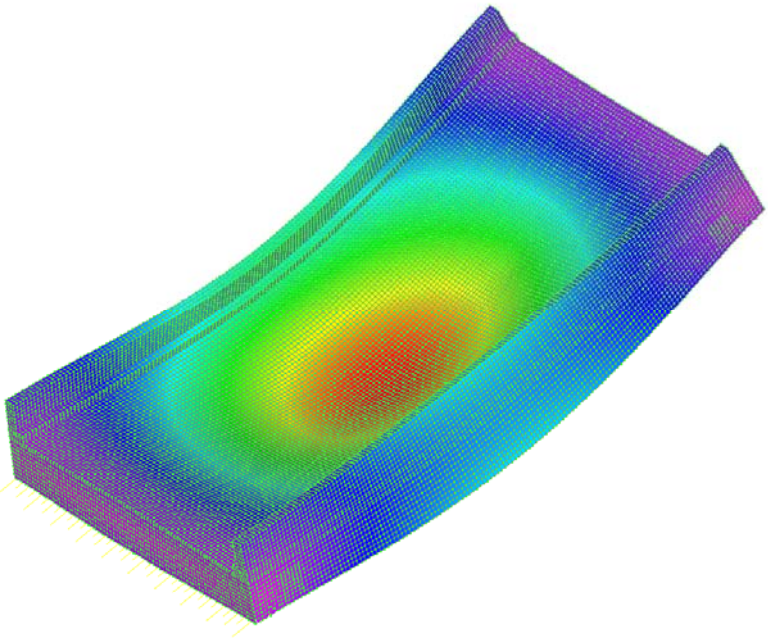

Figure 33: Vertical Deformation Contour Plot

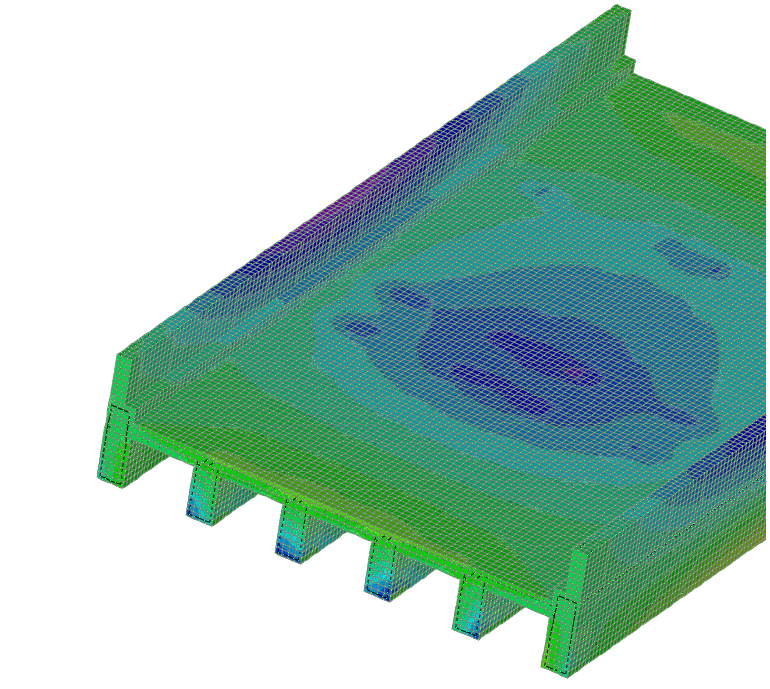

Figure 34: In-plane Stress View Cut

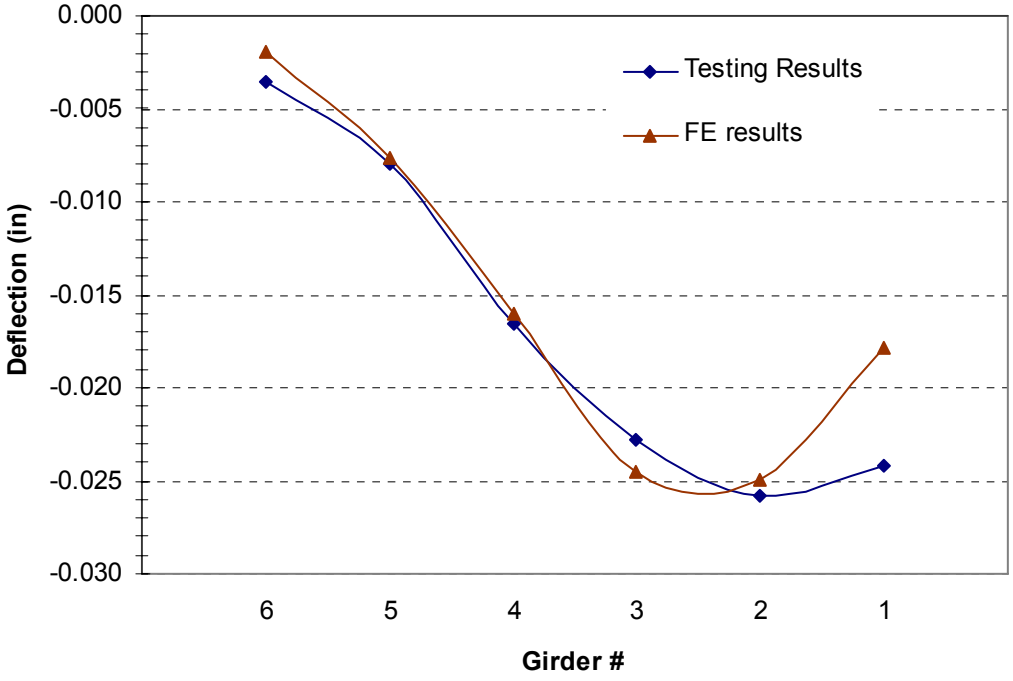

Figure 35: FEA Results for Mid-span Displacement, Case 6, PennDOT Tandem Truck

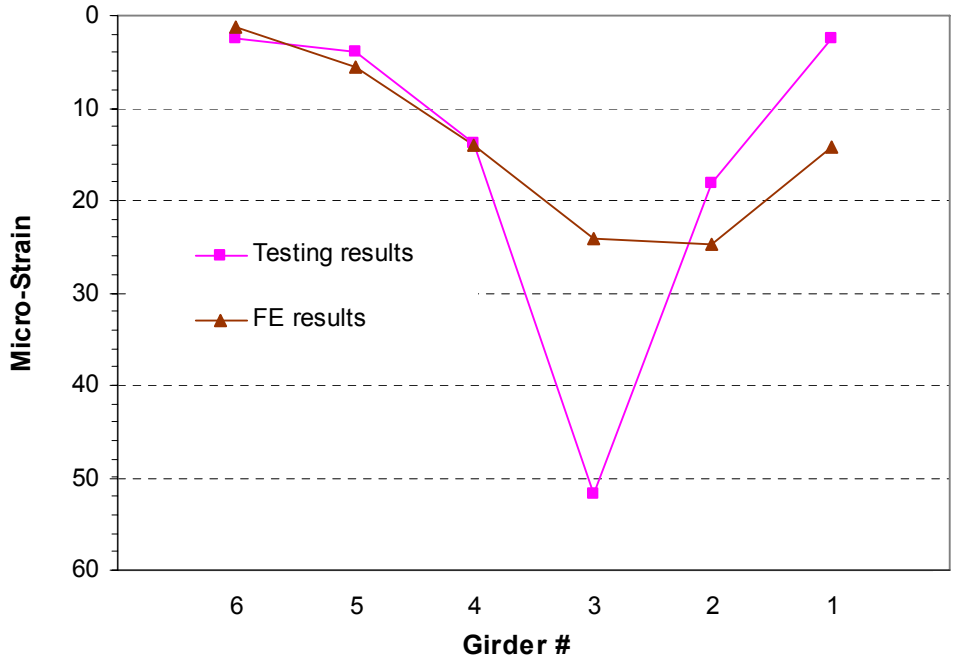

Figure 36: FEA Results for Mid-span Strain, Case 6, PennDOT Tandem Truck

4.1.2 Moment and Shear Force Computation

The output from the 3D solid and truss elements used in the FE modeling provides a stress profile, which is used to compute the girder moments. The effective slab width was calculated based on AASHTO specifications.

The most critical position for girder bending was determined to be at the mid-span of the girder for load Case 3, when the center of gravity of the truck was at mid-span. Load Case 1 was determined to be the most critical position for girder shearing when the rear wheels were near the support.

The normal and shear stresses were integrated to compute the resulting moment and shear force of the section. The maximum moments and shear forces under live load and dead load for girders are given in Table 5.

Table 5: Maximum Moments and Shear Forces for Girders at the Critical Cross-Section

			HS 20 Truck	Dead Load	Factored Load
Moment (k-ft)	Interior Girder		143.41	247.40	726.18
	Exterior Girder		59.06	91.25	285.24
Shear (kips)	Interior Girder	Section 1	27.96	28.04	115.31
		Section 5	11.08	20.53	57.95
		Section 6	11.11	16.99	53.43
		Section 8	7.11	7.35	29.62
	Exterior Girder	Section 1	12.25	29.80	73.28
		Section 5	4.37	16.21	33.40
		Section 6	4.29	13.40	29.52
		Section 8	2.26	5.85	13.97

4.1.3 Load Rating Factor Based on FE Model

Load rating calculations provide a basis for determining the safe load-carrying capacity of a bridge. Inventory and operating ratings are required using the Load Factor Method specified in AASHTO. The bridge should be rated at two load levels, the maximum load level called the Operating Rating and a lower load level called the Inventory Rating. The Operating Rating is the maximum permissible load that should be allowed on the bridge.

Exceeding this level could damage the bridge. The Inventory Rating is the load level the bridge can carry on a daily basis without damaging the bridge. For comparison, the rating factors are computed using the ultimate capacities calculated from the above described FE model. The Rating Factor *RF* is determined by

$$RF = \frac{C - A_1 D}{A_2 L(1+I)}$$

where C is the capacity of the member from cross-section analysis, D is the dead load effect on the member, L is the live load effect on the member, I is the impact factor to be used with the live load effect, A_1 is the factor for dead loads, and A_2 is the factor for live loads. A_1 is taken as 1.3 and A_2 is taken as 2.17 for Inventory Rating or 1.3 for Operating Rating.

Table 6: Rating Factors for the Girders

			Rating Factor Based on FE Analysis		Rating Factor Based on AASHTO		Ratio of Rating Factor (FE/AASHTO)	
			OR	IR	OR	IR	OR	IR
Moment (k-ft)	Interior Girder		3.55	2.13	1.69	1.02	2.10	2.10
	Exterior Girder		6.37	3.81	1.80	1.08	3.53	3.53
Shear (kips)	Interior Girder	Section 1	2.68	1.61	2.00	1.20	1.34	1.34
		Section 5	4.76	2.85	1.67	1.00	2.85	2.85
		Section 6	4.20	2.52	1.67	1.00	2.52	2.52
		Section 8	5.42	3.25	1.95	1.17	2.77	2.77
	Exterior Girder	Section 1	6.01	3.60	4.01	2.40	1.50	1.50
		Section 5	10.15	6.08	2.87	1.72	3.53	3.53
		Section 6	9.32	5.59	2.94	1.76	3.17	3.17
		Section 8	14.25	8.54	3.61	2.16	3.95	3.95

Load ratings were calculated for AASHTO truck HS20. The maximum shear and maximum moment were listed in Table 5. An impact factor was also taken into account for load rating. This value for the bridge studied is 30%. Table 6 gives the results of the Rating Factor for the girders. For comparison, the Rating Factor based on AASHTO

specifications is also listed in Table 6. They are based on girder analysis as previously provided by the WVU research team in the report "WVU Design Suggestions for FRP Strengthening Design of PennDOT Bridge #49-4012-0250-1032 on State Route 4012 in northumberland County, PA" and BASF final design calculations.

Table 6 indicates that the current flexural load capacity rating and shearing load capacity rating of the interior girder are at least as much as 2.1 times and 1.5 times higher, respectively, than the current load ratings based on AASHTO specifications. Note that the calibrated FE model simulates all of the situations that were identified during field assessment, including the bonding of FRP strips and concrete patching/replacement. This discrepancy is because of the conservatively imprecise nature of the lateral live-load distribution factors that have been recommended in the AASHTO specifications. In the current load capacity rating practice based on AASHTO specifications, an individual beam is taken out as a free-body, idealized as simply-supported, while the continuity of the bridge in the transverse direction is indirectly accounted by means of axle-load distribution factors. This approach is known to underestimate the plate contributions. It is expected that the differences in modeling assumptions between 3D FE bridge models and 2D AASHTO simplified beam models will lead to different load capacity ratings for the same structure. Support conditions and secondary structural elements also have significant effects on the response of the bridge. The diaphragm beams provide effective rotational restraints and thereby increase bending stiffness at the boundaries, which in turn reduce the critical flexural demand at the midspan.

Similarly, parapets help distribute the flexural stresses from the mid-span towards the edges by creating very stiff girders at the edges. The AASHTO method incorporates idealized pin-roller boundary conditions, increasing the flexural demand at the mid-span. However, this does not reflect the actual design and measured behavior of the bridge. Lateral and longitudinal movement is restrained with dowels at both ends. In addition, the lateral diaphragm beams restrain the movement of the superstructure.

Therefore, the actual boundary conditions do not conform to pin-roller boundary assumptions.

Comparing to the load rating results on un-repaired bridges, it can be noted that the load rating factors have been increased, illustrating the effectiveness of increasing section capacities using externally bonded FRP strips.

4.1.4 Dynamic Response Analysis

A dynamic analysis was also performed in order to determine the natural frequency of the bridge. The frequencies are based on a global response of the bridge. This is another parameter that can be used to verify the accuracy of the FE model developed. This information will provide verification that the FE model and the actual bridge are yielding the same results and responding to loading in similar fashions. The natural frequencies of the bridge were determined to be 13.44, 16.21, 20.92, 28.49, and 30.61 Hertz for Mode 1, Mode 2, Mode 3, Mode 4, and Mode 5, respectively. The Mode 1 natural frequency from field testing is 14.72 Hertz, which is about 9% higher than the predicted value. Figure 37 shows the first three mode shapes.

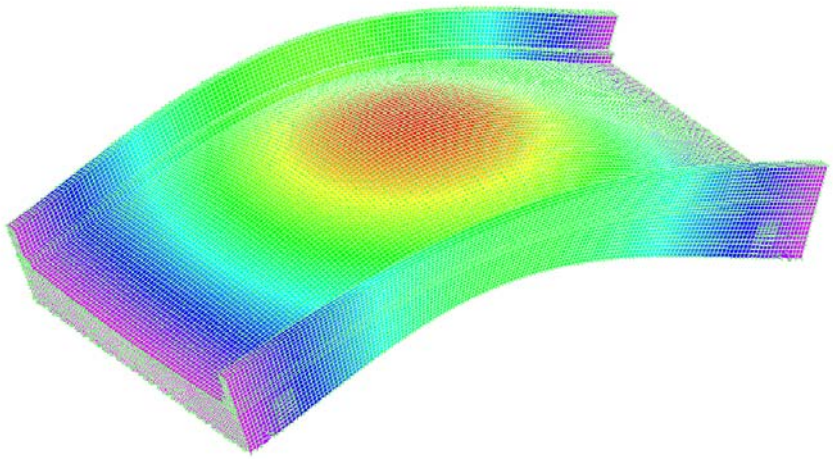

Mode 1 – 13.44 Hz

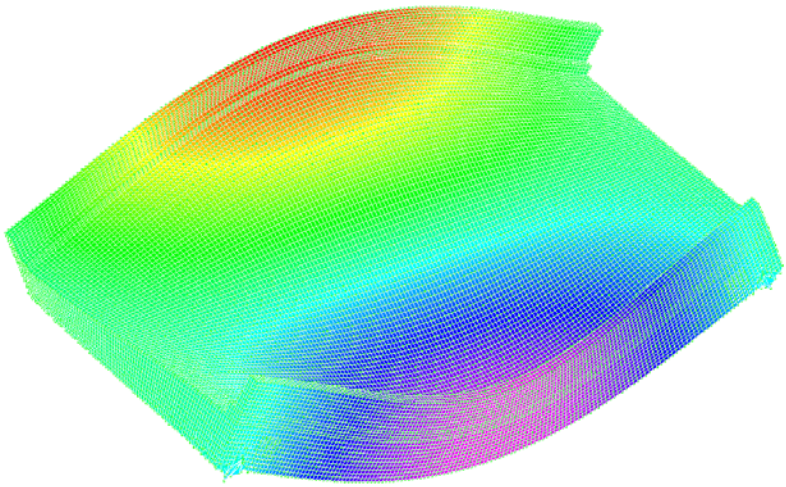

Mode 2 – 16.21 Hz

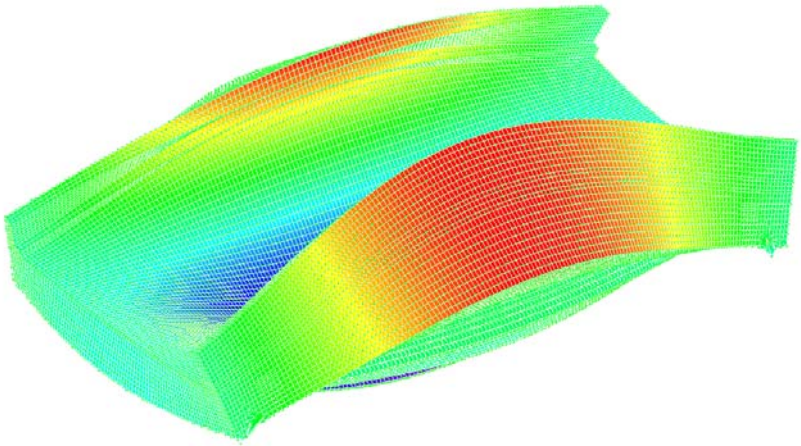

Mode 3 – 20.92 Hz

Figure 37: Mode Shapes and Frequencies

4.2 Testing of Repaired Bridge

The objectives of testing the repaired bridge were to acquire data that would be useful in correlating with results from the FE analysis, and for calibrating and improving the accuracy of the FE model, so that an accurate analysis of the bridge could be performed with allowances for unknown variables; and to compare with data obtained from testing the un-repaired bridge to illustrate the effectiveness of the repair technology.

4.2.1 Setup

Similar to the testing plan of the un-repaired bridge, strains and displacements were recorded at the center of the bridge span under each girder. Accelerations were recorded at the mid-span under Girder #4. See Figure 38 for position of instruments.

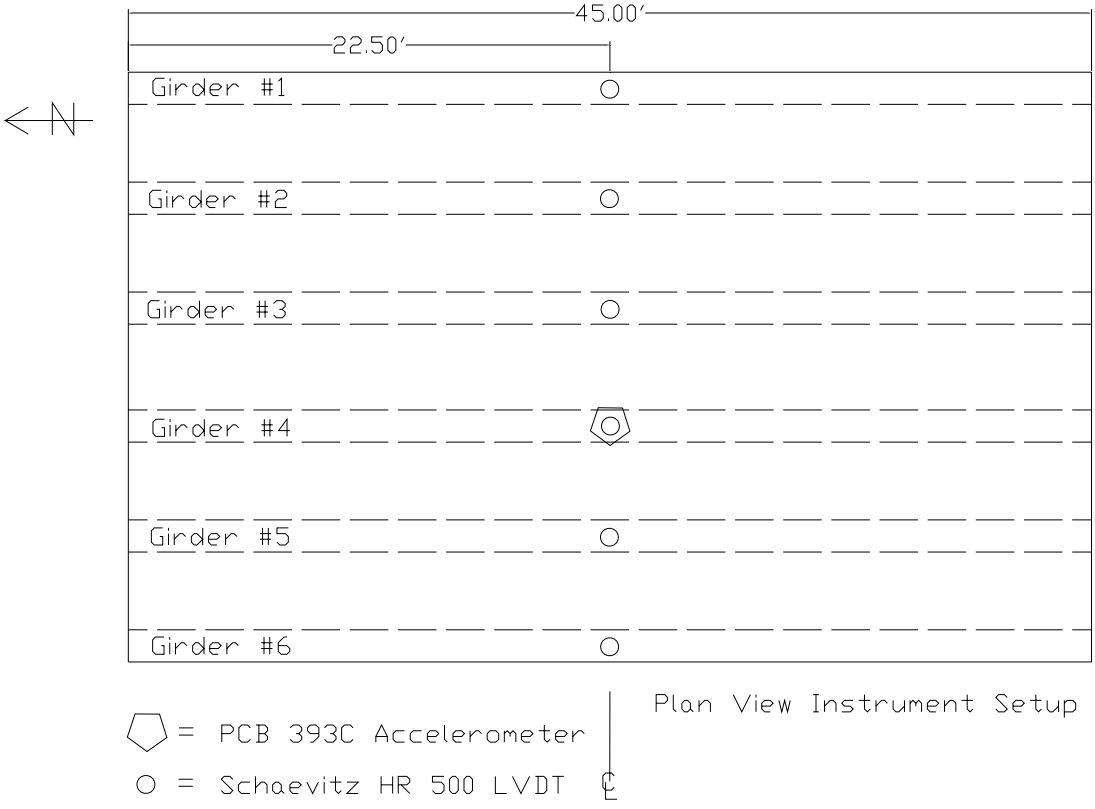

Figure 38: Plan View Instrumentation Placement

4.2.1.1 Strain Gages

In order to find the neutral axis of each girder under loading, four strain gages were to be placed on each girder. Three gages would be placed at the quarter, half, and three-quarter height of the girder web, measured from the bottom of the deck to the bottom of the T-beam. All of these gages would be bonded to concrete, with the exception of the gage at the three-quarter point of Girder #5 which was bonded to a shear reinforcing FRP strip due to the FRP design. It was observed that, as with most concrete surfaces, irregularities were present at some of these locations. As a result, those locations were altered slightly in an attempt to avoid irregularities and obtain better strain data. Refer to Figure 39 and Table 7 for a general layout on vertical girder faces and exact locations of strain gages, respectively. The fourth gage was placed at the center of the bottom face of the T-beam bonded to a flexural reinforcing FRP strip. All gages used on concrete were 4-inch general-purpose strain gages (Vishay Model N2A-06-40CBY-350/P), while all gages used on FRP were 2-inch general-purpose strain gages (Vishay Model N2A-06-20CBW-350/P).

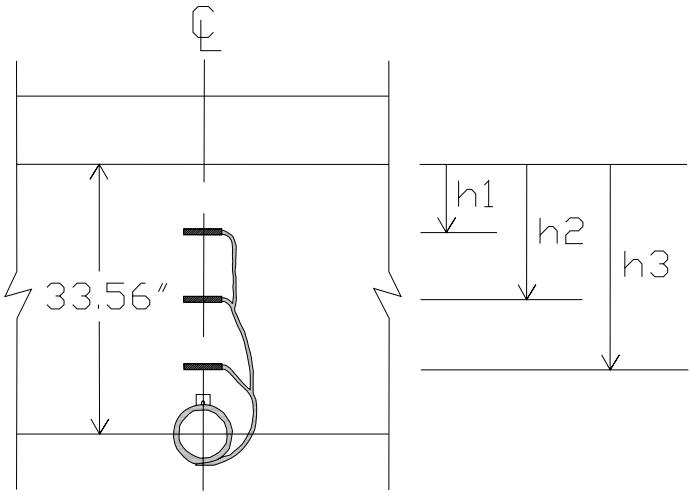

Figure 39: Strain Gage Layout on Web

Table 7: Exact Strain Gage Locations

		Girder #					
		6	5	4	3	2	1
Location (inch)	h1	9.3	8.5	8.3	8.9	9.0	9.2
	h2	15.8	16.5	17.6	17.8	17.2	17.8
	h3	25.5	25.5	25.5	26.0	25.6	26.4

For the un-repaired bridge testing, the concrete surface preparation was attempted but was not successful because the 100% solid adhesive chosen at that time, Vishay M-Bond AE-10, could not cure at temperatures below 75°F. In an effort to solve this problem, under the advice of Vishay applications engineers, a different adhesive was chosen for the void filling process during this test. This adhesive, Vishay M-Bond 300, would allow for curing under a much broader range of temperatures. The curing requirements were: 24 hours at +40°F, 18 hours at +60°F, and 12 hours at +75°F. With this wide range of curing temperatures, the surface preparation was successfully performed. When the preparation was complete, each gage was bonded using Vishay M-Bond 200 and covered with Vishay Barrier E for protection. Figures 40, 41, and 42 illustrate some of these aspects with the strain gage application process.

Figure 40: Surface Preparation

Figure 41: Gage on Flexural FRP

Figure 42: Concrete Gages with Barrier E Protective Coating

4.2.1.2 LVDT's

Six Shaevitz HR 500 LVDTs were placed each, at the bottom-inside face of every girder (see Figure 43). The LVDTs had a range of ±0.5 inches with a sensitivity of 0.001 inches. The LVDTs were held in place by rubber grip test tube holders that sat on scaffolding, as can be seen from Figure 44. Due to the clearing of the creek bed after the repair was completed, scaffolding served as a very convenient tool for both testing preparation and setup; providing a rigid and level surface. The displacements were taken at ten scans per second during the static load tests. Figure 45 illustrates this overall setup.

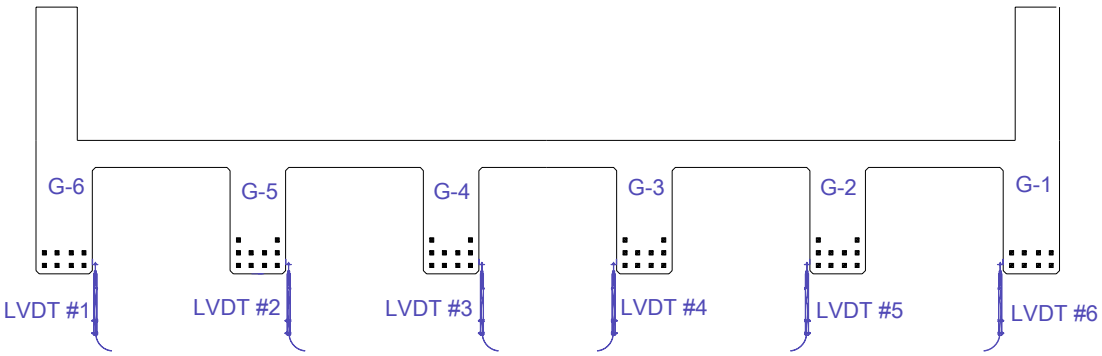

Figure 43: Cross-Section View LVDT Setup

Figure 44: LVDT Setup

Figure 45: Overall Test Setup

4.2.1.3 Accelerometer

A PCB Model 393C accelerometer was used to measure the vibration response of the bridge due to dynamic loading. The accelerometer was placed under the interior Girder #4 to closely reproduce the testing setup of the un-repaired bridge (see Figure 46). The data was collected using a Vishay System 6000 data acquisition system that allowed for using a data collection rate of 10,000 scans per second. Figure 47 illustrates the total instrumentation setup.

Figure 46: PCB 393C Accelerometer Mounted

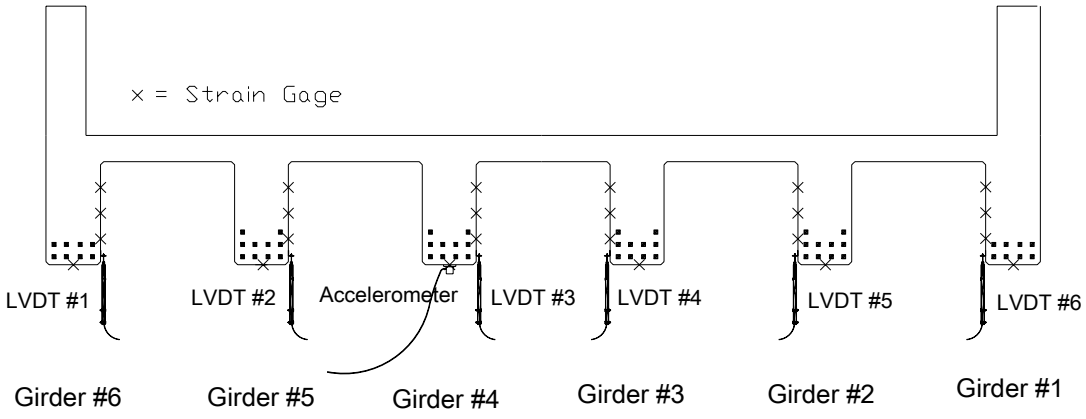

Figure 47: Cross-Section View Instrumentation Setup

4.2.2 Trucks

Similar to the testing of the un-repaired bridge, PennDOT provided two fully loaded tandem dump trucks for the load test. PennDOT personnel weighed the trucks' individual wheel loads using scales. The loads were then used to calculate the centroid of truck loading to define where to line up the trucks on the bridge during testing for maximum load effects. Figures 48 and 49, respectively, show details for each truck.

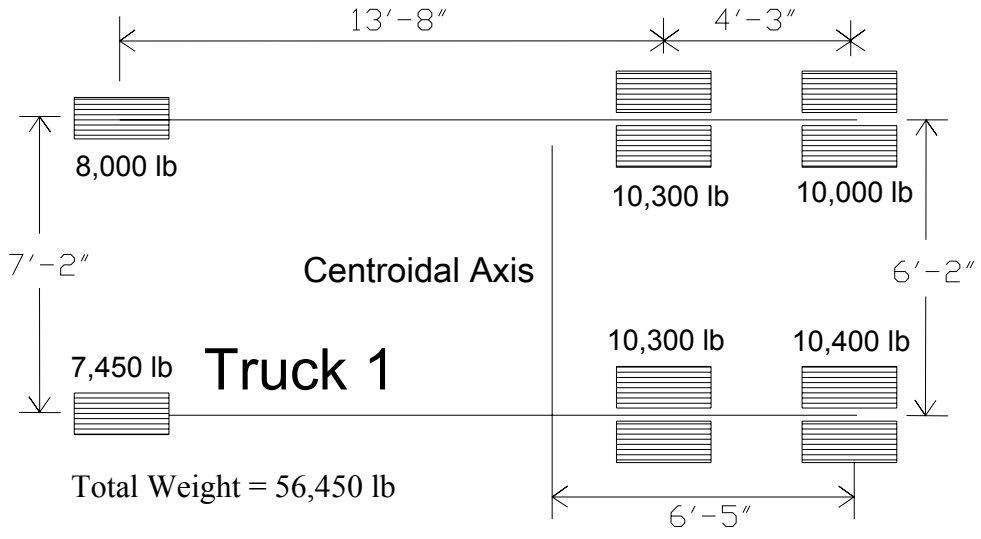

Figure 48: Truck 1

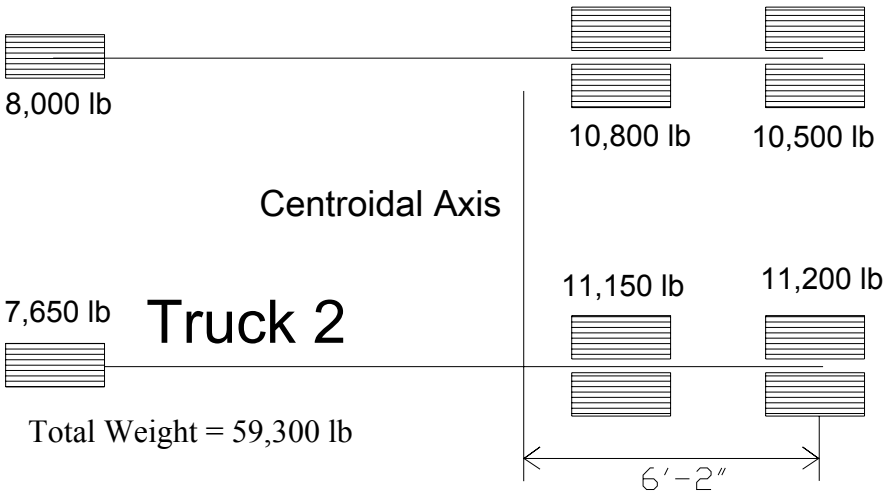

Figure 49: Truck 2

4.2.3 Static Load Cases

During testing of the un-repaired bridge, many of the load cases had to be altered due to the dimensions of the bridge and trucks. For comparison purpose, the same load cases with an addition of two more (Load Case #5 and Load Case #6) were used in this testing. Load Case #5 is a mirror load of Load Case #2-one truck, while Load Case #6 is a mirror load of Load Case #4-one truck. The same modified load cases #1 and #2 were also used in the repaired bridge testing. The goal of the modified load cases was to have an extreme loading event that could be modeled in FE. The trucks were placed back to back as close as possible over the centerline and straddling girder #3 for the modified load case #1, and straddling girder #4 for the modified load case #2. There are no AASHTO specifications for the modified load cases. Refer to Table 8 for a summary of static load cases and descriptions.

Table 8: Summary of Static Load Cases

Title	Description
Load Case #1	See Figure 50
Load Case #2 - two truck	See Figure 50
Load Case #2 - one truck	See Figure 50
Load Case #4 - one truck	See Figure 50
Load Case #5 - one truck	Mirror image of Load Case #2 - one truck
Load Case #6 - one truck	Mirror image of Load Case #4 - one truck
Modified #1	See Figure 51
Modified #2	See Figure 51

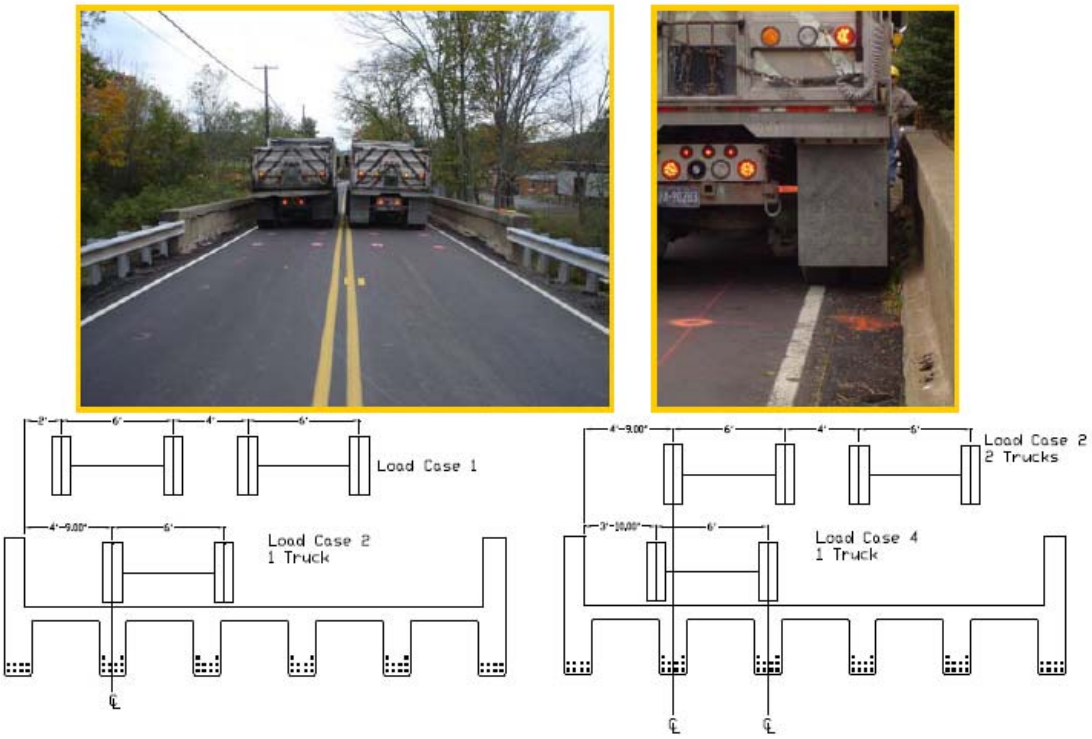

Figure 50: Load Cases

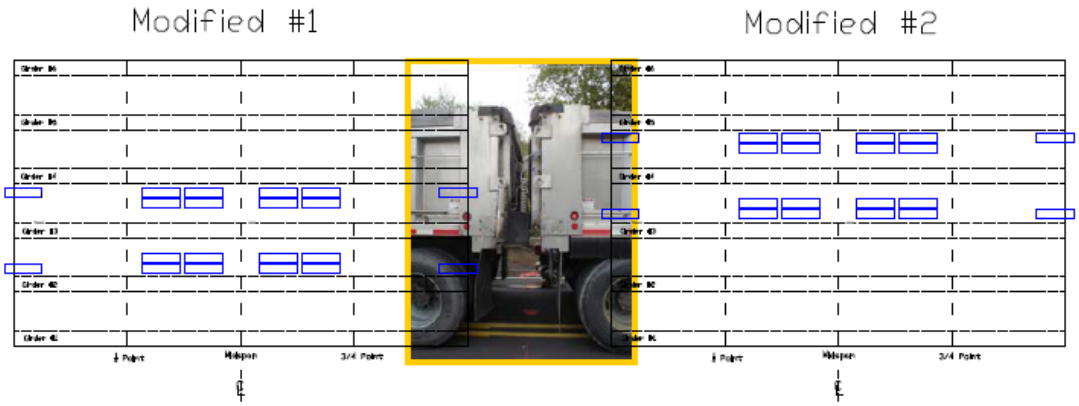

Figure 51: Modified Load Cases

The trucks were moved onto the bridge one at a time and the centroid of the trucks were lined up at the quarter, mid, and three-quarter points of the bridge. While continuous data was taken from the initial time the trucks were moved onto the bridge, 30 to 40 seconds were allowed at each placement to let the bridge dampen itself so that there would be no impact loads recorded in the results.

4.2.4 Dynamic Load Cases

For dynamic loading of the un-repaired bridge, six dynamic tests were run. Three tests used a 2x4 wood plank that was placed at one end of the bridge to excite the trucks suspension system and therefore excite the bridge under forced vibration. The other three consisted of the truck simply jamming on the brakes around the middle of the bridge at a speed ranging from 30 mph to 50 mph. It was concluded that brake jamming tests gave much better results compared to the wood plank tests. Therefore, it was decided to use only the brake jamming tests for dynamic loading on the repaired bridge. This brake jamming test for vibration response was repeated three times. The data was recorded at 10,000 scans per second, which was the limit of the data acquisition system.

4.2.5 Testing Results

The load testing deflection results are shown in Figures 52-55 for load cases #1, #2 – 1 truck, #2 – 2 trucks, and #4. The three curves on each figure represent the deflection under each girder when the truck centroid is positioned at quarter, mid, and three-quarter points along the span of the bridge. Deflection results for load cases #5 and #6 are shown in Figures 56 and 57. These load cases were not used in the un-repaired bridge testing and, as stated earlier, are mirror loads of load case #2 – 1 truck and #4 – 1 truck, respectively. Mid-span deflection data from load case #2 – 1 truck and load case #4 – 1 truck are plotted on the same figures to show symmetric stiffness of the repaired bridge. As can be seen from the figures, Girder 1 has nearly the same stiffness as Girder 6, Girder 2 has nearly the same stiffness as Girder 5, and Girder 3 has nearly the same stiffness as Girder 4. This comparison is made easy by flipping the data from load case #2 – 1 truck and load case #4 – 1 truck as can be seen from the data labels in the graphs. This method was further used in Figure 58 in which Modified #1 and Modified #2 are

compared to confirm symmetric stiffness throughout the repaired bridge. Deflection results for the repaired and un-repaired bridge based on Modified #1 and #2 are shown in Figures 59 and 60, respectively. It is important to note that all deflection values from testing of the un-repaired bridge were scaled up due to the weight difference of the trucks. During testing of the un-repaired bridge, the average of the two truck weights was 51,175 lb, whereas during testing of the repaired bridge, the average of the two truck weights was 57,875 lb. Based on this difference, a scale factor was used to compare deflection values at the same loading level. This scale factor was used to proportionally increase all un-repaired deflection values as

$$scale\ factor = 1 + \frac{repaired\ test\ weight - unrepaired\ test\ weight}{unrepaired\ test\ weight} = 1.131$$

It is noted that this method of obtaining comparable values is reasonable for symmetric loading conditions only, since each wheel loads is different for the tandem trucks provided. A more accurate analysis can be performed using the FE model to verify the testing data since the FE analysis can include more accurately the individual axel loads and their corresponding locations on the bridge as shown in Section 4.1. As illustrated in the aforementioned deflection graphs, no significant changes are observed in the deflections of the un-repaired bridge and repaired bridge, indicating minor change of stiffness from externally bonded FRP strips. The deflection results for load case #1 – 2 trucks and load case #4 – 1 truck seem to indicate a possible malfunction in LVDT #1.

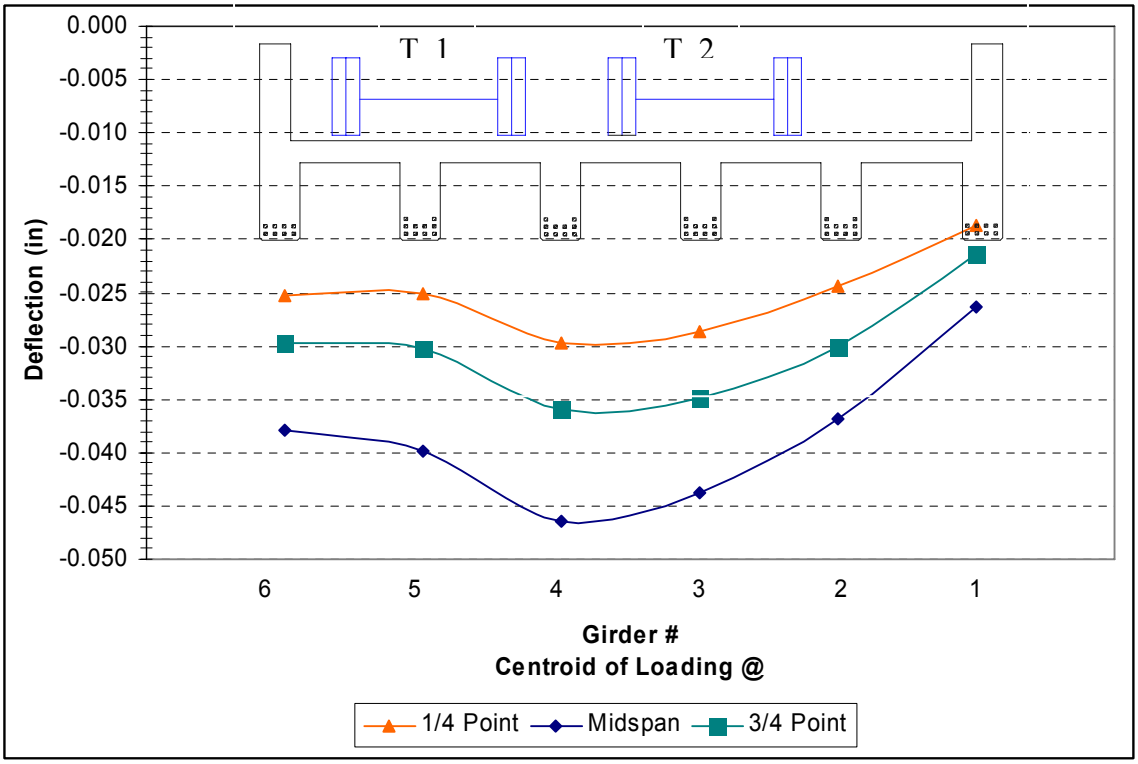

Figure 52: Load Case #1 – 2 Trucks

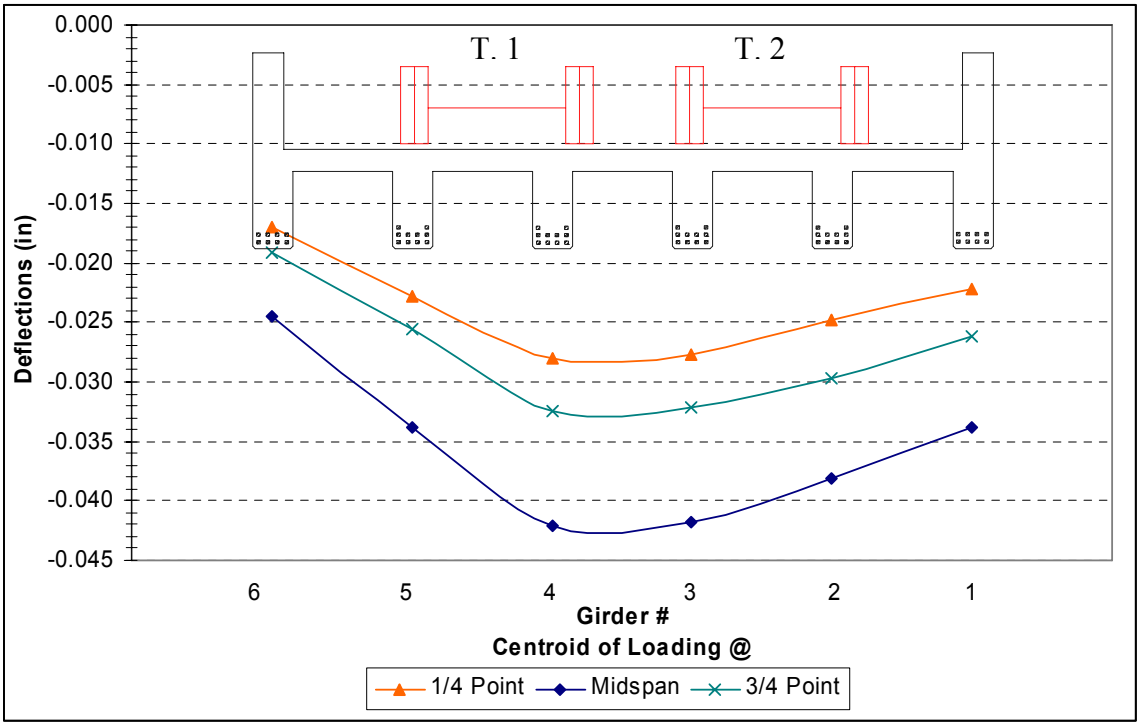

Figure 53: Load Case #2 – 2 Trucks

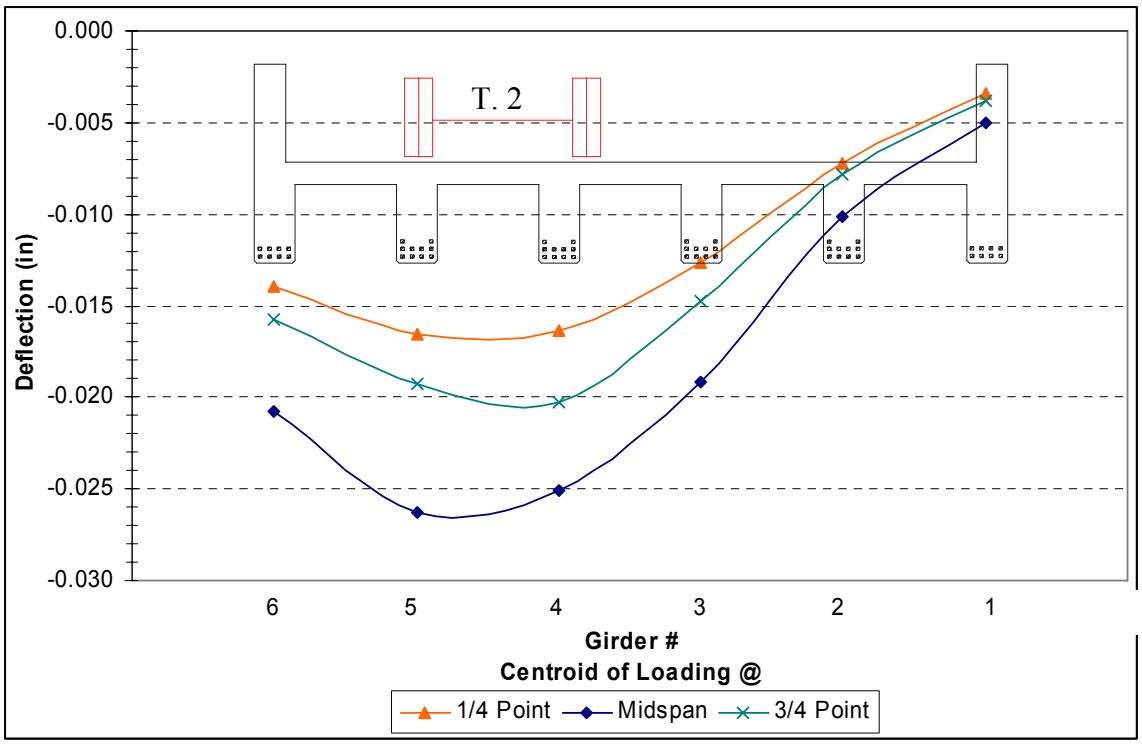

Figure 54: Load Case #2 – 1 Truck

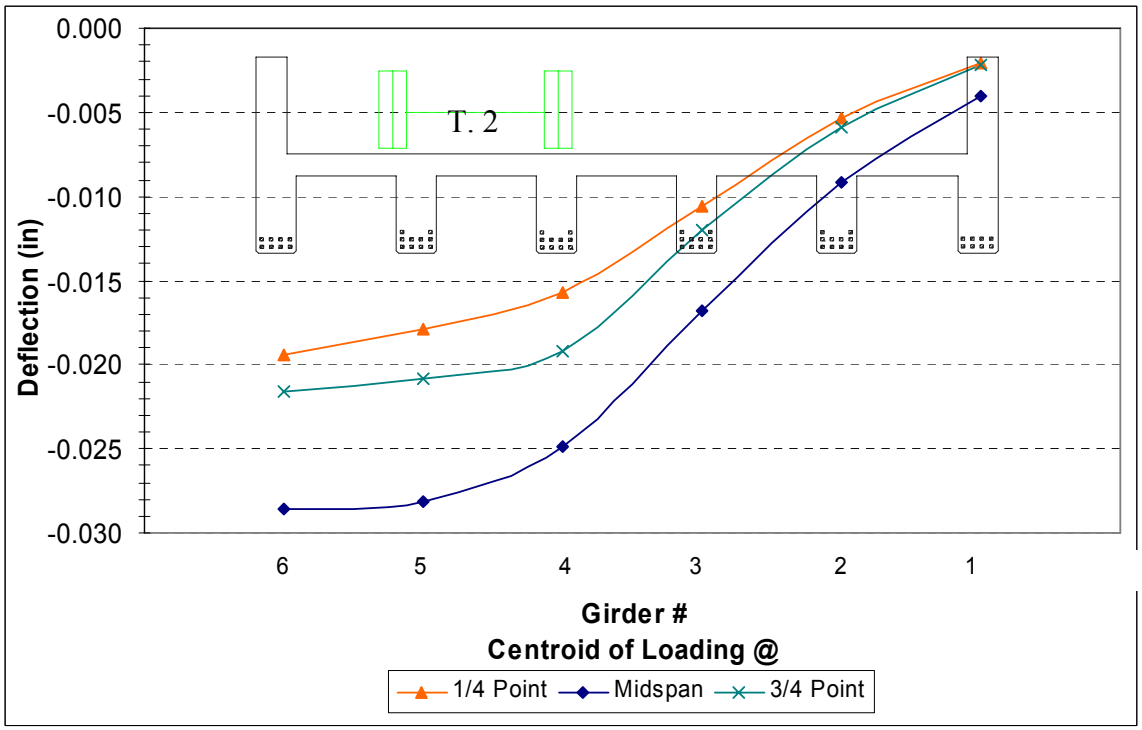

Figure 55: Load Case #4 – 1 Truck

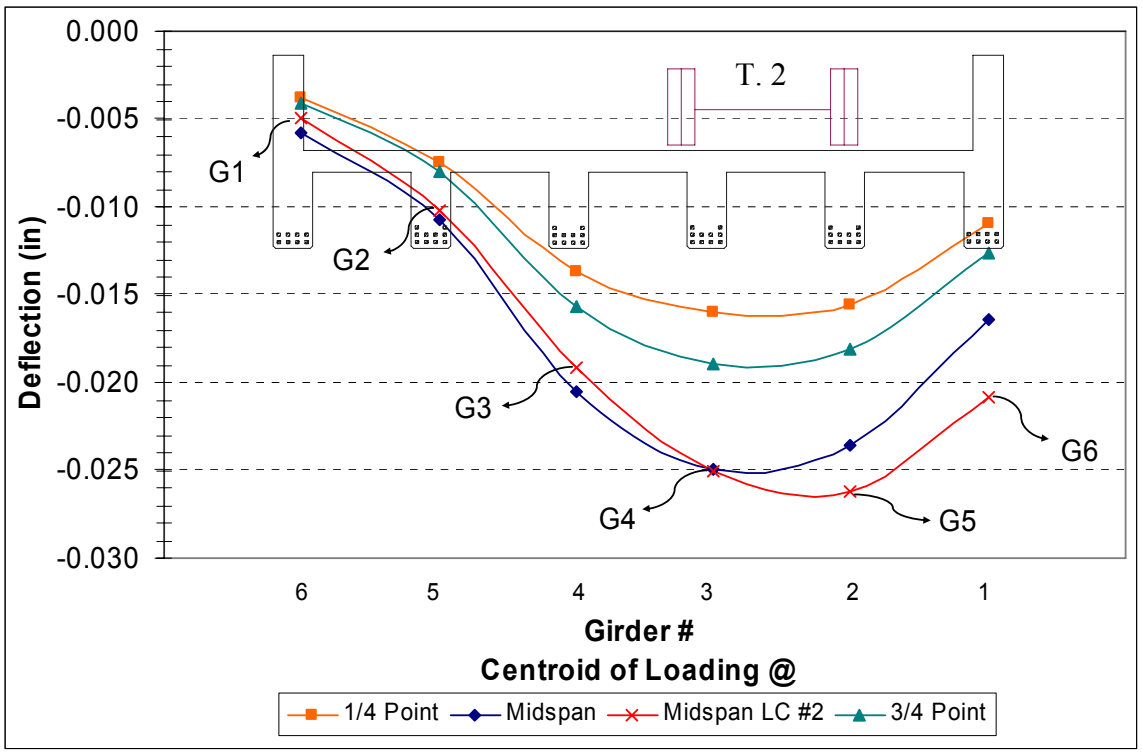

Figure 56: Load Case #5 – 1 Truck with Symmetry Check Using Load Case #2 – 1 Truck

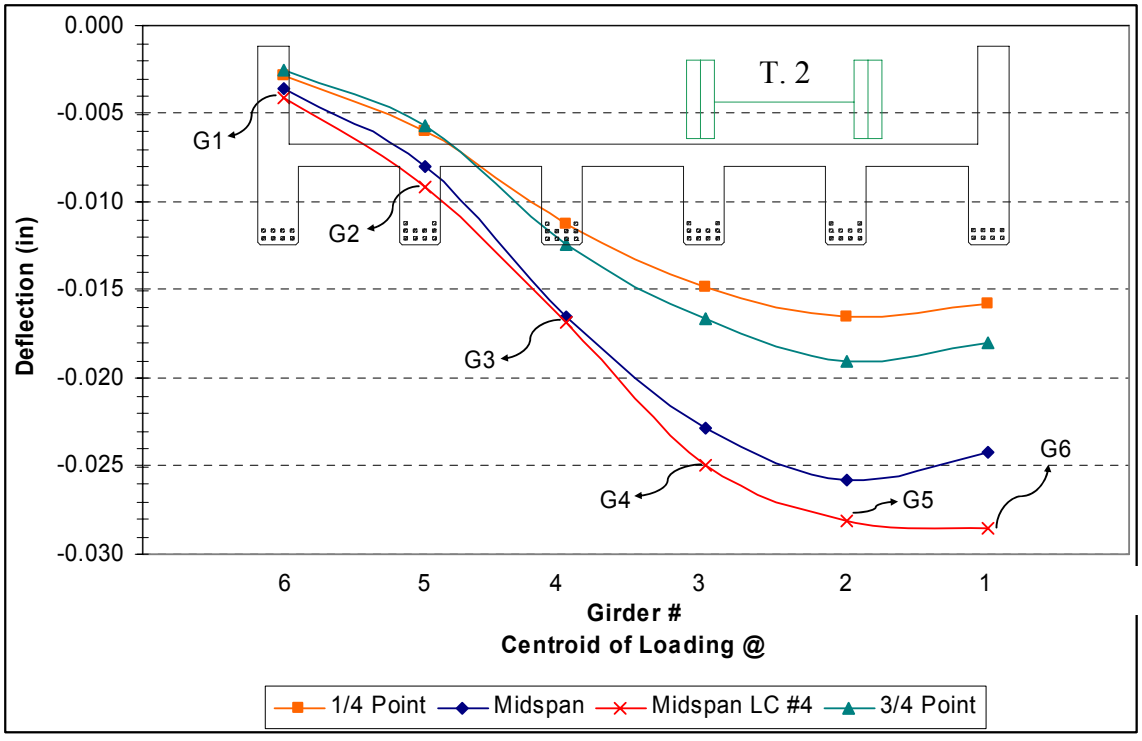

Figure 57: Load Case #6 – 1 Truck with Symmetry Check Using Load Case #4 – 1 Truck

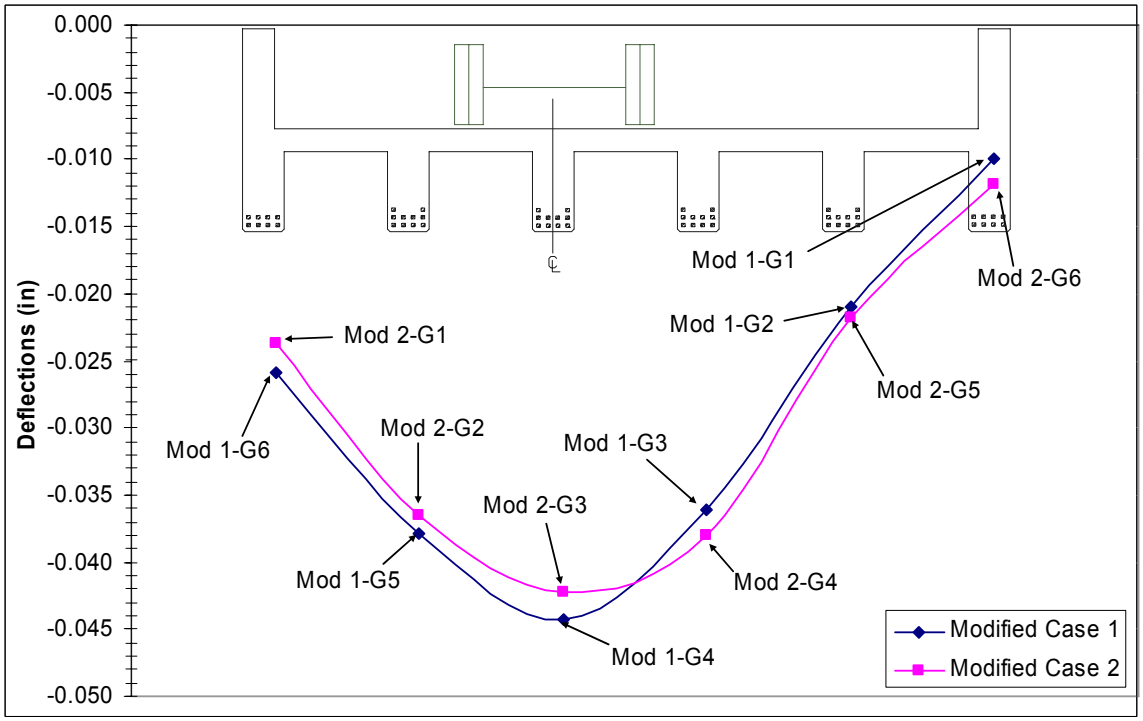

Figure 58: Symmetry of Repaired Bridge

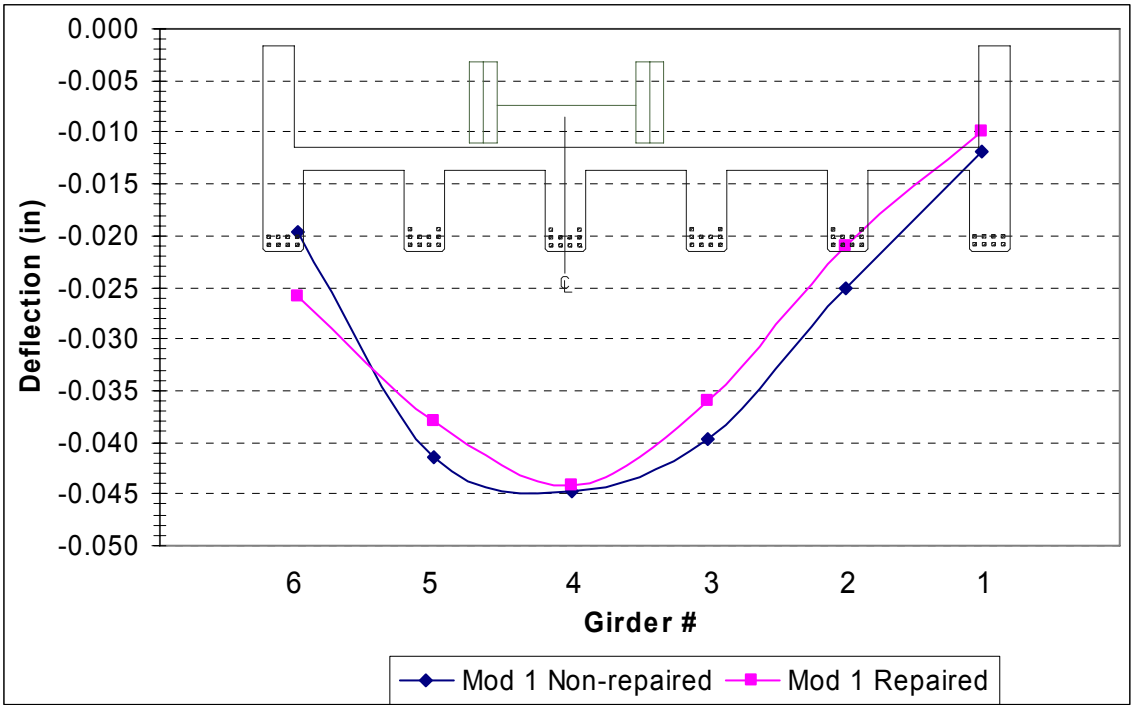

Figure 59: Modified #1 – Repaired vs. Non-repaired

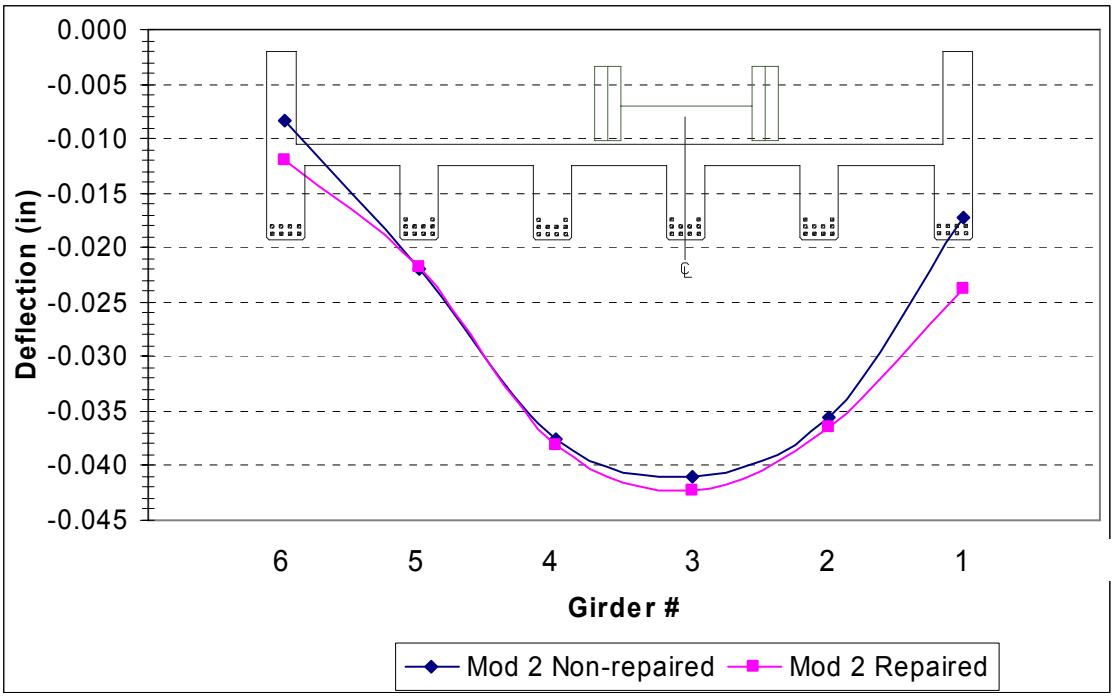

Figure 60: Modified #2 – Repaired vs. Non-repaired

Figures 61-67 show the strain results of the flexural FRP gages for each load case. The three curves on each figure represent the strains at the bottom face of each girder when the truck centroid is positioned at quarter, mid, and three-quarter points along the span of the bridge. Similar to the deflection figures, the transverse load placement is also shown in each figure. These figures indicate reasonable strain results with the exception of readings from Girders 2 and 6. The strain values from the gage on Girder 2 are significantly lower than expected as shown in Figures 61-64. This can indicate a possible malfunction of that gage. The strain values from the gage on Girder 6 show no relative strain throughout each load case. This, again, may represent a malfunction with that gage.

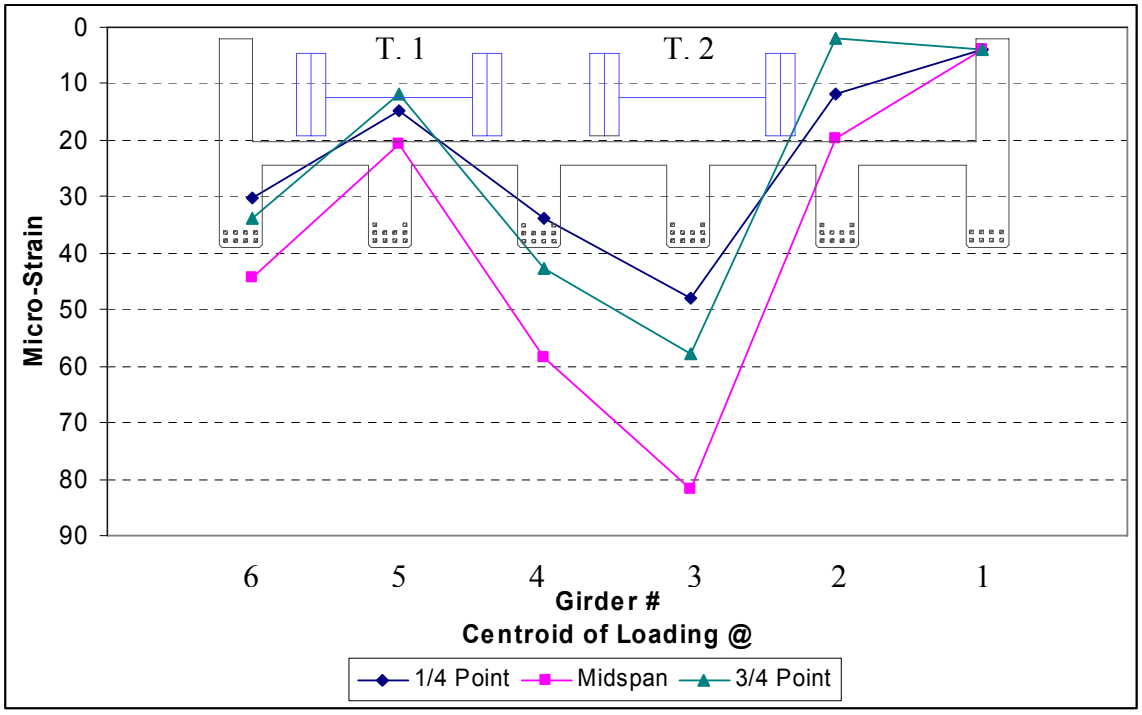

Figure 61: Load Case #1 – 2 Trucks

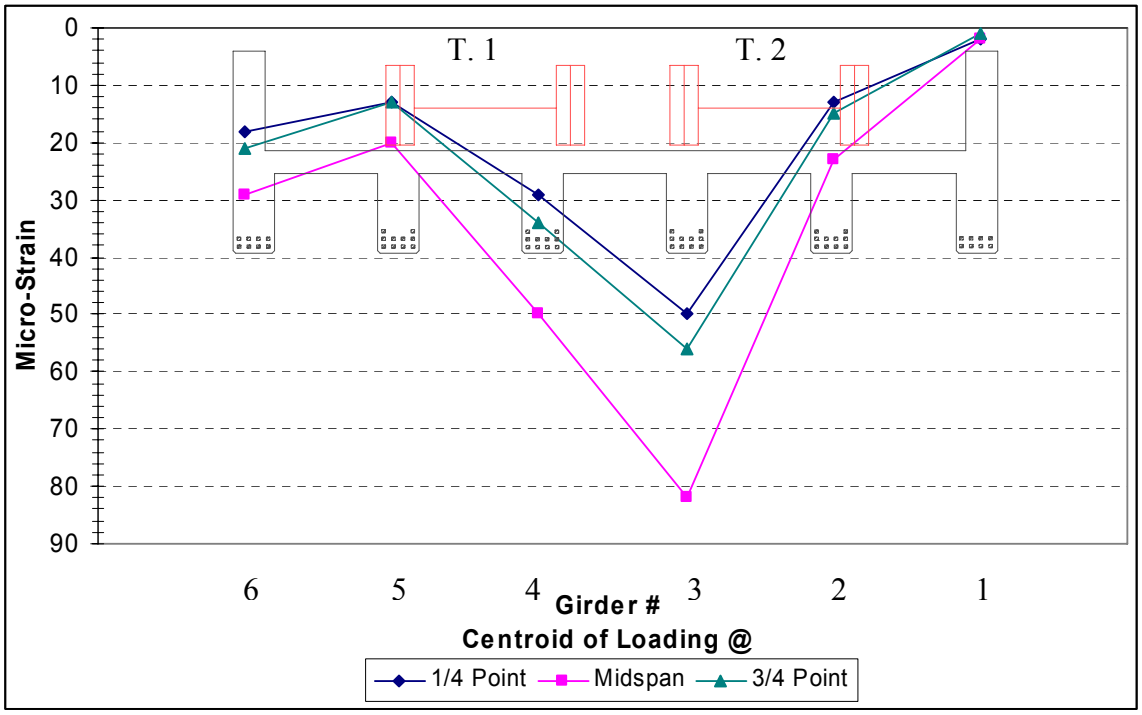

Figure 62: Load Case #2 – 2 Trucks

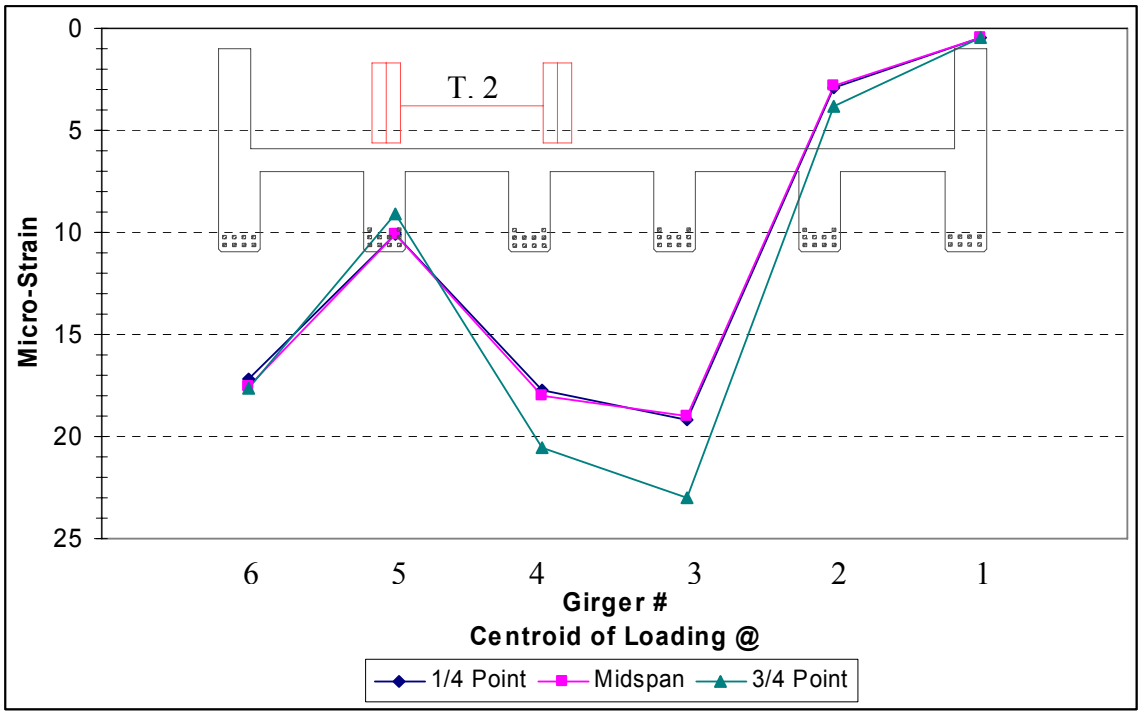

Figure 63: Load Case #2 – 1 Truck

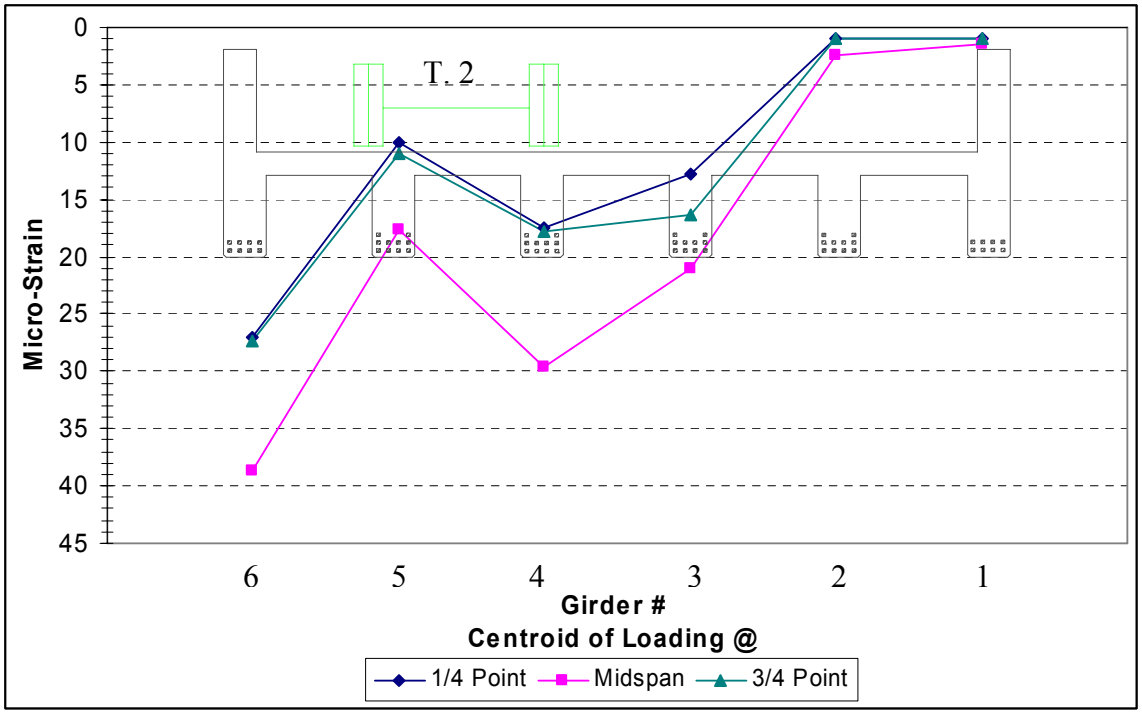

Figure 64: Load Case #4 – 1 Truck

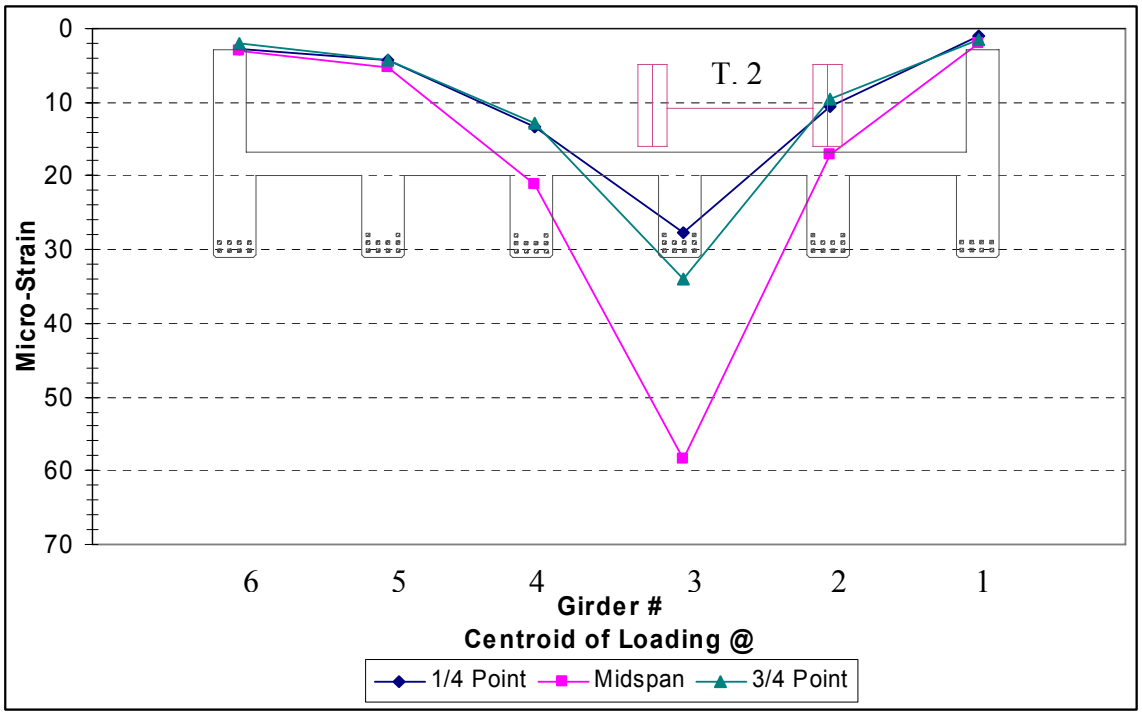

Figure 65: Load Case #5 – 1 Truck

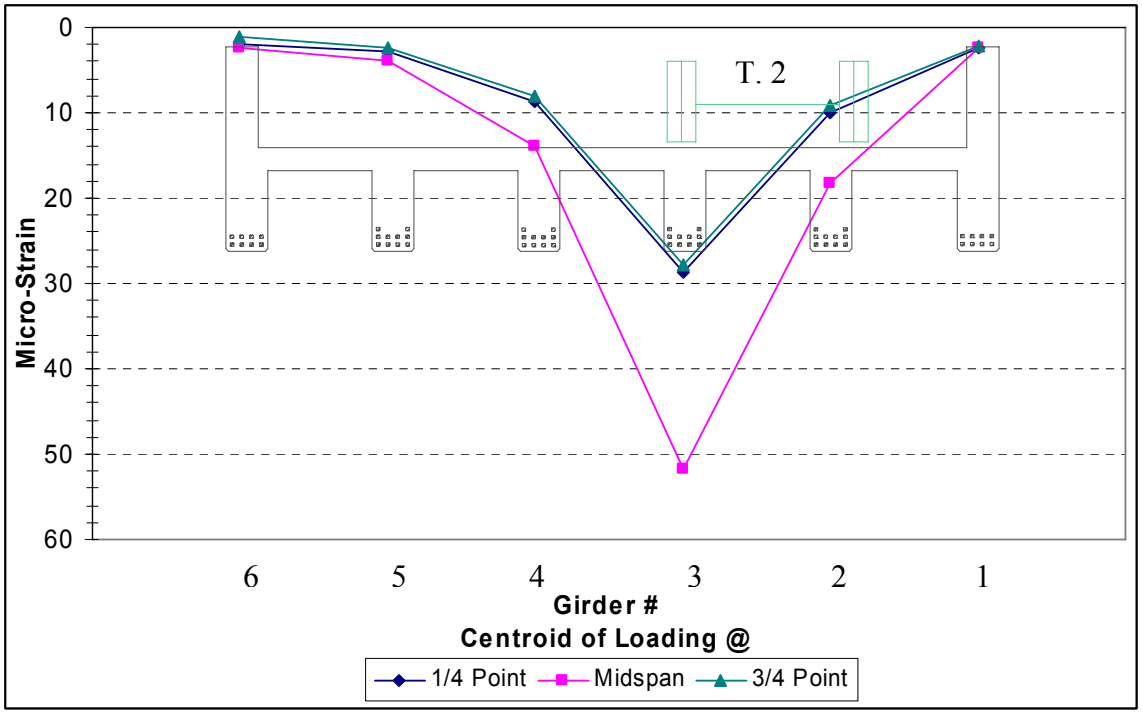

Figure 66: Load Case #6 – 1 Truck

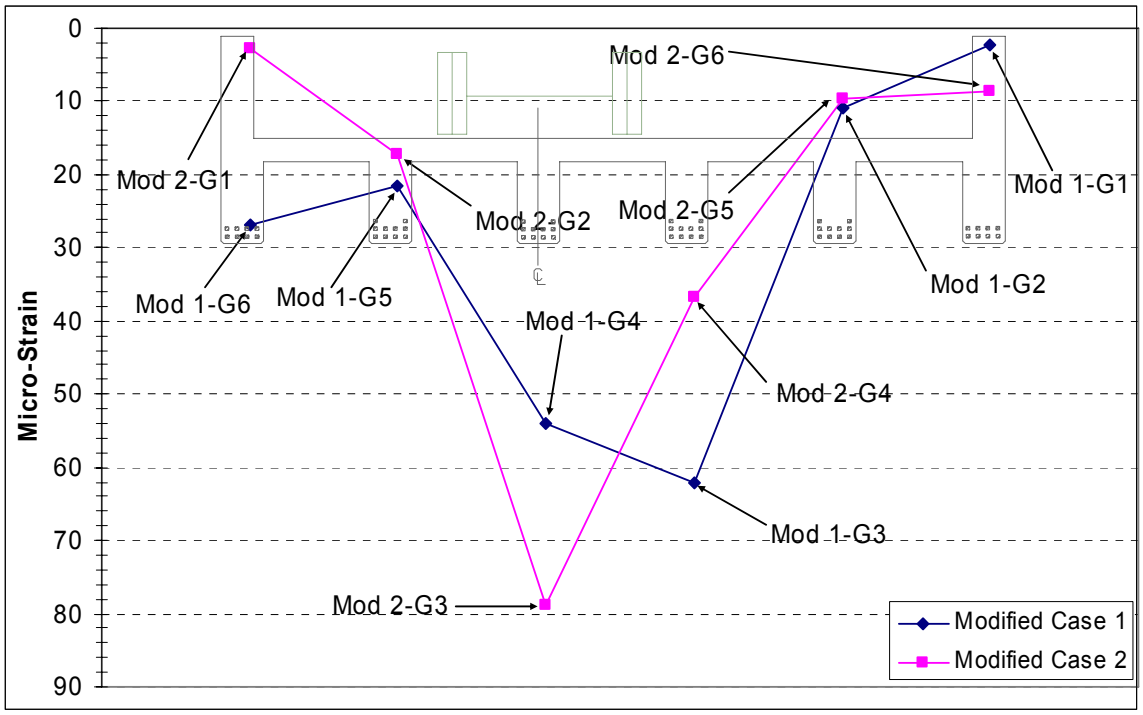

Figure 67: Modified Cases

Concrete strain gage readings are illustrated in Figures 68-74. One strain distribution diagram is shown for each girder, created from the load case which gave the highest FRP strain reading. The load case used is included in the figure description. As can be seen from these figures, the strain readings on the concrete surface seem to be reasonable and assume an approximate linear distribution.

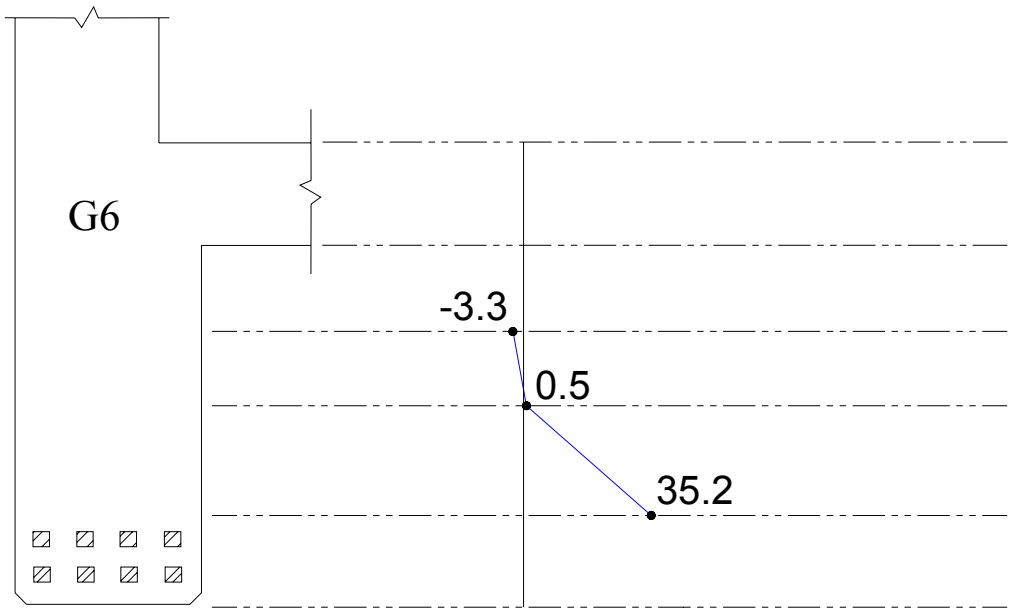

Figure 68: Strain from Load Case #1

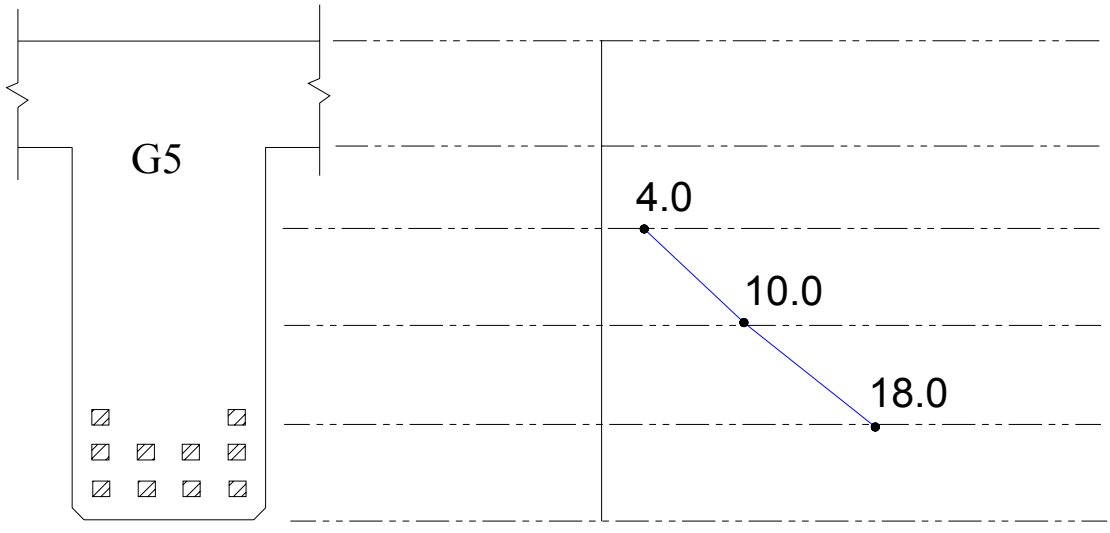

Figure 69: Strain from Modified #1

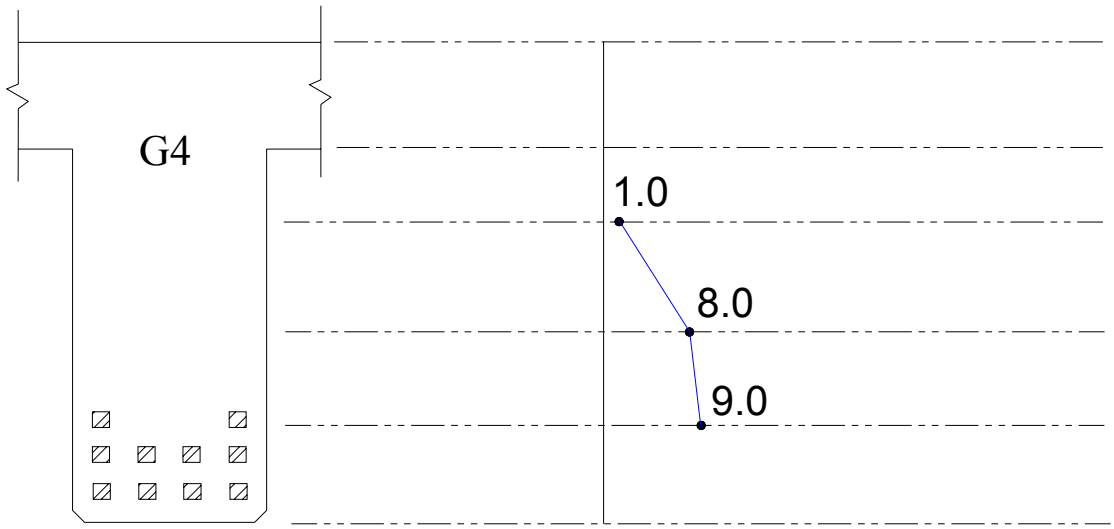

Figure 70: Strain from Modified #2

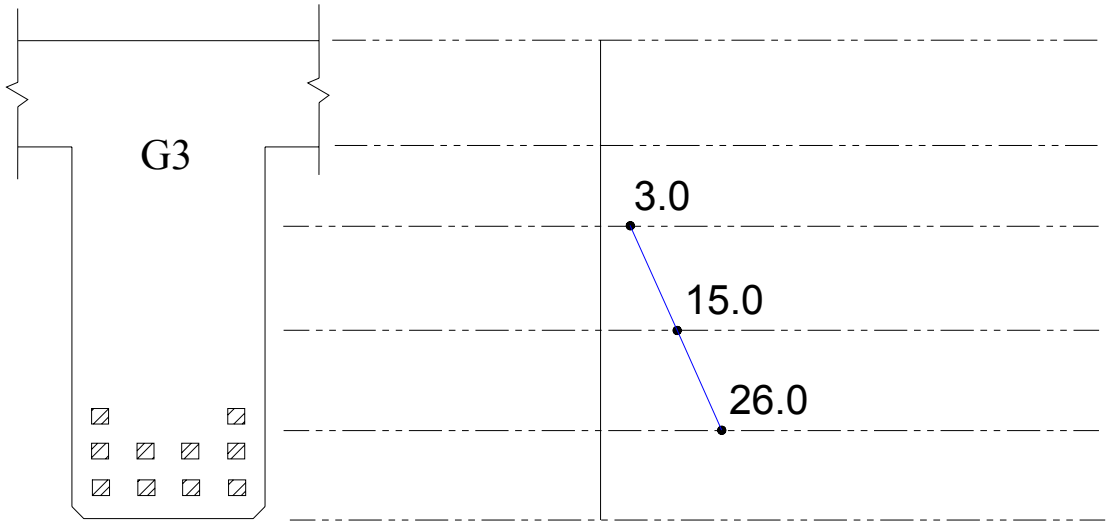

Figure 71: Strain from Load Case #1

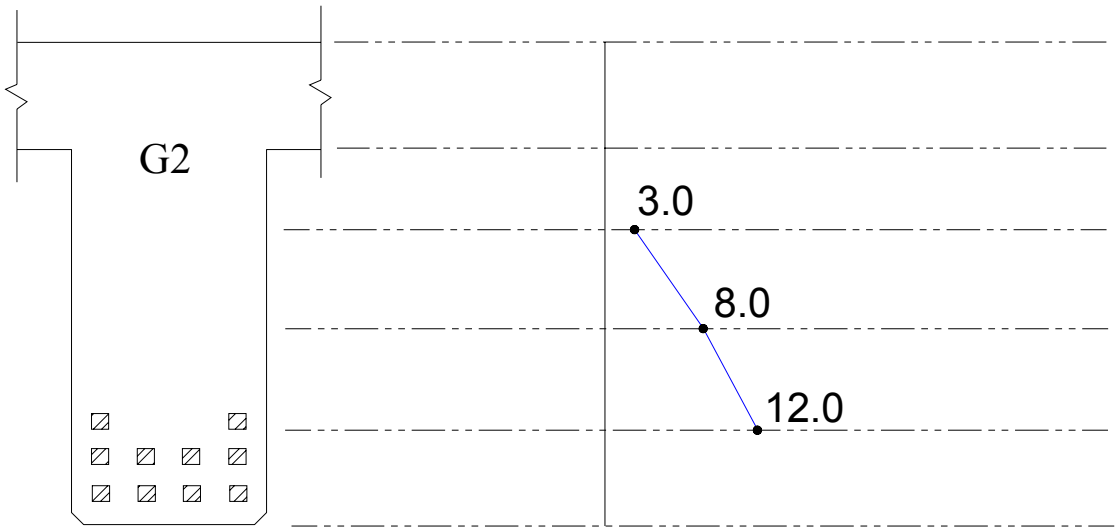

Figure 72: Strain from Load Case #2 – 2 Trucks

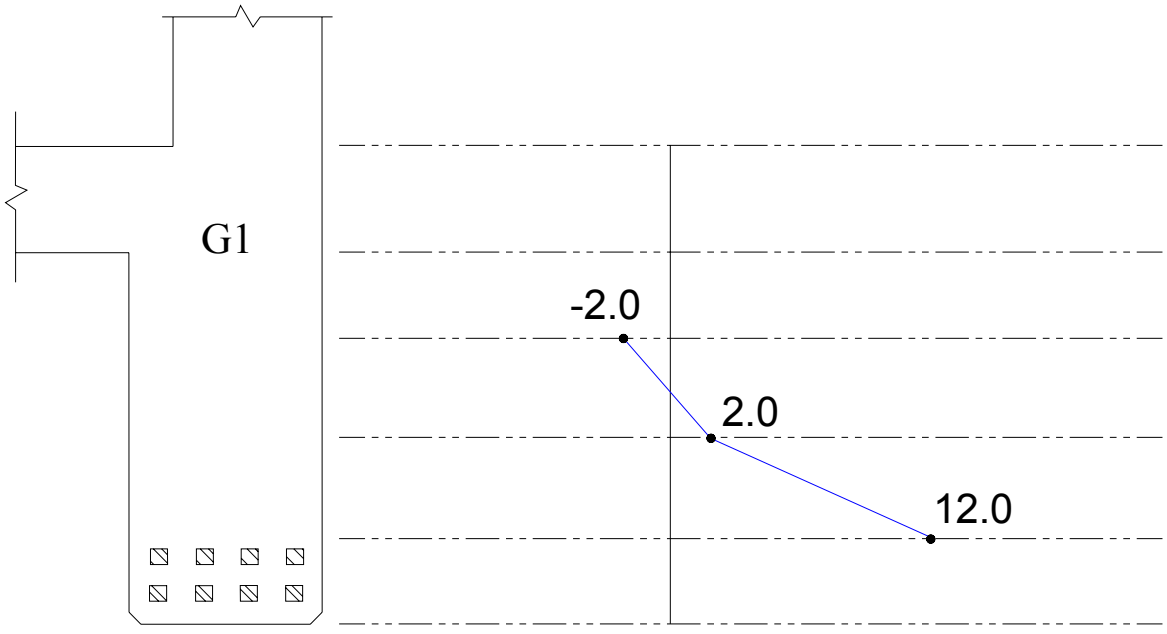

Figure 73: Strain from Modified #2

A sample natural frequency curve is shown in Figure 74. The data was analyzed through a Fast Fourier Transform (FFT) analysis available in the Strain Smart software. The values obtained correlated well with FE results. As seen in Figure 48, the field tests showed a first mode frequency of 14.72 Hz. This value is very close to that from testing of the un-repaired bridge, where the first mode frequency was 14.66 Hz. Once again this indicates that the externally bonded FRP strips do not contribute too much to the bridge stiffness.

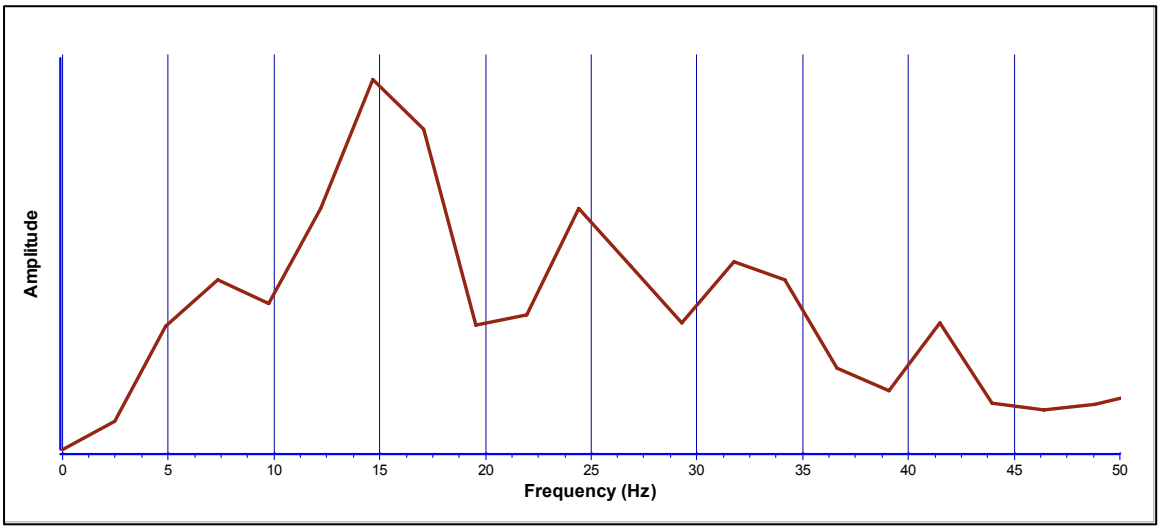

Figure 74: Natural Frequency Chart

4.3 Conclusions

The testing on the repaired bridge was conducted on October 20, 2008. An FE model was created to study the behavior of the concrete bridge repaired using FRP strips. It can be concluded that:

1) The testing data for the repaired structure seem to be reasonable;
2) The FE model was calibrated using the testing data and was used to calculate load rating factors;
3) Based on the loading factors along with previous research results at WVU and design documents from BASF, the moment and shear capacities of the repaired bridge have

increased. However, the stiffness of the repaired bridge has not changed much, as illustrated by both testing and FE analysis results.

Table 6 illustrates increased load rating factors for the repaired bridge. Based on bridge testing and study on lab-scale specimens, the stiffness of the FRP-strengthened structures is approximately the same as the un-strengthened one. Therefore, there is no direct way of showing the strengthening effect through a bridge loading test, where the maximum load is within service limits. There are, however, some indirect ways, such as based on strain readings from testing results, the FRP works compositely with the concrete beam. Based on this assumption, we can determine increases in the capacities using FE analysis or other design methodologies. This has been proven based on destructive testing on lab-scale specimens, where increases in moment and shear capacities after strengthening with externally bonded FRP were obtained.

Task 5 Conducting Supporting Lab-scale Studies

5.1 Effect of Concrete Substrate Repair Methods

5.1.1 Concrete Mix Design

In order to create a corroded beam specimen that simulates the field conditions in an actual aged, chloride-contaminated, reinforced concrete bridge girder, the first step was to determine the destructive sources of deterioration that are common in most concrete bridges. Based on the results from the material test descriptions above, it was determined that the beam test specimens in this study should exhibit the following deteriorated properties, considered to be common for aged concrete bridge girders before repair: (1) The concrete should be low-strength and porous; (2) the concrete should be contaminated with embedded chloride salts; (3) the reinforcing steel should be corroded, showing pitting corrosion; (4) the concrete cover layer should be cracked and/or delaminated due to expansive corrosion of the reinforcing steel; and (5) the specimens should have a high moisture content. Basic fundamentals of concrete mix technology were applied to produce a concrete that was low strength, porous, and salt contaminated. The concrete's low strength and high porosity were achieved by employing a high water-cement ratio of 0.60 and using air entraining admixture. Sodium chloride crystals (5% by weight of cement) were added directly to and dissolved into the mix water to create a corrosive environment for the reinforcing steel. In this concrete, 5% sodium chloride by weight of cement was equivalent to about 31.23 lb/cy, a value that far exceeds the commonly accepted corrosion threshold quantity of 1 lb/cy (when NaCl is added directly to the mix). The estimated soluble chloride content of the beam concrete samples extracted from the PennDOT bridge was 1.64% by mass of cement, while a commonly acceptable threshold limit for reinforcement corrosion is 0.15%. Table 9 shows details of concrete mix proportions, which resulted in a porous and low-strength concrete with compressive strengths shown in Table 10. This concrete can provide a favorable environment for corrosion of the reinforcement, as will be shown in a later section.

Table 9: Concrete Mix Proportions

Material	Material/Cement Ratio
# 8 Coarse Aggregate	2.42
Sand	1.92
Water	0.6
Sodium Chloride	0.05
Air Entraining Admixture	0.79 L/m^3 (22.4 mL /ft^3)

Table 10: Compression cylinder test results

Age	Corresponding Beams	Average Compressive Strength (psi)	Range (psi)
28 days	28-Day Pristine	3501	-
8 Weeks	Mild Corrosion Unrepaired	3505	20
25 Weeks	After First Corrosion Cycle I	3444	424
40 Weeks	After Concrete/FRP repair	3578	597
66 Weeks	After Corrosion Cycle II	3791	159

5.1.2 Testing Plan

The experimental program consisted of testing under 4-point bending load fifteen large-scale beams damaged by induced electric current. After repairing the concrete substrate using two different methods, and subsequent bonding of the CFRP flexural reinforcement and shear anchors after corrosion cycle I, some beam specimens were subjected to accelerated corrosion cycle II, and tested to failure in bending. The second-cycle corrosion-induced aging was used to indirectly evaluate long-term performance after CFRP retrofitting. As shown in Figure 75, the numerals indicate times at which static load tests were performed to failure. The numerals, which are lined up vertically in the figures, indicate control beams that were tested under flexure at the same age.

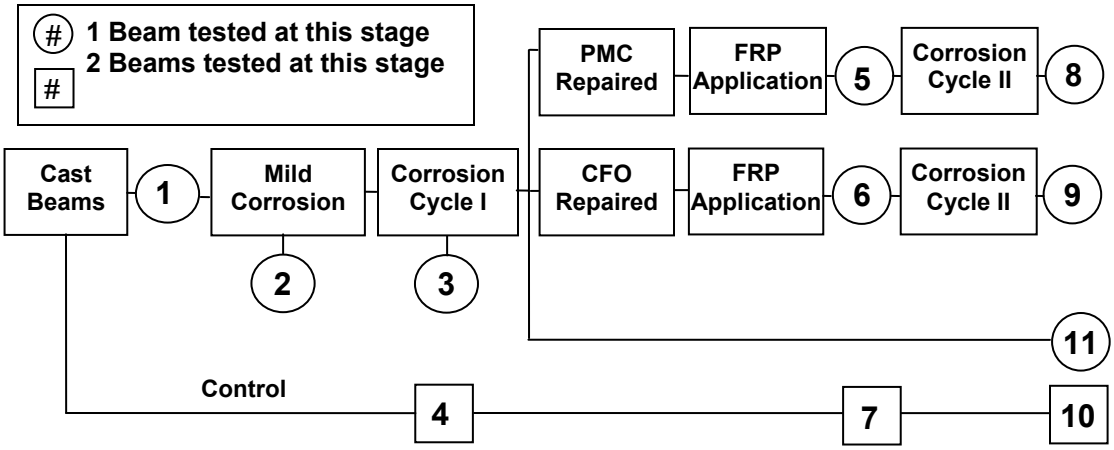

Figure 75: Schematic of experimental testing plan

5.1.3 Test Specimen

5.1.3.1 Dimensions

The beams were 6x8x108 in, which were tested on a span of 102 in. Steel reinforcement consisted of two #5 bars [⅝ in diameter] for tension, two #3 bars [⅜ in diameter] for compression, and twenty-two #3 stirrups for shear. One inch of concrete cover was provided around the perimeter of each rectangular stirrup. A smooth stainless steel tube with an outer diameter of ⅜ in and a wall thickness of 0.065 in was placed above and at the center of the tension reinforcing bars to serve as the cathode in the accelerated corrosion process. A diagram of the beam specimen is provided in Figure 76.

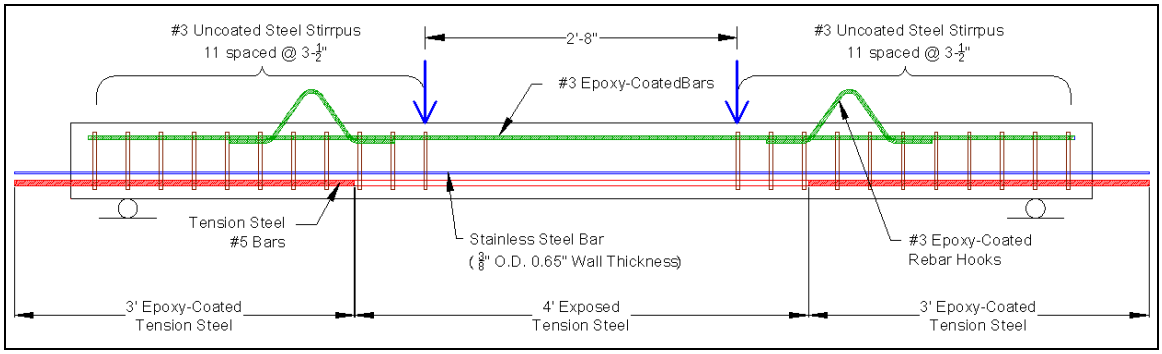

Figure 76: Beam Specimen

5.1.3.2 Materials

The concrete mix described in the previous section was used to cast the samples. All steel reinforcement consisted of Grade 60 (60*ksi*) steel. All tension steel except for that within a 4 ft section at the midspan was epoxy coated in the laboratory. This was done in an attempt to confine the corrosion to the mid-section of the tension reinforcement. The compression steel was coated with standard fusion-bonded epoxy. The tubing was made of seamless Type 304 stainless steel. All stirrup-bending was done professionally due to the large quantity required and need for all stirrups to effectively have the same dimensions. Electrical tape was wrapped around the four corners of each stirrup at locations where the stirrup made contact with tension or compression steel. This was done as an effort to prevent direct electrical contact between the reinforcing steel components, but this scheme did not perform as anticipated as will be discussed later. The stirrups were not insulated at any other location.

5.1.4 Repair of Beam Specimens

5.1.4.1 Beam Repair

Two distinct substrate repair methods, which are commonly used in practice, were used and compared in this study, while the FRP wrapping scheme was the same for all beams.

5.1.4.1.1 Two Substrate Repair Techniques

Substrate Repair Method 1-Crack Filling Only (CFO): For substrate repair method 1, which was performed on beams in Groups 6 (G-6) and 9 (G-9), none of the old deteriorated concrete was removed prior to FRP repair. Instead, Sikadur 52 epoxy was used to fill and structurally repair the corrosion-induced cracks.

Substrate Repair Method 2-Polymer Modified Concrete (PMC): For substrate repair method 2, which was performed on beams G-5 and G-8, the damaged old concrete was removed to the level of the reinforcement and replaced with high-strength polymer concrete containing corrosion inhibitor.

5.1.4.1.2 FRP Strengthening

The FRP wrapping scheme used consisted of one layer of flexural CFRP and two CFRP U-wrapped anchors, each located at a strategic distance from the end of each specimen. Leung (2006) stated that to maximize the total load carrying capacity, the U-anchor should be placed close to the initiation point of debonding so that its resistance is activated before significant debonding (and/or interfacial softening) has occurred. In an E-mail conversation (Leung, 2008), Leung stated that debonding initiates from a flexural or a flexural-shear crack that forms near the load application point. The crack propagates downward from the load application point at roughly 30º to the vertical. Therefore, Leung suggested that the U-anchor be placed at a location slightly beyond the point where this 30º line meets the tension face of the beam. His suggestion was followed in this research. The FPR wrapping scheme can be seen in Figure 77.

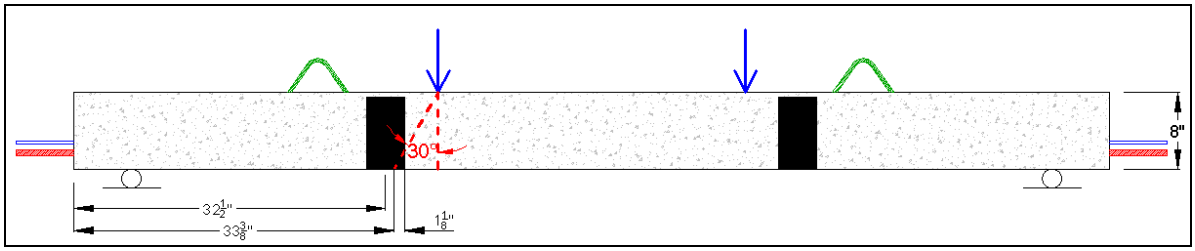

Figure 77: FRP Wrapping Scheme

5.1.5 Testing Method

5.1.5.1 Accelerated Aging

An accelerated aging approach was adopted by the application of direct electric current, and the addition of chloride to the concrete mix, while keeping the samples exposed to moisture. Either two or three beams were wired to each power supply as shown in Figure 78. In an attempt to maintain a constant moisture level within the beams, they were each partially covered with three layers of wet burlap and then were loosely covered with a plastic sheet. A dry cycle was also incorporated for two days per week by removing the burlap and plastic cover. A current density of 178 mA/cm^2 was applied. The first corrosion cycle subjected the beams to 1,200 *amp-hours* of constant current, except for

the trial beams G-2 subjected to 575 *amp-hours*, and the second corrosion cycle exposed the beams to an additional 1,200 *amp-hours* of constant current.

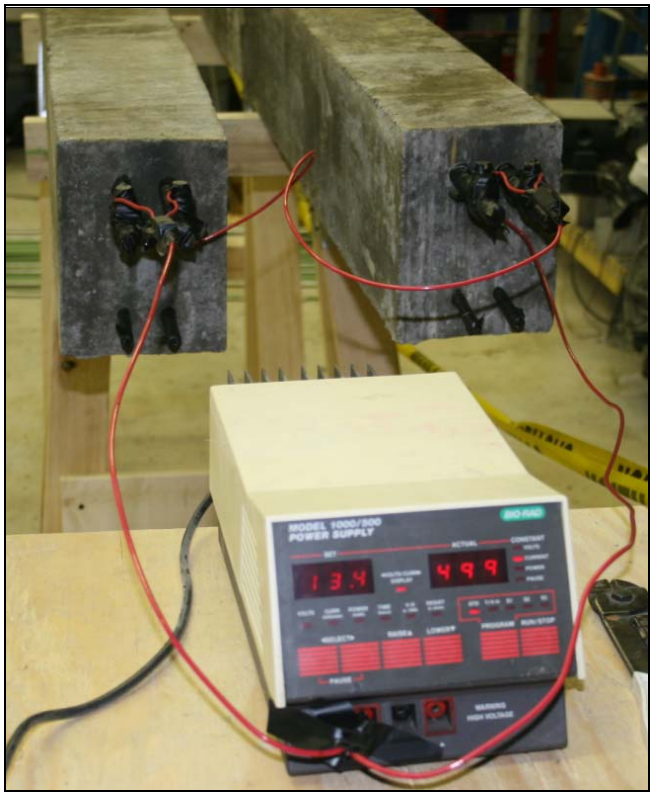

Figure 78: Beams wired to power supply

5.1.5.2 Static Flexural Testing

An MTS Actuator with a capacity of 110kips of compressive force was used to apply load to the beam specimens. Three LVDTs were used to measure displacements. Each beam was tested under 4-point bending, with a simply supported span of 8 ft, as shown in Figure 79. The static load test was performed at a constant load rate of 0.02 in/min using displacement control mode, as specified by ASTM C78-09.

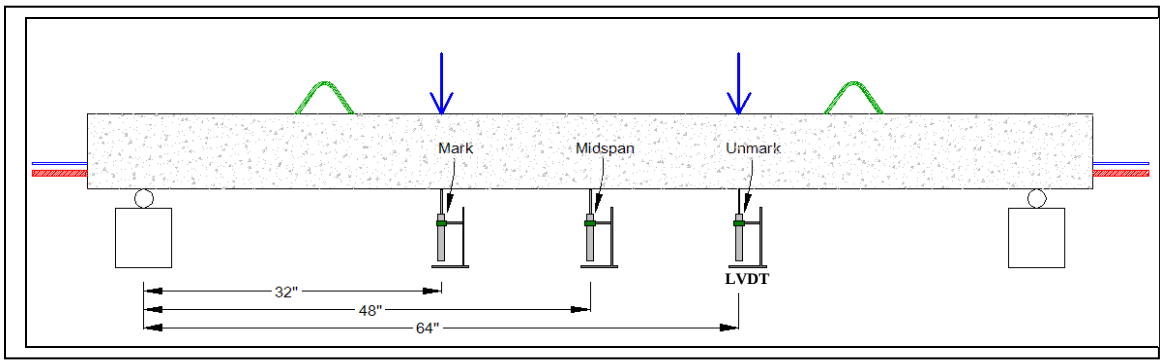

Figure 79: Testing Setup

5.1.6 Test Results and Discussions

5.1.6.1 Accelerated Aging Results

Figure 80: Typical extent of deterioration observed after initial corrosion

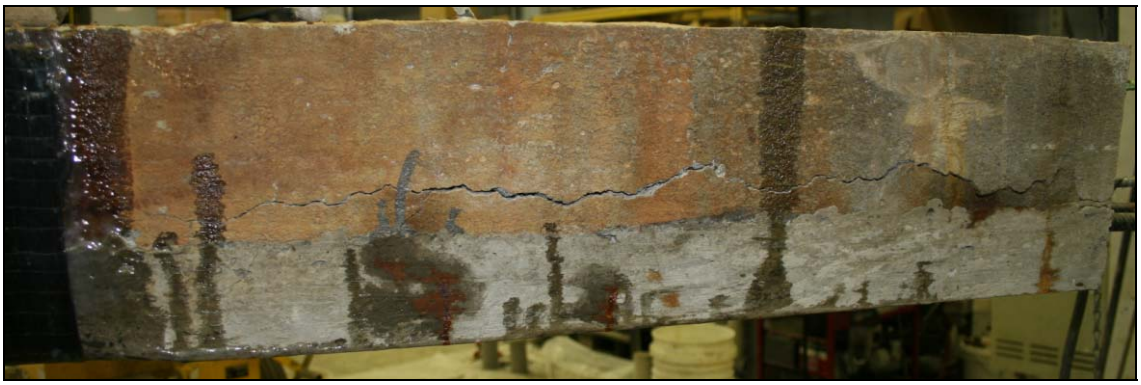

Figure 81a: Cracks in beam G-8 within the old concrete running parallel to patched concrete interface

Figure 81b: New crack running parallel to injection-repaired crack in beam G-9

Figure 82a: Corroded beam sample

Figure 82b: Corroded girder of a PennDOT bridge

Table 11: Mass Loss Summary

Description	Group (See Figure 75)	Mass Loss
Control Pristine Samples		
At 28 days	1	-
After Corrosion Cycle I	4	1.8
After Corrosion Cycle II	10	0.8
Control Corroded Unrepaired		
Mild Corrosion*	2	6.2
After Corrosion Cycle I	3	15.6
After Corrosion Cycle II	11	24.2
Concrete/FRP repair after Corrosion Cycle I		
PMC-repaired	5	17.4
CFO-repaired	6	17.2
Concrete/FRP repair after Corrosion Cycle II		
PMC-repaired	8	17.1
CFO-repaired	9	26.5

Note: * denotes the average value of two beam samples

Figures 80 and 81 show the beams after corrosion cycles I and II, respectively, where severe material deterioration can be observed. After corrosion cycle II, it was observed that, for the PMC-repaired beam, cracks occurred within the old concrete running parallel above the patched concrete interface; and for the CFO-repaired beam, the cracks filled with epoxy were not visibly damaged, but new cracks formed above and parallel to the major filled cracks. This is because the epoxy-concrete interface was stronger than the deteriorated concrete itself. As shown in Figure 82, the corrosion resulted in deterioration of the laboratory specimens with similar characteristics to what was observed of bridges in the field. Table 11 lists the mass loss from different aging protocols, showing that longer corrosion period resulted in greater mass loss. When CFO-repaired beams were subjected to corrosion cycle II, a significant mass loss was observed. However, when PMC-repaired beams were subjected to the same corrosion cycle II, virtually no additional mass loss was observed.

It is worth pointing out that some useful provisions are provided in this study to treat the reinforcing steel, such as all tension steel except for that within a 1.22 m (4 ft) section at the midspan was epoxy coated, the compression steel was coated with standard fusion-

bonded epoxy, and electrical tape was wrapped around the four corners of the stirrups. However, even by using such measures, it took significantly longer time than expected to achieve the desired corrosion and mass loss. Based on a preliminary accelerated corrosion tests with 36 in-long samples (Parish, 2008), it was expected that the accelerated aging process would sufficiently damage each beam within 5 to 6 weeks (350-*450 amp-hours*). However, when beams G-2 (Figure 75) were tested at 55 days (575 *amp-hours*), it was found that their respective mass losses were only 5.6% and 6.8%. This was equivalent to a steel cross-sectional loss of only about 0.04 in^2, which was significantly lower than what was initially expected. After removing the concrete from the entire shear span of the beams, it was observed that the extent of corrosion in the steel stirrups and portions of epoxy-coated tension steel was the same as that within the uncoated steel in the constant moment region, which indicated that the electric current spread over not only the surface area of the exposed tension steel, but also the entire surface area of all twenty-two stirrups, resulting in a larger surface area of steel that required a longer time to corrode. Thus, the remaining of the beams had to be subjected to an electric current for another 111 days until 1,200 *amp-hours* was reached. Based on this experience, it is suggested that in order to more effectively corrode beam specimens, all stirrups should be epoxy coated to decrease the exposed surface area of the steel and increase the current density, and the beam size should be reduced. This approach was successfully implemented in part II.

5.1.6.2 Static Flexural Testing

Table 12: Load, Deflection and Stiffness Summary

Description	Group (See Figure 75)	Service Load (lbs)	Maximum Load (lbs)	Deflection at Service Load (in)	Deflection at Maximum Load (in)	Stiffness (lbs/in)
Control Pristine Samples						
At 28 days	1	11,300	13,300	0.52	0.95	22,201
After Corrosion Cycle I*	4	11,850	13,500	0.7	0.88	15,246
After Concrete/FRP Repair*	7	13,000	14,350	0.77	1.13	16,708
After Corrosion Cycle II*	10	13,350	14,600	0.76	0.99	16,577
Control Corroded Unrepaired						
Mild Corrosion*	2	11,900	13,500	0.72	1.21	13,943

After Corrosion Cycle I	3	10,300	11,400	0.7	1.21	13,448
After Corrosion Cycle II	11	8,300	10,500	0.62	2.18	9,730
Concrete/FRP repair after Corrosion Cycle I						
PMC-repaired	5	11,600	13,300	0.78	1.51	13,358
CFO-repaired	6	12,800	14,800	0.72	1.26	14,942
Concrete/FRP repair after Corrosion Cycle II						
PMC-repaired	8	10,500	13,300	0.62	1.13	11,378
CFO-repaired	9	9,600	11,000	0.53	0.75	12,969

Note: * denotes the average value of two beam samples

Figure 83 displays comparisons of representative concrete/FRP-repaired beams, control corroded beams, and control pristine beams, respectively. Details of load capacities, deflections, and stiffness are shown in Table 12. The maximum service load is defined as the highest load observed within the nearly linear post-cracking region on the load-deflection curve. All loads presented in this table were rounded to the nearest 100 lb. The maximum service load deflection is the largest deflection observed in the post-cracking region of the load-deflection curve. All deflections presented in this table were rounded to the nearest 0.01 inch. The stiffness values reported were obtained by adding linear trend lines to the linear portions of the load-deflection curves and obtaining the slopes of these segments. The stiffness value was only used if the linear regression value R^2 was ≥ 0.99.

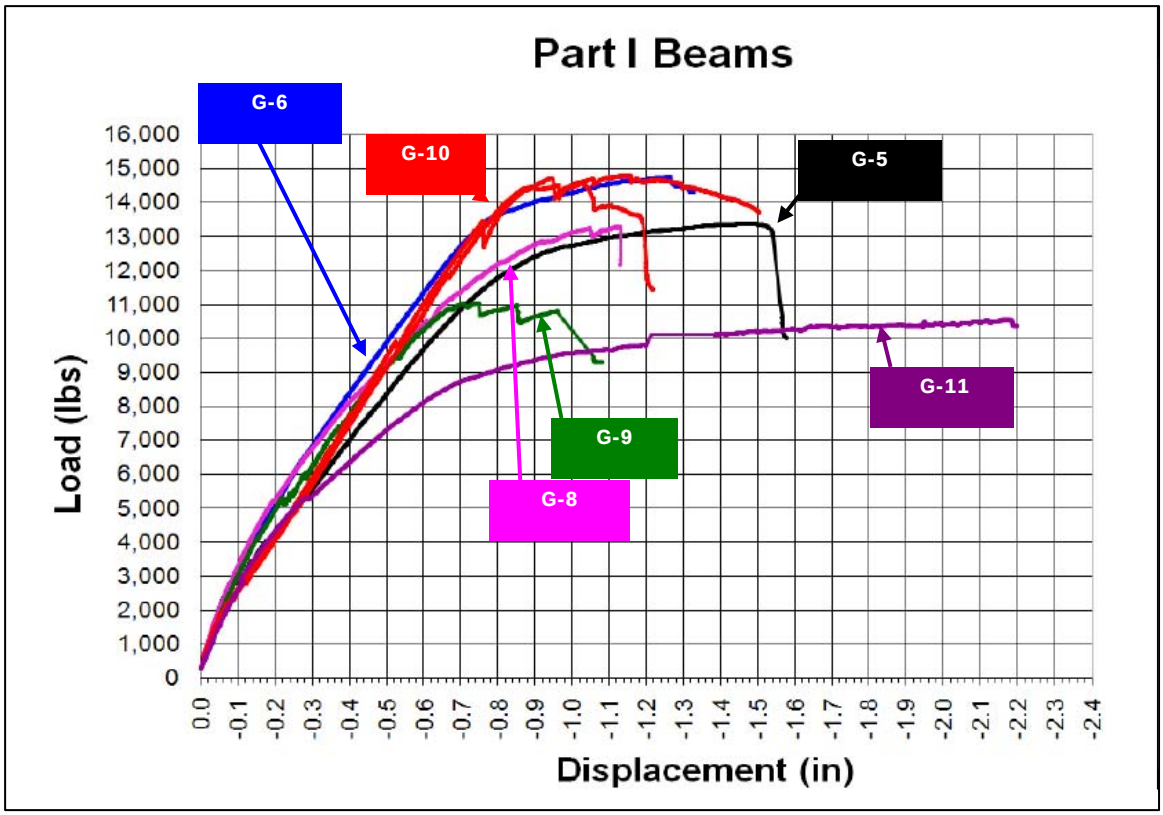

Figure 83: Load-deflection curves for representative beam samples

Effect of Corrosion

Un-repaired beams subjected to corrosion cycles I and II: The analysis following ACI guidelines predicted an un-factored service load of 6,198 lbs at each load point, or approximately 12,400lbs total. All control pristine beams (G1, G4, G7, and G10; Figure 75) yielded an average maximum service load of 12,529 lbs, and gained strength as they aged, which indicated that the beam specimens performed as designed.

Compared to the control pristine beam G-4, the aged beam G-3, which was subjected to corrosion cycle I, resulted in reductions of 13% for service load capacity, 16% for maximum load capacity, and 11.8% for stiffness, respectively; and beam G-11, which was subjected to two corrosion cycles, yielded reductions of 38% for service load capacity, 28% for maximum load capacity, and 41% for stiffness, respectively, compared

to the control pristine beam G-10. It can be seen that larger stiffness reduction occurred due to corrosion cycle II in relation to corrosion cycle I.

CFO-repaired beams subjected to corrosion cycle II: When subjected to corrosion cycle II after concrete repair and FRP application, CFO-repaired beam G-9 exhibited significant strength decrease. The service and failure loads were 25% and 29% less; the service and failure deflections were 26% and 50% less; and the stiffness was 15% less than those of CFO-repaired beam G-6, which was tested immediately after FRP application.

PMC-repaired beams subjected to corrosion cycle II: After corrosion cycle II, PMC-repaired beam G-8 exhibited some deterioration compared to its duplicate beam G-5, which was tested immediately after FRP application. Beam G-8 had a service load of 9% less; service and failure deflections of 21% and 25% less; and a stiffness of 15% less than those of beams G-5, respectively. The maximum load of the two beams was about the same.

Discussion: The loss of strength and stiffness as shown above clearly indicated the effect of accelerated aging. Corrosion cycle II produced an even greater loss in relative stiffness than did corrosion cycle I. FRP strengthened beams retained more stiffness than the equivalent control corroded beams. It seems that the deterioration of PMC-repaired beam was less significant than that of CFO-repaired beam, when both were subjected to corrosion cycle II, which will be discussed in detail in the following section.

Effect of Substrate Repair Method

Immediately after corrosion cycle I and concrete/FRP repair: As mentioned before, the same FRP strengthening scheme was used for both concrete-repaired groups of beams. They were designed to withstand an unfactored service load of approximately 11,630 lbs. The two FRP-strengthen beams yielded maximum service loads of 11,600 lbs for PMC-repaired (G-5) and 12,800 lbs for CFO-repaired (G-6) beams, in close correlation with

the analysis. The CFO-repaired beam G-6 showed substantial increases in load capacity of 10% and 11% for maximum service and failure loads, respectively, when compared to PMC-repaired beam G-5. The two control pristine beams of equivalent age, G-7, had the average maximum service and failure loads of 13,800 lbs and 14,350 lbs, respectively.

PMC-repaired beam G-5 yielded a maximum service deflection of 0.78 in, while CFO-repaired beam G-6 yielded a slightly lesser service deflection of 0.72 in. A similar trend was observed for failure deflection: Beam G-5 deflected a maximum of 1.51 in while beam G-6 deflected a 17% less at 1.26 in. Control pristine beams of equivalent age, G-7, had average service and failure deflections of 0.77in and 1.13 in, respectively. No significant differences were detected between the deflections of the repaired beams and control pristine beams.

The stiffness of PMC-repaired beam G-5 was 11% less than that of CFO-repaired beam G-6. The stiffnesses of beams G-5 and G-6 were 20% and 11% less than the average for control pristine beams G-7, but within the same range as for the control corroded beam G-3. The FRP strengthening did not appear to stiffen the specimens, which was also observed in a bridge testing (Davalos et al., 2009).

After corrosion cycle II: After exposure to additional corrosion cycle, the maximum service and failure loads of PMC-repaired beam G-8 were 9% and 21% higher than those of CFO-repaired beam G-9; and 21% and 9% less than the average for the control pristine beams of the same age (G-10). The CFO- and PMC-repaired beams had maximum service loads of 10% and 17% less than those predicted by the ACI design equations for a beam immediately after FRP application, showing the necessity of using conservative safety factors when designing an FRP strengthening system, since the strength loss due to continuing deterioration is inevitable.

The service and failure deflections were 0.63 inch and 1.14 inch for PMC-repaired beam G-8; 0.51 inch and 0.75 inch for CFO-repaired beam G-9; and 0.75 inch and 0.98 inch for control pristine beams G-10, respectively. Both of the repaired beams which were subjected to corrosion cycle II exhibited deflections that were similar to the control pristine beams. The fact that PMC-repaired beams yielded higher deflections both before and after corrosion cycle II suggests that this approach resulted in a more ductile failure mode.

The stiffness of PMC-repaired beam G-8 was 12% less than that of CFO-repaired beam G-9, similar to the difference between that of PMC-repaired beam G-5 and CFO-repaired beam G-6, which were tested immediately after concrete/FRP repair. PMC-repaired beam G-8 and CFO-repaired beam G-9 had stiffness values of 31% and 23% less, respectively, than the control pristine beam G-10; and 17% (G-8) and 33% (G-9) higher stiffness values than the control corroded beam G-11, respectively, which indicated that corrosion cycle II after FRP strengthening resulted in a loss of stiffness in the repaired beams, but not as significant as that for the control corroded beam.

Discussion: Immediately after corrosion cycle I and concrete repair/FRP strengthening, the CFO-repaired beam outperformed the PMC-repaired beam. This result changed, however, when the beams were subjected to additional aging. When CFO-repaired beams were subjected to corrosion cycle II, severe cracking, mass loss, and reduction in flexural strength ensued. However, when PMC-repaired beams were subjected to the same corrosion cycle II, only minor degradations were observed. The CFO-repaired beams had greater stiffness than the PMC-repaired beams, which indicated that the PMC-repair approach yielded a more ductile failure. The PMC-repair approach showed better durability when compared with the CFO-repair approach.

Interestingly, if we compare PMC-repaired beam G-8 and CFO-repaired beam G-9 with the control corroded beam G-3, which was subjected to only one corrosion cycle, the

repair and FRP-strengthening maintained the load capacities of the beams even after corrosion cycle II. In relation to beam G-3, the service and failure loads for PMC-repaired beam G-8 were 2% and 17% more; and for CFO-repaired beam G-9 were 7% and 4% less; illustrating that the PMC-repair approach behaved even better than the control corroded beam.

Figure 84: FRP Rupture on PMC-repaired beam G-5

Figure 85: FRP rupture on PMC-repaired beam G-8

Figure 86: FRP rupture on CFO-repaired beam G-6

Figure 87: FRP rupture on CFO-repaired beam G-9

Photos of the FRP rupture of beams G-5 and G-8 (PMC-repaired), and G-6 and G-9 (CFO-repaired), are shown in Figures 84 through 87. Both PMC-repaired beams failed via crack-induced debonding and subsequent FRP rupture. Crack-induced debonding initiates at the location of a flexure crack where there is a high stress concentration at the FRP-concrete interface. When the stress level reaches a critical value, the crack instantly propagates along the FRP-concrete interface resulting in dramatic debonding of the FRP from the concrete. Due to the rapid redistribution of stress, the FRP ruptures at a location near the original concrete flexure crack. This debonding can be attributed to the high strength of the PMC-repaired concrete. The bond between the FRP and the concrete seemed to be sufficient.

It was observed, however, that such sudden debonding did not occur for CFO-repaired beams. Instead, debonding occurred at the steel-concrete interface with subsequent cover delamination and FRP rupture. This behavior can be seen in Figures 86 and 87, which occurred probably because the steel-concrete bond was already weakened by corrosion cracking prior to static testing and the presence of corrosion products around the steel. It

appeared that FRP rupture via direct tension, instead of crack-induced debonding, was the failure mode for the CFO-repaired beams.

5.1.7 Conclusions

Based on this study, the following conclusions can be drawn:

(1) The accelerated corrosion method by direct induced current in combination with a mix design to produce porous, chloride-contaminated, and low-strength concrete has been shown to be effective and produce consistent results. The corrosion-induced damage resulted in deterioration of the laboratory specimens with similar characteristics to what was observed on bridges in the field. The beams which were unrepaired and subjected to corrosion cycles I and II exhibited large reductions in strength properties.

(2) Actual service loads immediately after corrosion cycle I and concrete/FRP repair either approximately matched or exceeded the value predicted by the ACI design equations, indicating that the guidelines are adequate and even conservative for newly repaired FRP strengthening systems. However, after corrosion cycle II, the service load capacities of FRP-strengthened beams were less than the ACI predicted values. Improved design equations considering materials and bonding degradations due to corrosion need to be developed, to account for long-term performance.

(3) Immediately after corrosion cycle I and concrete repair/FRP strengthening, the CFO-repaired beams outperformed the PMC-repaired beams. However, when subjected to additional aging (corrosion cycle II), severe cracking, mass loss, and reduction in flexural strength ensued for CFO beams, while virtually no additional mass loss and minor strength degradations were observed for PMC-repaired beams. The PMC-repair approach showed better durability when compared with the CFO-repair approach.

It is noted that the two methods, PMC-repair and CFO-repair, closely simulate the substrate repair methods that are being adopted in the field. For PMC-repair, old concrete, which was contaminated with chloride ions, was removed and repaired

with new concrete free of chloride ions, whereas for CFO-repair, chloride ions were still left unextracted. Naturally, the PMC-repair approach showed better durability. If chloride ions were extracted for the CFO-repair using an electrochemical extraction method, such as ECE, as will be described in Section 5.3, both repairs would probably have very similar corrosion and degradation with longer exposure. If this is the case, CFO-repair might be more favorable considering other factors such as labor and cost. It is therefore recommended that further study be conducted to compare the durability between the two repair methods, with the addition of electrochemical chloride extraction.

(4) The accelerated corrosion process reduced specimen stiffness, as expected. However, the stiffness of concrete/FRP-repaired beams was actually similar to the stiffness of control corroded unrepaired beams, illustrating the negligible effect of FRP strengthening on beam stiffness. Corrosion cycle II produced an even greater loss in relative stiffness than did corrosion cycle I. For both corrosion cycles, the CFO-repaired beams exhibited greater stiffnesses than similar PMC-repaired beams, which indicates that the PMC-repair approach yields a more ductile failure. The FRP-strengthened beams retained more stiffness than the equivalent control corroded, unrepaired beams.

(5) The PMC-repaired beams failed via crack-induced debonding and FRP rupture while the CFO-repaired beams showed debonding of the concrete cover and subsequent FRP rupture. The FRP rupture on the CFO-repaired beams was likely caused by localized direct tension in areas of high stress concentration due to the substrate failure, and in this case, no significant debonding occurred between the concrete and FRP strips.

5.2 Effect of FRP Wrapping Scheme

5.2.1 Test Specimen

This study consisted of 21 large-scale reinforced concrete beam specimens which were cast using chloride contaminated, low-strength, highly porous concrete as described in Part I. The objective was to compare the performance of three unique FRP anchorage schemes under both static and cyclic loading. Scheme 1 consisted of flexural FRP only, scheme 2 consisted of flexural FRP plus two strategically placed anchor stirrups, and scheme 3 consisted of flexural FRP plus eight evenly spaced anchor stirrups.

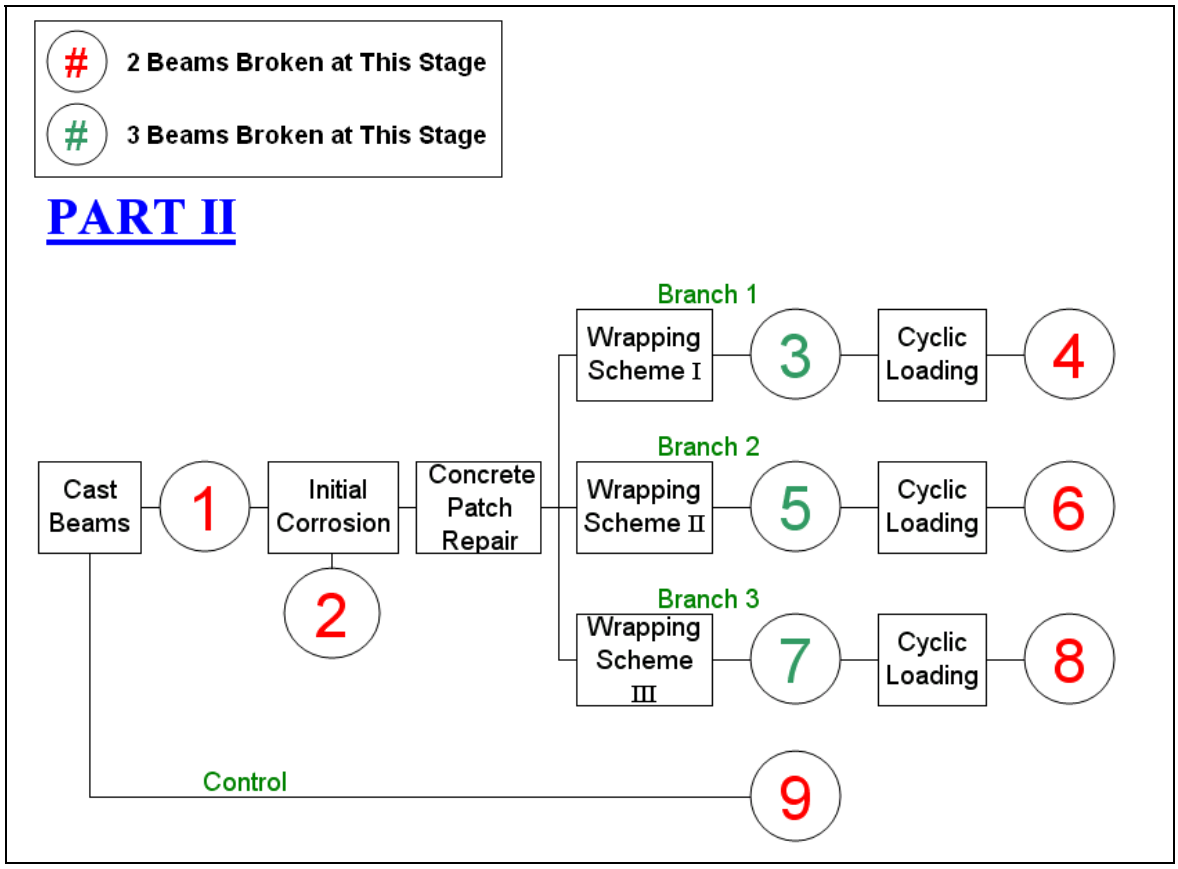

Figure 88: Schematic of experimental testing plan Part II

Figure 88 shows schematic drawings of the experimental testing plan. The circled numerals indicate points in which static load tests were performed to failure. The color of each numeral indicates the number of specimens tested at each given stage. Circles

which are lined up vertically in the figures indicate those beams were flexure tested at the same age.

5.2.2 Test Specimen

5.2.2.1 Dimensions

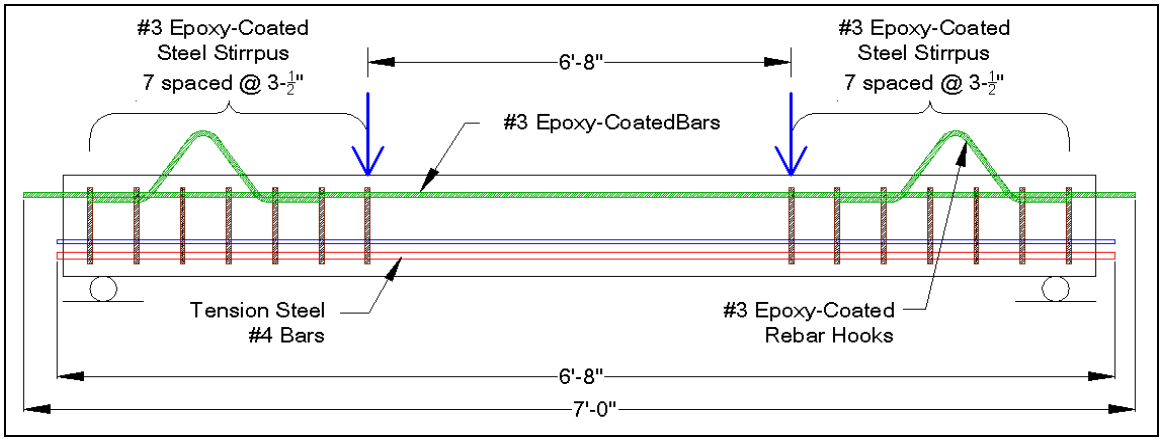

Figure 89: Beam Specimen (Reinforcement Diagram)

The beams had a dimension of 6"x 8"x78". Compare to Part I, the specimens were shortened and the rebar size was reduced in order to expedite the accelerated aging process. Steel reinforcement consisted of two #4 bars (½"diameter) for tension, two #3 bars (⅜" diameter) for compression, and #3 stirrups for shear. The dimensions of the stirrups, the stainless steel tubes, and the hooks were the same as that described for Part I specimens. Diagrams of the beams are given in Figure 89.

5.2.2.2 Materials

Mix proportions and materials in the concrete as well as the types and grades of steel and stainless steel were the same as those described for Part I specimens. In Part II, however, the entire surface area tension of steel was exposed to the surrounding concrete over the entire length of each beam and no epoxy coating was used. As in Part I, the compression steel was coated with standard fusion-bonded epoxy before purchase.

Due to corrosion of the shear reinforcement in Part I, it was decided that all stirrups in Part II specimens would be epoxy coated. Due to the large quantity and necessity for

quality and uniform coating, the epoxy coating was commercially done. Electrical tape was then wrapped around the four corners of each stirrup at locations where the tension or compression steel were to make contact to protect epoxy coatings from abrasion during assembly of the reinforcing cages

5.2.3 Beam Repair

5.2.3.1 Substrate Repair

The substrate repair method for the Part II beam repairs was identical to the polymer-modified concrete patch repair for Part I beams. First, deteriorated cover concrete was removed from each beam. Second, corrosion product was removed from the tension steel. Next, new polymer repair concrete was used to replace the old concrete that was removed. Finally, the surface of the repair concrete was prepared for the application of FRP.

5.2.3.2 FRP Repair Using Three Unique Wrapping Schemes

The effectiveness of three unique wrapping schemes was studied. The variable was the extent of U-wrap anchorage provided. Flexural FRP strengthening consisted of one ply of Tyfo SCH-7UP Composite, which is 0.007" thick for all Part II beams.

5.2.3.2.1 Wrapping Scheme I

No anchorage system was used so that the beam specimens with Wrapping Scheme 1 would serve as a base comparison to the anchored schemes 2 and 3. A schematic of Wrapping Scheme 1 is provided in Figure 90.

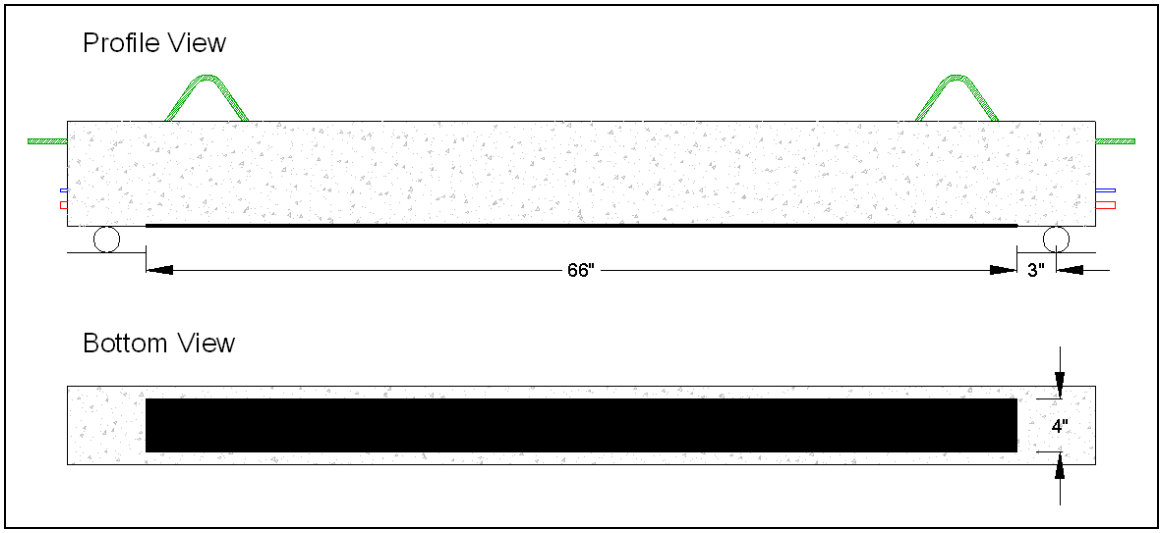

Figure 90: Schematic of Wrapping Scheme I

5.2.3.2.2 Wrapping Scheme 2

Two 4" wide U-wrap anchors, one on either side of the beam's midspan, were installed at strategic locations. The same FRP strip was used to make the anchor stirrups. The concept behind Dr. Chris Leung's advice regarding the location of these stirrups (Leung, 2006) was the basis of the locations chosen for this wrapping scheme. The locations were not decided upon until the Wrapping Scheme 1 beams were tested in 4-point bending and the rupture and debonding locations were discovered. It was finally decided that the U-wrap anchors be placed at locations of 17" from the supports (14" from the FRP termination points). This anchor location was slightly inside location Dr. Leung suggested (refer to Part I), because this appeared to be the initiation point of debonding for beams repaired using Scheme 1. A schematic of Wrapping Scheme 2 is provided in Figure 92.

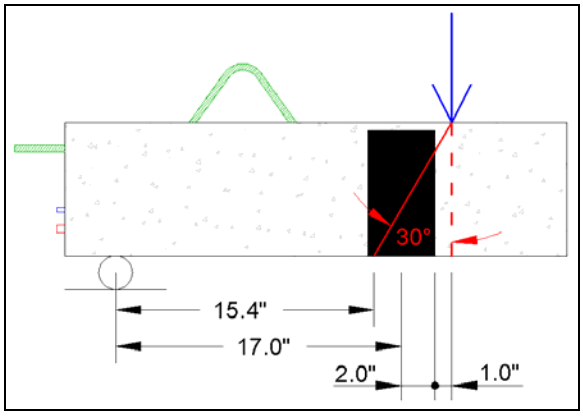

Figure 91: Stirrup Location for Wrapping Scheme II

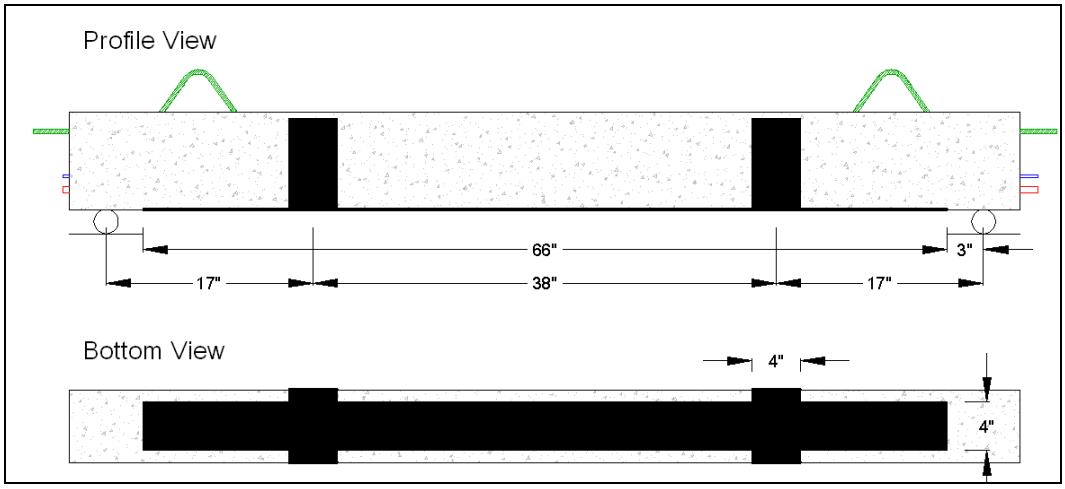

Figure 92: Schematic of Wrapping Scheme 2

5.2.3.2.3 Wrapping Scheme 3

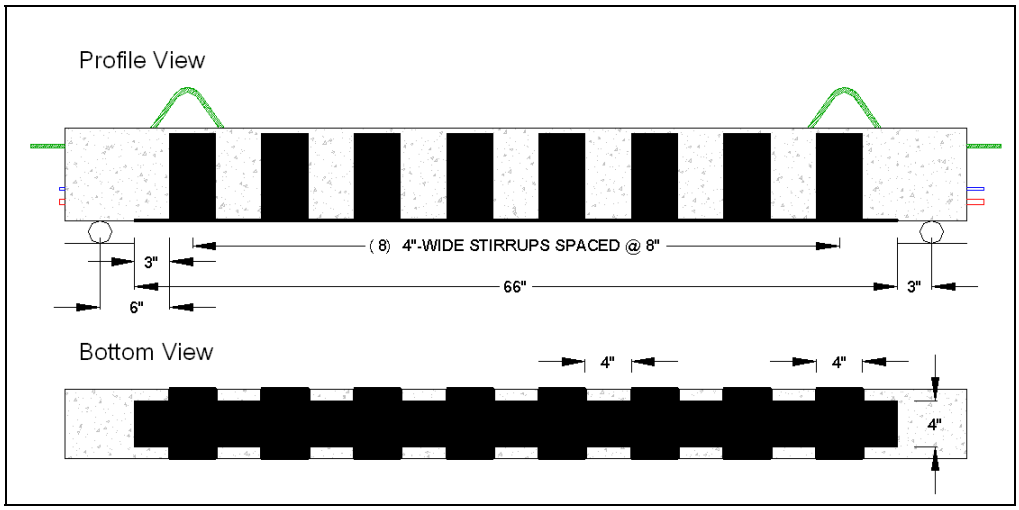

Figure 93: Schematic of Wrapping Scheme 3

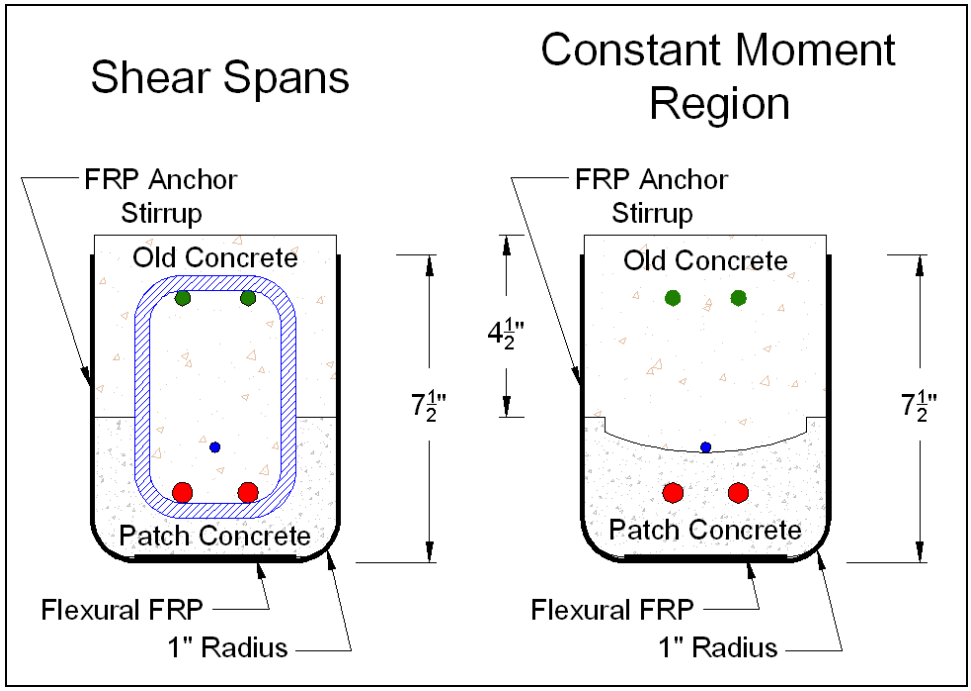

Figure 94: Cross-section of patch repaired beams with FRP at both shear and constant moment regions

Eight U-wrap anchors were evenly spaced 8" apart over the length of the span. The same FRP strip was used to make the anchor stirrups. A schematic of Wrapping Scheme 3 is provided in Figure 93. Figure 94 shows the cross-section of patch repaired beams strengthened with FRP at both the shear and constant moment regions.

5.2.4 Testing Method

5.2.4.1 Static Flexural Testing

An MTS Actuator capable of producing 110*kips* of compressive force was used to apply load to the beam specimens. Instrumentation included LVDT's to measure displacement, externally bonded strain gages to measure concrete strain, concrete embedment gages to measure concrete strain at reinforcement levels, and strain gages to measure both steel and FRP strain. The locations of the instrumentations are shown from Figure 95 through Figure 99.

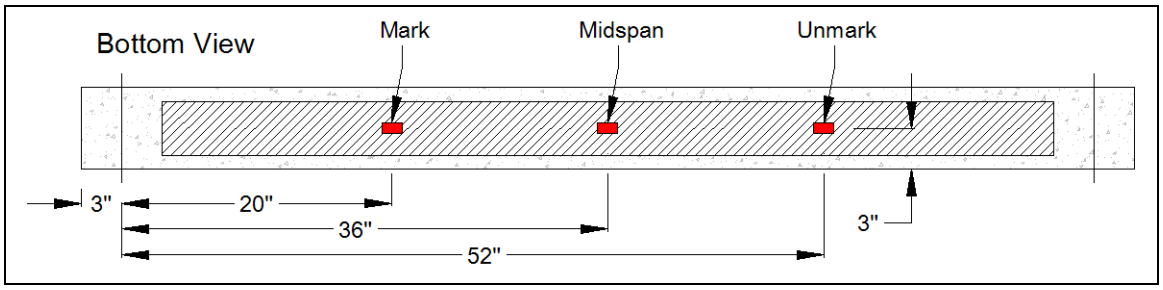

Figure 95: FRP strain gage locations

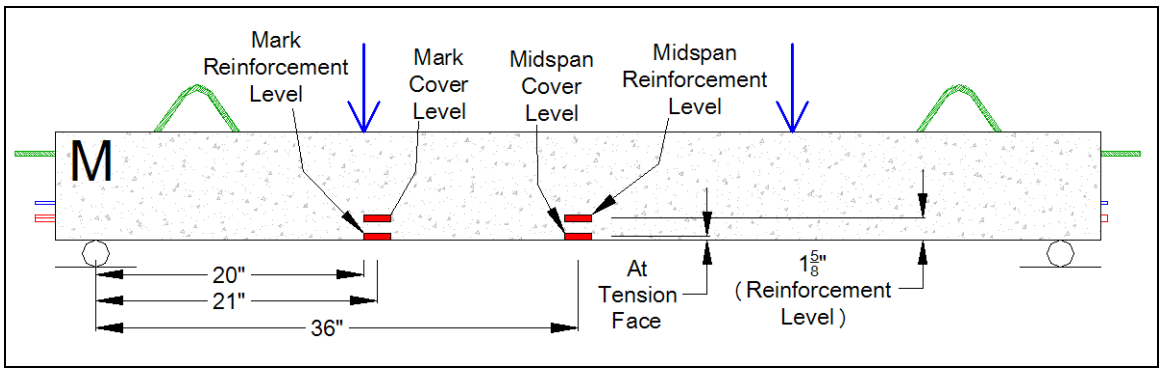

Figure 96: Externally-bonded concrete strain gage locations

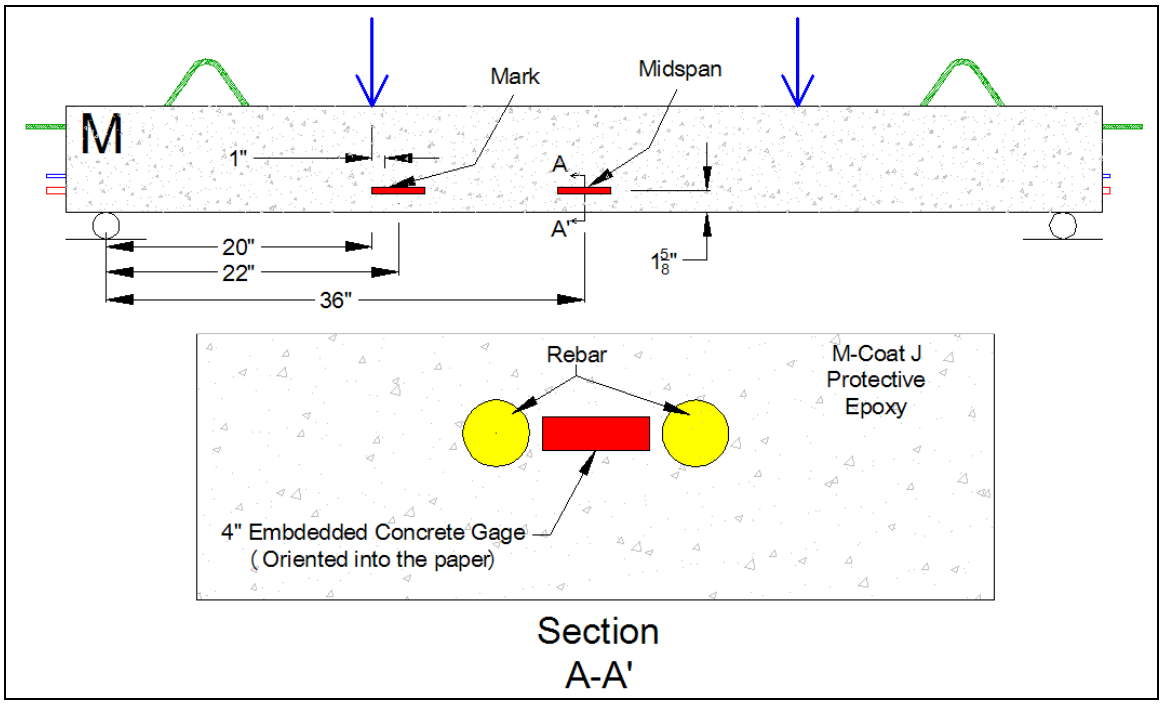

Figure 97: Externally-bonded concrete strain gage locations

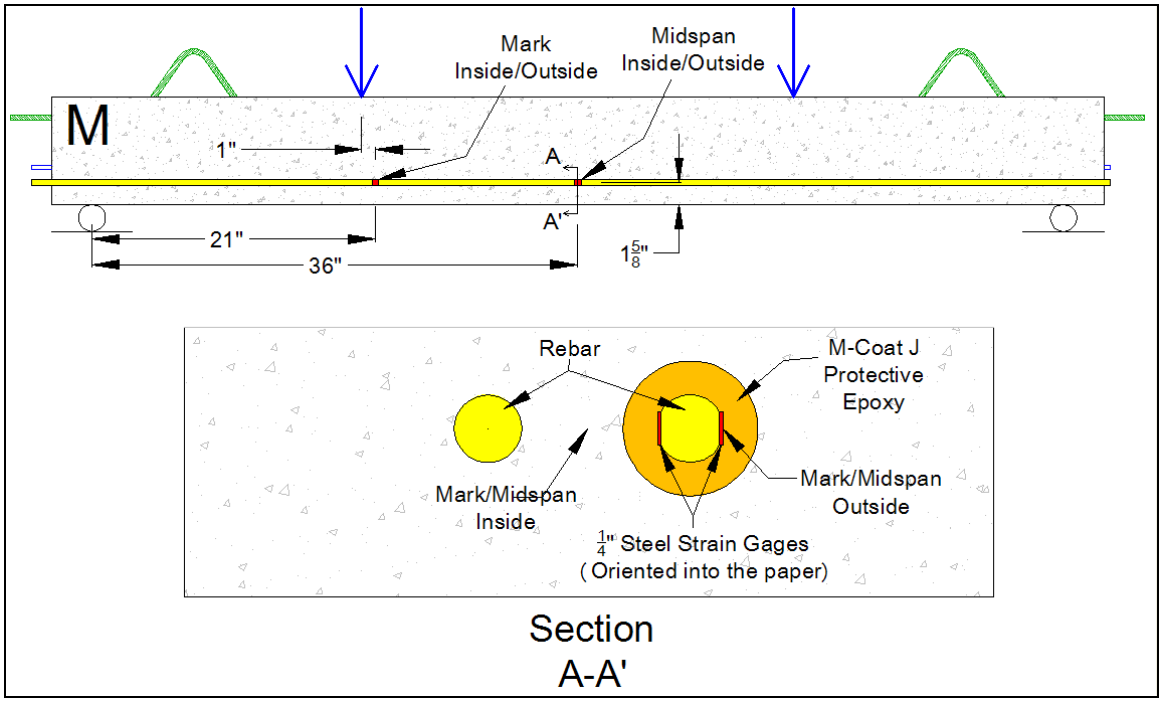

Figure 98: Steel strain gage locations

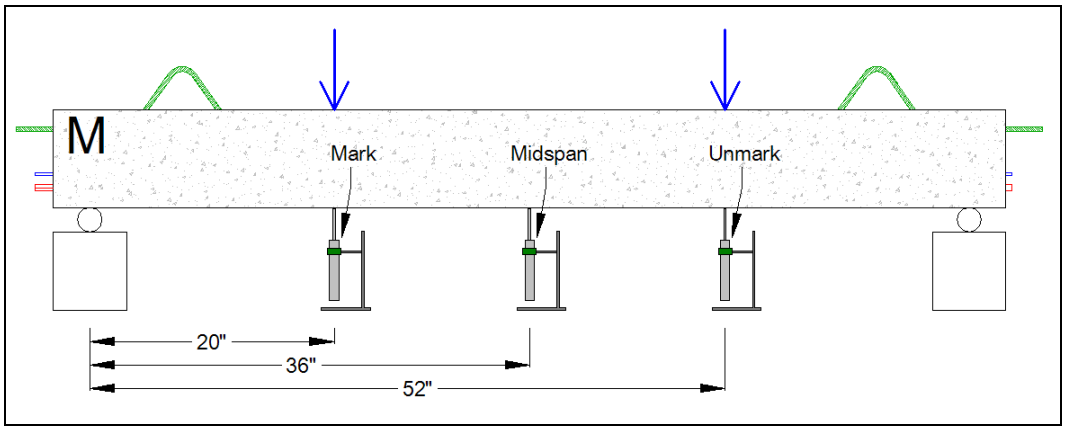

Figure 99: Part II LVDT locations

For the fully-instrumented pristine Beam 2, the externally bonded concrete gages and the concrete embedment gages were placed at the exact same locations as those beams with FRP repair. Two additional concrete embedment gages were attached between the compression steel bars to capture the compression strain at that depth. One gage was centered at the midspan and the other was placed at the load application point.

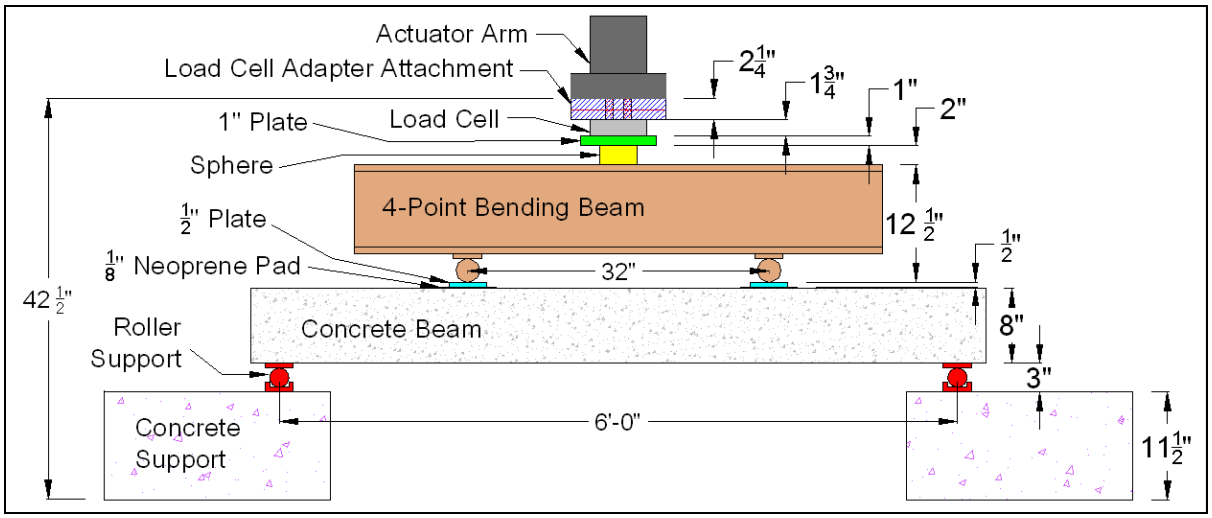

Figure 100: Part II Testing Setup

5.2.4.2 Testing Procedures

Each beam was tested in 4-point bending. Part II beams were tested across a span of 6'-0". Figure 100 shows the setup for Part II beams and displays labels on each item of the test setup. Static load tests were performed at a constant load rate of 0.5*mm/min* (0.02*in/min*) using displacement control mode, as specified by ASTM. Each sensor

recorded two data points per second. Beam specimens were tested to failure. After failure, the static load was removed, the cracks were traced, and photos were taken.

For cyclic loading, the test parameters were set up so that the actuator provided a sinusoidal cyclic load with a frequency of 3.0*Hz* and a range between 3,200*lbs* and 6,400*lbs*, corresponding to 20 and 40% of the ultimate load recorded from the three static tests of Beams 5, 8, and 9. At 250,000 cycle increments, the cyclic loading was paused and a static load was applied to the peak load of 6,400*lbs* and then removed at a rate of 0.5*mm/min* (the same rate as used for static tests to failure) while data was recorded. These static load tests provided insight into the decay of the beam specimens at various stages during fatigue loading.

5.2.5 Testing results

5.2.5.1 Accelerated Aging

The outstanding observation in Table 13 is the consistency of the accelerated aging process. The range of total percent mass loss for all fifteen FRP-repaired beam specimens was only 2.7% with a percent difference of 11.9%. This data shows that the modified specimen and the finely-tuned accelerated aging procedure is a very dependable method for creating low-variability aged reinforced concrete beam samples.

The average percent mass loss for the FRP repaired beams subjected to 1,100*amp·hours* (2,200 hours at a current of 500*mA*) was 22.5%. This magnitude of mass loss of produced a substantial amount of concrete cover cracking and deterioration of steel-to-concrete bond. It should be noted that the average mass loss observed in the corroded unrepaired Beams II-3 and II-4 averaged a 1.7% greater mass loss than did the repaired beams. This difference is probably because these bars were encased in the chloride-contaminated concrete for a slightly longer amount of time than were the fifteen repaired beams. Typical deterioration of the beams are shown in Figures 101 and 102. A photo of Beam II-3 prior to concrete removal and steel extraction is provided in Figure 103. It should be noted that a natural mass loss of only 0.7% was observed in the long-term pristine beam at 34 weeks of age.

Table 13: Part II Mass Loss Summary

Description	Group (Refer to Figure 5.2)	Beam	Mass Loss (%)	Average Mass Loss by Group (%)	Range of Mass Loss by Group (%)	Percent Difference by Group (%)	Total Average Mass Loss (%)	Total Range of Mass Loss (%)	Total Percent Difference (%)
Pristine (28-day)	1	2	0.5	-	-	-			
Pristine (Long-Term)	9	12	0.7	-	-	-			
Corroded Unrepaired	2	3	24.2	24.2	0.2	0.6			
		4	24.3						
Repaired with Wrapping Scheme 1	3	5	22.5	22.6	2.6	11.4	22.5	2.7	11.9
		8	22.3						
		9	21.3						
	4	7	23.9						
		14	23.2						
Repaired with Wrapping Scheme 2	5	13	22.1	22.2	2.4	10.5			
		15	21.2						
		17	21.7						
	6	18	23.5						
		20	22.2						
Repaired with Wrapping Scheme 3	7	21	22.6	22.6	1.2	5.1			
		22	22.4						
		24	22.4						
	8	20	22.2						
		23	23.4						

Figure 101: Typical deterioration of Part II beams prior to repair

Figure 102: Typical deterioration of Part II beams prior to repair

Figure 103: Corrosion observed in Beam II-3 after cover delamination

5.2.5.2 Cyclic Flexural Testing

Figure presents the normalized maximum deflection obtained during each static load test within the serviceability region up to 7,000*lbs*. Normalized deflection is calculated by dividing the actual maximum deflection at "*i"* cycles by the initial maximum deflection at 0 cycles. The specimen size, reinforcement ratio, and deflections were similar to those studied in the literature.

The maximum deflection increase due to fatigue occurred during the first 250,000 cycles for all specimens. On average, the second largest increase occurred between 250,000 and 500,000 cycles. Between 500,000 and 2,000,000 cycles, the maximum deflection increased more uniformly. A significant increase in maximum deflection occurred between 750,000 and 1,000,000 cycles for Beam II-14 and between 1,000,000 and 1,250,000 cycles for Beam II-7, each of which were repaired using Wrapping Scheme 1. A similar increase was not noticed within these intervals for the other four fatigue-loaded beams repaired using Wrapping Schemes 2 or 3.

The maximum deflection for beams repaired using Wrapping Scheme 1 was significantly higher than for beams repaired using Wrapping Schemes 2 or 3. The average normalized maximum deflection for Wrapping Scheme 1 beams was 2.38, while the average normalized maximum deflections for Wrapping Schemes 2 and 3 were 2.01 and 1.93, respectively. Therefore, when at least minimum anchorage was provided, deflections due to fatigue loading decreased significantly. More anchorage further reduced deflections, but only by a small amount. The range was largest for beams repaired with Scheme 1 and smallest for beams repaired with Scheme 3.

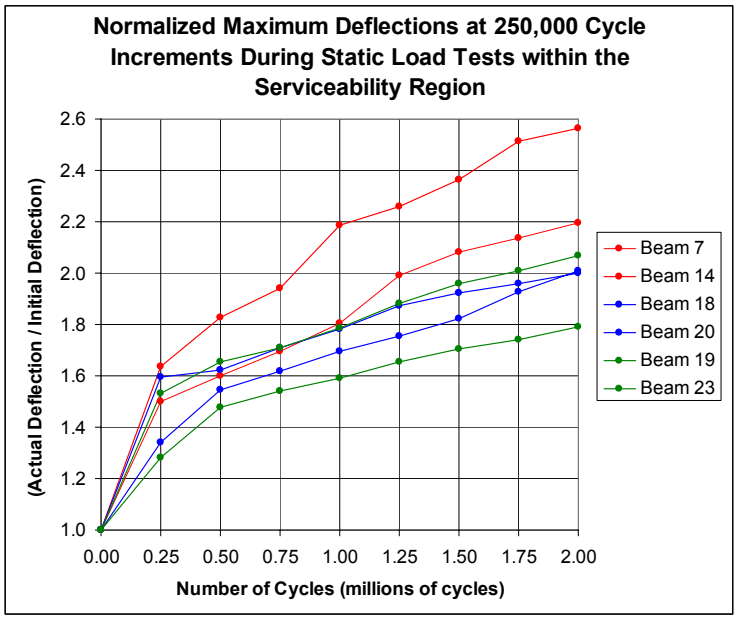

Figure 104: Decay of Part II fatigue-loaded beams as illustrated by normalized deflections at 250,000 cycle increments during static load tests within the serviceability region

Figure 105 presents the permanent deflections observed at each 250,000 cycle increment. The trends observed in Figure 104 and Figure 105 were very similar. The maximum permanent deflection increase occurred within the first 250,000 cycles for all fatigued specimens. Between 250,000 and 2,000,000 cycles, the permanent deflection increased more uniformly. A significant increase in maximum deflection occurred between 750,000 and 1,000,000 cycles for Beam II-14 and between 1,000,000 and 1,250,000 cycles for Beam II-7, each of which were repaired using Wrapping Scheme 1. This jump was not observed for Wrapping Schemes 2 or 3.

As were the maximum deflections, the average permanent deflections for Wrapping Scheme 1 beams were significantly higher than for beams repaired using Wrapping Schemes 2 or 3. Again, when at least minimum anchorage was provided, deflections due to fatigue loading decreased. Overall, the final average permanent deflection observed for Wrapping Scheme 1 beams was 0.174*in*, which was 12% larger than for Scheme 2 beams and 14% larger than for Scheme 3 beams. More anchors did not appear to further

reduce the permanent deflection, as Schemes 2 and 3 had similar averages. The range was largest for beams repaired with Scheme 2 and smallest for beams repaired with Scheme 3.

Figure 106 presents the normalized stiffness obtained during each static load test within the serviceability region up to 7,000*lbs*. Normalized stiffness is calculated by dividing actual stiffness at "*i*" cycles by initial stiffness at 0 cycles.

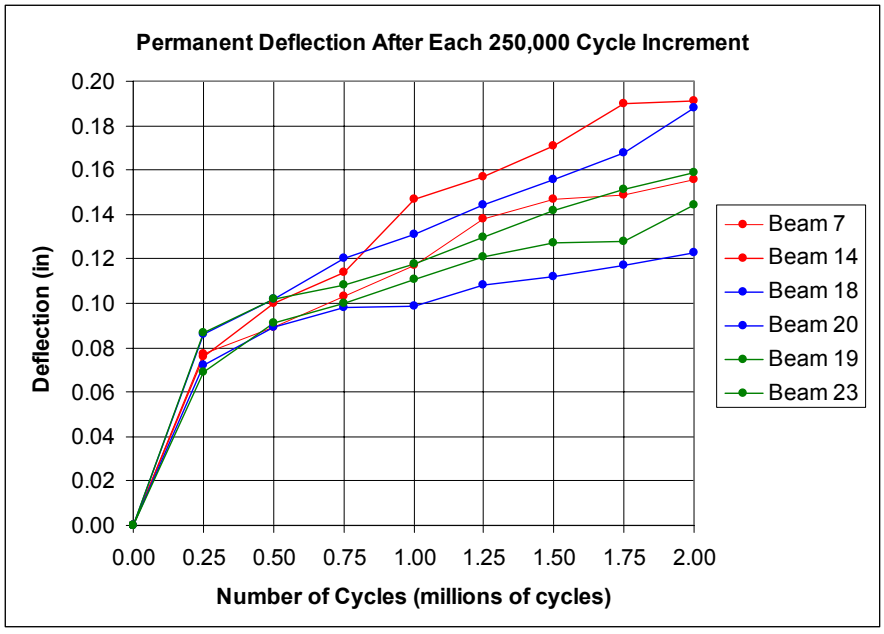

Figure 105: Decay of Part II fatigue-loaded beams as illustrated by permanent deflections after each 250,000 cycle increment

The stiffness of all beams decreased by 55-60% between the static test at 0 cycles and the incremental static test at 250,000 cycles. A majority of this stiffness loss occurred because the concrete cracked at around 4,000*lbs* load. For beams 19 and 20, a second static load test was performed at 0 cycles. The results from these additional static tests showed that between 65 and 72% of the total stiffness loss observed between 0 and 250,000 cycles was due to the fatigue loading (the remaining 28-35% was due to cracking during static loading at zero cycles).

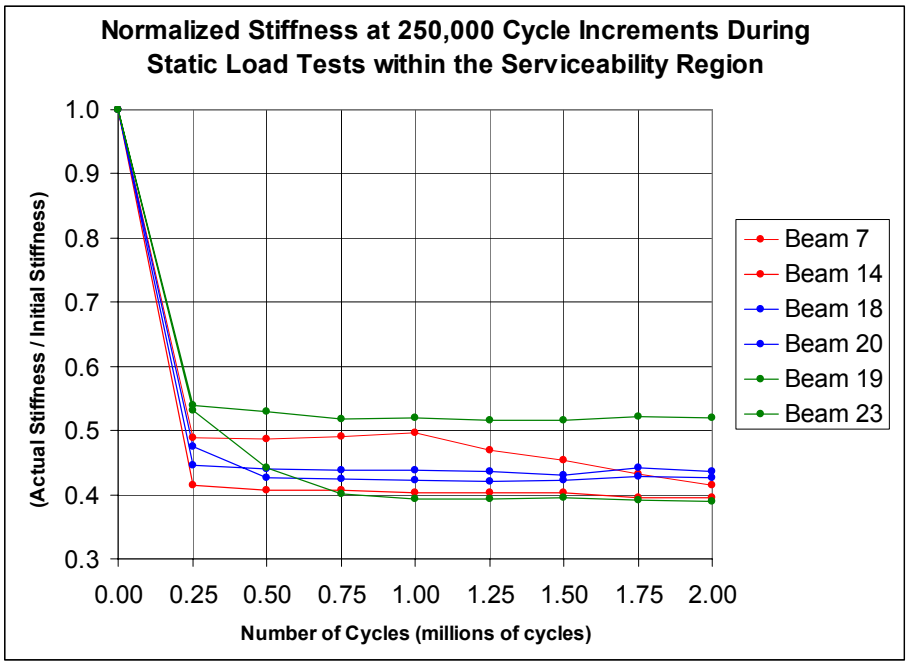

Figure 106: Decay of Part II fatigue-loaded beams as illustrated by normalized stiffness at 250,000 cycle increments during static load tests within the serviceability region

Stiffness remained fairly constant (perhaps decreasing only slightly) between 250,000-2,000,000 cycles for Beams II-14, II-18, II-19, and II-20. Beam II-23 stiffness decreased between 250,000 and 750,000 cycles before becoming fairly constant up to 2,000,000 cycles. Beam II-7 exhibited a fairly constant stiffness between 250,000 and 1,000,000 cycles, but then began to decrease (and almost linearly) between 1,000,000 and 2,000,000 cycles. All fatigued beams had a similar average stiffness after 2,000,000 cycles that ranged between 39,000 and 43,000*lbs/in*. The range of values for Wrapping Schemes 1 and 2 was very small, while the range for Wrapping Scheme 3 was much larger.

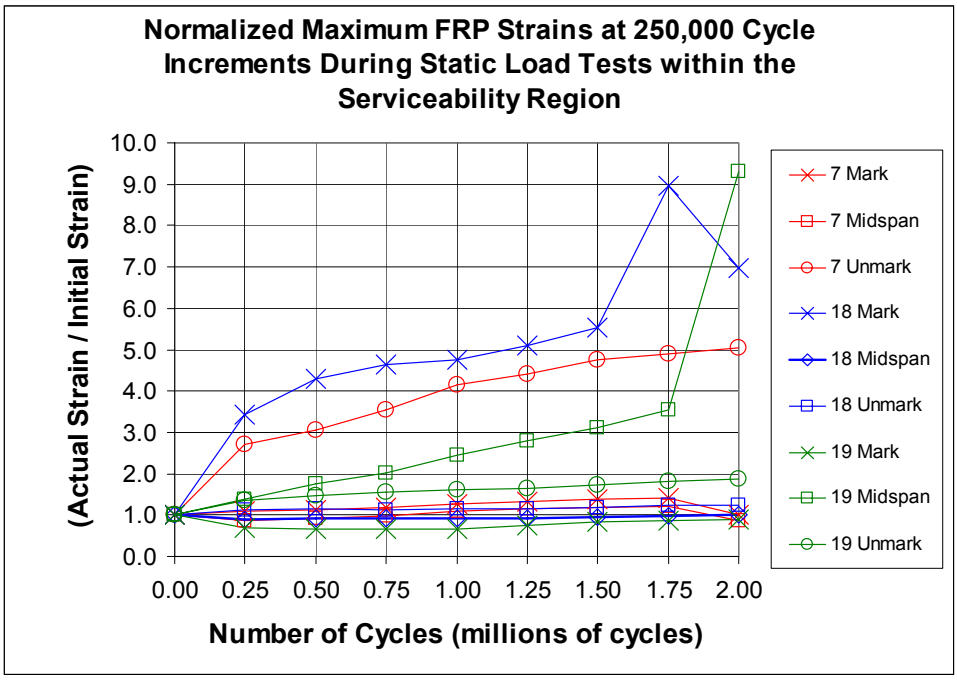

Figure 107: Decay of Part II fatigue-loaded beams as illustrated by normalized FRP Strain at 250,000 cycle increments during static load tests within the serviceability region (with outliers)

Figure 107 and Figure 108 shows the normalized FRP strains obtained during the static load tests conducted at every 250,000 cycles. "Mark" strain gages were located at the loading point toward the marked end of the beam, midspan strain gages were located at the midspan of the beam, and "unmark" strain gages were located at the load point toward the unmarked end of the beam. One FRP strain gage from each beam provided outlying results. These outliers are shown in Figure , however, to illustrate the necessity of using many FRP strain gages on actual field tests due to high variability. If only few strain gages are used during testing, very inaccurate results will likely be obtained. Outliers are eliminated from the same plot in Figure .

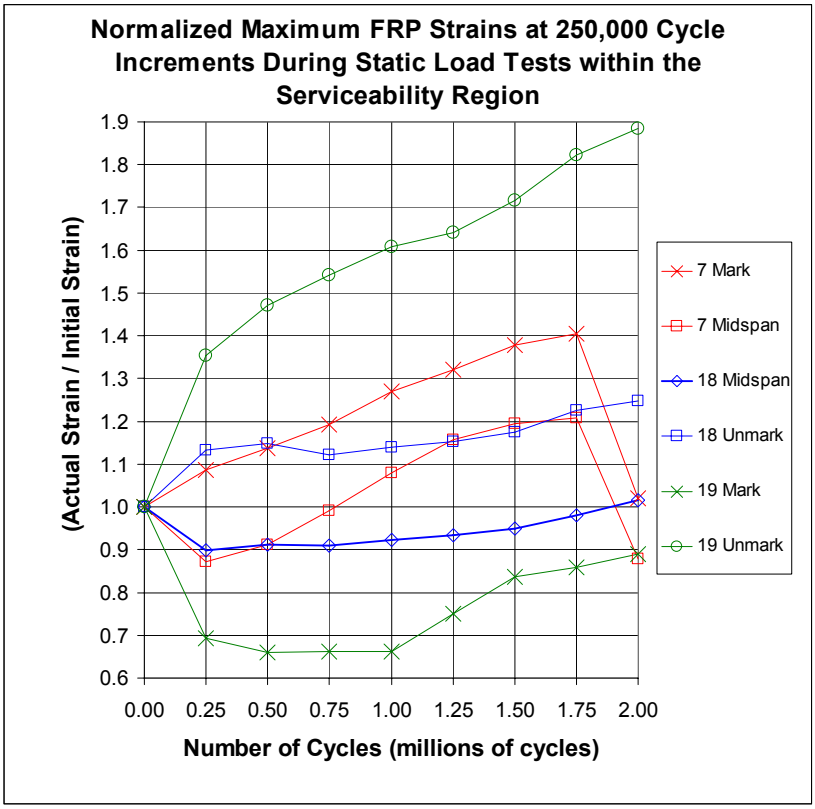

Figure 108: Decay of Part II fatigue-loaded beams as illustrated by normalized FRP Strain at 250,000 cycle increments during static load tests within the serviceability region (outliers removed)

The FRP strain gages yielded inconsistent values for fatigue-loaded beams. However, a general trend of increasing FRP strains with an increasing number of cycles can be seen, with a maximum normalized FRP strain of 1.88. FRP strains on Beam II-7 (repaired with Wrapping Scheme 1) tended to steadily increase up to 1,750,000 cycles and then decrease at 2,000,000 cycles. FRP strains on Beam II-18 (repaired with Wrapping Scheme 2) tended to steadily increase over 2,000,000 cycles. This indicates that strains may not be uniform (as in theory) across the entire constant moment region of the beam, but instead may be highly localized due to cracking. This is illustrated more emphatically when comparing the "mark" and "unmark" strain results for Beam II-19 (repaired with Wrapping Scheme 3).

Figure 109 shows the normalized steel strains obtained during the static load tests that were conducted every 250,000 cycles. "Mark inside" and outside "mark outside" gages were located beneath the load point toward the marked end of the beam on the vertical centerline of the rebar. Midspan inside and outside strain gages were located at the midspan of the beam on the vertical centerline of the rebar.

Most normalized steel strains increased to a range of 1.20 and 1.45 after the first 250,000 cycles and then tended to continue increasing less dramatically to a range of 1.45 and 1.80. Several outlying curves that may be attributed to localized strain differences due to cracking or to statistical variability of the strain gages were obtained. Again, the presence of these outliers emphasizes the necessity of using a large quantity of steel strain gages during actual field tests. Also, gages with 350Ω resistance are more accurate and consistent than gages with 120Ω resistance like the ones used in this research and should be used in field studies.

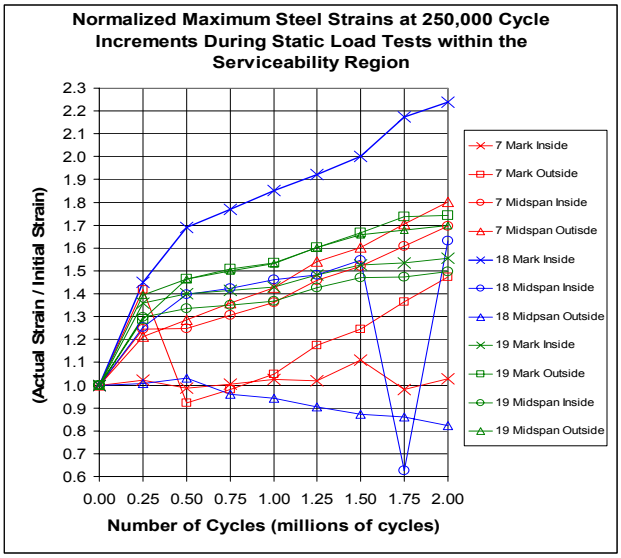

Figure 109: Decay of Part II fatigue-loaded beams as illustrated by normalized steel strain at 250,000 cycle increments during static load tests within the serviceability region

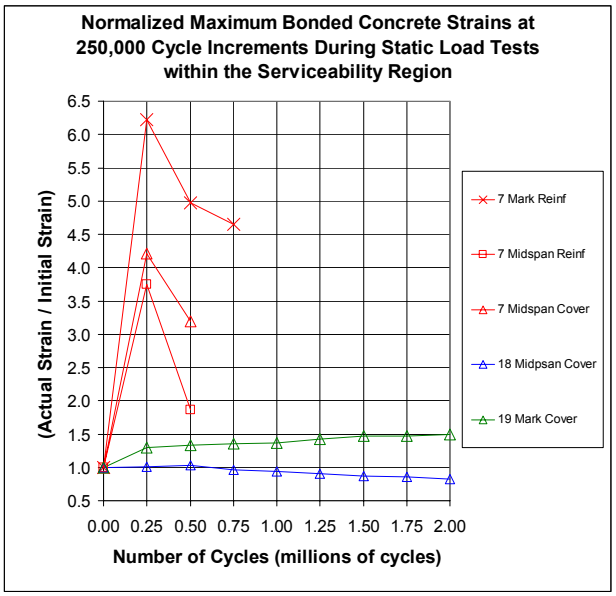

Figure 110: Decay of Part II fatigue-loaded beams as illustrated by normalized bonded concrete strain at 250,000 cycle increments during static load tests within the serviceability region

Figure 110 presents normalized concrete strains obtained from surface-bonded gages during the static load tests performed at every 250,000 cycles. "Mark reinf" and "midspan reinf" gages were bonded to the concrete at the depth as the tension steel centerline at the "mark" load point and at midspan, respectively. "Mark cover" and "midspan cover" gages were bonded to the concrete at the tension face of the beam at the mark load point and at the midspan, respectively.

Again, highly variable results were obtained from the concrete strain gages with many outliers due to cracking. These outliers are not shown in Figure 110. In fact, many of these bonded gages failed during the static load test at 0 cycles due to the formation of cracks beneath the gages.

Meaningful results were obtained, however, from several concrete strain gages. Beam II-7 (repaired with Scheme 1) gages showed large maximum strain increases, Beam II-18

(repaired with Scheme 2) gages showed slowly increasing maximum strains, and Beam II-19 (repaired with Scheme 3) gages showed slightly decreasing maximum concrete strains. These results are logical since the least-confined concrete in Wrapping Scheme 1 beams yielded the most dramatic increase in concrete strain and the most-confined concrete in Wrapping Scheme 3 beams yielded a slight decrease in concrete strain.

Embedded concrete strain gages did not perform well in fatigued beams and failed within the first 250,000 cycles.

Table 14 presents the permanent microstrains recorded after 2,000,000 fatigue loading cycles in all materials. Beam II-18 yielded the largest average permanent FRP microstrain of 2,019. All permanent microstrain values were similar. The permanent strain at midspan was slightly larger than at the load points on each of the gaged and fatigued beams. Average permanent steel strains were similar at all locations. Beam II-7 yielded the largest average permanent steel microstrain of 802.

Table 14: Part II permanent strains after 2,000,000 loading cycles

Gage	Location	Part II Beam			Average
		7	18	19	
FRP	Mark	1,171	1,442	1,407	1,340
	Midspan	2,625	1,937	1,527	2,030
	Unmark	1,174	2,678	1,136	1,663
	Average	1,657	2,019	1,357	
Steel	Mark Inside	78	1,089	757	641
	Mark Outside	684	-	905	795
	Midspan Inside	736	672	615	674
	Midspan Outside	986	267	742	665
	Average	802	470	754	

5.2.5.3 4-point bending test

Figure 111 through 114 show various sets of load-deflection curves grouped together for comparison. Figure 111 provides the superposition of all curves obtained in Part II. Figure 112 displays comparisons of all pristine and corroded unrepaired control beams.

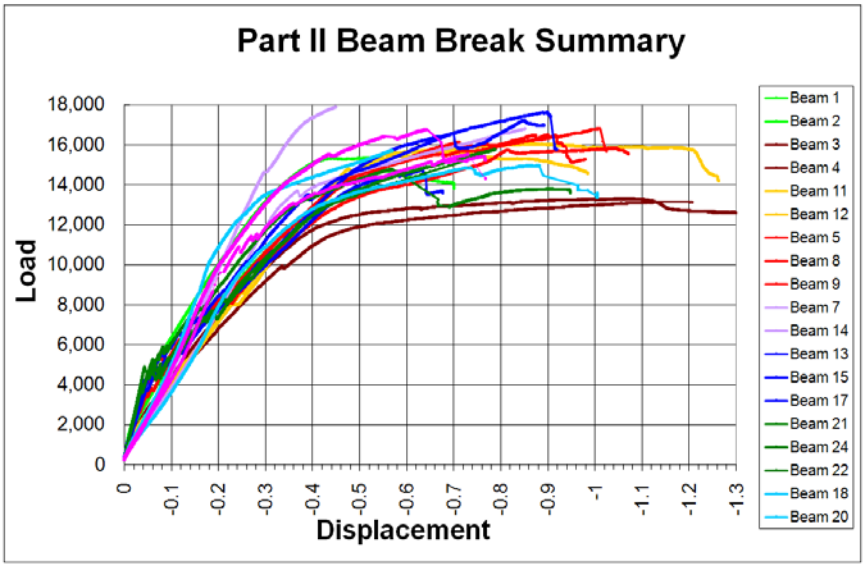

Figure 111: Part II load-deflection curves

Figure 113 shows load-deflection curves for the Part II beams repaired with FRP Wrapping Schemes 1, 2, and 3. Figure 114 shows a comparison of all beams subjected to cyclic loading before repair. The curves in these figures are analyzed in the following commentary.

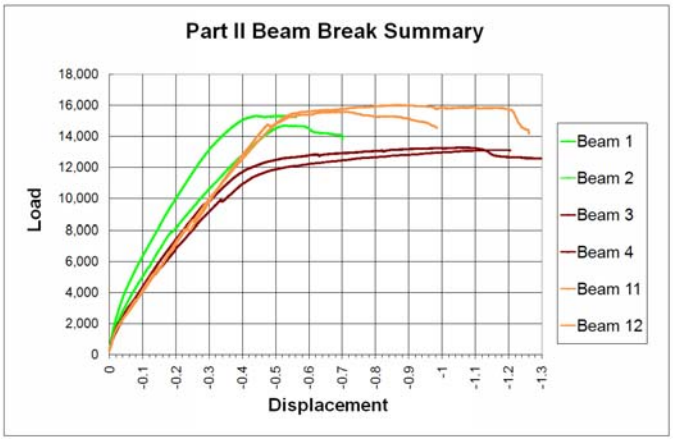

Figure 112: Comparison of Part II load-deflection curves for both pristine and corroded unrepaired control beams

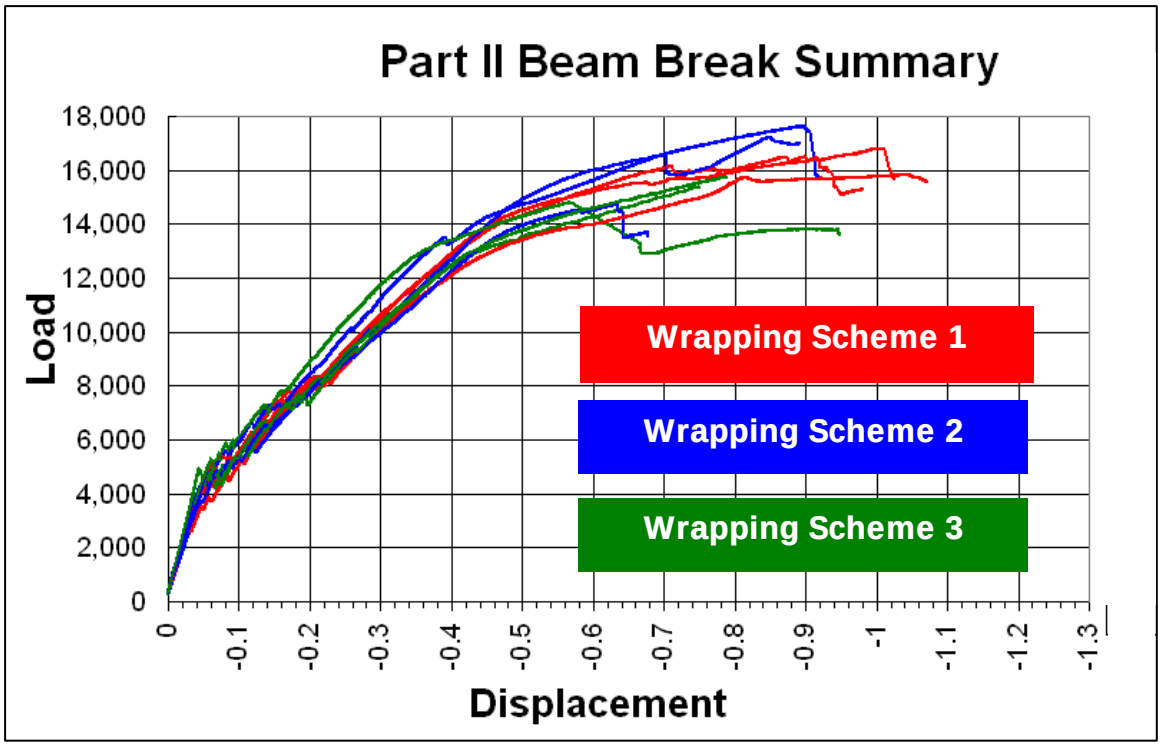

Figure 113: Comparison of Part II load-deflection curves

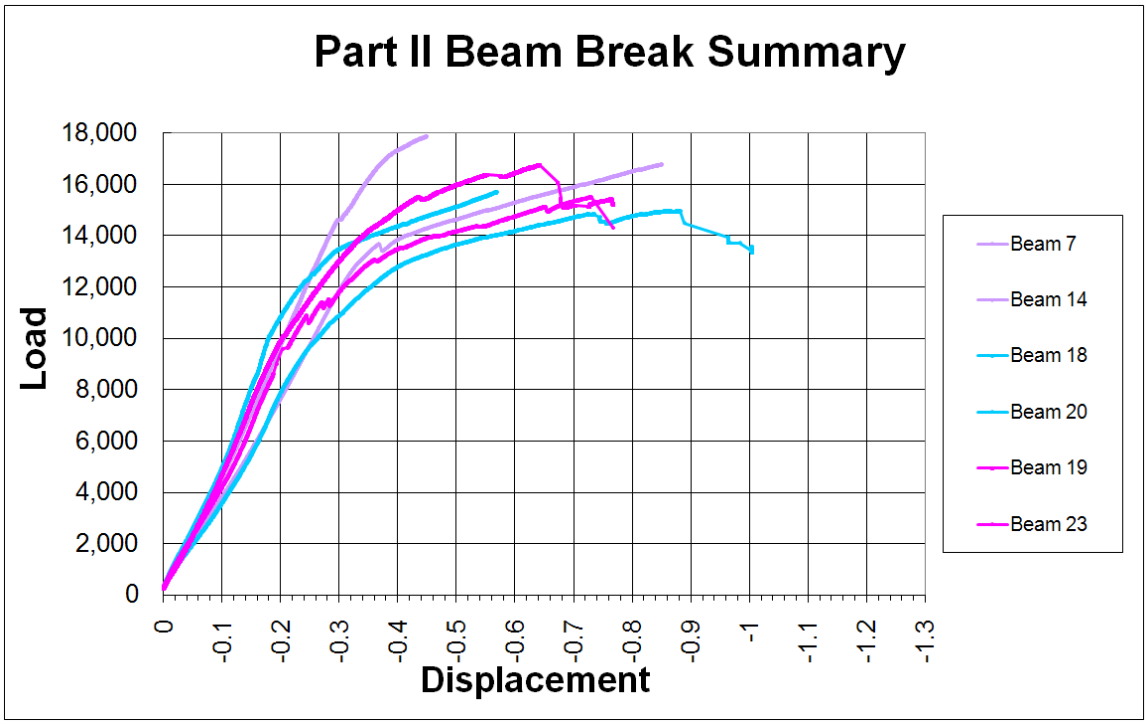

Figure 114: Comparison of Part II load-deflection curves for repaired beams subjected to fatigue loading prior to loading statically to failure

Table 15 presents a summary of both maximum service load and maximum load at failure. The maximum service load is the highest load observed within the post-cracking region of the load-deflection curve. All loads presented in this table were rounded to the nearest 100*lbs*

.

Reinforced concrete beam deflection analysis equations predicted an ultimate load of 6,488*lbs* applied at each load points, or approximately 12,976*lbs* total. The pristine beams yielded average maximum service loads of 13,500*lbs* (28-day) and 15,100*lbs* (27 weeks). These were good for quality control since they verified the beam specimens performed according to the conservative ACI design guidelines.

Table 15: Part II Load Capacity Summary

Description	Beam	Maximum Load Within Servicability Range (lbs)				Total Maximum Load (lbs)			
		Load	Mean	Range	% Diff.	Load	Mean	Range	% Diff.
28-Day Pristine	1	13,000	13,500	1,000	7.41	15,300	15,000	600	4.00
	2	14,000				14,700			
Corroded Unrepaired	3	9,700	9,850	300	3.05	13,200	13,150	100	0.76
	4	10,000				13,100			
Long-Term Pristine Control	11	14,600	15,100	1,000	6.62	16,000	15,100	1,800	11.92
	12	15,600				14,200			
Repaired using Wrapping Scheme 1	5	10,100	12,233	3,400	28.81	15,700	16,300	1,100	6.77
	8	13,100				16,400			
	9	13,500				16,800			
Repaired using Wrapping Scheme 1 + Cyclic Load	7	14,600	13,850	1,500	10.83	17,900	17,350	1,100	6.34
	14	13,100				16,800			
Repaired using Wrapping Scheme 2	13	13,500	13,700	600	4.35	17,400	16,533	3,000	18.63
	15	14,100				17,600			
	17	13,500				14,600			
Repaired using Wrapping Scheme 2 + Cyclic Load	18	12,400	12,750	700	5.49	15,000	15,350	700	4.56
	20	13,100				15,700			
Repaired using Wrapping Scheme 3	21	12,300	12,267	500	4.08	15,700	15,300	900	5.90
	22	12,000				15,400			
	24	12,500				14,800			
Repaired using Wrapping Scheme 3 + Cyclic Load	19	14,000	12,450	3,100	24.90	16,800	16,150	1,300	8.05
	23	10,900				15,500			

On average, corroded unrepaired Beams II-3 and II-4 suffered a 35% decrease in service load capacity and a 13% decrease of failure load compared to the long-term control specimens II-11 and II-12. ACI design equations predicted that the FRP-repaired beams in Part II would have a maximum service load capacity of 11,893*lbs*. Beams repaired with Wrapping Scheme 1 (II-5, II-8, and II-9) had an average maximum service load of 12,233*lbs* and an average failure load of 16,300*lbs*. Beams repaired with Wrapping

Scheme 2 (II-13, II-15, and II-17) had an average maximum service load of 13,700*lbs* and an average failure load of 16,533*lbs*. Beams repaired using Wrapping Scheme 3 (II-21, II-22, and II-24) had an average maximum service load of 12,267*lbs* and an average failure load of 15,300*lbs*.

FRP strengthening with Wrapping Schemes 1, 2, and 3 yielded maximum service load increases of 24, 39, and 25% compared to the corroded unrepaired samples. One of the three beams repaired with Scheme 1 and all three of the beams repaired with Scheme 2 were restored to at least their original service capacities, although the specimens were not designed to fully restore these capacities. Recall that this slight under-reinforcement guarded against possible crushing of the intentionally poor-quality concrete if too much tension reinforcement was provided. Beams II-5 and II-8 had service capacities that were 75% and 97% that of the 28-day pristine beams, respectively. Beams II-9, II-13, and II-17 had service capacities equaling that of the 28-day pristine specimens, and Beam II-15 had a capacity of 104% that of the 28-day pristine specimens. Beams repaired using Wrapping Scheme 3 had service load capacities less than that of the 28-day pristine beams (91, 89, and 93% that of the 28-day pristine beams). Wrapping Schemes 1, 2, and 3 yielded percent increases in service load of 24, 39, and 12% compared to the corroded unrepaired Beams II-3 and II-4, respectively.

FRP-repair of beams using Wrapping Schemes 1, 2, and 3 yielded 9, 10, and 2% increases in failure load compared to the 28-day pristine specimens, respectively. These wrapping schemes yielded 24, 26, and 16% increases in failure load compared to corroded unrepaired Beams II-3 and II-4, respectively. FRP repair of beams using Schemes 1, 2, and 3 had service load capacities that were 3, 15, and 3% higher than predicted, respectively.

Cyclic loading did not appear to have a significant effect on load capacity. There was not consistency between duplicate beams in Part II of this experiment. The capacity difference between most specimens in defined beam groups was less than 10%.

Table 16 shows the Part II service and failure deflections. The predicted service deflection was 0.37*in* and the average deflection of the 28-day pristine specimen was 0.38*in*, a good result for quality control showing that the beams were performing as designed. The average service deflection of the long-term control beams was a larger 0.48*in*. The corroded unrepaired beams II-3 and II-4 each exhibited an average service deflection of 0.32*in*. Large differences existed between the failure deflections of duplicate beam specimens.

Non-fatigued beams repaired with Wrapping Schemes 1, 2, and 3 yielded service deflections of 0.38, 0.44, and 0.36*in*, respectively. Fatigue loading appeared to reduce the service deflection for Schemes 2 and 3. The service defection of Scheme 1 beams was not significantly affected by fatigue loading.

The average failure deflection for 28-day pristine beams was 0.56*in*. Long-term pristine control beams exhibited a scattered average failure deflection ranging between 0.72 and 1.17*in*. Corroded unrepaired beams yielded a 100% increase in failure deflection compared to that of the 28-day pristine beams.

Table 16: Part II Deflection Summary

Description	Beam	Maximum Deflection at Initiation of Postservicability Cracking Stage (in)				Deflection @ Maximum (Failure) Load (in)			
		Δ	Mean	Range	% Diff.	Δ	Mean	Range	% Diff.
28-Day Pristine	1	0.30	0.38	0.16	42.1	0.53	0.56	0.05	9.0
	2	0.46				0.58			
Corroded Unrepaired	3	0.29	0.32	0.06	18.8	1.10	1.12	0.03	2.7
	4	0.35				1.13			
Long-Term Pristine Control	11	0.48	0.48	0.01	2.1	1.17	0.95	0.45	47.6
	12	0.47				0.72			
Repaired using Wrapping Scheme 1	5	0.30	0.38	0.13	35.6	1.05	0.80	0.60	80.0
	8	0.41				0.91			
	9	0.43				0.45			
Repaired using Wrapping Scheme 1 + Cyclic Load	7	0.52	0.43	0.18	41.9	0.60	0.73	0.25	34.5
	14	0.34				0.85			
Repaired using Wrapping Scheme 2	13	0.39	0.44	0.07	16.5	0.84	0.79	0.26	33.8
	15	0.46				0.90			
	17	0.46				0.64			
Repaired using Wrapping Scheme 2 + Cyclic Load	18	0.37	0.33	0.09	27.7	0.88	0.73	0.31	42.8
	20	0.28				0.57			
Repaired using Wrapping Scheme 3	21	0.39	0.36	0.06	16.7	0.79	0.70	0.22	32.4
	22	0.37				0.75			
	24	0.33				0.57			
Repaired using Wrapping Scheme 3 + Cyclic Load	19	0.34	0.29	0.10	34.5	0.64	0.69	0.09	13.1
	23	0.24				0.73			

The average failure deflections for non-fatigued beams repaired with Schemes 1, 2, and 3 were 0.80, 0.79, and 0.70*in*, respectively. Cyclic loading reduced the failure deflection for Schemes 1, 2, and 3 by 9, 8, and 1%, respectively.

Table 17 presents both the post-cracking and the post-serviceability stiffness observed for each Part II beam. The average 28-day pristine post-cracking stiffness was 29,280*lbs/in*. The average post-cracking stiffness for the corroded unrepaired beam was 26,360*lbs/in*, a 7% decrease compared to that of the long-term pristine control specimens. Large differences were observed between the stiffness of two 28-day pristine beams.

The average post-cracking stiffness increased as more anchorage was added. Beams repaired with Schemes 2 and 3 exhibited 1 and 11% post-cracking stiffness increases (respectively) over those repaired with Scheme 1.

Table 17: Part II Stiffness Summary

Description	Beam	Initial Stiffness (lbs/in)				Secondary Stiffness (lbs/in)			
		Stiffness	Mean	Range	% Diff.	Stiffness	Mean	Range	% Diff.
28-Day Pristine	1	34,550	29,280	10,541	36.00	2,012	1,969	87	4.42
	2	24,009				1,925			
Corroded Unrepaired	3	27,751	26,360	2,782	10.55	1,199	1,505	611	40.61
	4	24,969				1,810			
Long-Term Pristine Control	11	28,634	28,236	797	2.82	1,658	1,251	814	65.07
	12	27,837				844			
Repaired using Wrapping Scheme 1	5	21,864	24,483	3,928	16.48	6,021	7,076	2,470	34.04
	8	25,792				8,491			
	9	25,792				6,717			
Repaired using Wrapping Scheme 1 + Cyclic Load	7	51,655	46,950	9,410	20.04	11,744	9,002	5,485	60.93
	14	42,245				6,259			
Repaired using Wrapping Scheme 2	13	27,494	24,712	5,181	20.80	9,422	7,350	3,846	51.29
	15	24,330				5,576			
	17	22,313				7,053			
Repaired using Wrapping Scheme 2 + Cyclic Load	18	42,409	53,004	21,190	39.98	5,623	6,772	2,297	33.92
	20	63,599				7,920			
Repaired using Wrapping Scheme 3	21	26,573	27,191	2,971	10.80	6,240	7,414	2,348	31.67
	22	26,014				7,414			
	24	28,985				8,588			
Repaired using Wrapping Scheme 3 + Cyclic Load	19	31,429	42,832	22,806	53.25	8,784	7,293	2,982	40.90
	23	54,235				5,802			

Table 18 presents a summary of strains and corresponding loads recorded during the Part II static tests. The average strain at peak of the linear region and its corresponding load is given in the "max in linear region" rows. The average maximum strain recorded and its corresponding load is provided in the "failure" rows. These values are the average of all gages in similar locations by material. Values recorded from the four steel gages, the three FRP gages, the two bonded concrete reinforcement level gages, the two bonded concrete cover level gages, and the two embedded concrete gages were each averaged together, respectively. Each respective group of gages should theoretically have the same strain at the same load since they were all located within the constant moment region of the beam specimen.

Table 18: Part II Strain Summary

Gage / Material			Part II Beam and Description									
			28-Day Pristine	Long-Term Pristine		Severely Corroded	Wrapping Scheme 1	Wrapping Scheme 1 (Fatigued)	Wrapping Scheme 2	Wrapping Scheme 2 (Fatigued)	Wrapping Scheme 3	Wrapping Scheme 3 (Fatigued)
			2	11	12	3	5	7	17	18	24	19
Steel	Max in Linear Region	Microstrain	2,466	2,439	2,465	-	2,358	3,172	1,791	2,390	2,286	2,911
		Load (lbs)	14,321	14,724	14,331	-	11,293	16,652	13,381	11,703	11,946	11,837
	Failure	Microstrain	8,050	16,986	10,629	-	11,085	4,527	5,117	9,218	8,641	11,820
		Load (lbs)	13,830	15,777	14,546	-	14,601	17,878	14,436	14,043	14,128	16,074
FRP	Max in Linear Region	Microstrain	-	-	-	-	299	5,830	211	6,902	247	3,903
		Load (lbs)	-	-	-	-	9,510	16,775	8,717	12,281	5,284	11,013
	Failure	Microstrain	-	-	-	-	9,731	6,803	3,377	10,755	8,954	7,320
		Load (lbs)	-	-	-	-	15,513	17,879	14,471	14,830	14,784	15,724
Bonded Concrete Reinf. Level	Max in Linear Region	Microstrain	2,529	-	-	141	88	-	174	-	108	-
		Load (lbs)	14,459	-	-	1,866	3,370	-	5,736	-	4,930	-
	Failure	Microstrain	8,050	-	-	9,303	6,220	-	4,601	-	10,793	-
		Load (lbs)	13,830	-	-	11,124	10,615	-	13,994	-	9,711	-
Bonded Concrete Cover Level	Max in Linear Region	Microstrain	2,425	-	-	152	88	-	154	-	-	-
		Load (lbs)	14,680	-	-	1,195	3,370	-	5,669	-	-	-
	Failure	Microstrain	-	-	-	15,844	5,488	-	6,734	-	-	-
		Load (lbs)	-	-	-	3,945	5,353	-	13,578	-	-	-
Embedded Concrete	Max in Linear Region	Microstrain	-	660.5	391	-	57	-	90	-	106	-
		Load (lbs)	-	12771	8492	-	3,362	-	4,382	-	7,122	-
	Failure	Microstrain	846	1521	588	-	248	-	660	-	8,959	-
		Load (lbs)	14,216	15413	15438	-	15,430	-	10,434	-	11,525	-

5.2.5.4 Failure modes

All beams failed via crack-induced debonding and subsequent FRP rupture. Recall that crack-induced debonding initiates at the location of a flexure crack where there is a high stress concentration at the FRP-concrete interface. When the stress level reaches a critical point, the crack instantly propagates along the FRP-concrete interface. Due to the rapid redistribution of stress, the FRP ruptures at a location near the original concrete flexure crack.

Table 19 shows the primary locations of FRP rupture on Part II beams. The reported locations were measured from the marked end support location. Please note that the

marked end support was located 3” from the beam ends and the FRP termination points were located 3” to the inside of each support. Therefore, a reported FRP rupture location of 3’-9” would have been located 3’-6” from the FRP termination point. Recall that the locations of the beams’ midspan are 3’-0”.

Table 19: Part II FRP Rupture Locations

Description		Beam	Distance from the Mark Support to the Primary Location of FRP Failure
Wrapping Scheme 1	Non-Fatigued	5	1' - 6¾" -- 1' - 10½
		8	1' - 11⅜" -- 2' - 3⅞"
		9	1' - 4¾" -- 2' - 3"
	Fatigued	7	2' - 3" -- 2' - 9½"
		14	3' - 9"
Wrapping Scheme 2	Non-Fatigued	13	2' - 6" -- 2' - 9"
		15	3' - 6½" -- 3' - 9½"
		17	1' - 10¾" -- 1' - 11¾"
	Fatigued	18	1' - 8¼" -- 2' - 6¼"
		20	3' - 8" -- 3' - 11"
Wrapping Scheme 3	Non-Fatigued	21	2' - 7½" -- 2' - 8"
		24	1' - 7" -- 1' - 8"
	Fatigued	19	2' - 11½" -- 3' - 2½"
		23	3' - 8"

The FRP rupture locations for non-fatigued Scheme 1 beams ranged between 1’-4¾” and 2-3⅞”. Non-fatigued Scheme 2 rupture locations ranged between 1’-10¾” and 3’-9½”. Recall that, for Scheme 2, a 4”-wide FRP anchor stirrup was located at locations of 1’-3” – 1’-7” and at 4’-3” – 4’-7” (measured from the marked end support). These failure locations (including debonding) were contained to within the regions between the two anchor stirrups. Scheme 2 ruptures tended to occur nearer to the midspan than did Scheme 1 ruptures. Non-fatigued Scheme 3 rupture locations ranged between 1’-7” and 2’-8”. Recall that for Scheme 3, 4” wide FRP anchor stirrup were present at locations between 0’-6” and 0’-10”, 1’-2” and 1’-6”, 1’-10” and 2’-2”, 2’-6” and 2’-10”, 3’-2” and 3’-6”, 3’-10” and 4’-2”, 4’-6” and 4’-10”, and 5’-2” and 5’6”. Scheme 3 rupture locations were scattered.

The FRP rupture locations for fatigued Scheme 1, 2, and 3 beams ranged between 2’-3” and 3-9”, 1’-8¼” and 3’-11”, and 2’-11½” and 3’-8”, respectively . These ruptures were nearer to the midspan than for the non-fatigued ruptures of the same scheme.

Figure 115 displays photos of the statically-failed non-fatigued beams that were repaired using Wrapping Scheme 1. Top left is Beam II-5, top right is Beam II-8, bottom left is Beam II-9, bottom center shows a typical FRP failure surface, and bottom right shows a vee-shaped crack that will be discussed next. As evidenced in the photos, widespread delamination occurred due to crack-induced debonding. The vee-shaped crack is also visible at the initiation point of crack-induced debonding in the top left photo. Similar pronounced vee-shaped cracking was very common among most of the non-fatigued FRP-repaired beams. Debonding occurred primarily within the epoxy-concrete interface, with very thin localized patches of concrete remaining adhered to the FRP. The debonding would have likely occurred within the concrete cover layer if normal concrete were used for repair, but due to the high strength of the polymer concrete, failure occurred primarily at the bonded interface.

Figure 116 presents photos of the statically-failed beams that were fatigued and beams that were repaired using Wrapping Scheme 1. The photo on the left is of Beam II-7 and the photo on the right is of Beam II-14. For the fatigued beams, vee-shaped cracking was not as prevalent (there were still very small v-shaped patches, but they were not nearly as pronounced as those observed on the non-fatigued beams). A possible reason for this was that either localized debonding or weakening of the epoxy-concrete interface occurred within the constant moment region during fatigue loading, which caused non-composite behavior. The strong bond closer to the beam ends may have held the FRP system in place, resembling the behavior of the prestressed beam. It should be noted that no visual observation could be made that suggested the weakening of the bond during fatigue loading or during static loading prior to failure.

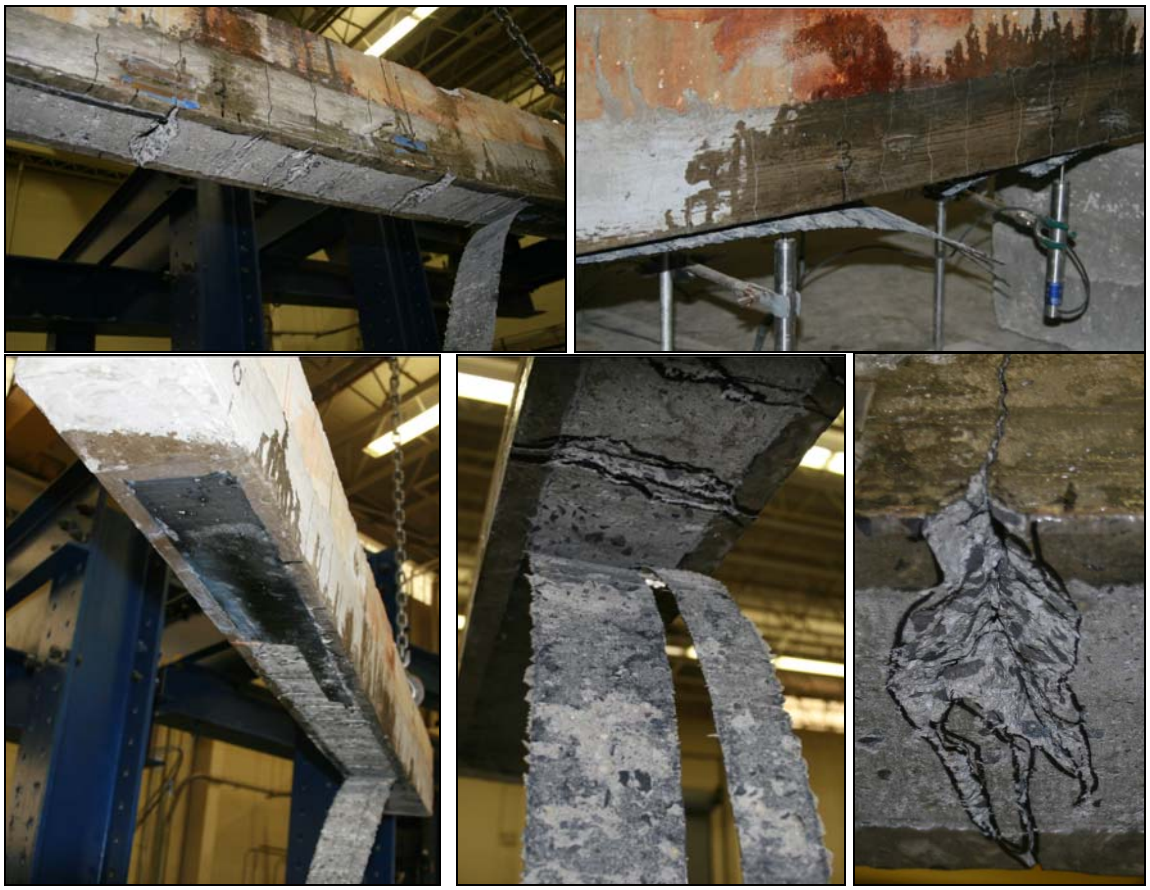

Figure 115 Photos of non-fatigued Part II beams repaired using Wrapping Scheme 1 after failure

Figure 116: Photos of fatigued Part II beams repaired using Wrapping Scheme 1 after failure

Figure 117 shows photos of the statically-failed non-fatigued beams that were repaired using Wrapping Scheme 2. The top photo is of Beam II-13, the middle photo is of Beam II-15, and the bottom photo is of Beam II-17. Regions of dramatic delamination, as for

Scheme 1, were also observed to either side of the crack where crack-induced debonding occurred on Beams II-13 and 15. The anchors prevented the delamination from continuing beyond the stirrup locations. A very small area of delamination was observed adjacent to the rupture location on Beam II-17, which was near the anchor stirrup. Figure 118 displays photos of the statically-failed fatigued beams that were repaired using Wrapping Scheme 2. The photo on the left is of Beam II-18 and the photo on the right is of Beam II-20. The FRP rupture and delamination on these beams support the conjecture proposed for the fatigued Wrapping Scheme 1 beams. Notice how the FRP freely delaminated from Beams II-18 over almost the entire constant moment region and had multiple locations of partial rupture. Also, observe the lack of pronounced vee-shaped notches on the concrete tension face of Beam II-20.

Figure 117: Photos of non-fatigued Part II beams repaired using Wrapping Scheme 2 after failure

Figure 119 presents photos of the statically-failed non-fatigued beams that were repaired using Wrapping Scheme 3. The top left photo is of Beam II-21, the top right photo is of Beam II-24, the bottom left photo is of Beam II-23, and the bottom right photo shows the pronounced vee-shaped crack on beam II-24 after the FRP was locally removed. The evenly spaced anchors greatly limited the size of FRP debonding areas at the time of failure. Failure in Beam II-21 occurred directly beneath the anchor stirrup, so no delamination was observed. The anchor stirrups confined the delamination on Beams II-22 and II-24 to within the 4*in* region between the transverse reinforcement.

Figure 118: Photos of fatigued Part II beams repaired using Wrapping Scheme 2 after failure

Figure 119 displays photos of the statically-failed fatigued beams that were repaired using Wrapping Scheme 3. The photo on the left is of Beam II-19 and the photo on the right is of Beam II-23. Again, the pronounced vee-shaped cracking is not prevalent in the fatigue-loaded beams, suggesting that a localized weakening of the bond layer may have still occurred between the anchor stirrups as a result of fatigue.

Figure 119: Photos of non-fatigued Part II beams repaired using Wrapping Scheme 3 after failure

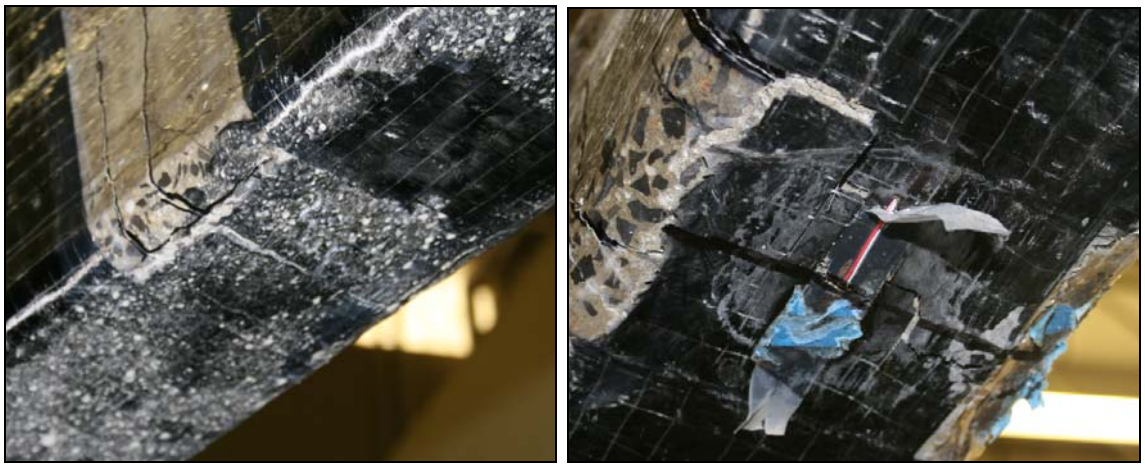

Figure 120: Photos of fatigued Part II beams repaired using Wrapping Scheme 3 after failure

Observations of the corroded unrepaired beams during static flexure testing were very interesting since the deterioration closely resembled that typically seen in the field, as shown in Figure 122 Figure 122, which depicts what was observed on the severely-deteriorated exterior girder of #49-4012-0250-1032.

Figure 121: Failure of Beam II-4

Figure 122 Figure Corroded exterior girder of PennDOT Bridge #49-4012-0250-1032

Another observation to note is the formation of a shear-flexure crack on most beams. This crack would begin on most beams as a flexure crack, and then begin to propagate at a 45º upward and toward the midspan as the load increased. Some examples of these shear-flexure cracks are displayed in Figure 123; from top to bottom are photos of Beams II-1, II-11, II-15, and II-21 respectively. Interestingly, these shear-flexure cracks were not observed in the corroded unrepaired specimens nor were they observed in the non-fatigued beams repaired with Wrapping Scheme 1 (they were observed on fatigued Scheme 1 beams). For beams repaired with Scheme 3, as in the bottom photo of Figure 123, multiple shear-flexure cracks were typically observed within the same region. The transverse FRP, however, appeared to terminate the growth of these cracks once they reached and propagated beneath the stirrups.

Figure 123: Typical shear flexure cracks observed on Part II beams

Figure 124: Composite action between old and new concrete on Part II beams as evidenced by cracking continuity across interface

After witnessing all the Part II static tests, it was determined that there was an excellent bond and composite action between old concrete and the polymer-modified repair-concrete. This is illustrated by the cracking seen in Figure 124. Cracks propagated across the interface of the two materials as if they were one material. Even in the shear spans where the patch material did not completely encase the steel, no horizontal cracking was observed along the interface and no debonding of the patch material was detected.

5.2.6 Results

Pristine beams performed slightly better than predicted by ACI guidelines. The accelerated corrosion process yielded a 13% decrease in failure load and a substantial 35% loss of service load capacity. As the corroded unrepaired beams were statically tested to failure, they had the appearance of deteriorated concrete bridge girders in the field. Longitudinal cracks grew, cover delamination occurred, and corroded rebar became exposed. Again, this substantiates the successfulness of the accelerated aging process as it simulated field conditions in a laboratory environment.

Beams repaired with Wrapping Schemes 1, 2, and 3 had service load capacities between 3 and 15% higher than that predicted by ACI design equations. The average failure load

for each group of the FRP-repaired beams was also higher than that of the pristine control samples of equivalent age. Although these equations are conservative immediately after repair, they may be somewhat non-conservative for long-term performance, as demonstrated in Part I.

No clear trend was observed in either failure or service load capacity as more anchorage was added, as was expected since flexural performance is not at all related to extent or quality of anchorage used in ACI's flexure FRP design. Cyclic loading did not appear to significantly affect the flexural strength capacity of the beams for any of the three schemes, and no clear trend in load capacity was detected as more anchorage was added. Duplicate FRP-repaired beams showed excellent consistency in service load capacity and deflection, as evidenced by the comparison tables and curves presented.

The extent of anchorage did not significantly influence the maximum service deflection, but the addition of evenly spaced anchors tended to reduce the failure deflection. For fatigued beams, the maximum service deflections were reduced as more anchorage was added. As expected, the corroded unrepaired beams yielded much higher deflections than did the pristine beams.

The accelerated aging process resulted in a 7% decrease in stiffness for unrepaired beams. The average post-cracking stiffness increased as more anchorage was added with the greatest increase between Schemes 2 and 3.

Pristine beams showed very uniform steel strains, but steel strains in repaired beams were more scattered. It could be seen that, although FRP repair did not significantly affect the maximum linear steel strain, it did tend to reduce the load at which the strain became non-linear. The maximum linear steel strain was also higher for fatigued beams than it was for non-fatigued beams.

The maximum linear FRP strains[1] were very similar amongst the three wrapping schemes, but the loads at which the linearity of the strain was terminated varied significantly. FRP strains tended to remain linear to a higher flexural load for beams with less anchorage.

Both the bonded and the embedded concrete gages provided very inconsistent strain data, which was likely due to the variable location of crack formation within the gage length on different beams.

All beams failed via some extent of crack-induced debonding and subsequent FRP rupture. It was found that FRP rupture was contained between the anchor stirrups for beams repaired with Schemes 2 and 3. Rupture of Scheme 2 beams occurred closer to the midspan than for Scheme 1 beams. Dramatic debonding occurred in unanchored Scheme 1, dramatic debonding occurred in Scheme 2 but was contained to between the anchors, and small areas of debonding occurred between anchors in Scheme 3.

It can be concluded that vee-shaped portions of concrete remaining adhered to the FRP coupled with bond failure at the FRP-concrete interface provides an indicative sign of crack-induced debonding. Pronounced vee-shaped notches were prevalently observed in all non-fatigued beams. The vee-shaped cracking was not nearly as prevalent in fatigued beams, although very small vee-shaped notches were still present on the concrete substrate. It is theorized that the fatigue loading weakened the epoxy-concrete interface within the constant moment region, and perhaps even caused some localized debonding. This yielded non-composite action between the FRP and the concrete, and the FRP failure was more due to direct tension than actual instantaneous crack-induced

[1] Please note that FRP strain is linear to rupture for direct tension coupon tests involving the FRP alone. However, when FRP is bonded to the concrete, the two materials behave compositely, resulting in a non-linear portion of the load-strain curve.

debonding. Contrary to hypothesis, the presence of shear-flexure cracks actually appeared to increase as more transverse stirrups were added.

Overall, the wrapping scheme did not appear to cause dramatic differences in overall performance. More anchorage was found to reduce the area of FRP debonding, but also to create a slightly stiffer reinforced concrete member. Cyclic loading seemed to shift the failure mode from instantaneous crack-induced debonding to weakening of the FRP-concrete interface and then tension failure of the FRP for all wrapping schemes. It is extremely important to note that, since all these beams were tested immediately after repair, that additional aging would very possibly yield widespread differences between the performances of the wrapping schemes. Additional corrosion on the three schemes could not be investigated in this research due to time constraints, but the results of Part I prove that additional aging definitely changes the performance of an FRP repair. It can be very easily hypothesized that more anchorage would provide a safer long-term repair.

5.3 ECE Technique for Chloride Extraction

5.3.1 Testing Protocol

The current study involves casting 6" x 8" x 78" (15.24 x 20.32 x 198.12cm) reinforced concrete beams with chlorides included within the concrete mix in the cover areas as shown in Figure 125. This casting scheme was selected to closely simulate an actual environment while coping with time constraints that prevented us from corroding the beams by natural means (i.e. exposure to saltwater). The top concrete cover does not contain chlorides, on the basis that actual bridge beams are connected to and protected by a deck slab. The concrete mix was produced with a w/c ratio of 0.6 to create weak, porous concrete similar to conditions found in deteriorated bridges. The beam size and reinforcement layout (shown in Figures 125 and 126) were selected to be the same as those shown in the previous section in order to correlate the results.

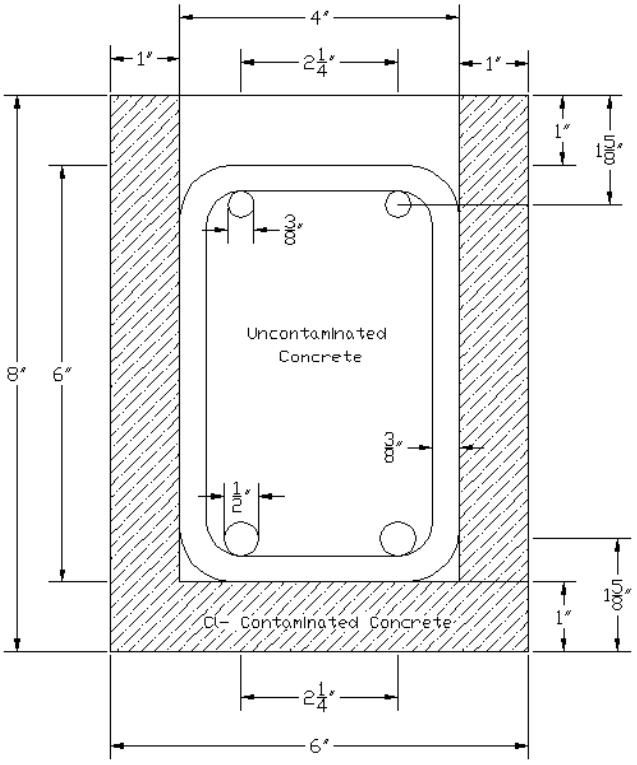

Figure 125: Beam Cross-Section (1" = 25.4mm)

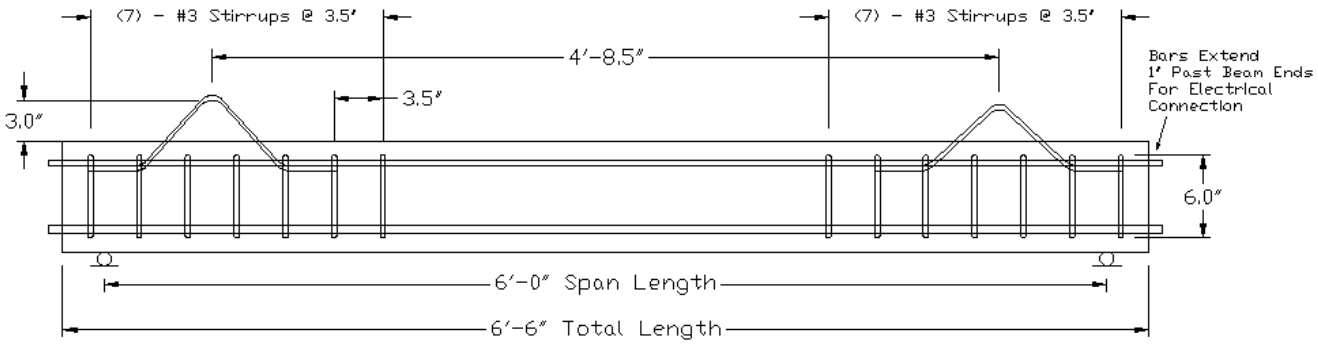

Figure 126: Beam Specimen (Profile Dimensions) to Show Reinforcement Layout (1" = 25.4mm)

The exterior concrete was contaminated with 5% NaCl by weight of cement, added during mixing (Note: 5% NaCl corresponds to 3.03% Cl). The two types of concrete within the cross-section were separated using two 1/8" thick stainless steel plates. The 78" long plates extended 7" downward into the forms, leaving the bottom 1" open for contaminated concrete to flow from the sides to the bottom 1". Utilizing two concrete mixers; one holding normal concrete and one with chloride contaminated concrete, the bottom 1" of concrete was poured first, followed by the simultaneous pouring of the remaining normal and contaminated concretes. Once each form was filled, the steel plates were removed, allowing the two types of concrete to adhere to one another before curing. Beams were removed from their forms after two days and moist-cured under wet burlap for 28 days before testing began.

A representative beam was selected to be used for concrete powder sample collection prior to testing; to serve as a baseline to compare with the results of the trial test. The samples were obtained using a drill with a ¼" diamond drill bit from extracted 2"-diameter cores. The powder samples were used to perform a chloride content analysis following ASTM designation C 1152/C 1152M-04; Standard Test Method for Acid-Soluble Chloride in Mortar and Concrete. The results are shown in Figures 127 and 128.

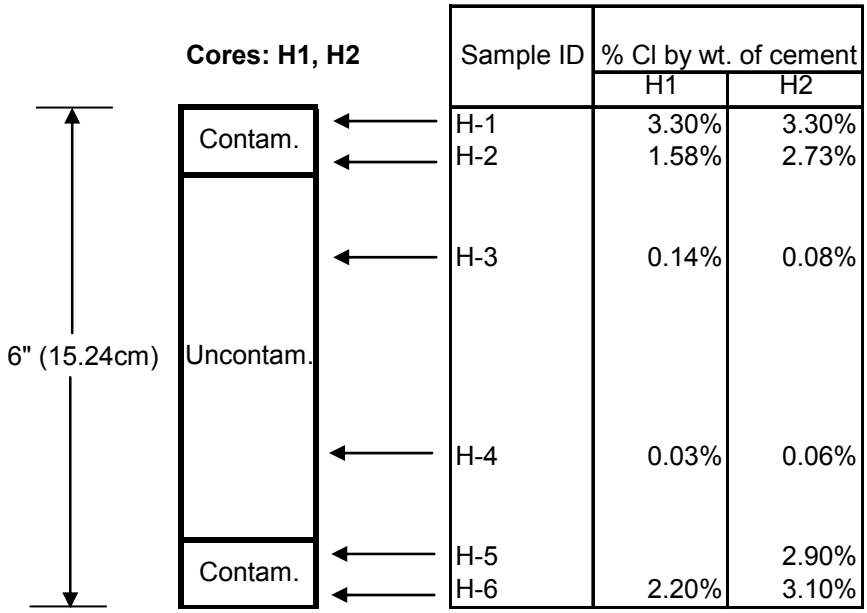

Sample ID	% Cl by wt. of cement	
	H1	H2
H-1	3.30%	3.30%
H-2	1.58%	2.73%
H-3	0.14%	0.08%
H-4	0.03%	0.06%
H-5		2.90%
H-6	2.20%	3.10%

Figure 127: Chloride Analysis Results – Horizontal Cores H1 and H2

Horizontal cores were taken from the midspan, through the cross-section of the beam. The horizontal core samples provided promising results, showing a maximum chloride content of 3.30% by weight of cement at the exterior with lower values near the contaminated/uncontaminated interface as expected. The traces of chloride found in the uncontaminated region were consistent with expectations for the concrete mix produced with tap water. The cores also displayed a perfect bond between the two concrete types.

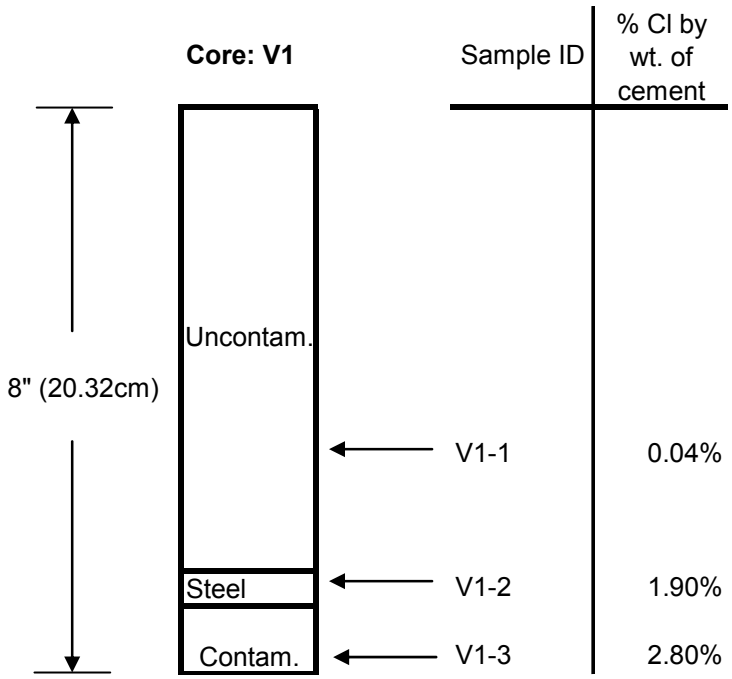

Figure 128: Chloride Analysis Results - Vertical Core

Data from the vertical cores also produced approximately the anticipated results, with similar relationships as the analyses for the horizontal cores: maximum chloride near the estimated 3.03% designed in the mix, with less near the interface and negligible within the uncontaminated region.

5.3.1.1 Beams without FRP Wrapping

The ECE was performed on three beams without FRP wrapping at a high current density of 2 A/m^2 (of steel area) and terminated after 600 A*hr/m^2. The photographs of Figure 129 illustrate the test setup. Spots of brown, rusty staining were observed on samples in the electrolyte after only a few days of current, indicating that the ECE was working properly. Electrical continuity on all beams was routinely checked using a clamp meter capable of reading to the nearest 0.1A, and the electrolyte (tap water) was replenished daily using irrigation drip lines embedded in the anolyte media (wet cellulose fibers). After achieving a cumulative current density of 600 A*hr/m^2, concrete powder samples were drilled. Samples were taken with a ¾" concrete masonry bit and hammer drill,

greatly simplifying the collection process. Samples were analyzed in the chemical laboratory, and the results of the chloride analysis are given in Table 20:

Table 20: Chloride Analysis Results – Trial Test

Sample ID	Sample Location	Sample Depth	% Cl by wt. of cement
1	Side A	0 - 1/2" (12.7mm)	1.42%
2	Side A	0 - 1/2" (12.7mm)	1.20%
3	Side B	0 - 1/2" (12.7mm)	0.71%
4a	Bottom	0 - 1/2" (12.7mm)	0.53%
4b	Bottom	1/2 - 1" (12.7 - 25.4mm)	0.30%
5a	Bottom	0-1/2" (12.7mm)	0.61%
5b	Bottom	1/2 - 1" (12.7 - 25.4mm)	0.59%
6	Bottom	0 - 1/2" (12.7mm)	0.70%
7	Bottom	0 - 1/2" (12.7mm)	0.72%

All samples were drilled from the same beam. All bottom samples were taken at locations 8” (20.32cm) from the beam ends, directly below the steel, and side samples were taken near the beam midspan, midway up the cross-section. The results indicated that over 50% of chlorides were removed from the beam sides, and over 75% (on average) were removed from the bottom.

(a) Beam Configuration Details

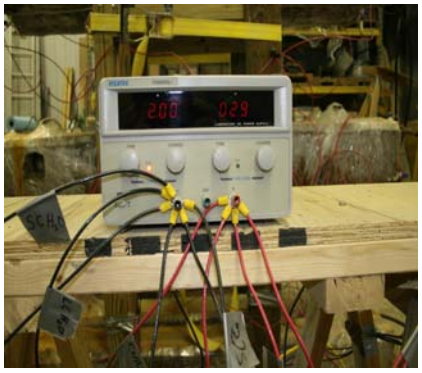

(b) DC Power Supply

Figure 129: Photographs of Test Setup

5.3.1.2 Beams with FRP Wrap

The FRP wrapping scheme is shown in Figure 130, with a single longitudinal strip running along the bottom of each beam and two strategically placed U-wrap anchors. Two beams were treated with different types of electrolyte: tap water for Beam 1; and a mixture of tap water and 5g/L of calcium hydroxide for Beam 2.

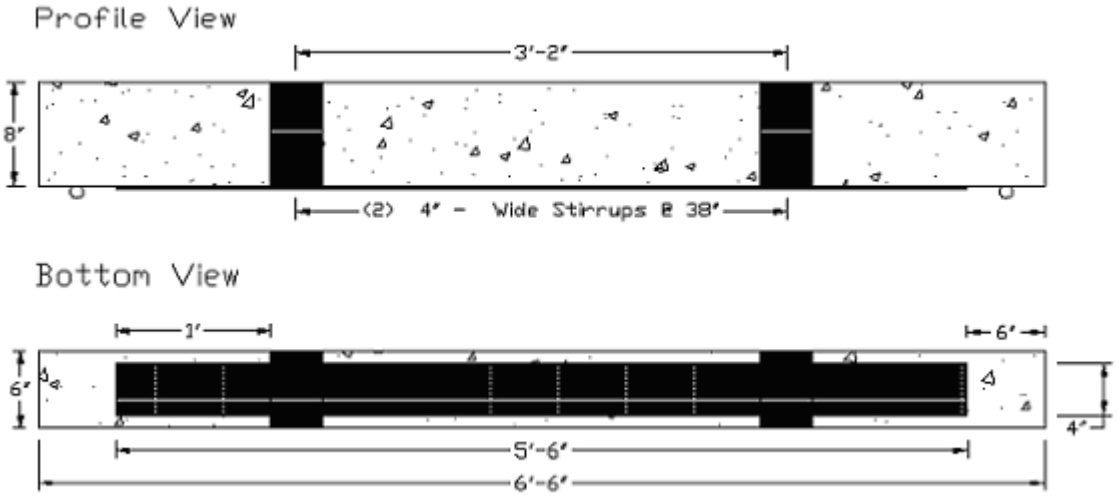

Figure 130: FRP U-wrap Anchoring Scheme (1" = 25.4mm)

ECE was performed on the two beams for a cumulative current density of 600 A*hr/m^2 of embedded steel area; the established termination time of the process. The beams were sampled using a hammer drill and 1" masonry bit. At each sample location, two samples were taken. The first sample was from the concrete surface to ½", and the second was from ½" to 1" into the cross-section. Three holes were made on the side and bottom of each beam in identical locations, totaling six holes for 12 samples per beam. Side samples were taken through the FRP, next to the FRP, and in the middle of the side. At the bottom, samples were drilled through and next to the FRP near its termination point, as well as in the middle of the beam. The figure below outlines the sampling locations, which are numbered from left to right for each beam face.

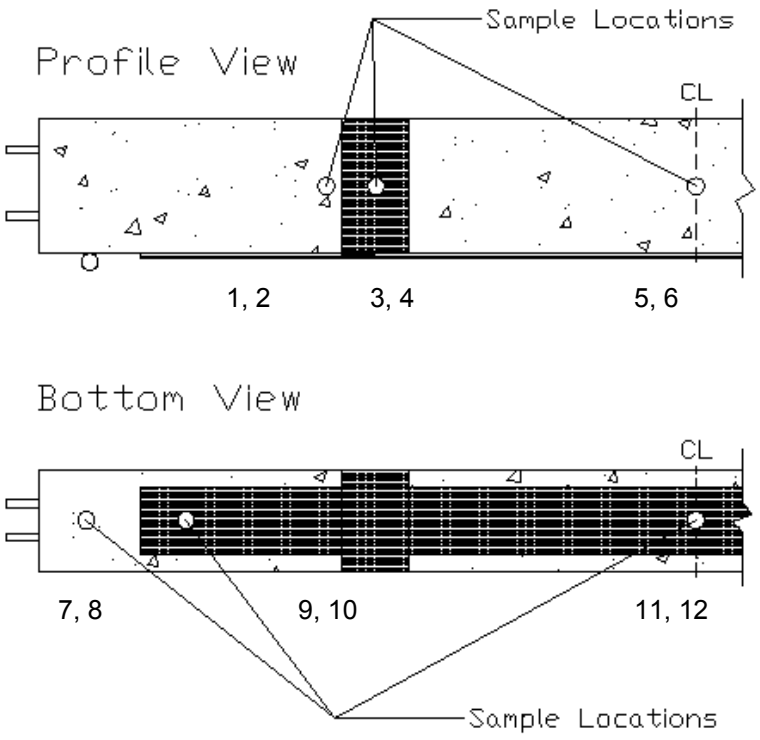

Figure 131: Sampling Location Detail

Based on the sample locations shown in Figure 131, the results of the laboratory chloride analysis are displayed in Table 21. They are in relative values, using the amount of chloride ion extracted at locations 5 and 6 as base values (100%), which can be interpreted as extraction effectiveness.

Table 21: Extraction Effectiveness at Different Locations

Location	Sample ID	Sample Depth	Relative Cl Removal, %, Beam 1	Relative Cl Removal, %, Beam 2
S-M	1	0 - 1/2" (12.7mm)	85%	62%
S-M	2	1/2 - 1" (12.7 - 25.4mm)	96%	100%
S-Next to FRP	3	0 - 1/2" (12.7mm)	33%	62%
S-Next to FRP	4	1/2 - 1" (12.7 - 25.4mm)	98%	81%
S-Through FRP	5	0 - 1/2" (12.7mm)	100%	100%
S-Through FRP	6	1/2 - 1" (12.7 - 25.4mm)	100%	100%
B-M-Through FRP	7	0 - 1/2" (12.7mm)	122%	122%
B-M-Through FRP	8	1/2 - 1" (12.7 - 25.4mm)	98%	108%
B-E-Through FRP	9	0 - 1/2" (12.7mm)	122%	16%
B-E-Through FRP	10	1/2 - 1" (12.7 - 25.4mm)	108%	100%
B-E Next to FRP	11	0 - 1/2" (12.7mm)	133%	91%
B-E Next to FRP	12	1/2 - 1" (12.7 - 25.4mm)	108%	104%

From Table 21, it can be observed that:

(1) Locations between 0” to 0.5” immediately behind FRP were significantly affected, with extraction effectiveness of 33% for Beam 1 and 62% for Beam 2. Locations between 0.5” to 1” were not affected too much.
(2) Locations next to FRP were also affected, but not as significantly as those locations directly behind FRP.
(3) FRP has not effect on chloride extractions at the bottom of the beams, indicating that the ions move horizontally to the exposed side surfaces.
(4) It seems that tap water was more effective for bottom extraction, whereas solution with calcium hydroxide was more effective for side extraction.

Based on this exploratory study, it seems that ECE technique can be effectively used to extract chloride ions for concrete beams with and without FRP wrapping. Since the chloride ions will accumulate directly behind FRP within 0” to 0.5”, the number of U-wraps should be limited. It is recommended that further study be conducted on this topic to optimize the combination of ECE and externally bonded FRP wrap repair methods.

Task 6 Guidelines for Project Selection and Management

Guidelines and recommendations are needed for the effective implementation of surface bonded FRP on concrete T-beam bridges. This section of the report describes guidelines for project selection and management. The guidelines for project selection include procedures for determining suitable T-beam bridges for FRP retrofit and the level of FRP-repair needed, and the guidelines for project management include procedures for effective bidding, contracting, and overall management.

6.1 Project Selection

The importance of selecting a bridge that would benefit from repair with surface-bonded composites is inherently obvious. Along with a proposed FRP repair project, the extensiveness of the repair needs to be defined so that the scope of work can be foreseen and allow for proper management decisions.

6.1.1 Suitability for FRP Repair

Suitability for FRP repair shall be determined either based on level of damage as described in Section 6.1.1.1 or bridge classification from Section 6.1.1.2. A suitability analysis based on level of damage may only incorporate field inspections, whereas a suitability analysis based on bridge classification shall incorporate a number of classification categories as introduced in Section 6.1.1.2.

6.1.1.1 Assessment based on Level of Damage

Level of damage shall be considered as the primary factor in determining the suitability for FRP repair. Deck and sub-structure shall be evaluated for a cost-benefit analysis to determine whether FRP repair is a viable method. Inquiries such as the following should be completed based on the field assessment to determine the level of damage.

- The availability of bridge plans and the level of confidence that the plans agree with the as-built conditions;
- Area-specific damage as opposed to global damage;
- Adequacy of concrete cover;
- Type of aggregate within the structure;

- Deck and substrate unit condition;
- Chloride-ion content or amount of visible efflorescence; and
- Any issues observed that may inhibit the proper installation of the FRP system, such as accessibility.

6.1.1.2 Assessment based on Bridge Classification

This section discusses the procedure for classifying bridges as being suitable for FRP repair. The classification is based on relevant criteria such as the condition of the bridge and various bridge inventory parameters. In assessing the condition of the bridge, photographic indication of damage is assessed. Bridge inventory parameters used in the classification include: age, span length, ADT/ADTT, functional class of highway the bridge serves, and the bridge capacity appraisal. For each of these characteristics, scores are assigned based on favorability for repair. Each score (generally 1-10) is assigned in an attempt to place bridges into one of three classes that represent the potential for repair. These classes are as follows: prime (class #1) – greatest potential; moderate (class #2) – medium potential; and low (class #3) – least potential.

6.1.1.2.1 Condition of the Bridge

6.1.1.2.1.1 Photographical Evidence of Damage

For the purpose of classification, damages indicated by photographical evidence are scored into the following rating categories: 3, 2, 1, and 0. Based on NCHRP Report 514 pages I-12 thru I-13 and a journal article by Kutarba et al. (2004), bridges should be evaluated based on the similarity in damage when compared to those damages described in the literature. This is illustrated in Appendix A, in which examples are provided.

Bridges that receive a rating of 3 are possibly prime candidates for repair. Bridges that receive a rating of 2 may be candidates for repair; however, field inspection is strongly suggested to determine if the damage on these bridges is suitable for repair. Bridges with a rating of 1 are either not likely candidates for repair based on the photographical evidence, or the photographical evidence may be unclear in regard to the damage. Bridges with a rating of 0 are, judging by photographical evidence, either not requiring any repairs or not applicable for repairs.

For numerical scoring of the bridges, each bridge with a rating of 3 receives a score of 10, while each bridge with a rating of 2 receives a score of 6.67. Each bridge with a rating of 1 receives a score of 3.33, and finally, all bridges with a rating of 0 receive a score of 0, as shown in Table 22.

Table 22: Score Based on Photographical Evidence

Rating	Score
3	10
2	6.67
1	3.33
0	0

6.1.1.2.2 Bridge Inventory Parameters

6.1.1.2.2.1 Age

For the purpose of classification, the ages of the bridges are assigned a rating of 1 through 10, where a bridge with a rating of 10 is most favorable for repair and a bridge with a rating of 1 is least favorable for repair. Older bridges are rated lower in this category because these bridges are closer to their designed life-span. Also, due to the factor of age and/or global deterioration of the bridge, replacement rather than repair may be the most economical alternative. The scores are assigned for each age category following Table 23. This table assumes that all bridges were built under the same condition. If any special treatments, such as epoxy-coated rebar, corrosion inhibitor, etc., were included, the bridge should be evaluated separately based on Section 6.1.1.1.

Table 23: Score Based on Age

Age Category	Score
1955-1973	10
1950-1954	9
1944-1949	8
1942-1945	7
1940-1941	6
1935-1939	5
1930-1934	4
1925-1929	3
1920-1924	2
Older than 1920	1

6.1.1.2.2.2 Span Length

For the purpose of classification, the span lengths of the bridges are assigned a rating of 1 through 10 as shown in Table 24, where a bridge with a rating of 10 is most favorable for repair and a bridge with a rating of 1 is least favorable for repair. Because of the similarity in beam size and spacing, a longer span will experience more critical loads than a shorter span. Hence, a longer span is more favorable for repair because of strength concerns. Also, longer bridges are inherently more costly for replacement. The repair cost effectiveness is assumed to be more favorable for longer bridges.

Table 24: Score Based on Span

Span (ft)	Score
80+	10
60-79	9
50-59	8
45-49	7
40-44	6
35-39	5
30-34	4
25-29	3
20-24	2
Less than 20	1

6.1.1.2.2.3 ADT and ADTT

For the purpose of classification, the ADT and ADTT (average daily traffic and average daily truck traffic respectively) of the bridges are assigned a rating of 1 through 10, where a bridge with a rating of 10 is most favorable for repair and a bridge with a rating of 1 is least favorable for repair, as shown in Table 25 and Table 26. A bridge which is carrying more volume of traffic is more favorable for repair than a bridge that does not carry much traffic at all. Because of limited resources, it is more sensible to repair bridges that are used more frequently. Also, with the increase of truck traffic, the probability of carrying future critical loads increases.

Table 25: Score Based on ADT

ADT	Score
10,000 +	10
5,000-9,999	9
3,000-4,999	8
2,500-2,999	7
1,500-2,499	6
1,000-1,499	5
500-999	4
300-499	3
150-299	2
Less than 150	1

Table 26: Score Based on ADTT

ADTT	Score
1,000 +	10
500-999	9
400-499	8
300-399	7
200-299	6
100-199	5
75-99	4
50-74	3
25-49	2
Less than 25	1

6.1.1.2.2.4 Functional Class of Highway

The functional class of highway that the T-beam bridge serves is an important aspect to consider when determining suitability for repair with externally bonded FRP. The point system for classifying a bridge based on functional class is presented in Table 27. Bridges serving a functional class with a rating of 10 shall be more favorable for repair whereas a bridge serving a functional class of 1 is least favorable for repair.

Table 27: Score Based on Functional Class of Highway

Functional Class of Highway	Score
Interstate	10
Principal Arterial	8
Minor Arterial	7
Major Collector	5
Minor Collector	4
Local	2
Other	1

6.1.1.2.2.5 Bridge Capacity Appraisal

The appraisal of the load capacity of the bridge, as detailed in Publication 100A BMS2 Coding Manual, shall be considered important in determining a bridge's suitability for FRP repair. The bridge capacity appraisal is determined by evaluating the load capacity of the bridge in comparison with the state legal load; this is similar to a bridge superstructure rating. Substructure ratings are not considered. In this system, a bridge's load capacity is compared to the legal load by using the ratio of the actual load capacity to the legal load. A coding system is developed which classifies the ratios for easy referencing. This coding system and corresponding ratios of load capacity to legal load capacity are presented in Table 28 in accordance with the Coding Manual.

Table 28: Bridge Capacity Appraisal Coding System

Code	Capacity % above or below Legal Load	Lowest Ratio
9	31% or more above	1.31 or more
8	21-31% above	1.21-1.30
7	11-20% above	1.11-1.20
6	1-10% above	1.06-1.10
5	Equal to legal loads	1.00-1.05

4	0.1-9.9% below	0.91-0.99
3	10.0-19.9% below	0.81-0.90
2	20.0-29.9% below	0.71-0.80
1	30.0-39.9% below	0.61-0.70
0	>39.9% below	0.60 or less

As the intent of this scoring system is to rate T-beam bridges as being suitable for FRP repair, those with a bridge capacity appraisal code of 0 (ratio of 0.6 or less) will not be included, since replacement rather than repair would be more logical. Based on the bridge capacity appraisal coding system, a coding is assigned to a score as indicated in Table 29. A high score of 10 shall signify more favorability for FRP repair, while a lower score such as 2 shall signify less favorability for FRP repair.

Table 29: Score Bases on Bridge Capacity Appraisal

Bridge Capacity Appraisal Code	**Score**
1 - 4	10
5	8
6	6
7	4
8 or 9	2

6.1.1.2.2.6 Function Obsolete Bridges

For function obsolete bridges, other assessment, such as road width assessment, shall be made to determine whether FRP repair is a viable solution.

6.1.1.2.3 Weighted Values for Classification

In order to aid in the selection of bridges for further evaluation and potential for FRP rehabilitation, the scores assigned for each characteristic as detailed in Section 6.1.1.2 are tabulated and averaged based on weighted averages. Each characteristic is weighted as follows:

1. Photographic Indication of Damage (40%)
2. Age (10%)
3. Span Length (6%)
4. ADT/ADTT (20%) (10% & 10%)
5. Functional Class of Highway (12%)

6. Bridge Capacity Appraisal (12%)

6.1.1.2.4 Class Assignment

Once a total score is calculated, the bridges are classified into three tentative groups for visitation. Visitation is necessary for re-evaluation of visual damage provided by available photographs. The visual damage ranking performed from photographic indication may be modified upon a more thorough visual inspection. Typically, photographs only illustrate local damage whereas visitation can give more insight into the overall damage of a bridge.

Class 1: Prime Candidate for Repair (Score of 68-100%). This set of bridges is likely a prime candidate for FRP retrofit technology. Field investigation is suggested for the following purpose: On some of these bridges, the damage may be so severe that the most economical course of action may be to replace these structures.

Class 2: Moderate Candidate for Repair (Score of 50-68%). These bridges are likely candidates for repair. However, field investigation of these bridges is suggested to closely examine the type and extent of damage, as well as the cost-benefit of applying FRP technology to these bridges.

Class 3: Low Candidate for Repair (Score of 0-50%). Because of age, size, level of traffic, damage type or lack of damage, these bridges are not the prime focus for FRP retrofit technology. Some of these bridges may benefit from FRP technology, but these bridges may not be the most economical choice for this type of repair.

The breakdown of bridge class ratings is shown in Table 30. Appendix A provides examples. Appendix B provides a form that can be filled out to calculate the total score percentage for class rating purposes.

Table 30: Class Rating

Rating	Score
Class 1	68-100%
Class 2	50-68%
Class 3	0-50%

6.1.2 Level of Repair

Analysis, design and specification of the repair can be performed either by an outside consultant/contractor, or in-house by District personnel. Depending on the overall scope of work, the FRP-repair may be defined at three levels: (1) major, with all work contracted out; (2) moderate, with combined outside consultant and in-house personnel; and (3) minor, with all work accomplished in-house.

6.1.2.1 Level 1 (Major)

This level addresses a bridge requiring extensive FRP repair. At this level the engineering is performed by a consultant and the actual repair is contracted out through competitive bid.

The preparatory concrete work and application of the surface bonded FRP would be performed per project specifications and construction drawings. It is expected that the overall scope of work may include other pay items such as abutment repair, bearing repair, and possible expansion joint repair. While the application of the FRP may represent a smaller portion of the overall project cost, the scale of the project can offer sufficient opportunities for developing expertise with FRP technology.

As a result of the significant damage of such structures that fall within this level of repair, the use of FRP for additional strengthening is possible, such as in areas deficient in shear or areas that require confinement of reinforcing steel due to low cover or inadequate splice length.

6.1.2.2 Level 2 (Moderate)

This level of repair addresses a bridge showing moderate levels of damage. A combination of work performed by District forces and some contracting through specialty trades or engineering by a consultant is suggested.

Most field activities can be accomplished by District forces. However, because there may be a need for injecting cracks with either epoxy or urethane, or the overall cost may

exceed allocated District limits, it may be necessary to advertise portions of the project for competitive bids. Several possibilities could be explored, such as: (1) retaining a consultant for the engineering portion and using District forces for labor (possible in phases); (2) performing the engineering in-house and contracting out the specialty items (crack injection or application of the FRP), with District forces acting as a general contractor; or (3), performing the engineering in-house and contracting out the field work.

6.1.2.3 Level 3 (Minor)

This level should address bridges with minor to moderate levels of damage. In general, a structure with moderate and localized damage should be considered a likely candidate for the implementation of any new repair technology.

At this level the anticipated scope of work, although detailed, is small and it is realistic to assume that the District could accomplish this using in-house engineering and District forces. Funding for this type of maintenance construction is realistically within the limits of a District force account.

A repair project at this scale will aid in further training personnel and evaluating FRP-repair technology. Experience gained at this level can be built on to better understand the complexities associated with moderate and major FRP-repair bridges.

6.2 Management Considerations

Given the complexities of repair projects incorporating the use of surface-bonded composites, much attention has to be devoted to overall management. The success of a project is closely related to the implementation of effective bidding, contracting, and project management.

6.2.1 Bidding

To develop adequate bidding practices for an FRP retrofit project, all protocols for effective technology implementation and work completion will need to be considered.

The appropriate sections of existing guidelines, standards and published documents, and acceptance by District engineers are to be followed when performing concrete and steel repairs; surface preparations and installation of FRP systems; acceptance of testing requirements and inspections; and provisions for authorizing rework and repairs. Guidelines relating to the aspect of concrete and reinforcement steel repair, surface preparation, and installation of FRP are given in the construction specifications. Every stage of the work requires approval from the engineer of record. Depending on in-situ findings, the contractors or applicators may suggest some necessary changes to these proposed guidelines if needed.

With the added qualifications needed from the materials, manufacturer, and applicator for an FRP repair project, top bids may best be chosen by considering price estimates and a technical score. The technical score shall be closely related to the mandatory qualifications specified before the start of a project. Along with qualifications, such aspects as construction management practices and safety plans can be evaluated and included within the technical score. In this way, many important aspects other than price estimates will be included in determining the winning bid.

6.2.1.1 Quantities/Payment Method

Material quantities and payments for construction processes can be defined by the following method:

- Substrate repair, consisting of removal of unsound concrete, sandblasting, cleaning of reinforcement and concrete, placing new concrete, surface preparations, and any other supplementary work by lump sum;
- Epoxy injection for crack repair by the linear meter/foot of the injected cracks;
- Supply and placement of corrosion inhibitors by the square meter/foot of concrete surface;
- Supply and placement of the wet lay-up FRP system by the square meter/foot of each layer applied;

- Supply and placement of the precured FRP system by the square meter/foot of each layer applied and accounting for different layer thicknesses;
- Supply and placement of the protective coating for the FRP system by the square meter/foot of each coating layer applied.

Various aspects shall be given special consideration. FRP roll width may not be the same for different suppliers, but the typical width varies from 20 to 24 in. Commonly, upon removal of concrete, additional deteriorated areas may be located that require more undercutting and repair of the substrate and reinforcement. The contractor may be required to obtain approval from the Chief Engineer before extending the limits of concrete removal beyond that which is clearly specified in the contract documents.

6.2.1.2 Submittals

To adequately bid on FRP retrofit projects, it is important that the contractor submit all required documentation as specified herein. Documentation should include but not be limited to: working drawings, quality assurance and quality control plans, and qualifications. The contractor shall submit all required documentation for approval before starting the work.

6.2.1.2.1 Working Drawings

Working drawings may contain the type of FRP system and the plan of work along with the relevant pre-preparations of the existing structure. Along with the shop drawings, the manufacturer's system data sheets identifying mechanical, physical, and chemical properties of all components of the FRP system; design calculations, and all relevant MSDS should be included. Also, an application guide presenting the installation and maintenance procedures and a time schedule for various portions of the repair process should accompany the drawings. The procedure for installation must clearly recognize the environmental and substrate conditions that may affect the application process.

The necessary information for each FRP system can be different. As an example, shop drawings for wet lay-up systems can include such details as: fiber orientation, nominal

thickness, number of layers, fiber volume fraction, weight fraction, location and length of lap splices, weight per unit area of dry fabric, end arrangements, and anchoring.

6.2.1.2.2 Quality Assurance and Quality Control Plans

A comprehensive quality control and quality assurance (QC/QA) plan should be implemented that covers all aspects of the FRP-repair project. The plan should consist of a complete set of inspections and tests to determine the acceptability of construction tasks performed. Details of the plan may be developed to conform to the size and complexities of a given project. A pre-installation meeting between the owner and the contractor is recommended for development and approval. The contractor shall have a preliminary plan, at the time of the meeting, to evaluate for further discussion and detailing.

The contractor may be largely responsible for the processes and materials associated with a given project. The District must approve any QC and QA plan. Any aspect of work that does not comply with the requirements set forth in the contract documents may be rejected by the project engineer and replaced or corrected at the contractor's expense in order to comply fully with the contract documents. Included in these documents may be the following: personnel safety procedures, tracking and inspection of all FRP components before installation, inspection of all prepared surfaces prior to any material application, inspection during various stages of the work to ensure compliance with specifications, QA sampling, inspection of any completed work for approval including possible testing and test results, and clean-up.

6.2.1.2.3 Qualifications

The manufacturer or supplier should be considered to be prequalified for a project only after all required information has been submitted for review and has been accepted. The information that is required from the manufacturer or supplier can vary with project size and complexities and with District expectations. Recommended information to be received from a given manufacturer or supplier as presented in NCHRP Report 514 (2004) is as follows:

1) System data sheets and Material Safety Data Sheets (MSDS) information for all components of the FRP system;
2) A minimum of 5 years of documented experience or 25 documented similar field applications with acceptable reference letters from respective owners;
3) A minimum of 50 test data sets (total) from an independent agency approved by the owner on mechanical properties, aging and environmental durability of the system; and
4) A comprehensive hands-on training program for each FRP system to qualify contractors/applicators.

The contractor or applicator should be prequalified for a project only after all required information has been submitted for review and has been accepted. As with required information from the manufacturer or supplier of the technology, the required qualifications for the contractor or applicator may vary with project size or complexities and with District expectations. Recommended information to be received from a given contractor or applicator as presented in NCHRP Report 514 (2004) is as follows:

1) A minimum of 3 years of documented experience or 15 documented similar field applications with acceptable reference letters from respective owners, and
2) A certificate of completed training from the manufacturer/supplier for at least one field representative who will be present on site throughout the project.

6.2.2 Contracting

The method in which contracting is performed should correspond to the level of repair associated with a given FRP rehabilitation project. This level of repair is based on overall damage and is categorized into three repair levels: repair level 1 (major), repair level 2 (moderate), and repair level 3 (minor). A large-scale repair (repair level 1) is most likely contracted out to a 3rd party company, whereas a small-scale repair (repair level 3) could be performed by a trained, "in-house" work force. Bridges that fall between these two ranges (repair level 2) could be repaired via a joint effort between a contractor and Department forces. For any given case, the selected contractor or District personnel shall subcontract the technology/material supplier. An outside consultant, such

as a university research team, could be used in an enhanced effort to provide higher levels of quality control and assurance, with the quality assurance aspects being the most important. This can also promote continued education and research while incorporating knowledge from both industry and academia.

Because of the nature of FRP repair, any possible defect cannot be observed from outside once the FRP installation has been completed. This makes QA even more important during the FRP installation. Therefore, the authors suggest a third-party consultant be hired to oversee the repairing process. It can be any qualified party, and one example is a university team. The advantage of the university team is that such a team may be more experienced and knowledgeable and well equipped to perform the testing needed for proper QA for this relatively new repairing technique.

6.2.2.1 Contract Items

Contract items for FRP retrofit projects will include any number of items commonly incorporated in normal highway construction projects. Items more specifically related to FRP strengthening projects shall include, but not be limited to, the following:

- Temporary Support and Protection System
- Repair of Deteriorated Concrete
- Construction Restrictions
- Maintenance and Protection of Traffic during Construction
- Cement Concrete Modified (Class AA – Class AAA)
- FRP Repair of Concrete T-Beam
- Removal of Portion of Existing Bridge
- Reinforcement Bars Epoxy Coated
- Epoxy Injection Crack Seal

Items to be placed within a contract may include sub-sections on details relating to general work description, materials, construction aspects, design, qualifications, and measurement/payment. Reference to relevant documentation such as Publication 408, ACI, ICRI, etc. shall be stated accordingly.

6.2.2.1.1 Temporary Support and Protection System

Contained within this section should be a detailed description of the design, furnishing, installation and removal of a temporary support and protection system for the existing superstructure and deck.

Material should be provided as approved by the Project Manager and as specified by a Professional Engineer registered in the Commonwealth of Pennsylvania. Materials provided should also be in accordance with salvage design values from AASHTO Guide Design Specification for Bridge Temporary Works for used steel.

Design of the temporary support and protections system should be in accordance with AASHTO LRFD Bridge Design Specifications and Design Manual, Part 4 Specifications, current FHWA guidelines and AASHTO Guide Spec. The design should be analyzed for final conditions and all construction conditions. Sets of design calculations and completed detail drawings should be submitted for review. Calculations and drawings should include all material properties, design loads, and design assumptions. Submissions should be made with allowance of sufficient time for review.

Installation of the temporary support and protection system should be performed in accordance with the applicable sections of Publication 408. This work should be undertaken with coordination to the construction and removal of any bridge sections as indicated.

As for qualifications, the work must be supervised by a superintendent or foreman who is experienced in the construction of the temporary support and protection system proposed. Lists of previous projects should be submitted as deemed necessary.

Measurement and payment shall be taken as lump-sum.

6.2.2.1.2 Repair of Deteriorated Concrete

Contained within this section should be a detailed description for repairing the spalled and deteriorated concrete areas.

Materials to be used should be listed with adequate descriptions along with reference to all necessary documentation such as ASTM standards and Publication 408. Such materials can include types of modified concretes, admixtures, and steel.

Construction aspects should be described in much detail. The extent of all repair areas should be clearly presented. It should be clear that all necessary precautions need to be taken in order to not damage existing structural components. If undesirable damages do occur, they should be repaired to the satisfaction of the Project Manager. All exposed reinforcement and exposed inner concrete surfaces should be cleaned as specified. The details of the construction process should be well organized.

Equipment to be used should be described in detail along with any restrictions to be placed on such use of equipment.

Measurement and payment shall be taken by the square foot. Specific items of the construction that are to be paid separately shall be stated.

6.2.2.1.3 Construction Restrictions

Contained within this section should be a well organized list of all requirements placed on the contractor. This list should include, but not be limited to, various aspects such as the following: deadlines, responsibilities, submittals, requests, and record keeping.

6.2.2.1.4 Maintenance and Protection of Traffic during Construction

All requirements and limitations of the traffic control plan should be clearly stated within this section. Referral to Publication 408 may be necessary to provide the contractor with required information to achieve the highest standards of traffic control.

6.2.2.1.5 Cement Concrete Modified (Class AA – Class AAA)

This section should contain all requirements and construction uses for the type of modified concrete specified. Curing materials and admixtures along with any limitations should be well documented. More thorough descriptions can be made available by properly referencing corresponding sections of Publication 408.

Details to be placed on the construction process should be well documented. These details should include, but not be limited to, aspects relating to the following: curing, protection, temperature recordings, falsework and forms, and quality control. Corresponding sections of the ACI Manual of Concrete Practice should be referenced accordingly.

6.2.2.1.6 FRP Repair of Concrete T-Beam

This section should present information on designing, furnishing, and installing the FRP system for the damaged areas as specified.

Types of materials to be used and any restrictions should be addressed. The material suppliers and their contact information should be listed. Any mandatory qualifications for a selected repair system such as any number of successful, previous repairs should be stated. Mandatory qualifications and submittals required by the proposed Project Manager should be described as well. The manufacturer must indicate a chosen system's compliance with environmental durability requirements such as those of ICBO AC 125. ICBO Evaluation Services, Inc. (ICBO ES) is a leading source of information on building codes, building products, and building technology. This is a subsidiary corporation of the International Corporation of Building Officials. A nonprofit corporation, ICBO ES does technical evaluations of building products, components, methods, and materials. ICBO AC 125 is acceptance criteria for concrete and reinforced and unreinforced masonry strengthening using fiber-reinforced polymer (FRP) composite systems. The system needs to have been satisfactorily tested to any such requirements. If warranted, evidence of similar successful tests other than those prescribed by ICBO AC 125 may suffice.

All specified documentation to be used in designing and constructing the repair system should be presented. The newest addition of the ACI 440.2R should be adhered to. The objective of the design should be clearly stated. For example, the objective may be to restore the section to achieve a specified ultimate flexural and shear strength. Also, the FRP repair may need to be designed at working stress levels for fatigue stress ranges produced by a specified loading. Requirements, if any, of an acceptable stress-strain model for the reinforced concrete compression zones should be described. The desire for ductile behavior of the beams needs to be considered in the design.

Submittals to be received by the Department should be stated along with corresponding deadlines for the submittals, as they require adequate time for review. Such submittals include: information concerning the prequalified system to be used, design calculations, signed and sealed working drawings, and detailed installation procedures.

A proper installation plan shall include, but not be limited to, the following: general procedures, product delivery, storage and handling, all aspects of surface preparation, restrictions, repair of defective work, and quality-control measures. It should be made known that the contractor is to provide the Department with all maintenance and inspection requirements for the installed system.

The construction of the FRP system should follow strict guidelines. If more stringent requirements are imposed by the system manufacturer, those requirements will govern. The construction of the FRP system will include, at a minimum, the following work items:

- Deteriorated or damaged concrete removal;
- Cleaning of reinforcement;
- Surface preparation;
- FRP installation;
- Inspection and acceptance criteria; and
- System protection.

Measurement and payment shall be taken as lump-sum. This lump-sum amount will include the complete cost for the design, manufacture, and installation. It should be made clear that any repairs to correct insufficient bond, lack of cure or other deficient work are to be made at no additional cost to the Department.

6.2.2.1.7 Removal of Portion of Existing Bridge

Removal of portions of the existing bridge is a common part of the repair process due to the presence of spalling and defected concrete as a result of reinforcing steel corrosion. Removal of portions or all of concrete T-beams (essentially replacing the entire beam) and other bridge components such as any parapets or barriers is applicable. Barriers may need to be removed to provide access for concrete restoration on exterior beams. In general, a plan for concrete bridge portions removal shall be submitted during the pre-construction conference.

Concrete removal shall be in accordance with construction specifications, with removal being performed to a minimum of 3/4" beyond the existing reinforcing steel or ¼" larger than the largest aggregate used in the repair material, whichever is greater, as stated by ICRI 03730. This section shall contain the general restrictions as to the extent of bridge removal that can be made before the passage or transport of construction equipment on the bridge is prohibited. All defective material obtained during the removal process shall be removed from the project site in accordance with construction specifications and to the satisfaction of the Project Manager. It should be made clear that any material removed or damaged in excess of the material that was intended, will be repaired or replaced at no additional cost to the Department. Any disassembled and removed material that is unwanted by the Department shall be clearly appointed ownership to the contractor, and therefore responsibility for removal or recycle is acknowledged. All applicable laws, regulations, and guidelines shall be adequately referenced. This shall include but not be limited to: Publication 408 (Seciton 1018), OSHA regulations, DEP regulations, federal law 40 CFR 261, and any applicable state regulations such as Section 25 PA Code 260.

6.2.2.1.8 Reinforcement Bars, Epoxy Coated

All reinforcing bars shall be prepared and applied in accordance with Section 1002 of Publication 408. All epoxy coatings shall be provided as specified in Section 709.1(c). Details relating to storage, placing and fastening, and splicing and lapping shall be clearly presented.

6.2.2.1.9 Epoxy Injection Crack Seal

Section 1091 of Publication 408 present the provisions for epoxy injection crack seal. ACI 224.1R or the manufacturer's requirements may also be followed for epoxy injection crack seal. In general, cracks greater than 0.01 inches in width must be sealed. Inspection for epoxy injection crack seal shall be performed after removal of defected concrete and cleaning and after cross-section restoration and cleaning before FRP application.

6.2.3 Project Management

Management of an FRP retrofit project is vital for successful implementation of the technology. The entities involved will include: (1) District Bridge Engineers, who will be responsible for supervising and approving the work at each stage; (2) the contractor, who will carry out the work according to contract documents, plans, specifications, and other official documentation; and (3) an outside consultant such as a university research team, serving in an advisory capacity and to provide QC assistance to the contractor while providing improved QA to the District engineer. The outside consultant shall also review all working drawings.

The project management aspect of the rehabilitation should include a thorough understanding of all works associated with the project from start to end. The implementation of a thorough management control manual, that takes into account every possible aspect of the project, can be followed to ensure all goals are met.

6.2.3.1 Management Control Manual

This section briefly describes recommended divisions that should be considered when creating a management control manual that can be followed to ensure overall project

success. Great consideration should be given to all items described in sections 6.2.3.1.1 – 6.2.3.1.7.

6.2.3.1.1 Start-Up

Before any construction work can be performed, contractor submittals relating to the construction aspects of the project, such as shop drawings, should be reviewed to ensure conformance with contract documents while referencing design plans and specifications. All material information should be reviewed and approved. The intended locations and quantity along with details such as splices and fiber orientation should be specified. Contractor submittals relating to qualifications should be reviewed and approved. Judgment should be used to ensure that the project is properly staffed for the given size and complexities. Any apparent conflicts should be resolved by mutual discussion as a first step.

6.2.3.1.2 Faulty Concrete Removal and Restoration

This item covers all aspects that are associated with the removal of defective concrete followed by the use of polymer or latex modified concrete to restore the cross-section. Sections of the management control manual that set forth guidance to ensure the effective completion of this construction task should follow all relevant guidelines and specifications.

6.2.3.1.3 Concrete Substrate Inspection

Inspection and acceptance of the concrete surface before application of the FRP is mandatory. The required smoothness or roughness should be verified and any unwanted imperfections repaired.

6.2.3.1.4 Conditions at Time of Application

All specifications should be adhered to when checking conditions such as ambient temperature and surface dryness. The application should be rescheduled if rain is imminent. If by chance, precipitation starts after the application process has begun, the contractor should provide methods of protecting the installations that have been completed.

6.2.3.1.5 Application Procedure

Sections of the management control manual relating to the application procedure should be concerned with a variety of topics that may affect the overall performance of the FRP in repairing the structure.

Records on the quantity of mixed resin, the day and time of mixing, the proportions and components of mix, the ambient temperature and any other factor that may affect the resin properties as explained in all relevant documentation should be kept. Also, records providing details for the FRP sheeting used on a given day and time and other pertinent information such as ply count or the orientation of the application should be maintained. A sampling plan shall be determined before application in which FRP specimens can be fabricated with the same ambient temperature and application procedure as used on the structure being repaired. Specimens shall be tested with reference to relevant ASTM standards to assess quality. Resin samples may also be obtained or by visually observing resin thickness and hardness on the construction site. Waviness and fiber orientation should be visually inspected after application to ensure conformity with drawings. Fiber orientation differing by more than five degrees from that which has been specified should be reported, as it may adversely affect the performance of the system. Different types of FRP systems will require dissimilar information or additional information. In general, for overall application management, all documented specifications and guidelines should be followed in an effort to obtain adequate results.

6.2.3.1.6 Identification of Defects and Re-application

An overall inspection program should be implemented to assess FRP system quality. Inspection should be focused on, but not necessarily limited to, extent of delaminations, adhesion, laminate thickness, and fiber orientation.

If detected, delaminations shall be assessed while considering their size and frequency for a given application area. Another important aspect to consider for delaminations is their location with respect to key load transfer areas between the structure and the FRP system. Visual assessment, acoustic sounding, thermography, and ultrasonics are some of the inspection methods that may be used. ACI 503R or ASTM D4541 should be referenced

when performing tension adhesion tests on cored samples. Cored samples may also serve to provide verification of the laminate thickness and number of plies. All repairs should be made with compliance to specifications. A second inspection shall be performed, following the repairs, and a comparison made of each inspection to verify the effectiveness of the repair. Adequate records need to be filed for all inspections and testing data.

6.2.3.1.6 Administration Concerns

An adequate management control manual should contain sections for various forms and checklists that address administration aspects such as claims and change orders, estimates and payments, and scheduling. This section may be slightly modified depending on various types of projects and project conditions.

Task 7 Developing Guidelines for Concrete T-Beam Bridge Design and Construction

The work of Task 7 resulted in the development of three separate documents, each created in different formats. Because formatting of the documents does not match conventional formatting, each document is presented in the appendices. The Design Guidelines were to be created in PennDOT's DM-4 format and are given in Appendix C. It is proposed that these design guidelines be added to DM-4 as a new section titled "FRP Strengthening Design." Construction Guidelines were to be drafted in PennDOT Publication 408 format and are presented in Appendix D. It is proposed that these construction guidelines be added to Publication 408 within Section 1000 as indicated in Appendix D. Guidelines for Bridge Testing and Long-term Monitoring are presented in Appendix E.

Summary and Conclusions

Based on the research study conducted, the following can be summarized and concluded:

1) Through the repair contract, lab studies and post-construction load testing, it can be concluded that Externally Bonded FRP Composites are a viable means to rehabilitate concrete T-beam bridges. A sound employment strategy for this technology can result in considerable economic savings for PennDOT, as many concrete T-beam bridges are in need of repair.

2) A criterion was developed for ranking the PennDOT D3 concrete T-beam bridges into three categories as candidates for possible repair with FRP and applied to the bridges in the PennDOT D3. Selection criteria relating to the functional class of highway that the bridge serves and the bridge capacity appraisal were added to the ranking system as recommended by PennDOT D3. Repair levels of 1, 2, and 3 were assigned to candidate bridges based on severity of deterioration. Repair level 1 would most likely be contracted out through competitive bid. Repair level 2 may consist of a combination of a contractor and District forces. Repair level 3 may consist of only District forces. At each repair level, it is suggested that the use of a third company (outside consultant) may provide increased QA. It was recommended that the field implementation phase follow sequentially bridge projects beginning with Level 1, followed by Levels 2 to 3. Implementation of this nature can allow for efficient knowledge transfer to District forces.

3) A Level 1 bridge was selected to demonstrate the technical and cost-effective application of externally bonded FRP. Visual inspection, in-situ non-destructive concrete tests, and laboratory tests showed that the quality of concrete in the exterior and first interior girders was poor. Prior to retrofitting, the deteriorated concrete surface required major removal and replacement. The quality of concrete in the interior girders was within a typical range and can be used after filling the internal voids and cracks by injection grouting. Minor void filling and localized spalling patching were needed for the deck slab.

4) The FRP repair system was designed based on current ACI 440.2R-02 design guidelines. It was noticed that some reinforcing were missing based on design drawings. Rather than being concerned with any discrepancies between original design plans/specifications and as-built conditions, using FRP strengthening was recommended to sustain a current AASHTO design load. The capacity required to achieve a load rating factor of 1 based on an AASHTO design load was suggested for strengthening requirements.

5) An FE model was built using available as-built drawings and field information. This model was calibrated using the field test results and modified as needed to increase its accuracy. The verification of the model permitted its confident use in designing the FRP reinforcement.

6) Based on the loading factors from unrepaired and repaired bridges and design documents from the contractor, the moment and shear capacities of the repaired bridge increased. Overall, the stiffness of the repaired bridge did not change much, as illustrated by both testing and FE analysis results, which were also verified by the lab-scale studies.

7) Based on the lab-scale studies, it was concluded that corrosion produced by the accelerated aging technique resulted in deterioration of the laboratory specimens that was very similar to what was observed on bridges in the field. The polymer patch repaired beams outperformed the crack-injected beams in long-term behavior.

8) Using results from the study, draft PennDOT design guidelines, construction specifications, and bridge testing and long-term monitoring guidelines were developed. The objective is to incorporate all drafted guidelines into official PennDOT specifications, such as DM-4 and Publication 408.

It is noted that no de-corrosion technique was considered in this report. There is an ongoing study on the effectiveness of electro-chemical chloride extraction (ECE)

technique on the concrete beams strengthened with FRP strips at WVU. If ECE technique is proven to be beneficial and cost-effective, this process can be applied to the demonstration bridge project after retrofit. Although specific to PennDOT D3, this report presents a general prescription for the possible adoption of FRP repair as a viable and cost-effective method for rehabilitation of deficient concrete bridges to promote a sustainable infrastructure system.

REFERENCES

AASHTO, "Manual for Condition Evaluation of Bridges," 2nd Edition, pp 49-72, 1994.

AASHTO, "Standard Specifications for Highway Bridges," 16th Edition, 760 pp., 1996.

ACI Concrete Repair Manual

ACI 318-08 (2008), Building Code Requirements for Structural Concrete and Commentary (318R-08), American Concrete Institute, Farmington Hills, MI.

ACI 440.2R-08. Guide for the Design and Construction of Externally Bonded FRP Systems for Strengthening Concrete Structures. Farmington Hills, MI: American Concrete Institute, 2008.

ACI 440R-07 (2007). Report on Fiber-Reinforced Polymer (FRP) Reinforced for Concrete Structures. American Concrete Institute.

Bousselham, A., and Chaallal, O., 2006, "Behavior of Reinforced Concrete T-Beams Strengthened in Shear with Carbon Fiber-Reinforced Polymer—An Experimental Study," *ACI Structural Journal*, V. 103, No. 3, May-June, pp. 339-347.

Davalos, Julio F., Karl E. Barth, Indrajit Ray, Chunfu Lin, Adam L. Justice, and Matt D. Anderson. District 3-0 Investigation of Fiber-Wrap Technology for Bridge Repair and Rehabilitation (Phase-3). Morgantown, WV: West Virginia University, 2008.

Deniaud, C., and Cheng, J. J. R., 2003, "Reinforced Concrete T-Beams Strengthened in Shear with Fiber Reinforced Polymer Sheets," *Journal of Composites in Construction*, ASCE, V. 7, No. 4, pp. 302-310.

Funakawa, I.; Shimono, K.; Watanabe, T.; Asada, S.; and Ushijima, S., 1997, "Experimental Study on Shear Strengthening with Continuous Fiber Reinforcement Sheet and Methyl Methacrylate Resion," *Third International Symposium on Non-Metallic (FRP) Reinforcement for Concrete Structures (FRPRCS-3)*, V. 1, Japan Concrete Institute, Tokyo, Japan, pp. 475-482.

Green, M.; Bisby, L.; Beaudoin, Y.; and Labossiere, P., 1998, "Effects of Freeze-Thaw Action on the Bond of FRP Sheets to Concrete," *Proceedings of the First International Conference on Durability of Composites for Construction*, Sherbrooke, QC, Canada, Oct., pp. 179-190.

Khalifa, A.; Alkhrdaji, T.; Nanni, A.; and Lansburg, S., 1999, "Anchorage of Surface-Mounted FRP Reinforcement," *Concrete International*, V. 21, No. 10, Oct., pp. 49-54.

Malek, A.; Saadatmanesh, H.; and Ehsani, M., 1998, "Prediction of Failure Load of R/C Beams Strengthened with FRP Plate Due to Stress Concentrations at the Plate End," *ACI Structural Journal*, V. 95, No. 1, Jan.-Feb., pp. 142-152.

Okeil, A. M.; Bingol, Y.; and Alkhrdaji, T., 2007, "Analyzing Model Uncertainties for Concrete Beams Flexurally Strengthened with FRP Laminates," *Proceedings of the Transportation Research Board 86th Annual Meeting*, Jan. 21-25, 2007, Washington, DC, 15 pp. (CD-ROM)

Parish, George C. CFRP Repair of Concrete Beams Aged by Accelerated Corrosion. Thesis. West Virginia Univ., 2008. Morgantown, WV: West Virginia University, 2008

Pellegrino, C., and Modena, C., 2002, "Fiber Reinforced Polymer Shear Strengthening of Reinforced Concrete Beams with Transverse Steel Reinforcement," *Journal of Composites in Construction*, ASCE, V. 6, No. 2, pp. 104-111.

Priestley, M.; Seible, F.; and Calvi, G., 1996, *Seismic Design and Retrofit of Bridges*, John Wiley and Sons, New York, 704 pp.

Quattlebaum, J.; Harries, K. A.; and Petrou, M. F., 2005, "Comparison of Three CFRP Flexural Retrofit Systems Under Monotonic and Fatigue Loads," *Journal of Bridge Engineering*, ASCE, V. 10, No. 6, pp. 731-740.

Roberts, T. M., and Haji-Kazemi, H., 1989, "Theoretical Study of the Behavior of Reinforced Concrete Beams Strengthened by Externally Bonded Steel Plates," *Proceedings of the Institute of Civil Engineers*, Part 2, V. 87, No. 9344, pp. 39-55.

Sasher, William C. Testing, Assessment and FRP Strengthening of Concrete T-Beam Bridges in Pennsylvania. Thesis. West Virginia Univ., 2008. Morgantown, WV: West Virginia University, 2008

Soudki, K. A., and Green, M. F., 1997, "Freeze-Thaw Response of CFRP Wrapped Concrete," *Concrete International*, V. 19, No. 8, Aug., pp. 64-67.

Triantafillou, T. C., 1998a, "Shear Strengthening of Reinforced Concrete Beams Using Epoxy-Bonded FRP Composites," *ACI Structural Journal*, V. 95, No. 2, Mar.-Apr., pp. 107-115.

University of Missouri-Rolla. Preservation of Missouri Transportation Infrastructures; Validation of FRP Composite Technology Through Field Testing; Strengthening of Bridge P-0962 Vol. II: Master Design. Rolla, MO: University of Missouri-Rolla, 2004.

Appendices

Appendix A

Bridge Classification Examples

Example #1
Class #1: Overall Score (84.8/100)

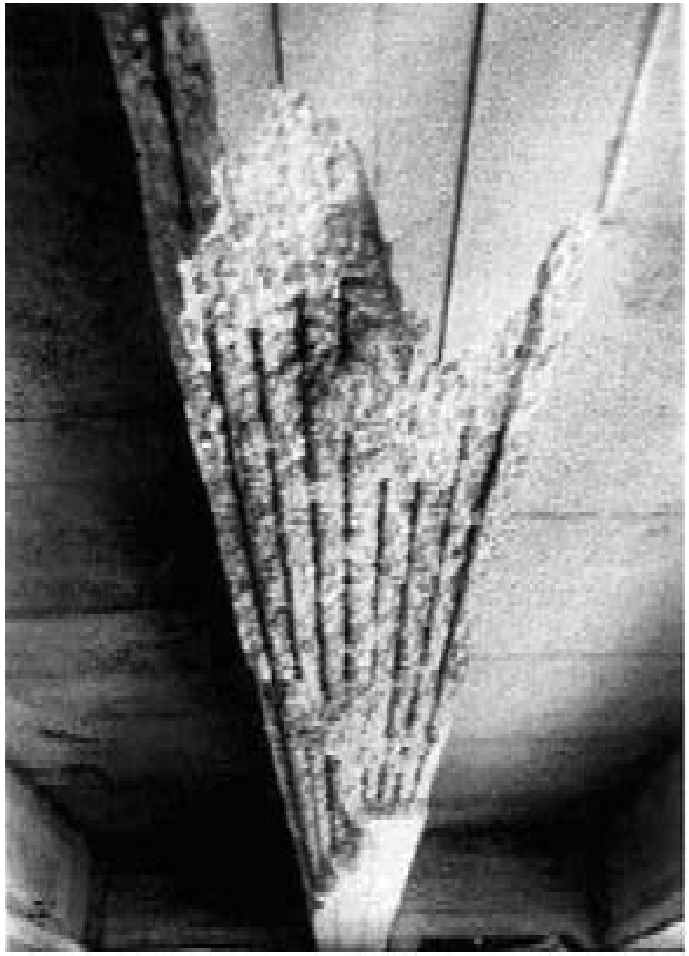

Details:

Span(ft): 30
Ranking: 4/10

Year Built: 1938
Ranking: 5/10

ADT: 10310
Ranking: 10/10

ADTT: 648
Ranking: 9/10

Visual Damage:
Ranking: 10/10

Number of Spans: 1

Status: Open

Road: SR 45

Photo on left: NCHRP Report 514, an example of a T-beam suitable for FRP-wrap technology

Photo on right: Provided by PennDOT for bridge #59-0045-0310-2011

Note: This is a likely candidate for repair. This bridge scored high because of its high traffic volume and similarities in damage to the NCHRP Report 514. This bridge ranked high even though it scored relatively low in the span and age categories.

Example #2
Class #2: Overall Score (65.4/100)

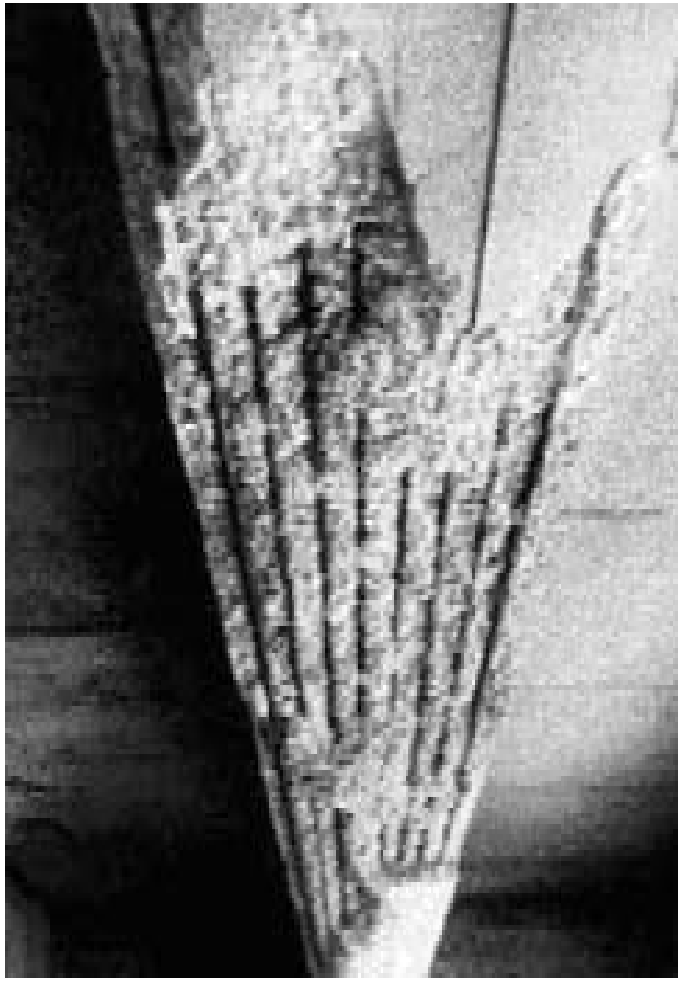

Details:

Span (ft): 55
Ranking: 8/10

Year Built: 1929
Ranking: 3/10

ADT: 4195
Ranking: 8/10

ADTT: 299
Ranking: 7/10

Visual Damage:
Ranking: 6.67/10

Number of Spans: 2

Status: Open

Road: SR 522

Photo on left: NCHRP Report 514, an example of a T-beam suitable for FRP-wrap technology

Photo on right: Provided by PennDOT for bridge #54-0522-0090-1932

Note: Though this bridge carries a lot of traffic, and ranked high in the span category, it is ranked into Class #2 because of the extent of the visual damage. This bridge would be suitable for repair by fiber-wrap technology.

Example #3
Class #3: Overall Score (39.9/100)

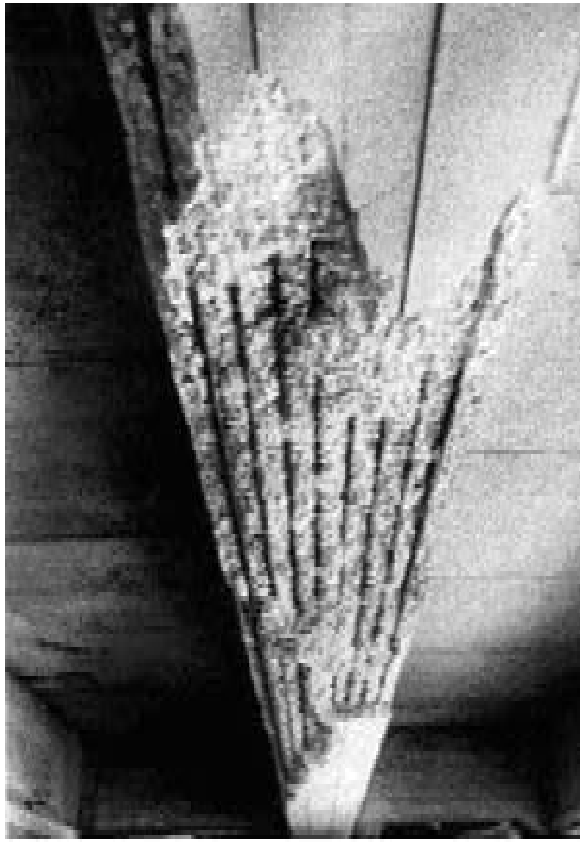

Photo on left: NCHRP Report 514, an example of a T-beam suitable for FRP-wrap technology

Photo on right: Provided by PennDOT for bridge #19-3008-0100-0039

Details:

Span (ft): 23
Ranking: 2/10

Year Built: 1933
Ranking: 4/10

ADT: 265
Ranking: 2/10

ADTT: 20
Ranking: 1/10

Visual Damage:
Ranking: 3.33/10

Number of Spans: 1

Status: Open

Road: SR 3008

Note: This bridge ranked low overall because of low traffic volume, short span, and old age. Also, the visual damage was not as severe as many of the other bridges. This is an example of a bridge which may not be a good candidate for FRP technology.

Appendix B

Project Selection Forms

A convenient pull-down form in word is provided to the user, as shown in the example below:

Form for Assessing the Suitability of a Concrete T-Beam Bridge for Repair with FRP (Based on Bridge Classification)	
Scoring Category (weight percentage)	**Score**
1. Photographic Indication of Damage (40%)	6.67
2. Age (10%)	10
3. Span Length (6%)	10
4. ADT & ADTT (10% & 10%)	10 & 10
5. Functional Class of Highway (12%)	10
6. Bridge Capacity Appraisal (12%)	10
Total Weighted Score	86.68%

Instructions:

1. A score shall be assigned for each category as specified in Section 6.1.1.2.
2. The score column on the right contains drop down menus that offer the score values recommended for bridge classification.
3. Select the appropriate score for each category from the drop down menus.
4. After the scores have been chosen, right click the total weighted score field and click update field. The total weighted score will be calculated based on the individual scores chosen. Based on this score, a class rating will be assigned with reference to Table 30; see Section 6.1.1.2.4.

A convenient self executable program was created in MATLAB that allows for quick and easy suitability analyses as shown below:

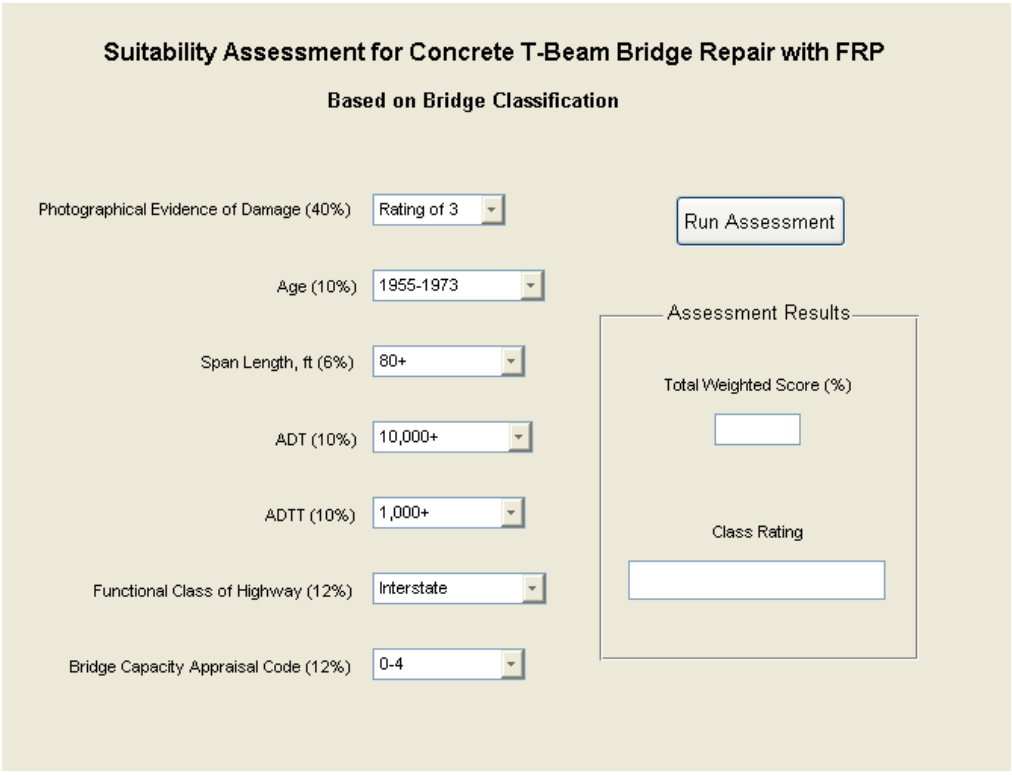

Appendix C

Design Guidelines

PENNSYLVANIA DEPARTMENT OF TRANSPORTATION
DESIGN MANUAL

PART 4
PART B: DESIGN SPECIFICATIONS

SECTION 1 – FRP STRENGTHENING DESIGN

SECTION 1 – TABLE OF CONTENTS

SPECIFICATIONS COMMENTARY

1.1 GENERAL

These design specifications are recommended for the repair of reinforced concrete T-beam bridges using FRP. Sections 1.2 through 1.5 present general material and analysis considerations. Sections 1.6 through 1.8 lay out the design procedures. Prestressed components are not discussed in this document.

1.2 DEFINITIONS

AFRP – Aramid fiber-reinforced polymer.

CFRP – Carbon fiber-reinforced polymer (includes graphite fiber-reinforced polymer).

Creep-rupture – The gradual, time-dependent reduction of tensile strength due to continuous loading that leads to failure of the section.

Debonding – A separation at the interface between the substrate and the adherent material.

Delamination – A separation along a plane parallel to the surface, as in the separation of the layers of the FRP laminate from each other.

Epoxy – A thermosetting polymer that is the reaction product of epoxy resin and an amino hardener (see also **Epoxy resin**).

Epoxy Resin – A class of organic chemical-bonding system used in the preparation of special coating or adhesives for concrete and as binders in epoxy-resin mortars and concretes.

Fiber-reinforced Polymer (FRP) – A general term for a composite material that consists of a polymer matrix reinforced with cloth, mat, strands, or any other fiber form.

GFRP – Glass fiber-reinforced polymer.

Inside Corner – Corner such as that found on the inside of hollow rectangular members.

Outside Corner – Corner such as that found on the outside of a hollow rectangular member.

Ply – A single layer of fabric or mat; multiple plies, when molded together, make up the laminate.

Resin – Polymeric material that is rigid or semi rigid at room temperature, usually with a melting point or glass transition temperature above room temperature.

SPECIFICATIONS COMMENTARY

Sheet, FRP – A dry, flexible ply used in wet lay-up FRP systems. Unidirectional FRP sheets consist of continuous fibers aligned in one direction and held together in-plane to create a ply of finite width and length. Fabrics are also referred to as sheets.

1.3 NOTATION

a = depth of equivalent stress block, in.
a_b = depth of equivalent rectangular stress block for balanced strain conditions, in.
A_f = area of external FRP reinforcement, nt_fw_f, in^2
A_{fv} = area of FRP shear reinforcement with spacing s, in^2
A_s = area of steel tension reinforcement, in^2
A'_s = area of compression steel reinforcement, in^2
b = width of compression face of member, in.
b_w = web width, in.
c = distance from extreme compression fiber to neutral axis, in.
C_E = environmental reduction factor
d = distance form extreme compression fiber to centroid of tension reinforcement, in.
d' = distance form extreme compression fiber to centroid of compression reinforcement, in.
d_c = distance measured from extreme tension fiber to center of the closest bar or wire in inches. For calculation purposes, the thickness of clear concrete cover used to compute d_c shall not be taken greater than 2 inches.
d_f = distance form the extreme compression fiber to centroid of FRP reinforcement, in.
d_{fv} = depth of FRP shear reinforcement, in.
d_L = distance form the extreme compression fiber to the top of the lateral FRP plies, in.
E_f = tensile modulus of elasticity of FRP, psi
E_c = modulus of elasticity of concrete, psi
f'_c = specified compressive strength of concrete, psi
f_f = stress level in the FRP reinforcement, psi
$f_{f,s}$ = stress level in the FRP caused by a moment within the elastic range of the member, psi
f_{fe} = effective stress in the FRP; stress level attained at section failure, psi
f^*_{fu} = ultimate tensile strength of the FRP material as reported by the manufacturer, psi
f_{fu} = design ultimate tensile strength of FRP, psi
f_r = modulus of rupture of concrete, psi
f'_s = stress in compression reinforcement, psi
f_s = tensile stress in nonprestressed steel reinforcement, psi
$f_{s,s}$ = stress level in nonprestressed steel reinforcement at service loads, psi

f_y = specified yield strength of reinforcement, psi
h_f = compression flange thickness of T – sections, in.

SPECIFICATIONS COMMENTARY

I_e = effective moment of inertia for computation of deflection, in^4
I_g = moment of inertia of the gross concrete section about the centroidal axis, neglecting reinforcement, in^4
k = ratio of the depth of the neutral axis to the reinforcement depth measured on the same side of the neutral axis
k_1 = modification factor applied to κ_v to account for the concrete strength
k_2 = modification factor applied to κ_v to account for the wrapping scheme
L_e = active bond length of FRP laminate, in.
M_a = maximum moment in member at stage for which deflection is being computed
M_{cr} = cracking moment
M_n = nominal moment strength of a section
M_s = moment within the elastic range of the member, in-lb
M_u = factored moment at the section under consideration
n = number of plies of the FRP reinforcement
n_f = modular ratio of FRP to concrete
n_s = modular ratio of steel to concrete
R_n = nominal strength of a member
S_{DL} = dead load effects
s_f = center-to-center spacing of FRP shear reinforcement, in.
S_{LL} = live load effects
t_f = nominal thickness of one ply of the FRP reinforcement, in.
V_c = nominal shear strength provided by the concrete with steel flexural reinforcement, lb
V_f = nominal shear strength provided by the FRP stirrups, lb
V_n = nominal shear strength, lb
V_s = nominal shear strength provided by the steel stirrups, lb
V_u = factored shear force at the section under consideration
w_f = width of FRP reinforcing plies, in.
y_t = distance form the centroidal axis of the gross section, neglecting reinforcement, to extreme fiber in tension
α = angle between inclined shear reinforcement and longitudinal axis of the member
α_L = longitudinal coefficient of thermal expansion, in/in/°F
β_1 = ratio of depth of equivalent compression zone to depth from extreme compression fiber to the neutral axis
ε_{bi} = strain level in the concrete substrate at the time of the FRP installation, in/in
ε_{cu} = maximum usable compressive strain of concrete, in/in
ε_{fe} = effective strain level in FRP reinforcement; strain level attained at section failure, in/in
ε_{fu} = design rupture strain of FRP reinforcement, in/in
ε^*_{fu} = ultimate rupture strain of the FRP reinforcement, in/in
ε_s = strain level in the nonprestressed tension steel reinforcement, in/in
ε'_s = strain level in the compression steel reinforcement, in/in
Φ = strength reduction factor
γ = multiplier for f'_c to determine the intensity of an equivalent rectangular stress distribution for concrete

SPECIFICATIONS COMMENTARY

κ_m = bond-dependent coefficient for flexure
κ_v = bond-dependent coefficient for shear
ρ_f = FRP reinforcement ratio
ρ_s = steel reinforcement ratio
Ψ_f = additional FRP strength reduction factor

1.4 MATERIAL

1.4.1 General

Materials to be considered in designing an FRP system for strengthening reinforced concrete components consist of the concrete, whether it be the existing or the replacement material, and all materials comprising the FRP system.

1.4.2 Concrete

C1.4.2

The substrate material for the application of the proposed FRP system should be of sound quality such that the FRP system will be allowed to perform as intended. The substrate material shall be prepared in a way that conforms to ICRI 03730 and/or the construction specifications.

In order for the FRP system to achieve its design objectives, it is imperative that a clean and sound substrate is prepared. Important considerations to consider are the quality and strength of the patch material, as well as its bond with the existing concrete.

1.4.3 FRP System

C1.4.3

Materials comprising the FRP repair system include fibers and all resins such as primers, putties, saturants, and adhesives. Brief descriptions of these FRP materials are given in Sections 1.4.3.1 – 1.4.3.5. The design engineer should consult with the FRP system manufacturer for more detailed aspects of these materials and the importance of these aspects in design.

The plans should include type of fiber, type of resin, tensile strength, f_{fu}, modulus of elasticity, E_f, and ultimate strain, ε_{fu}. FRP reinforcement shall conform to the specifications of ACI 440.3R-04.

All constituent materials used in FRP systems have been developed for the strengthening of structural concrete members through material and structural testing. The characteristics of an FRP material are greatly influenced by aspects such as fiber volume, type of fiber, type of resin, fiber orientation, and quality control during the manufacture process.

The most widely used forms of FRP system include wet layup, precured, and near-surface mounted (NSM) systems.

SPECIFICATIONS

1.4.3.1 FIBERS

FRP systems commonly incorporate the use of continuous glass, aramid, and carbon fibers. Fibers provide the FRP system with its strength and stiffness. ACI 440R can be referenced for a more detailed discussion of fibers.

1.4.3.2 RESINS

An extensive range of polymeric resins are used with FRP systems. These resins include primers, saturants, adhesives, and putty fillers as described herein. Frequently used resin types such as epoxy, vinyl esters, and polyesters have been formulated for use in many different environments.

Primer – Primer penetrates the surface of the substrate concrete and provides an improved bond for the saturating adhesive.

Saturants – Saturants are used to impregnate the fibers so as to provide a shear load path for the effective transfer of load between fibers. The saturant is also used as the adhesive for wet layup systems and as a result provides the shear
load path between the concrete and the FRP.

Adhesive - Adhesives are used for bonding precured FRP laminates and NSM systems. A shear load path is created. Adhesives are also used if it is necessary to bond multiple layers of precured FRP laminates.

Putty fillers – The use of putty is necessary to fill small surface voids in the

COMMENTARY

C1.4.3.2

Resins are broken into two broad categories: thermoset and thermoplastic. Thermoplastic resins are normally solid in their initial form and may be shaped or molded while in a heated semi-fluid state. Thermosetting resins are closer to a liquid form in their initial state and are more commonly used in the composites industry. Thermosetting resins are cured with a catalyst, heat, or a combination of the two. Once formed, they cannot be reshaped. The softening of a cured resin can be determined by the measurement of a heat distortion temperature and a glass transition temperature. Epoxy, vinyl esters, and polyesters are common types of thermosetting resins used. For a more informative discussion on various types of resins, refer to ACI 440R.

SPECIFICATIONS

concrete substrate and to provide a smooth
surface for the FRP system.

1.5 ANALYSIS

1.5.1 General

In order to design an FRP system to achieve a desired capacity, the existing capacity of the member considered needs to be determined in accordance with acceptable engineering principals. A load rating analysis may be used to assess the existing and desired structural capacity. The increase in structural capacity can be determined with the goal of reaching a desirable load rating factor. With an existing and required capacity established, the FRP strengthening system can be designed.

A realistic representation of the bridge's material strength and geometric properties is necessary to accurately determine the bridge's existing structural capacity. If available, documentation of the original material properties and any drawings should be used. In absence of original documentation, material strength values are suggested by AASHTO for unknown material properties in the *Manual for Condition Evaluation of Bridges* in accordance with the year a structure was built. As a more reliable alternative, AASHTO guidelines allow for the use of experimental values when available.

1.5.2 Concrete Material Properties

For all relevant material properties for concrete structures refer to Article 5.4.

1.5.3 FRP System Material Properties

1.5.3.1 GENERAL

COMMENTARY

C1.5.1

The repair process should be analyzed in an effort to achieve the most efficient design possible. FRP composite strengthening systems shall be designed to increase the flexural capacity, shear capacity, axial capacity, and ductility, or any combination thereof.

It has been found that there are several failure modes controlling the ultimate strength in concrete beams strengthened with FRP laminates. These failure modes consist of the following:

- Crushing of the concrete in compression before yielding of the reinforcing steel;
- Yielding of the steel in tension which is followed by rupture of the FRP laminate;
- Yielding of the steel in tension which is followed by concrete crushing;
- Delamination of the concrete cover due to shear or tension; and
- FRP debonding from the concrete substrate

C1.5.3.1

Factors such as loading history and duration, temperature, and moisture affect the properties of FRP material. The physical and mechanical properties discussed are the most relevant for concrete structure rehabilitation.

SPECIFICATIONS

Relevant material properties are presented in this section. Included, is a section for thermal expansion, general tensile and compressive behavior, and design material properties.

1.5.3.2 EXPANSION AND CONTRACTION

The manufacturer shall supply the coefficient of thermal expansion and contraction. Typical values for coefficients of thermal expansion for FRP materials are presented in ACI 440.2R-08 and are reprinted in Table 1.5 – 1.

Table 1.5 – 1 - Typical Coefficients of Thermal Expansion for FRP Materials

Direction	Coefficient of thermal expansion, x 10^{-6}/°F (x 10^{-6}/°C)		
	GFRP	CFRP	AFRP
Longitudinal, α_L	3.3 to 5.6 (6 to 10)	-0.6 to 0 (-1 to 0)	-3.3 to -1.1 (-6 to -2)
Transverse, αL	10.4 to 12.6 (19 to 23)	12 to 27 (22 to 50)	33 to 44 (60 to 80)

Note that negative values of coefficients of thermal expansion indicate that the material contracts with increased temperature and expands with decreased temperatures.

1.5.3.3 TENSILE AND COMPRESSIVE BEHAVIOR

With respect to mechanical properties, the tensile behavior of FRP materials should be very well understood. Under direct tension, unidirectional FRP materials do not display any yielding before rupture. Therefore, FRP consisting of one type of fiber will exhibit a linear elastic stress-strain relationship until failure. This results in a sudden and brittle failure which should be avoided in design.

COMMENTARY

C1.5.3.2

Unidirectional FRP materials have differing coefficients of thermal expansion in the longitudinal and transverse directions. Thermal expansion properties will depend on the types of fiber, resin, and volume fraction of fiber.

Often, thermal expansion properties of the fiber and polymer constituents will vary and be different from that of concrete. Polymers used in FRP strengthening systems normally have coefficients of thermal expansion nearly five times that of concrete. It has been shown (Motavalli et al. 1997; Soudki and Green 1997; Green et al. 1998) that although there are great thermal expansion differences in materials, the effect is not significant for small ranges of temperature change, within ±50 °F (±28 °C).

.

C1.5.3.3

The fiber in an FRP system is the main load-carrying material. Therefore, the tensile strength and stiffness of a system are strongly dependant on fiber type, fiber orientation, and fiber quantity. Due to this significant role of fibers, FRP system properties are often reported based on net-fiber area. Alternatively, and used with precured systems, properties can be reported based on gross-laminate area.

Mechanical properties of FRP systems should be based on testing of laminate samples with known fiber content. The FRP system manufacturer shall supply the tensile properties of any particular FRP system.

SPECIFICATIONS

Insufficient testing has been performed to permit the use of externally bonded FRP systems for compression reinforcement. Compression strength of externally bonded FRP shall be omitted in design.

1.5.3.4 DESIGN MATERIAL PROPERTIES

Material properties reported by manufacturers, such as the ultimate tensile strength, should typically be considered as initial properties; as they do not account for long term exposure to environmental conditions. Long term exposure to various environmental conditions can lead to decreases in tensile property values and creep-rupture and fatigue endurance of laminates. As a result, the material properties that are to be used in design should be adjusted to account for the environmental exposure condition. Equations (1-1) through (1-3) should be used to obtain tensile properties to be used in all design equations.

$$f_{fu} = C_E f_{fu}^{*} \tag{1-1}$$

$$\varepsilon_{fu} = C_E \varepsilon_{fu}^{*} \tag{1-2}$$

$$E_f = \frac{f_{fu}}{\varepsilon_{fu}} \tag{1-3}$$

Table 1.5 – 2 - Environmental Reduction Factors for Various FRP Systems and Exposure Conditions

Exposure Conditions	Fiber and Resin Type	Environmental Reduction Factor C_E
Interior Exposure	Carbon/epoxy	0.95
	Glass/epoxy	0.75
	Aramid/epoxy	0.85
Exterior Exposure	Carbon/epoxy	0.85
	Glass/epoxy	0.65

COMMENTARY

C1.5.3.4

Due to the linear elastic nature until failure for unidirectional FRP materials, Hooke's law can simply be used to determine the design modulus of elasticity. Due to the use of the same reduction factor, the modulus is typically unaffected by environmental conditions.

Test data for the durability of FRP systems with and without protective coatings can be obtained from the manufacturer of the FRP system when and if they become available.

SPECIFICATIONS

(bridges, piers, and unenclosed parking garages)	Aramid/epoxy	0.75
Aggressive Environment (chemical plants and waste water treatment plants)	Carbon/epoxy	0.85
	Glass/epoxy	0.50
	Aramid/epoxy	0.70

C_E is the reduction factor and can be found from Table 1.5 – 2. The reduction factor can be altered to reflect the use of protective coatings only if it has been demonstrated through testing that the coating reduces the effects of environmental exposure and the coating is maintained throughout the life of the FRP system.

1.6 FLEXURAL DESIGN

1.6.1 Design Method

1.6.1.1 - FRP strengthening systems should be designed to withstand tensile forces while maintaining strain compatibility between the FRP and the concrete substrate.

1.6.1.2 - FRP systems should not be relied on to withstand compression forces, although it is acceptable to introduce compression forces to an FRP strengthening system due to moment reversals and points of contra-flexure.

1.6.1.3 - Limit-states design principles are used that set acceptable levels of safety for the occurrence of both serviceability limit states and ultimate limit states.

1.6.1.4 - In evaluating the nominal strength of a member, the possible failure modes and corresponding strains and stresses in each material should be assessed.

COMMENTARY

C1.6.1

Strain compatibility should be satisfied in the design method, meaning that the strain across the depth of the section follows a linear distribution as illustrated in Figure 1.6-1. The calculation procedure should consider the governing mode of failure and satisfy force equilibrium.

Transformed sections incorporating the use of modular ratios for the evaluation of serviceability provides a way to visualize and organize the calculations. The method consists of transforming the cross section of a composite beam into an equivalent cross section of an imaginary beam that is composed of only one material.

The additional reduction factor that is implemented for the FRP contribution is presented in Section 1.6.4.1. It helps to account for the varying failure modes experimentally seen for FRP strengthened members and improves the reliability of the strength prediction. The reduction factor was developed based on experimentally calibrated statistical properties of the flexural strength (Okeil et al. 2007).

SPECIFICATIONS

1.6.1.5 - Engineering principles such as modular ratios and transformed sections can be used when evaluating the serviceability of a member.

1.6.1.6 - ACI 318-08 strength and serviceability requirements should be adhered to along with implementing additional reduction factors to the FRP contribution.

1.6.2 Assumptions

As with any design, assumptions are made in order to decrease the computational efforts down to a practical matter. This section presents the assumptions used in FRP strengthening design.

1.6.2.1 - Calculations are based on actual dimensions, material properties, and arrangement and type of internal reinforcement for the existing member that is to be strengthened.

1.6.2.2 - The maximum usable compressive strain in the concrete is 0.003.

1.6.2.3 - The strains in the concrete and reinforcement are directly proportional to their distances from the neutral axis of the member.

1.6.2.4 - Tensile strength of concrete is neglected.

1.6.2.5 - Shear deformation within the adhesive layer is neglected noting that the adhesive layer is very thin with only slight variations in thickness.

1.6.2.6 - There is no relative slip between the concrete and the externally bonded composites.

1.6.2.7 - FRP reinforcement has a linear elastic

COMMENTARY

C1.6.2

Much of the assumptions are necessary for the sake of computational ease and do not perfectly portray the exact fundamental behavior of FRP flexural reinforcement. Although the assumptions are not completely accurate, the computed flexural strength of a strengthened member will not be significantly affected.

SPECIFICATIONS

stress-strain relationship to failure.

1.6.2.8 - The concrete compressive stress/strain distribution can be taken as any shape that results in strength predictions within agreement of testing data. Most often, a rectangular stress/strain block will be used.

1.6.2.9 - The parameters α_1 and β_1 are used to define a rectangular stress block equivalent to the nonlinear distribution of concrete stress. α_1 and β_1 should be taken as the values associated with the Whitney stress block, where α_1 is equal to 0.85 and β_1 can be taken as 0.85 for $f_c' \leq 4{,}000$ psi ; 0.80 for $f_c' = 5{,}000$ psi ; 0.75 for $f_c' \leq 6{,}000$ psi ; 0.70 for $f_c' \leq 7{,}000$ psi ; 0.65 for $f_c' \geq 8{,}000$ psi. Note that this approach will give good results if concrete crushing is the controlling mode of failure. If FRP rupture, cover delamination, or FRP debonding is the mode of failure, the approach will still yield reasonably accurate results.

1.6.3 Strengthening Limits

Strengthening limits should be imposed to guard against collapse of the structure if failure of the FRP system would occur due to damage, vandalism, or any other causes.

1.6.3.1 - The existing strength of the structure should be adequate to resist a level load as given by equation (1-4).

$$(\Phi R_n)_{existing} \geq (1.1S_{DL} + 0.75S_{LL})_{new} \qquad (1\text{-}4)$$

1.6.3.2 - If the member to be strengthened has a high likelihood of being subjected to a live load that is present for a sustained period of time, a live load factor of 1.0 should be used in equation (1-4) instead of 0.75.

1.6.3.3 - All members of a structure should be adequate to withstand the anticipated increase in loads that is associated with the

COMMENTARY

C1.6.3

Careful consideration should be given to strengthening limits. It is possible to obtain an accurate evaluation of existing dead loads on a structure, and therefore, a number close to unity, such as 1.1, is used for the dead load factor. As reported in ACI 440.2R-08 and taken from ASCE 7-05, a live load factor of 0.75 is incorporated to exceed the statistical mean of annual maximum live load factors set at 0.5.

Examples where a live load factor of 1.0 may be used instead of 0.75 can include any area along a bridge that may be used as a heavy storage area for any period of time.

Special care should be taken to see that all components of the structure can withstand the anticipated future loading. Increasing primary member capacities without a full analysis of remaining components can prove disastrous.

SPECIFICATIONS COMMENTARY

strengthened members.

1.6.4 Flexural Strengthening

Flexural strengthening is achieved by bonding FRP reinforcement to the tension face of flexural members. The FRP is bonded so that the fibers are oriented along the longitudinal length of the member. Strength increases of up to 40% are reasonable when strengthening limits are imposed.

1.6.4.1 NOMINAL STRENGTH

1.6.4.1.1 - The strength design approach is used. This requires that the design flexural strength (nominal flexural strength, M_n multiplied by a reduction factor, Φ) exceeds it required factored moment (M_u) as indicated in equation (1-5).

$$\Phi M_n \geq M_u \qquad (1\text{-}5)$$

1.6.4.1.2 - To maintain an adequate degree of ductility, the strain level in the steel at the ultimate limit state should be checked. The strength reduction factor, Φ should be determined with reference to this strain level by using equation (1-6). ε_t is the net tensile strain in the extreme tension steel at nominal strength.

$$\Phi = \begin{cases} 0.90 \quad for\ \varepsilon_t \geq 0.005 \\ 0.65 + \dfrac{0.25(\varepsilon_t - \varepsilon_{sy})}{0.005 - \varepsilon_{sy}} \quad for\ \varepsilon_{sy} < \varepsilon_t < 0.005 \\ 0.65 \quad for\ \varepsilon_t \leq \varepsilon_{sy} \end{cases}$$

(1-6)

1.6.4.1.3 - An additional reduction factor ψ_f is applied to the FRP strength contribution. The recommended value of

C1.6.4.1

Load factors in correspondence with ACI 318-05 are used in calculating the factored moment, M_u.

Using externally bonded FRP to strengthen concrete members will often result in a reduction of the original ductility. Significant losses in ductility should be carefully evaluated. Adequate ductility should be maintained through careful consideration of strain levels in the reinforcing steel. The strain level in the steel, ε_t, should be at least 0.005 in order for adequate ductility to be achieved. This is in accordance with the definition of a tension-controlled section as specified in ACI 318-05. Equation (1-6) is represented graphically in Figure C1.6-1.

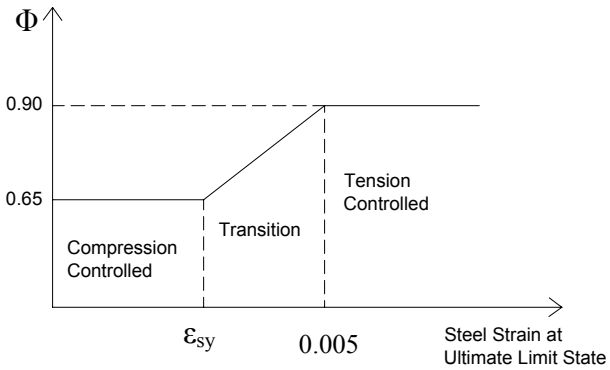

Figure C1.6-1 – Graphical Representation of Strength Reduction Factor

C1.6.4.2

The elastic analysis approach used based on cracked section properties neglects any contribution of tension-zone concrete to the stiffness of the cross

SPECIFICATIONS

ψ_f is 0.85.

1.6.4.2 INITIAL SUBSTRATE STRAIN

The substrate to which the FRP reinforcement is to be bonded will have an already existing strain due to self-weight and any sustained loads that may be present. These strains should be excluded from the strain in the FRP. An elastic analysis, considering all loads on the structure during application, can be used to determine the initial strain level on the bonded substrate (ε_{bi}) for a given member. The elastic analysis should be based on cracked section properties.

COMMENTARY

section. The moment of inertia of the cracked section, I_{cr}, shall be determined from the basic principles of mechanics.

With reference to Figure C1.6-2 and the accompanying discussion, the determination of the cracked section moment of inertia, I_{cr}, and therefore the initial substrate strain, ε_{bi}, can be made.

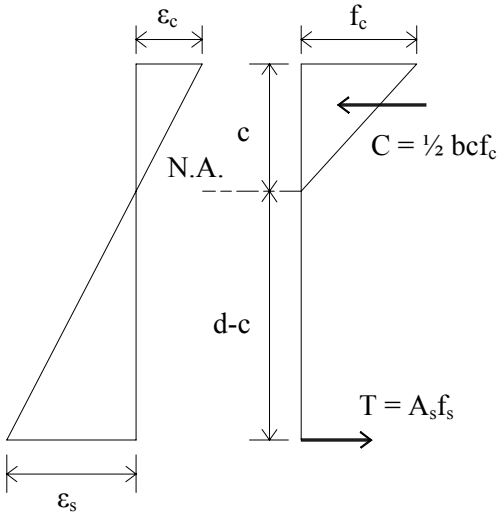

Figure C1.6-2 – Elastic Strain and Stress Across a Cracked RC Section

Horizontal force equilibrium should be used to calculate the moment of inertia.

$$A_s f_s = \frac{1}{2} bcf_c$$

$$f_s = E_s \varepsilon_s$$
$$f_c = E_c \varepsilon_c$$

Therefore, force equilibrium can be rewritten as follows:

$$A_s E_s \varepsilon_s = \frac{bc}{2} E_c \varepsilon_c .$$

By using similar triangles, we can obtain

SPECIFICATIONS

COMMENTARY

$$\frac{\varepsilon_c}{c} = \frac{\varepsilon_s}{d-c} \quad \Rightarrow \quad \varepsilon_s = \varepsilon_c \left(\frac{d}{c} - 1 \right)$$

And therefore force equilibrium may be written as follows:

$$A_s E_s \varepsilon_c \left(\frac{d}{c} - 1 \right) = \frac{bc}{2} E_c \varepsilon_c \Rightarrow \frac{A_s E_s}{E_c} \left(\frac{d}{c} - 1 \right) = \frac{bc}{2}$$

Replacing the modular ratio, E_s/E_c, with n, the force equilibrium equation can further be written as,

$$\frac{bc^2}{2} + nA_s c - nA_s d = 0 .$$

The quadratic equation can then be solved to determine the location of the neutral axis, c. Once c is found, the moment of inertia and the initial substrate strain can be found from the following two equations. It should be noted that the equation for the moment of inertia is in general for rectangular sections. Therefore, in a T-beam analysis, if the value c is found to be greater than the flange thickness, the equation should be altered slightly to account for the changing value of b as the concrete compression zone changes from flange to web.

$$I_{cr} = \frac{bc^3}{3} + nA_s \left(d - c \right)^2$$

$$\varepsilon_{bi} = \frac{M_{DL} \left(h - c \right)}{I_{cr} E_c}$$

C1.6.4.3

ε_{fd} in Equation (1-7) is the strain level at which debonding will occur and is determined in accordance with Section 1.6.4.6.4. Therefore, if the second expression in Equation (1-7) governs, FRP

SPECIFICATIONS

1.6.4.3 FRP REINFORCEMENT STRAIN AND STRESS

1.6.4.3.1 - The strain level in the FRP reinforcement at the ultimate limit state must be determined. FRP materials are linear elastic until failure and therefore the strain will directly dictate the stress level developed.

1.6.4.3.2 - The maximum strain level developed within the FRP will be that which occurs during concrete crushing, FRP rupture, or FRP debonding. This effective strain level can be determined from equation (1-7).

$$\varepsilon_{fe} = \varepsilon_{cu}\left(\frac{d_f - c}{c}\right) - \varepsilon_{bi} \le \varepsilon_{fd} \qquad (1\text{-}7)$$

1.6.4.3.3 - The maximum stress level developed within the FRP at failure can be found from the corresponding strain level. Equation (1-8) can be used to determine this effective stress level.

$$f_{fe} = E_f \varepsilon_{fe} \qquad (1\text{-}8)$$

1.6.4.4 SERVICEABILITY

1.6.4.4.1 - The serviceability of a bridge member under service loads should satisfy AASHTO specifications. The transformed-section analysis can be used to assess the FRP external reinforcement on the serviceability of a member.

1.6.4.4.2 - The existing internal steel reinforcement should be prevented from yielding under service loads in order to avoid inelastic deformations of reinforced concrete members.

1.6.4.4.3 - The stress in the internal steel under

COMMENTARY

debonding will be the failure mode, otherwise if the first expression governs; concrete crushing would be in the failure mode. If it is found that FRP does control the failure of the section, the concrete strain at failure, ε_c, may be less than 0.003 and can be calculated using similar triangles as presented in Equation (1-13).

C1.6.4.4

The procedure for applying a transformed-section analysis is presented in Section C1.6.4.2.

SPECIFICATIONS

service loads should be limited to 80% of its yield strength as shown in equation (1-9).

1.6.4.4.4 - The compressive stress in the concrete under service loading should be limited to 45% of the compressive strength as shown in equation (1-10).

$$f_{s,s} \le 0.80 f_y \quad (1\text{-}9)$$

$$f_{c,s} \le 0.45 f_c^{'} \quad (1\text{-}10)$$

1.6.4.5 CREEP-RUPTURE AND FATIGUE STRESS

Creep-rupture of the FRP reinforcement under sustained stresses and fatigue failure of the FRP due to cyclic stresses should be of great concern. The stress levels associated with these stress conditions, if present, should be checked. This section presents information to avoid these types of failure.

1.6.4.5.1 - To avoid failure of an FRP reinforced member due to creep-rupture and fatigue of the FRP, stress limits are imposed on the FRP reinforcement.

1.6.4.5.2 - The stress level in the FRP reinforcement can be found using an elastic analysis incorporating an applied moment due to all sustained loads plus the maximum moment induced in a fatigue loading cycle.

1.6.4.5.3 - The sustained stress should be limited as expressed by equation (1-11), where values of sustained plus cyclic stress limits are given in Table 1.6 – 1.

$$f_{f,s} \le sustained\ \ plus\ cyclic\ stress\ \text{lim}it \quad (1\text{-}11)$$

Table 1.6 – 1 - Sustained plus Cyclic Service Load Stress

COMMENTARY

C1.6.4.5

Creep-rupture is a type of failure in which a material is subjected to a constant load for such a time period known as the endurance time. It is when this endurance time has been reached, that the material can suddenly fail. Harsh environmental conditions, such as high temperatures, ultraviolet-radiation, and freeze thaw cycles, may decrease this endurance time. The most common type of FRP used for concrete rehabilitation, CFRP, is the most resistant to creep-rupture failure. The strength of the FRP is available for nonsustained loads if the sustained stress is kept below the creep-rupture stress limit.

As with creep-rupture, CFRP is the least susceptible to fatigue failure as well. With CFRP, an endurance limit of 60 to 70% of the initial static ultimate strength can be expected. This is in part due to the fact that CFRP is fairly unaltered by the moisture and temperature exposures of concrete structures unless environmental degradation of the fiber/resin interface is extensive.

SPECIFICATIONS COMMENTARY

	Fiber Type		
Stress Type	GFRP	AFRP	CFRP
Sustained plus cyclic stress limit	$0.20f_{fu}$	$0.30f_{fu}$	$0.55f_{fu}$

1.6.4.6 FAILURE MODES

1.6.4.6.1 - The controlling failure mode will govern the strength of a section. For a section strengthened with FRP, the following flexural failure modes, as listed in by ACI 440, should be investigated:

- Crushing of the concrete before yielding of the reinforcing steel
- Yielding of the steel in tension followed by rupture of the FRP laminate
- Yielding of the steel in tension followed by concrete crushing
- Shear/tension delamination of the concrete cover
- Debonding of the FRP from the concrete substrate

1.6.4.6.2 - Rupture of the externally bonded FRP is assumed to occur if the strain in the FRP reaches its design rupture strain ($\varepsilon_f = \varepsilon_{fu}$) before the concrete reaches its maximum usable strain ($\varepsilon_c = \varepsilon_{cu} = 0.003$).

1.6.4.6.3 - If the force within the FRP is too great to be sustained by the concrete substrate, cover delamination or FRP debonding can occur.

1.6.4.6.4 - To prevent the occurrence of a debonding failure mode, the effective strain developed within the FRP should be limited to the strain level at which debonding can occur, ε_{fd}. This limitation is defined in equation (1-12).

C1.6.4.6

The best fit coefficient of 0.083 in Equation (1-12) was developed by ACI Committee 440. The development resulted after assessing a significant data set of flexural beam tests focusing on FRP debonding failure. The reliability of Equation (1-12) to accurately portray FRP contribution to flexural strength is considered by imposing an additional strength reduction factor for FRP, ψ_f, as introduced in Section 1.6.4.1.

It is possible to improve the bond behavior in comparison to that determined by Equation (1-12) by use of transverse clamping as per procedure presented in Section 1.8.2.

$$\varepsilon_{fd} = 0.083\sqrt{\frac{f_c'}{nE_f t_f}} \le 0.9\varepsilon_{fu} \quad \text{in in.-lb units}$$

$$\varepsilon_{fd} = 0.41\sqrt{\frac{f_c'}{nE_f t_f}} \le 0.9\varepsilon_{fu} \quad \text{in SI units} \qquad (1\text{-}12)$$

In equation (1-12), n is the number of plies at the location along the length of the member where the flexural strength is being computed.

1.6.5 Method of Solution

Strain compatibility and force equilibrium should be satisfied when calculating the ultimate strength of a member reinforced with externally bonded composites. The calculation procedure should also consider the governing mode of failure. More than one calculation procedure can be derived to meet these conditions. A trial-and-error method is presented in this section.

In the trial-and-error procedure, an assumed depth to the neutral axis c is selected. Then, the strain level in each material is calculated using strain compatibility. With this strain, the corresponding stress levels are calculated and force equilibrium is checked. It these internal force resultants do not equilibrate, the neutral axis depth c is revised and the procedure is repeated.

1.6.5.1 STEP 1 – Preliminary Calculations

Before the trial-and-error procedure can be performed, some preliminary calculations need to be performed to obtain required

information. These preliminary calculations include the following:

- Calculate FRP system design material properties using the provisions of Article 1.5.3.4.
  - $f_{fu} = C_E f_{fu}^*$
  - $\varepsilon_{fu} = C_E \varepsilon_{fu}^*$

- Determine properties of the concrete, the existing reinforcing steel, and FRP.
  - Concrete – β_1(Article 1.6.2.9), E_c ($57{,}000\sqrt{f'_c}$)
  - Area of reinforcing steel – A_s
  - Area of external bonded FRP reinforcement - A_f

- Determine the initial substrate strain as explained in Article 1.6.4.2.

- Determine the design strain of the FRP system accounting for debonding failure using equation (1-12). Least value controls.

$$\varepsilon_{fd} = 0.083\sqrt{\frac{f'_c}{nE_f t_f}} \le 0.9\varepsilon_{fu} \quad \text{in in.-lb units} \qquad (1\text{-}12)$$

$$\varepsilon_{fd} = 0.41\sqrt{\frac{f'_c}{nE_f t_f}} \le 0.9\varepsilon_{fu} \quad \text{in SI units}$$

1.6.5.2 STEP 2 - Estimate the depth to the neutral axis, c

A reasonable first estimate can be taken as 0.20d.

1.6.5.3 STEP 3 – Calculate material strains

- Effective strain level in the FRP – equation (1-7)

SPECIFICATIONS COMMENTARY

$$\varepsilon_{fe} = \varepsilon_{cu}\left(\frac{d_f - c}{c}\right) - \varepsilon_{bi} \le \varepsilon_{fd} \qquad (1\text{-}7)$$

The controlling term in equation (1-7) signifies the controlling failure mode. If the first term controls, concrete crushing is the controlling failure mode; whereas if the second term controls, FRP rupture or debonding is the controlling failure mode.

If concrete crushing controls, the concrete strain is the maximum usable strain at 0.003. Otherwise, FRP failure controls and the concrete strain may be found using similar triangles as set in equation (1-13).

$$\varepsilon_c = \left(\varepsilon_{fe} + \varepsilon_{bi}\right)\left(\frac{c}{d_f - c}\right) \qquad (1\text{-}13)$$

- Strain in the existing reinforcing steel

This strain level can be found based off the strain level found in the FRP reinforcement using strain compatibility. Equation (1-14) provides this strain.

$$\varepsilon_s = \left(\varepsilon_{fe} + \varepsilon_{bi}\right)\left(\frac{d - c}{d_f - c}\right) \qquad (1\text{-}14)$$

1.6.5.4 STEP 4 – Calculate stresses in the reinforcing steel and FRP

Equation (1-8) of Article 1.6.4.3.3 can be used to find the effective stress in the FRP reinforcement.

$$f_{fe} = E_f \varepsilon_{fe} \qquad (1\text{-}8)$$

Equation (1-15) can be used to calculate the

stress in the reinforcing steel.

$$f_s = E_s \varepsilon_s \le f_y \qquad (1\text{-}15)$$

1.6.5.5 STEP 5 - Determine internal force resultants and check equilibrium

For T-beam analysis, two cases can occur. The depth of the rectangular stress block can be less than the flange thickness, in which the analysis is performed in the same manner as with a rectangular section. If the depth of the rectangular stress block (a) is greater than the flange thickness, the analysis has to account for it and hence, different equations are derived. In the following sections, equations are presented for each case that may be encountered. If force equilibrium is not satisfied for a given case, a different c value will be chosen and STEP 2 through STEP 5 should be repeated until force equilibrium is achieved.

1.6.5.6 STEP 6 - Compute nominal moment strength, M_n

With convergence on the correct neutral axis depth from STEP 5, the nominal moment strength can be calculated. As with the force equilibrium check, the equations used for the nominal moment strength are dependent on the analysis situation. These equations are presented in the following sections for each situation to be considered.

SPECIFICATIONS COMMENTARY

1.6.6 Tension Reinforcement Steel Only in Strengthened Section

1.6.6.1 DEPTH OF STESS BLOCK IS LESS THAN FLANGE THICKNESS

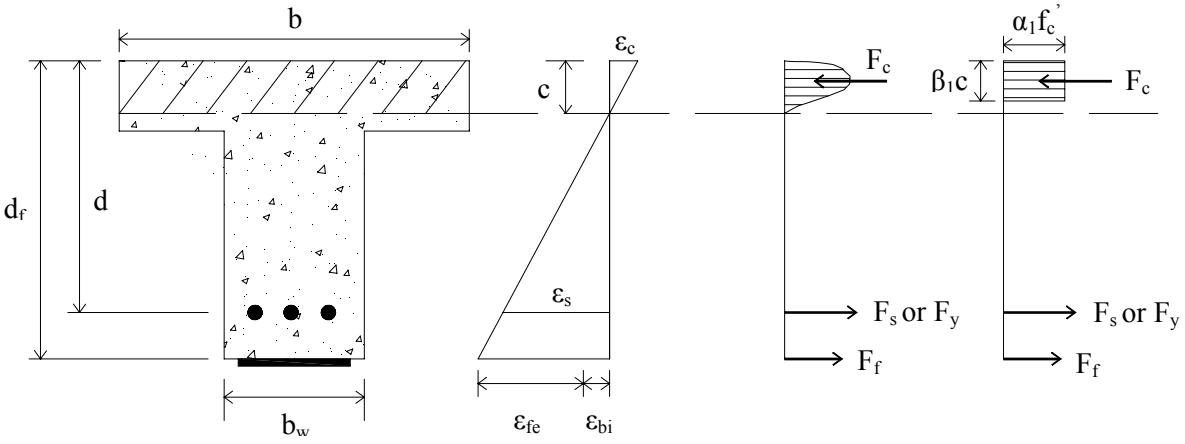

Figure 1.6 – 1 - Internal Strain and Stress Distribution at Ultimate Limit State ($\beta_1 c < h_f$)

1.6.6.1.1 This analysis is performed as if it were a rectangular section. Equation (1-16) may be used to check force equilibrium.

$$c = \frac{A_s f_s + A_f f_{fe}}{\alpha_1 f_c' \beta_1 b} \qquad (1\text{-}16)$$

The depth to the neutral axis is found by simultaneous satisfying equations (1-7), (1-8), (1-14), (1-15), and (1-16).

1.6.6.1.2 With the value of c known, the design moment strength can be determined using equation (1-17).

SPECIFICATIONS COMMENTARY

$$\Phi M_n = \Phi \begin{bmatrix} A_s f_s \left(d - \frac{\beta_1 c}{2} \right) + \\ \psi_f A_f f_{fe} \left(d_f - \frac{\beta_1 c}{2} \right) \end{bmatrix} \qquad (1\text{-}17)$$

1.6.6.1.3 Service condition properties are determined using a cracked section analysis as illustrated in Figure 1.6 – 2. The neutral axis depth at service loads, kd, can be calculated using equation (1-18).

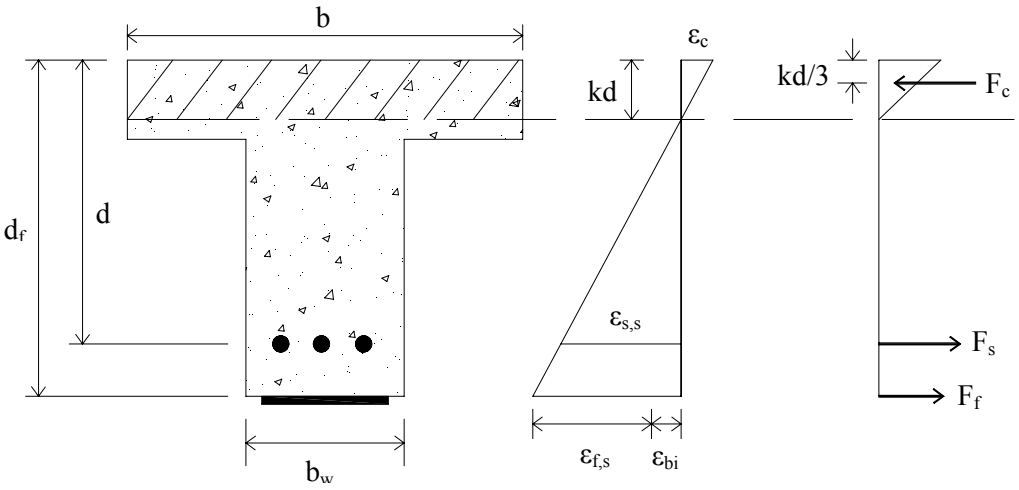

Figure 1.6 – 2 - Elastic Strain and Stress Distribution

$$k = \sqrt{\left(n_s \rho_s + n_f \rho_f \right)^2 + \left(2 n_s \rho_s + 2 n_f \rho_f \frac{d_f}{d} \right)} - \left(n_s \rho_s + n_f \rho_f \right) \qquad (1\text{-}18)$$

1.6.6.1.4 Equation (1-19) may be used to calculate the cracked moment of inertia, I_{cr}, of the section.

$$I_{cr} = \frac{b(kd)^3}{3} + n_s A_s \left(d - kd \right)^2 + n_f A_f \left(d_f - kd \right)^2 \qquad (1\text{-}19)$$

SPECIFICATIONS COMMENTARY

1.6.6.2 DEPTH OF STRESS BLOCK IS GREATER THAN FLANGE THICKNESS

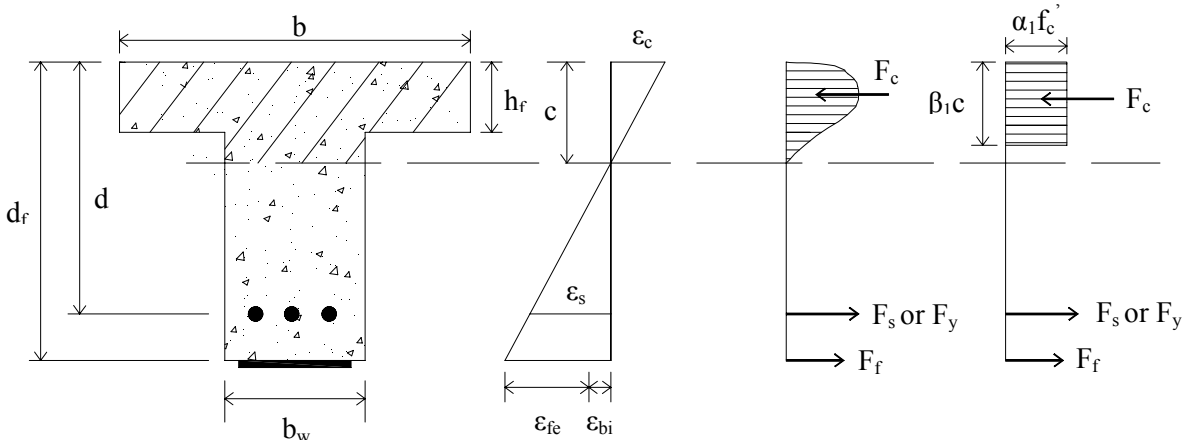

Figure 1.6 – 3 - Elastic Strain and Stress Distribution at Ultimate Limit State ($\beta_1 c > h_f$)

1.6.6.2.1 Force equilibrium may be checked by using equation (1-20) when the depth of the stress block is greater than the flange thickness.

$$c = \frac{A_s f_s + A_f f_{fe}}{\alpha_1 f_c' \beta_1 b_w} + \frac{t_f}{\beta_1 b_w}\left(b_w - b\right) \qquad (1\text{-}20)$$

The depth to the neutral axis is found by simultaneously satisfying equations (1-7), (1-8), (1-14), (1-15), and (1-20).

1.6.6.2.2 With the value of c known, the design moment strength can be determined using equation (1-21).

SPECIFICATIONS COMMENTARY

$$\Phi M_n = \Phi \begin{bmatrix} A_s f_s \left(d - \frac{\beta_1 c}{2} \right) + \\ \psi_f A_f f_{fe} \left(d_f - \frac{\beta_1 c}{2} \right) \end{bmatrix} \qquad (1\text{-}21)$$

1.6.6.2.3 Service condition properties are determined using a cracked section analysis. The neutral axis depth, kd, at service loads can be calculated by solving the polynomial of equation (1-22) using the coefficients given in equations (1-23), (1-24), and (1-25).

$$a_1 k^2 + a_2 k + a_3 = 0 \qquad (1\text{-}22)$$

$$a_1 = \frac{b_w d}{2b} \qquad (1\text{-}23)$$

$$a_2 = h_f \left(1 - \frac{b_w}{b} \right) + d \left(n_s \rho_s + n_f \rho_f \right) \qquad (1\text{-}24)$$

$$a_3 = \frac{h_f^{\,2}}{2d} \left(\frac{b_w}{b} - 1 \right) - n_s \rho_s d - n_f \rho_f d_f \qquad (1\text{-}25)$$

1.6.6.2.4 The cracked moment of inertia, I_{cr}, can be calculated using equation (1-26).

$$I_{cr} = \frac{b(h_f)^3}{3} + \frac{b_w (kd - h_f)^3}{3} + b h_f \left(kd \right) \left(kd - hf \right) + n_s A_s \left(d - kd \right)^2 + n_f A_f \left(d_f - kd \right)^2 \qquad (1\text{-}26)$$

1.6.7 Side Bonded FRP Laminates for Flexural Strengthening

The flexural properties of a member may also be increased by applying FRP reinforcement to the sides of a member. If this method is used for strengthening, the guidelines of Articles 1.6.7.1 and 1.6.7.2 shall apply.

SPECIFICATIONS

1.6.7.1 For any such side bonded FRP laminate, if the width of the laminate is less than $2d_c$, d_f may be taken as the distance from the extreme compression fiber to the centroid of the laminate. For laminate widths greater than $2d_c$, the laminate shall be divided into a series of equal width strips, with the width not exceeding d_c. d_f for each strip shall then be the distance from the extreme compression fiber to the centroid of that strip. This will help to more accurately account for the linear-elastic behavior of FRP.

1.6.7.2 The applicable sections contained in Article 1.6 shall be used in determining the contributions of externally bonded FRP applied in the manner presented in Article 1.6.8.

1.6.8 Stress in Reinforcing Steel Under Service Loads

The stress level in the reinforcing steel can be calculated using a cracked section analysis for the FRP strengthened section in accordance with equation (1-27). M_s is equal to the moment due to all sustained loads plus the maximum moment induced in a fatigue loading cycle.

$$f_{s,s} = \frac{\left[M_s + \varepsilon_{bi} A_f E_f \left(d_f - \frac{kd}{3}\right)\right](d - kd) E_s}{A_s E_s \left(d - \frac{kd}{3}\right)(d - kd) + A_f E_f \left(d_f - \frac{kd}{3}\right)(d_f - kd)} \quad (1\text{-}27)$$

This stress should be checked against the limits described in section 1.6.4.4.

1.6.9 Stress in FRP Under Service Loads

Equation (1-28) can be used to calculate the stress in the FRP reinforcement under service loads.

COMMENTARY

C1.6.8

Distributions of strain and stress are illustrated in Figure 1.6-2. In the same method as detailed in Section C1.6.4.2, the depth to the neutral axis, stated as kd, can be determined using a transformed section analysis. As opposed to conventional reinforced concrete analysis, the FRP component has to be incorporated, and therefore complicating the analysis. Similar to the transformed area of reinforcing steel, the transformed area of FRP can be obtained by multiplying the area of FRP with the modular ratio of FRP to concrete. This method doesn't consider the initial substrate strain as it causes a negligible difference in the depth of the neutral axis within the elastic range.

C1.6.9

The stress in the reinforcing steel under service loads can be directly related to the stress in the FRP under service loads as a result of a linear strain distribution and known material properties. Therefore, $f_{s,s}$ can be used in Equation (1-

SPECIFICATIONS

$$f_{f,s} = f_{s,s}\left(\frac{E_f}{E_s}\right)\frac{d_f - kd}{d - kd} - \varepsilon_{bi}E_f \qquad (1\text{-}28)$$

The stress calculated using equation (1-28) should be checked against the limits set forth in section 1.6.4.5.

1.7 SHEAR DESIGN

Wrapping or partially wrapping members can increase the shear strength. The fibers are oriented transverse to the longitudinal axis of beam members or perpendicular to potential shear crack locations in order to achieve this increase in shear strength.

This section presents guidance for determining the shear strength contributions of FRP when used as shear reinforcement.

1.7.1 Wrapping Schemes

Three types of wrapping schemes are typically used for shear reinforcement and are presented in Figure 1.7 – 1.

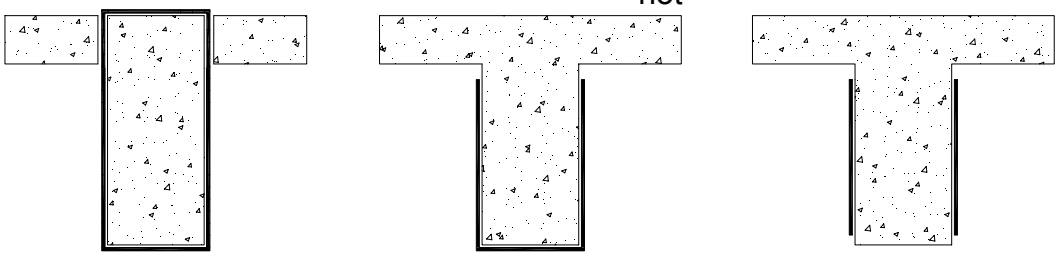

Completely Wrapped | 3 Sided "U-Wrap" | 2 Sides Wrapped

Figure 1.7 – 1 - Typical Wrapping Schemes for FRP Shear Strengthening

COMMENTARY

28) after it has been obtained from Equation (1-27). The stress level given by Equation (1-28) is the stress under an applied moment within the elastic response range of the member.

C1.7

The amount of additional shear strength that can be obtained by an FRP system is dependent of several factors. These factors include beam geometry, wrapping scheme, and the existing shear strength of the concrete.

C1.7.1

For RC T-beams, wrapping 3 sides or U-wrapping is the most efficient wrapping scheme since wrapping all four sides is not very practical. In any of the three wrapping schemes, the FRP system may be installed continuously along the longitudinal length of the member or

SPECIFICATIONS

COMMENTARY

applied as discrete strips. Many FRP systems are moisture impermeable, and hence, there is much concern with using continuously placed U-wrapping schemes as they may possibly entrap contaminants and accelerate the corrosion process. For this reason, FRP reinforcement that encases a member entirely and may prevent the passage of moisture is discouraged.

1.7.2 Shear Strengthening

1.7.2.1 The design shear strength can be calculated by multiplying the nominal shear strength by the strength reduction factor, Φ.

1.7.2.2 For an FRP-strengthened concrete member, the nominal shear strength can be determined by summing the contributions due to the FRP shear reinforcement, the reinforcing steel, and the concrete, as presented in equation (1-29).

$$V_n = V_c + V_s + \Psi_f V_f \qquad (1\text{-}29)$$

In equation (1-29),

V_n = nominal shear strength
V_c = nominal shear strength contribution from the concrete
V_s = nominal shear strength contribution from the steel
V_f = nominal shear strength contribution from the FRP
Ψ_f = reduction factor for the FRP shear strength contribution

Values for the reduction factor, Ψ_f, are given in Table 1.7 – 1.

Table 1.7 - 1 - Recommended Additional Reduction Factors for FRP Shear Reinforcement

C1.7.2

The current value of the strength reduction factor, Φ, is 0.75 for shear in accordance with ACI 318 – 08.

ACI recommends the reduction factor Ψ_f as presented in Table 1.7-1 based on a reliability analysis that uses data from Bousselham and Chaallal (2006), Deniaud and Cheng (2001, 2003), Funakawa et al. (1997), Matthys and Triantafillou (2001), and Pellegrino and Modena (2002).

SPECIFICATIONS COMMENTARY

$\Psi_f = 0.85$	Three sides and two opposite side schemes

1.7.2.3 The design of cross-sections for shear shall be based on equation (1-30).

$$\phi V_n \geq V_u \qquad (1\text{-}30)$$

1.7.3 Concrete and Steel Shear Strength Contribution

The contribution of shear strength provided by the concrete and steel can be determined with reference to Article 5.8.3.3.

1.7.4 FRP Shear Strength Contribution

The dimensional variables used in calculating the FRP contribution to shear strength are illustrated in Figure 1.7 – 1. Calculations are based off a proposed fiber orientation and an assumed shear crack pattern. The following sections present the applicable calculations.

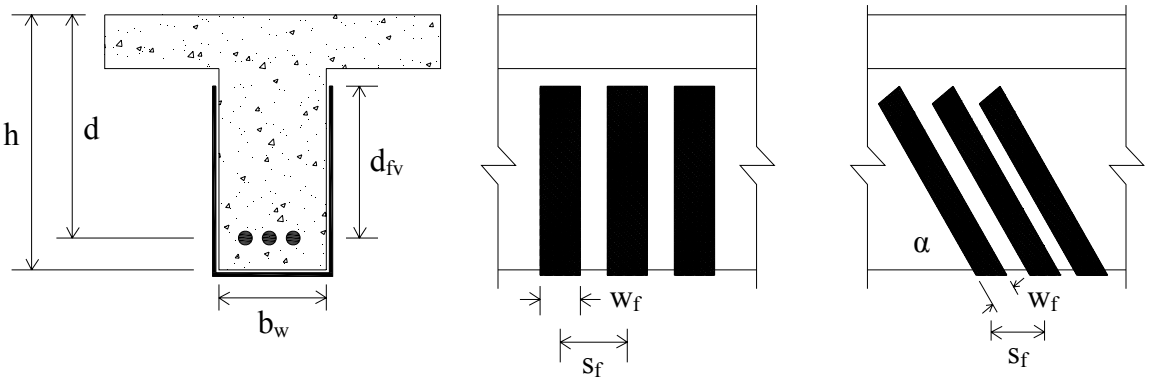

Figure 1.7 – 1 - Shear Strengthening Illustration Including Dimensional Variables Used

1.7.4.1 If the design shear strength provided by the concrete and steel, $\Phi(V_c + V_s)$, does not

SPECIFICATIONS

surpass the factored shear force, V_u, FRP shear reinforcement may be applied in order to satisfy equation (1-30). The FRP contribution to shear may not be less than that required in accordance with Article 1.7.5.

1.7.4.2 Where flexural capacity has been increased for an increase in loading condition, it is important to check that shear strength is adequate to withstand the corresponding increase in shear force. Shear reinforcing FRP may be required in this situation.

1.7.4.3 If FRP reinforcement perpendicular to the axis of the member is used, the contribution to shear strength may be computed using equation (1-31),

$$V_f = \frac{A_{fv} f_{fe} d_{fv}}{s_f} \qquad (1\text{-}31)$$

where,

$$A_{fv} = 2nt_f w_f \qquad (1\text{-}32)$$

1.7.4.4 If FRP reinforcement inclined to the axis of the member is used, the contribution to shear strength may be computed using equation (1-33).

$$V_f = \frac{A_{fv} f_{fe} \left(\sin\alpha + \cos\alpha\right) d_{fv}}{s_f} \qquad (1\text{-}33)$$

1.7.5 Effective Strain in FRP Shear Reinforcement

The effective strain is the strain that is achieved within the FRP system at the nominal strength. This strain is governed by the failure mode of the FRP system and the failure mode of the strengthened reinforced concrete member.

The sections that follow provide guidelines

COMMENTARY

C1.7.4.1 Article 1.7.5 is only relevant with completely wrapped members and is applied to prevent a mode of failure in which loss of aggregate interlock of the concrete occurs.

SPECIFICATIONS

on determining the effective strain for different configurations of FRP shear reinforcement.

1.7.5.1 SECTIONS COMPLETELY WRAPPED

To prevent a mode of failure in which loss of aggregate interlock of the concrete occurs, the maximum strain used for design should be limited to 0.4% when members are to be completely wrapped. This limit is shown in equation (1-34).

$$\varepsilon_{fe} = 0.004 \le 0.75\varepsilon_{fu} \qquad (1\text{-}34)$$

1.7.5.2 SECTIONS NOT COMPLETELY WRAPPED

For two and three sided wraps, delamination from the concrete has been shown to occur before loss of aggregate interlock. A bond-reduction coefficient, κ_v, is used in calculating the effective strain for this type of shear reinforcement layout. The procedure is presented in equations (1-35) through (1-39) as follows:

$$\varepsilon_{fe} = \kappa_v \varepsilon_{fu} \le 0.004 \qquad (1\text{-}35)$$

where,

$$\kappa_v = \frac{k_1 k_2 L_e}{468\varepsilon_{fu}} \le 0.75 \quad \text{in in.-lb units}$$

$$\kappa_v = \frac{k_1 k_2 L_e}{11{,}900\varepsilon_{fu}} \le 0.75 \quad \text{in SI units} \qquad (1\text{-}36)$$

and L_e is the active bond length, given by equation (1-37).

$$L_e = \frac{2500}{\left(n_f t_f E_f\right)^{0.58}} \quad \text{in in.-lb units}$$

COMMENTARY

C1.7.5.1

The strain limit presented was determined adequate through experience and testing (Priestley et al. 1996). Any higher strains for FRP applications in which the member is completely wrapped should not be used.

C1.7.5.2

The bond-reduction coefficient, κ_v, was developed after an analysis of bond stresses to determine the usefulness of two and three sided wraps and the effective strain level that could be achieved (Triantafillou 1998a).

The active bond length, L_e, is the length in which most of the bond stress is sustained.

The method used in this section to determine κ_v has been proven valid for regions of high shear and low moment. It has been suggested by ACI Committee 440 that although the method has not been validated for shear strengthening in regions of high flexural and shear stresses or sections where the web in mainly in compression, κ_v is sufficiently conservative to be used in such cases.

It is imperative that the effective strain in FRP laminates not exceed 0.004 in any circumstance.

SPECIFICATIONS

COMMENTARY

$$L_e = \frac{23{,}300}{\left(n_f t_f E_f\right)^{0.58}} \quad \text{in SI units} \tag{1-37}$$

Two modification factors, k_1 and k_2, are used to account for the concrete strength and the type of wrapping scheme and are determined by equations (1-38) and (1-39).

$$k_1 = \left(\frac{f_c'}{4000}\right)^{2/3} \quad \text{in in.-lb units}$$

$$k_1 = \left(\frac{f_c'}{27}\right)^{2/3} \quad \text{in SI units} \tag{1-38}$$

$$k_2 = \begin{cases} \dfrac{d_{fv} - L_e}{d_{fv}} & \text{for U - wraps} \\ \dfrac{d_{fv} - 2L_e}{d_{fv}} & \text{for two sides bonded} \end{cases} \tag{1-39}$$

1.7.6 Spacing Limits

The spacing limits for FRP shear reinforcing strips should conform to the limits set forth in Article 5.8.2.7 for internal steel reinforcement. Spacing of FRP strips is the distance between the center lines of the strips.

1.7.7 Reinforcement Limits

The shear strength provided by reinforcement alone is the sum of that contributed by steel and FRP. This shear strength contribution from reinforcement should be limited as stated in equation (1-40).

$$V_s + V_f \le 8\sqrt{f_c'}\, b_w d \quad \text{in in.-lb units} \tag{1-40}$$

C1.7.7

Equation (1-40) is the current limit for shear reinforcement in which more than one type of shear reinforcement is used as presented in ACI 318-08.

SPECIFICATIONS

$V_s + V_f \le 0.66\sqrt{f_c'}b_w d$ in SI units

1.8 DETAILING

Adequate FRP reinforcement details are necessary to ensure that the expected FRP system performance is achieved. This section presents guidance for detailing FRP sheets or laminates.

1.8.1 General Detailing Concerns

1.8.1.1 Do not turn inside corners. For example, do not turn the inside corner where a beam meets the bottom of the slab.

1.8.1.2 When turning an outside corner, provide at minimum, a ½ inch radius of curvature.

1.8.1.3 Provide adequate development length.

1.8.1.4 When splicing FRP plies, sufficient overlap should be provided.

1.8.2 Prevention of FRP End Peeling

1.8.2.1 Transverse FRP stirrups or anchorage can be used to prevent FRP end peeling failure.

1.8.2.2 Locating the curtailment as close as possible to the region of zero moment minimizes the stress at the FRP curtailment and can help mitigate FRP end peeling failure.

1.8.2.3 If the factored shear force at the termination point exceeds 2/3 the concrete shear strength, transverse reinforcement such as FRP anchors should be used to prevent the concrete cover layer from splitting.

1.8.2.4 Equation (1-41) can be used to

COMMENTARY

C1.8.2

FRP end peeling is also referred to as concrete cover delamination and can occur as a result of the normal stresses developed at the ends of externally bonded FRP reinforcement. These normal stresses are presented conceptually in Figure C1.8.2-1 along with the interfacial shear stresses as taken from ACI 440.2-08. In concrete cover delamination, the existing reinforcing steel may act as a bond separator in the horizontal plane and cause the concrete

SPECIFICATIONS

determine the area of the transverse clamping FRP U-wrap.

$$A_{fanchor} = \frac{\left(A_f f_{fu}\right)_{longitudinal}}{\left(E_f \kappa_v \varepsilon_{fu}\right)_{anchor}} \quad (1\text{-}41)$$

In equation (1-41), κ_v is calculated using equation (1-36).

1.8.2.5 CUTOFF POINTS

The following guidelines apply for both positive and negative moment regions.

1.8.2.5.1 In the case of simply supported beams, the termination point for a single-ply laminate should be at least a distance l_{df}, as determined by equation (1-42), past the point along the span that corresponds to the cracking moment, M_{cr}.

1.8.2.5.2 In the case of simply supported beams, the termination points for multiple-ply laminates should be tapered. The termination point for the outermost ply should be at a distance l_{df} past the point along the span that corresponds to the cracking moment, M_{cr}. Each additional ply should be terminated at least 6 inches past the previous ply.

1.8.2.5.3 In the case of continuous beams, the termination point for a single-ply laminate should be at least a distance d/2 or 6 inches beyond the inflection point.

1.8.2.5.4 In the case of continuous beams, the termination points for multiple-ply laminates should be tapered. at least a distance d/2 or 6 inches beyond the inflection point. The termination point for the outermost ply should be no less than 6 inches beyond the inflection point. Each additional ply should be terminated at least 6 inches past the previous

COMMENTARY

cover to pull away from the upper portion of the beam as presented in Figure C1.8.2-2 reprinted from ACI 440.2-08.

It should be considered good practice to incorporate transverse FRP stirrups as anchorage and locate the curtailment as close to the region of zero moment as possible to limit the possibility for FRP end peeling failure.

If end peeling has been adequately mitigated, or the member has a relatively long shear span, debonding can possible initiate at flexural cracks, flexural/shear cracks, or both, near the region of maximum moment. This can happen because when loaded, these cracks tend to open and create large interfacial shear stresses. In this case, debonding will propagate along the shear span in the direction of decreasing moment through the thin, largely mortar composed layer creating the surface of the concrete girder. This mode of failure can be more probable in sections having high shear-moment ratios.

The possibility for this debonding failure may be lessened by increasing the stress transfer through the effective implementation of mechanical anchorages (Khalifa et al. 1999). The success of such anchorages is believed not to result from an enhancement of interfacial shear capacity but rather from their ability to resist the tensile normal stresses (Quattlebaum et al. 2005). In any case, there is limited data that leads to the conclusion that only a modest increase in FRP strain at debonding can be obtained with anchoring FRP wraps (Reed et al. 2005).

SPECIFICATIONS

ply.

1.8.3 Development Length

The available anchorage length of FRP should surpass the value given by equation (1-42) in order to develop the effective FRP stress at a section.

$$l_{df} = 0.057\sqrt{\frac{nE_f t_f}{\sqrt{f_c'}}} \quad \text{in in.-lb units}$$

$$l_{df} = \sqrt{\frac{nE_f t_f}{\sqrt{f_c'}}} \quad \text{in SI units} \qquad (1\text{-}42)$$

1.8.4 Laps and Splices

Lap splices may be used to ensure that the fibers of FRP systems are continuous and oriented in the direction of the largest tensile forces. Fibers should be overlapped along their length. Ample overlap should be provided to support failure of the FRP laminate before debonding of the overlapped laminates.

1.8.4.1 The required overlap for individual FRP systems should be set forth by the material manufacturer and validated through testing which is independent of the manufacturer.

1.8.4.2 In the case of unidirectional FRP laminates, lap splices are only required in the

COMMENTARY

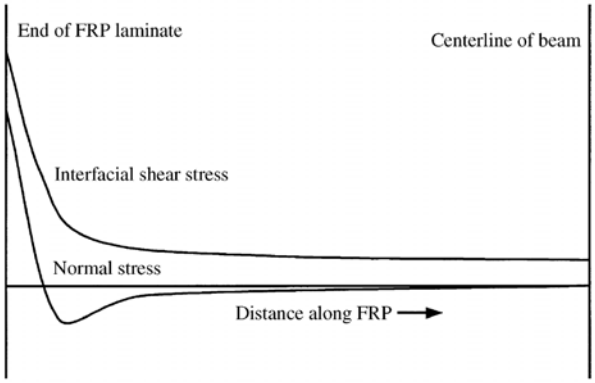

Figure C1.8.2-1 – Conceptual Interfacial and Normal Stresses along a Bonded FRP Laminate (Roberts and Haji-Kazemi 1989; Malek at al. 1998)

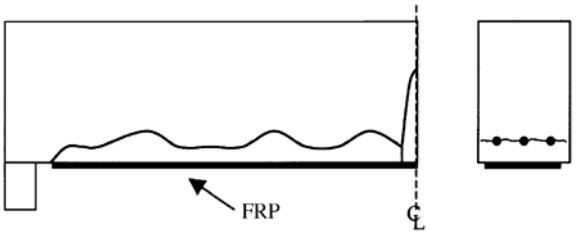

Figure C1.8.2-2 – Delamination Caused by Tension Failure of the Concrete Cover

C1.8.4

Splices for FRP laminates shall be placed in accordance with drawings,

SPECIFICATIONS

direction of the fibers.

1.8.4.3 To maintain the continuity of fibers and overall strength of the FRP laminates, multidirectional fabrics require lap splices in more than one direction.

1.8.4.4 Lap splices shall not be placed in the central third of simply supported spans.

1.8.4.5 Lap splices shall not be placed in the central quarter or the end 1/8 of continuous spans.

COMMENTARY

specifications, and as certified by the licensed design professional in agreement with recommendations from the system manufacturer. The thickness of the FRP system, tensile strength, and the bond strength between adjacent layer of laminates should control the required overlap for lap-splices.

1.9 EXAMPLE DESIGN PROBLEMS

1.9.1 Flexural Strengthening of a Reinforced Concrete T-beam with FRP laminates

After inspection and proper testing, it is determined that a reinforced concrete T-beam bridge is in poor condition and needs repair. The bridge is selected for retrofit with FRP.

Examining one of the interior beams, it is determined that only about 65% of the reinforcing tension steel remains after many years of deterioration. With 10 #11 bars being used in the original design, only 10 in^2 of steel area remains. The beam has the dimensions as shown in Figure 1.

A BAR7 analysis gives an inventory load rating factor of 0.83, and it is decided to strengthen the beam to achieve a minimum inventory load rating factor of 1.0. This requires increasing the nominal moment capacity of the beam from 1037 k-ft to 1138 k-ft.

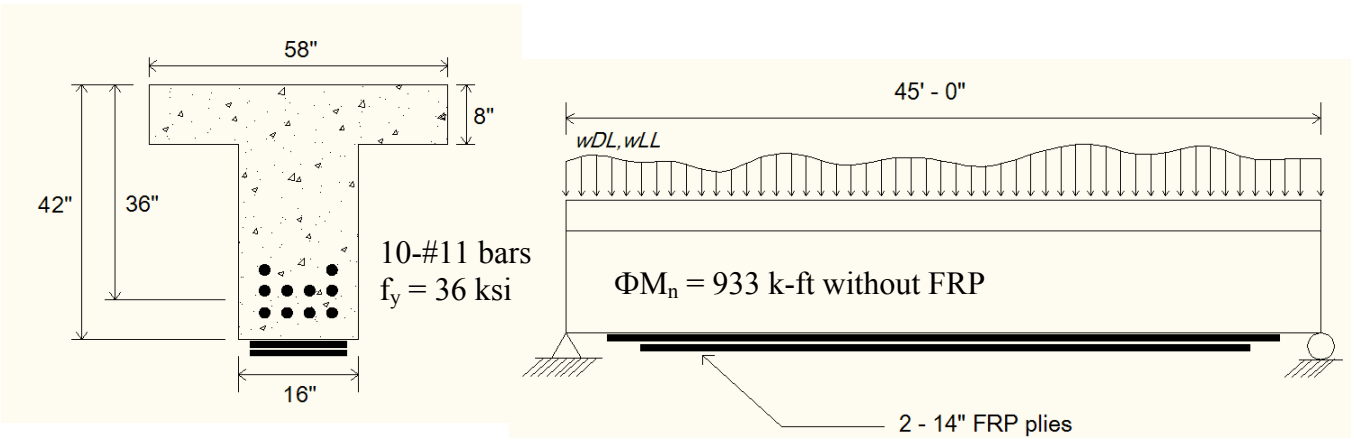

Cross-Section Elevation

Figure 1: Simply Supported T-Beam with Externally Bonded FRP

Beam dimensions and properties are presented in Table 1.

Table 1: Beam Dimensions and Properties

L	45 ft
b_w	16 in.
b	58 in.
h	42 in.
d	36 in.
f_c'	3000 psi
f_y	36 ksi
$A_{s\ original}$	15.6 in^2
$A_{s\ remaining}$	10 in^2
$\Phi M_{n\ existing}$	933 k-ft
$\Phi M_{n\ required}$	1024 k-ft
M_{DL}	415 k-ft
M_{LL}	214 k-ft
$1.1M_{DL} + 0.75M_{LL}$	617 k-ft

Note that the unstrengthened moment limit is less than the existing moment strength without FRP as per Equation (1-4). The beam is to be strengthened with an FRP system as detailed in Table 2. Two 14 in. wide layers will be applied using the wet layup technique.

Table 2: Manufacturer's Reported FRP System Properties

t_f	0.0065 in/ply
f_{fu}*	550 ksi
ε_{fu}*	0.0167 in/in
E_f	33000 ksi

The strengthening design calculations are as follows.

STEP 1 – Preliminary Calculations

SPECIFICATIONS COMMENTARY

- FRP system design material properties

Table 1.5-2 presents the environmental reduction factors.

Exterior exposure: $C_F = 0.85$

$$f_{fu} = C_E f_{fu}^{*} = 0.85(550) = 467.5 \ \ ksi$$
$$\varepsilon_{fu} = C_E \varepsilon_{fu}^{*} = 0.85(0.0167) = 0.0142 \ \ in/in$$

Equations (1-1) and (1-2)

- Properties of the concrete, steel, and FRP (Section 1.6.5.1)

$$E_c = 57000\sqrt{f_c'} = 57000\sqrt{3000} = 3122 \ \ ksi$$

$A_s = 10 \ \ in^2$ (as previously stated)

$$A_f = nt_f w_f = 2(0.0065)(14) = 0.182 \ \ in^2$$

- Initial substrate strain, ε_{bi} (Section 1.6.4.2)

A cracked section analysis provides that c = 9.26 in.
With this, $I_{cr} = 81821$ in^4

$$\varepsilon_{bi} = \frac{M_{DL}(h-c)}{I_{cr}E_c} = \frac{415(12000)(42-9.26)}{81821(3122)(1000)} = 0.00064$$ (See Section C1.6.4.2)

- Determine the design strain of the FRP system (Equation (1-12))

$$\varepsilon_{fd} = 0.083\sqrt{\frac{f_c'}{nE_f t_f}} \le 0.9\varepsilon_{fu}$$

$$\varepsilon_{fd} = 0.083\sqrt{\frac{3000}{2(33000000)(0.0065)}} = 0.0069$$

$$\varepsilon_{fd} = 0.0069 \le 0.9(0.0142) = 0.0128$$

Design strain is lower than the rupture strain and, therefore, debonding controls the design of the FRP system.

$$\varepsilon_{fd} = 0.0069$$

STEP 2 – Estimate the depth to the neutral axis, c

First estimate: c = 0.20d = 0.20(36) = 7.2 in.

STEP 3 – Calculate material strains

- Effective strain level in the FRP (Equation (1-7))

$$\varepsilon_{fe} = \varepsilon_{cu}\left(\frac{d_f - c}{c}\right) - \varepsilon_{bi} \le \varepsilon_{fd}$$

$$\varepsilon_{fe} = 0.003\left(\frac{42 - 7.2}{7.2}\right) - 0.00064 = 0.0139$$

$$\varepsilon_{fe} = 0.0139 > \varepsilon_{fd} = 0.0069$$

$$\therefore \quad \varepsilon_{fe} = \varepsilon_{fd} = 0.0069$$

Since the second expression controls, FRP debonding is the failure mode and hence, concrete strain may be less than 0.003 and can be determine by using similar triangles. (Equation (1-13))

$$\varepsilon_c = \left(\varepsilon_{fe} + \varepsilon_{bi}\right)\left(\frac{c}{d_f - c}\right) = \left(0.0069 + 0.00064\right)\left(\frac{7.2}{42 - 7.2}\right) = 0.0016$$

- Strain in the existing reinforcing steel (Equation (1-14))

$$\varepsilon_s = \left(\varepsilon_{fe} + \varepsilon_{bi}\right)\left(\frac{d - c}{d_f - c}\right)$$

$$\varepsilon_s = \left(0.0069 + 0.00064\right)\left(\frac{36 - 7.2}{42 - 7.2}\right) = 0.0062$$

$$\varepsilon_s = 0.0062$$

STEP 4 – Calculate stresses in the FRP and reinforcing steel

$$f_{fe} = E_f \varepsilon_{fe} = 33000(0.0069) = 227.7 \ \ ksi$$

$$f_s = E_s \varepsilon_s \le f_y \ \Rightarrow \ f_s = 29000(0.0062) = 179.8 \ \ ksi$$

$$\therefore \ \ f_s = f_y = 36 \ \ ksi$$

STEP 5 – Determine internal force resultants and check equilibrium

For a more accurate analysis, concrete stress block factors may be calculated based on the parabolic stress-strain relationship for concrete as follows:

$$\beta_1 = \frac{4\varepsilon_c^{'} - \varepsilon_c}{6\varepsilon_c^{'} - 2\varepsilon_c} \qquad \alpha_1 = \frac{3\varepsilon_c^{'}\varepsilon_c - \varepsilon_c^{\,2}}{3\beta_1 \varepsilon_c^{'2}}$$

Where $\varepsilon_c^{'}$ is the strain that corresponds to $f_c^{'}$ and is calculated as follows:

$$\varepsilon_c^{'} = \frac{1.7 f_c^{'}}{E_c}$$

$$\varepsilon_c^{'} = \frac{1.7(3000)}{3122000} = 0.0016$$

$$\beta_1 = \frac{4(0.0016) - (0.0016)}{6(0.0016) - 2(0.0016)} = 0.750$$

$$\alpha_1 = \frac{3(0.0016)(0.0016) - (0.0016)^2}{3(0.750)(0.0016)^2} = 0.889$$

With the stress block factors known, force equilibrium can be verified by computing the value of c.

$$c = \frac{A_s f_s + A_f f_{fe}}{\alpha_1 f_c^{'} \beta_1 b}$$

$$c = \frac{10(36) + 0.182(227.7)}{0.889(3)(0.750)(58)} = 3.46$$

$c = 3.46 \ \ in. \neq 7.2 \ \ in. \ \ \therefore NG$

As can be seen, the calculated value of c does not match the initial estimate. Steps 2 through 5 must be repeated until the initial estimate matches the calculate value, and hence, equilibrium is achieved.

This process was repeated several times with different values of c and the results of the finial iteration are shown below.

Final iteration results

$c = 4.82 \ \ in.; \ \varepsilon_s = 0.0063; \ f_s = f_y = 36 \ \ ksi; \ \beta_1 = 0.708; \ \alpha_1 = 0.676; \ f_{fe} = 227.7 \ \ ksi$

$$c = \frac{10(36) + 0.182(227.7)}{0.676(3)(0.708)(58)} = 4.82$$

$c = 4.82 \ \ in. \ \ OK$

STEP 6 – Compute nominal moment strength, M_n

The design flexural strength is calculated using Equation (1-17)

$$\Phi M_n = \Phi \begin{bmatrix} A_s f_s \left(d - \frac{\beta_1 c}{2} \right) + \\ \psi_f A_f f_{fe} \left(d_f - \frac{\beta_1 c}{2} \right) \end{bmatrix}$$

The reduction factor $\psi_f = 0.85$ is applied to the contribution of the FRP system.

- Steel contribution:

$$M_{ns} = A_s f_s \left(d - \frac{\beta_1 c}{2} \right)$$

$$M_{ns} = 10(36) \left(36 - \frac{0.708(4.82)}{2} \right)$$

$$M_{ns} = 12346 \ \ k - in. = 1023 \ \ k - ft.$$

- FRP contribution:

$$M_{nf} = A_f f_{fe}\left(d_f - \frac{\beta_1 c}{2}\right)$$

$$M_{nf} = 0.182(227.7)\left(42 - \frac{0.708(4.82)}{2}\right)$$

$$M_{nf} = 1670 \ \ k-in. = 139 \ \ k-ft.$$

- Design Flexural Strength:

$$\varepsilon_s = 0.0063 > 0.005$$

Therefore, a strength reduction factor of Φ = 0.9 is appropriate as in accordance with Section 1.6.4.1.

$$\Phi M_n = \Phi\left[M_{ns} + \psi M_{nf}\right]$$

$$\Phi M_n = 0.9\left[1023 + 0.85(139)\right] = 1027 \ \ k-ft.$$

$$\Phi M_n = 1027 \ \ k-ft > \Phi M_u = 1024 \ \ k-ft. \ \ OK$$

The strengthened section reaches the required moment capacity.

FINAL STEP – Check service stresses in the reinforcing steel and FRP

Calculate the elastic depth to the cracked neutral axis by using Equation (1-18).

$$k = \sqrt{\left(n_s\rho_s + n_f\rho_f\right)^2 + \left(2n_s\rho_s + 2n_f\rho_f\frac{d_f}{d}\right)} - \left(n_s\rho_s + n_f\rho_f\right)$$

$$k = \sqrt{\left((9.3)(0.00479) + (10.6)(0.000075)\right)^2 + \left(2(9.3)(0.00479) + 2(10.6)(0.000075)\frac{42}{36}\right)} - \left((9.3)(0.00479) + (10.6)(0.000075)\right)$$

$$k = 0.260$$

$$c = kd = 0.260(36) = 9.36 \ \ in$$

Next, the stress level in the reinforcing steel should be checked using Equation (1-27) as follows.

$$f_{s,s} = \frac{\left[M_s + \varepsilon_{bi} A_f E_f \left(d_f - \frac{kd}{3}\right)\right](d - kd) E_s}{A_s E_s \left(d - \frac{kd}{3}\right)(d - kd) + A_f E_f \left(d_f - \frac{kd}{3}\right)\left(d_f - kd\right)} \le 0.80 f_y$$

M_s is maximum distributed live load + impact factor ($M_{LL}(1.3)$) obtained from an HS20 Truck loading. M_s is determined to be (214 k-ft)(1.3) = 278 k-ft. in accordance with the AASHTO Standard Specification for Highway Bridges.

$$f_{s,s} = \frac{\left[278(12) + 0.00064(0.182)(33000)(42 - \frac{9.36}{3})\right](36 - 9.36)29000}{10(29000)(36 - \frac{9.36}{3})(36 - 9.36) + 0.182(33000)(42 - \frac{9.36}{3})(42 - 9.36)}$$

$$f_{s,s} = 10.3 \ \ ksi \le 0.8(36 \ \ ksi) = 28.8 \ \ ksi$$

Therefore, the stress level in the reinforcing steel is within the recommended limit.

The stress level in the FRP under service loads can be calculated using Equation (1-28). This stress needs to be less than the creep-rupture stress limit as given in Table 1.6-1.

$$f_{f,s} = f_{s,s}\left(\frac{E_f}{E_s}\right)\frac{d_f - kd}{d - kd} - \varepsilon_{bi} E_f$$

$$f_{f,s} = 10.3\left(\frac{33000}{29000}\right)\left(\frac{42 - 9.36}{36 - 9.36}\right) - \left(0.00064\right)\left(33000\right) = -6.76 \ \ ksi$$

Sustained plus cyclic stress limit = $0.55 f_{fu}$

$$f_{f,s} = -6.76 \ \ ksi \le (0.55)(467.5 \ \ ksi) = 257 \ \ ksi$$

Therefore, the stress level in the FRP is within the recommended sustained plus cyclic stress limit.

Note:
In detailing the FRP reinforcement, the FRP should be terminated a minimum of l_{df}, calculated in accordance with Equation (1-42), past the point on the moment diagram where cracking should occur. FRP end peeling should also be checked at the FRP termination point by seeing that the factored shear force at that point is not greater than 2/3 the concrete shear strength. If the factored shear force is greater than 2/3 the concrete

shear strength, the FRP flexural reinforcement should be terminated closer to the supports. U-wraps may also be used to eliminate cover delamination.

1.9.2 Shear strengthening of an interior reinforced concrete T-beam

A reinforced concrete T-beam (f_c' = 3000 psi) is shown to have approximately a uniform 20% decrease in shear reinforcing steel area as a result of many years of corrosion. It is found that this loss in area decreases the shear strength to an inadequate level. The nominal shear strength provided by the concrete is calculated to be V_c = 72 kips, and that provided by the remaining shear reinforcement steel is V_s = 31 kips. Therefore, in accordance with AASHTO Standard Specifications for Highway Bridges, $\Phi V_{n\ existing}$ = 0.85(72 + 31) = 87.6 kips. The factored required shear strength at a distance d from the support is V_u = 100 kips. The shear diagram showing the section of the span length where shear strengthening is required is illustrated in Figure 2.

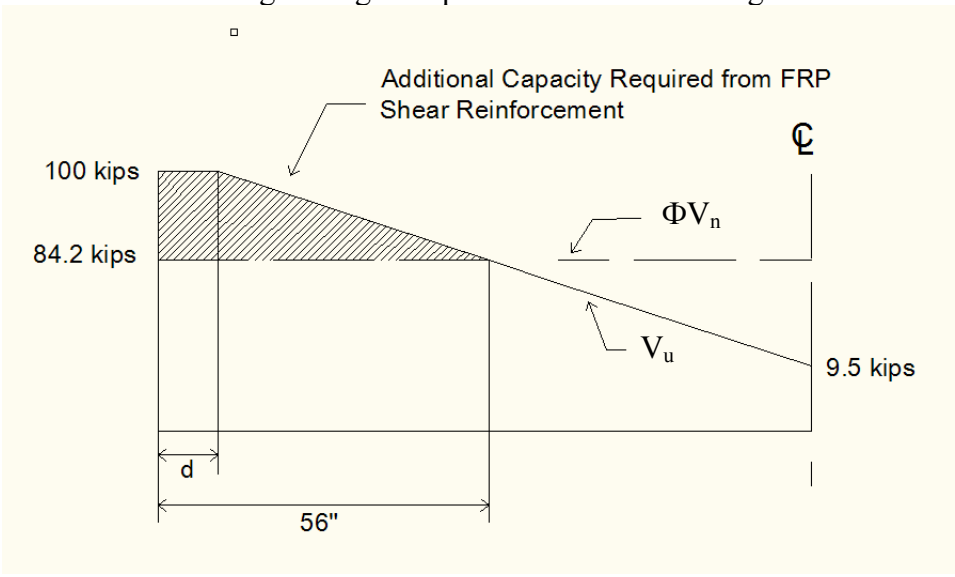

Figure 2: Shear Diagram

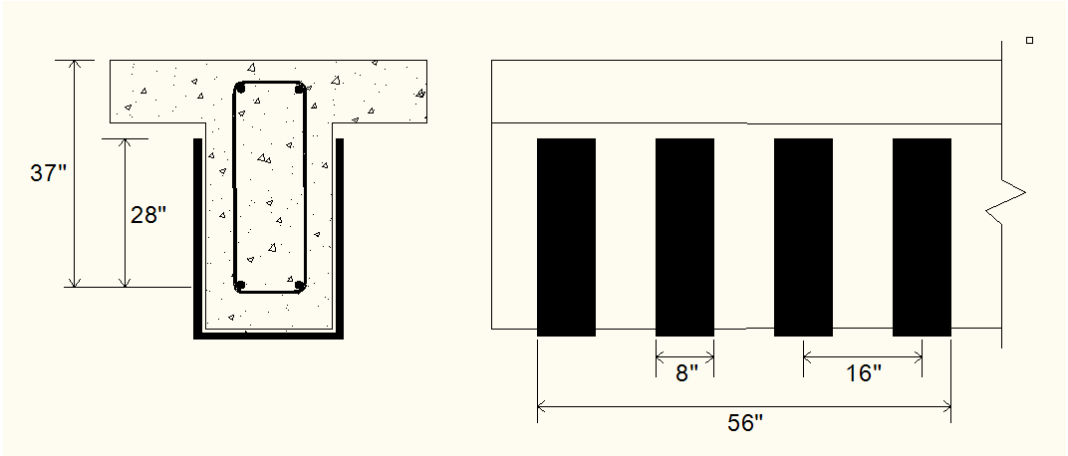

Figure 3: Schematics of FRP Shear Reinforcement

Figure 3 illustrates the schematics of the design which uses single ply U-wraps of CFRP. Table 3 summarizes the design configuration and Table 4 presents the manufacturer's reported FRP system properties.

Table 3: Configuration of Supplementary Shear Reinforcement

d	37 in.
d_{fv}	28 in.
Width of each sheet, w_f	8 in.
Span between each sheet, s_f	16 in.
FRP strip length	56 in.

Table 4: Manufacturer's Reported FRP System Properties

Thickness per ply, t_f	0.0065 in/ply
Ultimate tensile strength, f_{fu}^*	550 ksi
Rupture strain, ε_{fu}^*	0.0167 in/in
Modulus of elasticity, E_f	33000 ksi

The strengthening design calculations are as follows.

STEP 1 – Compute the design material properties

Table 1.5-2 presents the environmental reduction factors.

Exterior exposure: $C_F = 0.85$

$$f_{fu} = C_E f_{fu}^* = 0.85(550) = 467.5 \ \ ksi$$

$$\varepsilon_{fu} = C_E \varepsilon_{fu}^* = 0.85(0.0167) = 0.0142 \ \ in/in$$

STEP 2 – Calculate the effective strain level in the FRP shear reinforcement

The effective strain should be determined using the bond-reduction coefficient κ_v. The coefficient can be determined by using Equations (1-36) through (1-39).

$$L_e = \frac{2500}{\left(n_f t_f E_f\right)^{0.58}} = \frac{2500}{\left[(1)(0.0065)(33000000)\right]^{0.58}} = 2.0 \ \ in.$$

$$k_1 = \left(\frac{f_c^{'}}{4000}\right)^{2/3} = \left(\frac{3000}{4000}\right)^{2/3} = 0.825$$

$$k_2 = \frac{d_{fv} - L_e}{d_{fv}} = \frac{28 - 2.0}{28} = 0.929$$

$$\kappa_v = \frac{k_1 k_2 L_e}{468\varepsilon_{fu}} \le 0.75 \ \Rightarrow \ \kappa_v = \frac{(0.825)(0.929)(2)}{468(0.0142)} = 0.2307 \le 0.75$$

Now, the effective strain can be computed using Equation (1-35).

$$\varepsilon_{fe} = \kappa_v \varepsilon_{fu} \le 0.004 \ \Rightarrow \ \varepsilon_{fe} = 0.2307(0.0142) = 0.0033 \le 0.004$$

STEP 3 – Calculate the contribution of the FRP reinforcement to the shear strength

- Area of FRP shear reinforcement

$$A_{fv} = 2nt_f w_f = 2(1)(0.0065)(8) = 0.104 \ \ in^2$$

- Effective stress in the FRP

$$f_{fe} = \varepsilon_{fe} E_f = 0.0033(33000) = 108.9 \ \ ksi$$

Now, the shear contribution of the FRP can be calculated from Equation (1-31) since the FRP is oriented perpendicular to the longitudinal axis of the member.

$$V_f = \frac{A_{fv} f_{fe} d_{fv}}{s_f} = \frac{0.104(108.9)(28)}{16} = 19.8 \ \ kips$$

STEP 4 – Calculate the shear strength of the section

The design shear strength can be computed from Equation (1-29) with $\Psi_f = 0.85$ in accordance with Table 1.7-1.

SPECIFICATIONS COMMENTARY

$$\Phi V_n = \Phi\left[V_c + V_s + \Psi_f\left(V_f\right)\right]$$

$$\Phi V_n = 0.85\left[72 + 31 + 0.85(19.8)\right] = 102 \ \ kips$$

$$\Phi V = 102 \ \ kips > V_u = 100 \ \ kips \qquad \textbf{OK}$$

The shear strength is now adequate.

Reinforcement Limit: $V_s + V_f = 50.8$ kips $< 8\sqrt{f_c'}b_w d = 259$ kips **OK**

REFERENCES

AASHTO, "Manual for Condition Evaluation of Bridges," 2nd Edition, pp 49-72, 1994.

AASHTO, "Standard Specifications for Highway Bridges," 16th Edition, 760 pp., 1996.

ACI Concrete Repair Manual

ACI 318-08 (2008), Building Code Requirements for Structural Concrete and Commentary (318R-08), American Concrete Institute, Farmington Hills, MI.

ACI 440.2R-08. Guide for the Design and Construction of Externally Bonded FRP Systems for Strengthening Concrete Structures. Farmington Hills, MI: American Concrete Institute, 2008.

ACI 440R-07 (2007). Report on Fiber-Reinforced Polymer (FRP) Reinforced for Concrete Structures. American Concrete Institute.

Bousselham, A., and Chaallal, O., 2006, "Behavior of Reinforced Concrete T-Beams Strengthened in Shear with Carbon Fiber-Reinforced Polymer—An Experimental Study," *ACI Structural Journal*, V. 103, No. 3, May-June, pp. 339-347.

Davalos, Julio F., Karl E. Barth, Indrajit Ray, Chunfu Lin, Adam L. Justice, and Matt D. Anderson. District 3-0 Investigation of Fiber-Wrap Technology for Bridge Repair and Rehabilitation (Phase-3). Morgantown, WV: West Virginia University, 2008.

Deniaud, C., and Cheng, J. J. R., 2003, "Reinforced Concrete T-Beams Strengthened in Shear with Fiber Reinforced Polymer Sheets," *Journal of Composites in Construction*, ASCE, V. 7, No. 4, pp. 302-310.

Funakawa, I.; Shimono, K.; Watanabe, T.; Asada, S.; and Ushijima, S., 1997, "Experimental Study on Shear Strengthening with Continuous Fiber Reinforcement Sheet and Methyl Methacrylate Resion," *Third International Symposium on Non-Metallic (FRP) Reinforcement for Concrete Structures (FRPRCS-3)*, V. 1, Japan Concrete Institute, Tokyo, Japan, pp. 475-482.

Green, M.; Bisby, L.; Beaudoin, Y.; and Labossiere, P., 1998, "Effects of Freeze-Thaw Action on the Bond of FRP Sheets to Concrete," *Proceedings of the First International Conference on Durability of Composites for Construction*, Sherbrooke, QC, Canada, Oct., pp. 179-190.

Khalifa, A.; Alkhrdaji, T.; Nanni, A.; and Lansburg, S., 1999, "Anchorage of Surface-Mounted FRP Reinforcement," *Concrete International*, V. 21, No. 10, Oct., pp. 49-54.

Malek, A.; Saadatmanesh, H.; and Ehsani, M., 1998, "Prediction of Failure Load of R/C Beams Strengthened with FRP Plate Due to Stress Concentrations at the Plate End," *ACI Structural Journal*, V. 95, No. 1, Jan.-Feb., pp. 142-152.

Okeil, A. M.; Bingol, Y.; and Alkhrdaji, T., 2007, "Analyzing Model Uncertainties for Concrete Beams Flexurally Strengthened with FRP Laminates," *Proceedings of the Transportation Research Board 86th Annual Meeting*, Jan. 21-25, 2007, Washington, DC, 15 pp. (CD-ROM)

Parish, George C. CFRP Repair of Concrete Beams Aged by Accelerated Corrosion. Thesis. West Virginia Univ., 2008. Morgantown, WV: West Virginia University, 2008

Pellegrino, C., and Modena, C., 2002, "Fiber Reinforced Polymer Shear Strengthening of Reinforced Concrete Beams with Transverse Steel Reinforcement," *Journal of Composites in Construction*, ASCE, V. 6, No. 2, pp. 104-111.

Priestley, M.; Seible, F.; and Calvi, G., 1996, *Seismic Design and Retrofit of Bridges*, John Wiley and Sons, New York, 704 pp.

Quattlebaum, J.; Harries, K. A.; and Petrou, M. F., 2005, "Comparison of Three CFRP Flexural Retrofit Systems Under Monotonic and Fatigue Loads," *Journal of Bridge Engineering*, ASCE, V. 10, No. 6, pp. 731-740.

Roberts, T. M., and Haji-Kazemi, H., 1989, "Theoretical Study of the Behavior of Reinforced Concrete Beams Strengthened by Externally Bonded Steel Plates," *Proceedings of the Institute of Civil Engineers*, Part 2, V. 87, No. 9344, pp. 39-55.

Sasher, William C. Testing, Assessment and FRP Strengthening of Concrete T-Beam Bridges in Pennsylvania. Thesis. West Virginia Univ., 2008. Morgantown, WV: West Virginia University, 2008

Soudki, K. A., and Green, M. F., 1997, "Freeze-Thaw Response of CFRP Wrapped Concrete," *Concrete International*, V. 19, No. 8, Aug., pp. 64-67.

Triantafillou, T. C., 1998a, "Shear Strengthening of Reinforced Concrete Beams Using Epoxy-Bonded FRP Composites," *ACI Structural Journal*, V. 95, No. 2, Mar.-
Apr., pp. 107-115.

University of Missouri-Rolla. Preservation of Missouri Transportation Infrastructures; Validation of FRP Composite Technology Through Field Testing; Strengthening of Bridge P-0962 Vol. II: Master Design. Rolla, MO: University of Missouri-Rolla, 2004.

Appendix D

Construction Guidelines

SECTION 1000
STRUCTURES

SECTION 1002—RC T-Beam Bridge Rehabilitation with Externally Bonded FRP Strips

1002.1 DESCRIPTION----The intended use of these specifications is directed to the construction process incorporating repair by use of externally bonded FRP systems. The expected outcomes of such FRP retrofit are to enhance the shear strength, flexural strength, or ductility of members.

1002.2 MATERIALS----

(a) Resins. A broad range of polymeric resins are used with FRP systems. These resins include primers, putty fillers, saturants, and adhesives. Environmental conditions should be taken into account when selecting and using resins. The most commonly used resin types, such as epoxy, vinyl ester, and polyester, have been further formulated for use in many different environmental conditions. Resins that are used by FRP system manufacturers have compatibility and high adhesion properties with concrete substrates and FRP composite systems; are resistant to environmental effects associated with exposed concrete on bridges; have filling and workability; have adequate pot lives; and develop the appropriate mechanical properties for strengthening.

- Primer----Primer provides an improved adhesive bond for the saturating resin or adhesive by penetrating the surface of the concrete.

- Putty fillers----Small surface holes in the substrate should be filled with putty. The putty provides a smooth surface for which to apply the FRP system and can prevent bubbles from developing during the saturating resin curing process.

- Saturating resin----Saturating resin must be used to impregnate the fibers and therefore provide a shear load path between the fibers for the effective transfer of load. In wet layup systems, the saturating resin also serves as the adhesive to provide a shear load path between the FRP and the concrete substrate.

- Adhesive----Adhesives are resins that are used when bonding precured or Near-Surface Mounted (NSM) systems to concrete substrate. As with saturating resins, the adhesive provides a shear load path between the FRP system and the concrete substrate.

(b) Fibers. Fibers give the FRP system its strength and stiffness. Common reinforcing fibers used are continuous glass, aramid, and carbon fibers. Ranges of tensile properties for common types of fibers are presented in ACI 440.2R-08.

(c) Protective coatings. A protective coating should be used to greatly decrease the chances of the FRP system becoming damaged by environmental or mechanical effects. Once the saturating resin or adhesive has cured, the protective coating should be applied to the exterior of the FRP system in accordance with the manufacturer's recommendations. There are a wide range of forms available for protective coatings. Forms include: Polymer coatings; Acrylic coatings; cementitious systems; and intumescent coatings. The major reasons why protective coatings are used on finished FRP systems include: ultraviolet light protection; fire protection; vandalism; impact; abrasion; wear; aesthetics; and chemical resistance.

1002.3 SPECIAL CONSIDERATIONS----

(a) Product Shipping Dimensions. FRP shipping roll widths may not be the same for different suppliers, but the typical width varies from 20 to 24 in. For this reason, it is important that the shipped width be known when determining the quantity to be ordered. If the design width for the flexural reinforcing FRP is less than the shipping width (which is normally the case) the strips will have to be cut to size and the excess may not be a width usable in the design. Therefore, care may have to be taken so that the correct quantity of FRP area above the design area can be ordered, to avoid a shortage of material.

(b) Long Term Structural Performance. It is important that all construction aspects be performed as economically as possible while achieving the greatest increase in life for the structure. New technologies and additional construction works may be incorporated into the rehabilitation project to provide for enhanced life expectancy. This concept should also be taken into careful consideration during the design phase as detailed in Section 1002.3(b)2.

1. Waterproofing. Limiting further ingression of chlorides should be a major consideration with any concrete bridge rehabilitation. Membrane waterproofing can be used to form an impermeable water barrier between the concrete deck and overlay surfacing material. The intent of applying a membrane is to prevent moisture, salts and deicing chemicals from infiltrating through the concrete surface, and thereby reducing damage caused by steel corrosion and freeze-thaw cycles. Royston Bridge Membrane – 10A Easy Pave has been successfully used for this application.

2. Design. There has been much debate concerning the question as to whether or not certain FRP design configurations can potentially increase rates of deterioration. Other considerations include aspects such as reinforcement details that can seem adequate in accordance with design guidelines, but when viewed as achieving the greatest increase in life for the structure, may seem inadequate.

2.a Web Encasement. Continuous FRP reinforcement along the web of a beam that completely encases the member and potentially prevents the migration of contaminants and moisture is not recommended, as it can possibly increase the rate of deterioration. Up to three layers of flexural reinforcing FRP strips may be applied to the soffit of a beam as recommended by ACI. This type of layout is, in the majority of cases, is sufficient to provide the increase in moment capacity required. Therefore, the use of continuous U-wraps or continuous side flexural reinforcing strips should be avoided, in order to enhance longer anticipated life for the structure.

2.b Design Requirement. The FRP strengthening design may be based on the required moment and shear to bring the member back to its original capacity or it may be based on the required moment and shear to satisfy a specific AASHTO truck loading, such as an HS20 truck loading. In most cases, it may be more appropriate to bring the structure to a level that satisfies a specific truck loading, based either on actual or anticipated loss of steel reinforcement area and full strengthening with externally bonded FRP.

2.c FRP Wrapping Scheme. The quantity of transverse FRP anchorage used in design shall, at minimum, meet the requirements of design guidelines. It has been found that using the minimum transverse FRP anchorage, as required by design guidelines, results in the same short-term performance as when more anchorage than required is used (Parish, 2008). Although the short-term performance may not be affected by using more anchorage, it is likely that long-term performance will be improved (Parish, 2008). For this reason, it is suggested that using more transverse FRP anchorage than that required may lead to increased life expectancy for the structure.

1002.4 CONSTRUCITON----

(a) General. The intended use of these specifications is directed to the construction process incorporating repair by use of externally bonded FRP systems. The expected outcomes of such FRP retrofits are to enhance the shear or flexural strength or ductility of members such as beams or columns.

(b) Pre-repair Work. Care should be taken to ensure that proper methods are used in performing all tasks that are to precede the actual construction and those that arise as a result of the construction. Such tasks include, but are not limited to, comprehending all tolerances that may be set forth by the owner or manufacturer, attainment and proper review of submittals, evaluating all site considerations and challenges, and handling of materials from delivery to disposal.

1. Tolerances. Tolerances stated within these specifications or within the contract documents shall be followed unless more strict requirements are recommended by the manufacturer. Any uncertainties with respect to required tolerances shall be clarified by the engineer before proceeding.

2. Site Considerations. All site challenges or obstacles shall be dealt with accordingly after approval from the engineer. The contractor shall make arrangements for all necessary removal of obstructions such as pipes, conduits, wiring, fences, or vegetation. Any necessary removal should only take place upon approval from the engineer and after all records have been taken so that proper replacement can take place at project completion. Required means of access for personnel, material, and equipment such as scaffolding and pathways should be provided by the contractor.

3. Submittals. Prior to the start of construction work, all required documentation must be submitted. Submittals should consist of working drawings, qualifications, and quality control and assurance plans.

3.a Drawings. Working drawings should include all relevant information, such as the type of FRP system, repair locations and dimensions, and the work plan. The work plan should be composed of all necessary preparations of the existing structure. Design calculations, MSDS, and the manufacturer's system data sheets that provide physical, mechanical, and chemical properties of the system components should accompany the drawings along with an application guide that shall state all aspects concerning installation and maintenance.

3.b Qualifications. Documentation proving the required level of qualifications shall be submitted by the system manufacturer/supplier and the contractor. Recommended information to be provided by the manufacturer/supplier includes the following:

- System data sheets and MSDS for each component of the FRP system;
- A minimum of 5 years documented experience or 25 documented similar field applications with acceptable reference letters form the respective owners;
- A minimum of 50 total test data sets from an independent agency approved by the owner on mechanical properties, aging, and environmental durability of the system; and
- A thorough hands-on training program for each FRP system to qualify contractors/applicators.

Whereas recommended information to be provided by the contractor includes the following:

- A minimum of 3 years of documented experience or 15 documented applications with acceptable reference letters form the respective owners;

- A certificate of completed training from the manufacturer/supplier for at least one field representative who will be present on site throughout the project.

3.c QA/QC Plan. The contractor should be held responsible for the quality control of materials and the construction process. QC and QA plans submitted will be approved by the owner or the owner's representatives. Depending on the size of the project and the entities utilized, a third party such as a consulting firm or a University research team may greatly assist in the quality assurance and approval of QC and QA plans. The QC/QA plan should include at a minimum, detailed procedures for personnel safety, tracking and inspection of all FRP components before installation, inspection of prepared surfaces prior to FRP application, inspection of the work in progress, QA sampling, inspection of all completed work including necessary tests for approval, repair of defective work if applicable, and clean-up aspects. All work must comply with the contract documents and may otherwise be altered at the expense of the contractor.

4. Material Shipping. All applicable federal and state packaging and shipping codes must be followed when shipping FRP materials. CFR 49 is the controlling regulatory code for packaging, labeling, and shipping of thermosetting resins.

5. Material Storage.

5.a General. Components of the FRP system must be stored according to the manufacturer's recommendations. Normally in original factory-sealed and unopened packaging or in containers with proper labels that state the manufacturer, brand name, system ID number, and the date. Materials should be kept out of contact with anything that may cause physical damage, such as direct sunlight, dust, moisture, excess temperatures as specified in the material data sheets, and harmful chemicals. Components of the FRP system that are used as catalysts or inhibitors should be stored separately.

5.b Shelf Life. A set shelf life is recommended by the system manufacturer. Any duration of storage which is longer than the specified shelf life may result in property changes for the resin-based materials and therefore, the expected performance of such materials may be compromised. Any material that has reached its shelf life should not be used and disposed of in accordance with Section 1002.4(b)7.

6. Material Handling.

6.a General. When handling FRP system constituent materials, great care should be taken to ensure protection of the material and safety of work personnel. The MSDS for each component and all relevant information sources such as any literature provided by the system manufacturer, ACI, or ICRI reports should be present on site and used to aid in proper handling.

6.b Material Protection. All material must be handled according to manufacturer's recommendations to ensure that no damage is caused that may compromise the system performance. With respect to causing damage, emphasis should be placed on proper handling of fiber sheets to decrease the chances of misalignment or breakage of the fibers. This can be caused by pulling, separating, wrinkling or folding the sheets. After sheets have been measured and cut, they can be rolled or stacked before installation. If stacked, they should be stacked dry with the use of separators. If rolled, they should be rolled gently at a radius not less than 12 in. (305 mm) or as specified by the system manufacturer.

6.c Personnel Safety. Safety hazards to work personnel can be avoided if all components of the FRP system are handled with care. Emphasis should be placed on proper handling of adhesives and resins to decrease the chances of safety hazards to personnel. Safety hazards can include skin sensitization, breathing in of harmful vapors, possible explosion or fire, and inhalation of fiber fly. Mixing of resins shall be monitored to avoid any of the preceding hazards. Hazards may vary with different FRP systems and the manufacturer's literature should be consulted for more detailed information.

To protect against hazards, personnel should be equipped with the proper clothing and accessories. The use of disposable suits and gloves that are resistant to resins and solvents are recommended when handling fiber and resin materials. The contractor is responsible for providing the proper means of protection for the personnel and the workplace, including informing personnel of the dangers associated with any aspect of the construction. Other forms of protection that should be provided include safety glasses or goggles and respiratory protection, such as dust masks or respirators.

Conformance to local, state, and federal environmental and worker's safety laws and regulations is required throughout all stages of the work and is the responsibility of the contractor.

7. Cleanup and Disposal. Cleanup is the responsibility of the contractor. Safety and environmental concerns are important issues to consider with cleanup as it often involves the use of flammable solvents. System data sheets should be referred to in an effort to perform the cleanup in the most efficient way possible while obeying all regulations prescribed by the established environmental authority.

FRP system components that have exceeded their shelf life or pot life or have not been stored properly shall be disposed of in a method that conforms to the MSDS recommendations and environmental regulations.

(c) Pre-installation Repair Work.

1. General. All repair work should conform to ACI 546R and ICRI No. 03733. FRP rehabilitation should be performed through four main stages of work. These stages of work are the following: removal of defective concrete, restoration of cross-section, surface preparation, and FRP system installation. The success of the repair project strongly relies on satisfactory completion of each construction stage.

2. Removal of Defective Concrete. It is imperative that any defective concrete be removed and replaced, thus providing sound concrete substrate for the

installation. Removal shall be in accordance with ACI 546R and ICRI No. 03730, which may include the use of proper equipment such as a saw and an air-powered or electric-powered jack hammer. An adequate depth of at least ½ inch beyond the repair area should be reached to expose sound aggregates. In general, removal should reach a depth in which no loose aggregate is easily falling out of the concrete. When exposing reinforcing steel that is deteriorated or has lost its bond with the concrete, an additional ¾ inch or ¼ inch larger than the largest aggregate in the repair material shall be removed from behind the reinforcement. Restoration of the cross-section shall not take place until all sources of corrosion are located and properly treated. Research by Parish (2008), was conducted in which this traditional removal and restoration of defective concrete was compared with a method of repair in which only crack injection as presented in Section 1002.4(c)4.d was performed. The defective concrete removal and patch method demonstrated superior durability, compared to using only the crack injection method (Parish, 2008), and should be adopted where applicable.

3. Restoration of Cross-Section.

3.a General. After the concrete removal process is completed, work can be started to restore the cross-section. For proper concrete restoration, consideration should be given to repairing exposed reinforcement if necessary, surface cleaning, and the repair material.

3.b Repair of Reinforcement. Repair of defective reinforcement shall be performed in accordance with ICRI No. 03730 and to the satisfaction of the engineer. Corroded reinforcement can be prepared by abrasive cleaning or it can be replaced. If replaced, reinforcement should be cut out at a sufficient length as specified in the contract documents or to the approval of the engineer to ensure that only sound material remains. Splice lengths for replacement reinforcement shall be provided at sufficient length in accordance with contract documents or to the approval of the engineer.

3.c Surface Cleaning. To ensure adequate bond between the repair material and the newly exposed concrete substrate, proper surface preparations should be made prior to applying the repair material. Cracks within the solid concrete in the substrate shall be pressure injected with epoxy as specified in Section 1002.4(c)4.d. The substrate shall be cleaned from any dust, laitance, grease, oil, curing compounds, impregnations, foreign particles, wax, and other bond-inhibiting materials in the same manner of cleaning before FRP application as called for in Section 1002.4(c)4.f. After cleaning and just prior to applying the repair material, a water-based epoxy cementitious bonding agent shall be applied to the concrete and exposed reinforcement.

3.d Repair Material. Repair material shall conform to ICRI No. 03733. The mix design for any repair material shall be approved by the engineer. The FRP system manufacturer should be consulted on the compatibility of the FRP system with the repair material proposed. Repair materials that have been successfully used include Class AAA Polymer Modified Concrete and a BASF bag material product known as Emaco S66 C1 which is a flowable structural-repair concrete with integral corrosion inhibitor.

The compressive strength of the repair material shall be at least the compressive strength of the original concrete, but it should be no less than 4,500 and 5,500 psi at 7 and 28 days, respectively. It is important that the bond strength developed between the repair material and the existing concrete be adequate. This bond strength can be determined by pull-off tests in accordance with ASTM D4541 and must be, at minimum, 200 psi. A minimum of 7 days, unless a shorter time period for cure and strength is verified through testing, should be allowed for the repair material to cure before installing the FRP system.

4. Surface Preparation.

4.a General. Surface preparation should not begin until all concrete removal, cleaning and cross-section restorations have been approved by the engineer. The intended application of the FRP system normally determines the required surface preparation methods. FRP applications are termed as either bond-critical or contact-critical. In bond-critical applications, an adhesive bond is mandatory between the FRP and the concrete. Whereas, contact-critical applications only require intimate contact between the concrete and FRP, but often an adhesive is used anyway to aid in the installation. Since both applications require intimate contact between concrete and FRP and adhesives are commonly used in contact critical application, these specifications detail the same surface preparation to be used in either application. Recommendations given by ACI 546R and ICRI 03730 should be followed. In general, a clean, smooth, and flat or convex surface shall be provided. Key aspects of surface preparation include surface grinding, chamfering corners, crack injection, surface profiling, and cleaning. Once the surface has been prepared and approved by the engineer, work may begin on the installation.

4.b Surface Grinding. Disk grinders or other similar devices shall be used to remove all irregularities, unevenness, sharp protrusions such as form lines, and surface substances such as stains or paints. After grinding, all protrusions must be less than 1/32 inch (1 mm) or less than the requirements specified by the system manufacturer. If such variations are very small, it may be adequate to avoid grinding and simply smooth over the surface with resin-based putty.

4.c Chamfering Corners. When FRP is to wrap around corners of rectangular cross-sections, the corners should be rounded to a minimum radius of ½ inch to reduce stress concentrations and eliminate voids that may develop between the FRP and concrete. Putty should be used to smooth over roughened corners. Inside corners and concave surfaces are problematic and may require special detailing if bond between the concrete and FRP system is to be sustained.

4.d Crack Injection. The performance of an externally bonded FRP system can be affected by cracks that are wider than 1/100 inch (0.3 mm). Cracks of this size can cause delamination or fiber crushing and shall be filled using pressure injection of epoxy in accordance with ACI 224.1R. If aggressive environments are present, smaller cracks may require resin injection or sealing to prevent possible corrosion of reinforcing steel. ACI 224.1R gives crack width criteria for various exposure conditions.

FRP systems shall not be installed until at least 24 hours after crack injection is completed and after any surface variations caused by crack injection have been repaired in accordance with Section 1002.4(c)4.b.

4.e Surface Profiling. A minimum concrete surface profile (CSP) of No. 3 should be prepared as identified by the ICRI surface-profile chips. The FRP system manufacturer shall be consulted if a stricter surface-profile is required. This CSP shall be prepared using putty made of epoxy resin mortar or polymer cement mortar with strength equal to or greater than that of the original concrete. A minimum of 7 days must be provided for curing of this patching material before installation of the FRP system.

4.f Cleaning. Cleaning shall remove any dust, laitance, grease, oil, curing compounds, impregnations, stains, paint coatings, or any other type of bond inhibiting materials. Cleaning shall be performed to the approval of the engineer. Any cleaned surface should be protected from possible redeposit of any bond inhibiting materials. It is important that the surface be allowed to dry thoroughly before the installation of FRP if a power wash system is used in the cleaning process. The recommended moisture content can be evaluated with reference to ACI 503.4.

(d) FRP System Installation.

1. General. This section discusses issues related to installing the FRP system. The procedures specified for the installation may vary slightly depending on the type of system and the manufacturer. Specific aspects to be discussed include: environmental conditions during installation, shoring, equipment, and the type of FRP system to be used. The two types of FRP systems to be described are wet lay-up and precured.

2. Environmental Conditions at Installation. Environmental conditions such as temperature, relative humidity, and surface moisture at the time of installation can affect the performance of the FRP system. Therefore, these conditions should be examined before and during the installation process to ensure conformity with contract documents and any manufacturer's recommendations. Primers, saturating resins, and adhesives shall not be applied to cold or frozen surfaces. Resins and adhesives in general should never be applied to damp or wet surfaces unless they have been formulated for such applications. The installation should not proceed if the surface moisture is greater than 10% as evaluated by ACI 503R. Pressurized air may be used to help dry the surface. The minimum level of the concrete surface temperature should be set forth by the system manufacturer, with a general range being 50–95 °F (10-35 °C). A heat source may be used to raise the ambient and surface temperature during installation. Moisture vapor transmission is a problem that may be encountered during installation and usually appears as surface bubbles. FRP systems should never be applied to surfaces subject to moisture vapor transmission as this can greatly affect the bond.

3. Shoring. Conventional methods can be used to temporarily shore repaired members if necessary. Any shoring shall remain in place until the FRP system has completely cured and gained its design strength, as approved by the engineer.

4. Equipment. All necessary equipment shall be provided by the contractor. Equipment shall be in clean, working condition. The amount and types of equipment shall be such that continuous installation can be performed.

5. Wet Layup Systems.

5.a General. This section describes the process used in applying wet lay-up systems. This system can be dry or prepreg fiber sheets. Saturants are used to impregnate the fiber sheets at installation. Details from resin mixing to stressing applications are included.

5.b Mixing Resins. The process of mixing resins should always be performed in a way consistent with the manufacturer's recommended procedure. All resin components must be mixed at the proper ratios and specified temperature until consistency is achieved. Often, the components are different colors and consistency has been obtained when the mix reaches one color and no streaks are visible. Batches can be stirred by hand, but are most commonly stirred by some type of electrically powered mixing blades. Batch sizes, mix ratios, and mixing times should be supplied by the material manufacturer. In general, the quantities of mix shall be small enough to ensure use of all material before the pot life has been reached. If the pot life has been exceeded or the mix begins to show signs of exceeded pot life such as increase in viscosity, the mix shall not be used and it should be disposed of in accordance with Section 1002.4(b)7. Mixing should be performed in an area with adequate ventilation, as some resins can give off harmful fumes that can adversely affect the environment or work personnel.

5.c Primer. Primer application typically precedes the application of any FRP system. Primer should be applied in one or two coats or to manufacturer's specifications. The concrete surface and ambient temperatures should be within the range specified in Section 1002.4(d)2. If it is realized that the desired CSP as described in Section 1002.4(c)4.e has not been prepared, putty may need to be used to smooth the surface. If the use of putty is needed, it should be applied at the time the primer is no longer sticky to the touch. Putty should be applied in thin coats of one or two layers to smooth over the surface and adequately fill any voids, cracks, or uneven areas. As with any prepared surface, the primer and putty should be protected from dust, moisture, and any other contaminants that may arise at the site. If contamination does occur, the surface shall be cleaned as specified in Section 1002.4(c)4.f before the application of FRP.

5.d Fiber Sheet and Saturant Application. The procedure for applying the fiber sheet and saturant should be performed without interruption. This procedure can be explained in general as three basic steps: first layer of saturant, fiber sheet, and second layer of saturant. The first layer of saturant shall be applied to all areas on the concrete surface where the FRP system is to be applied. It shall be applied in a uniform layer and have a viscosity that will allow for full impregnation of the fiber sheets. The proper viscosity can be maintained by ensuring that the ambient and the concrete surface

temperatures are within the range specified in Section 1002.4(d)2. Once this first layer of saturant has been applied, work should begin immediately on applying the fiber sheet. Therefore, the fiber sheet must already be cut to the correct length as specified in the contract documents. The fiber sheet shall be placed on the intended area and gently pressed onto the wet saturant, allowing for full impregnation. Rollers can be used to further impregnate the fiber sheet while helping to eliminate any entrapped air between the fiber and concrete surface. Rollers should only be rolled across the sheet in the direction parallel to the fibers so as to help the fibers attain intimate contact with the substrate. If bidirectional fabrics are used, rolling should be performed in the fill direction end to end and then in the warp direction.

After the fiber sheet has been properly placed, a sufficiently thick layer of saturant shall be applied. This second layer of saturant ensures full saturation of the fibers and serves as an overcoat. It is important that this three step process be performed without interruption.

5.e Multiple Plies and Lap Splices. Multiple plies can be installed using the same procedure described in Section 1002.4(d)5.d. The overcoat saturant for each underlying ply should be applied with some excess so that it can also serve as a first layer for the overlying ply. If the plies are to be applied on the same day, the viscosity of the saturant must be maintained until all layers have been installed. The manufacturer should be consulted for the number of plies that can be installed in one day. The multiple ply installation shall meet the approval of the engineer. If all plies are not to be installed on the same day and intermediate layers are allowed to cure, surface preparation is needed before installation of the next layer. This surface preparation can include light sanding and filling with putty as specified in Section 1002.4(d)5.c.

It may be inconvenient to use exceptionally long pieces of fabric to strengthen long spans. Therefore, multiple lengths of fiber sheets can be used by incorporating lap splices to continuously transfer load. Lap splices should be detailed in accordance with the manufacturer's recommendations. The lap length of any lap splice should be as specified within contract documents but be no less than 6 in. (152 mm) in accordance with ACI 440.2-08. Lap splices should be staggered or meet the approval of the engineer with reference to the contract documents.

5.f Alignment of FRP Materials. The contract documents should specify the alignment of fiber plies. Variations as small as 5 degrees in angle from the design direction of plies can significantly change the strength and modulus and should not be accepted. The fiber sheets should be free of kinks and folds. Fiber orientation is discussed further in Section 1002.4(e)5.

6. Precured FRP Systems.

6.a General. Precured systems are normally installed with an adhesive and can include shells, strips, and open grid forms. The installation of these systems is generally similar to that of the single-ply wet lay-up. In instances of concrete confinement, adhesive may not be required. The surface for the precured system to be

bonded should be prepared as specified in Section 1002.4(c)4 to a minimum concrete surface profile (CSP) 3.

6.b Adhesive. The adhesive should be applied uniformly to all surface areas to receive the procured system. The rate of application, thickness, and viscosity at which the adhesive is to be applied to the concrete substrate should be in accordance with the manufacturer's recommendations. The ambient and concrete surface temperatures should be within the range as specified in Section 1002.4(d)2 during the application. Care should be taken so that the adhesive's pot life is not exceeded.

6.c Placement. As with the wet lay-up systems, precured system strips and shells shall be clean and cut to the correct size prior to the installation. They shall be placed onto the adhesive immediately after the adhesive has been applied, within the adhesive's pot life. Air trapped within the system shall be released in the same manner as described in Section 1002.4(d)5.d. All excess adhesive should be removed without disturbing the applied FRP system.

6.d Grouting. Pressure grouting may be performed on precured shells used for confinement of concrete columns. The grouting process should be in accordance with contract documents and to the manufacturer's recommendations. Grouting should take place no earlier than 24 hours after installation. The shrinkage strain of the grout shall be no less than 0.0005 and have a minimum compressive strength of 4,000 psi (27.6 MPa).

7. Anchoring of FRP Systems. If specified in contract documents or requested by the engineer, it may be required to anchor FRP sheets to the concrete substrate. Mechanical anchorages can be effective in increasing stress transfer. If mechanical anchorages such as clamps or fasteners are used, the installment should be used in a careful manner to avoid causing damage to the FRP or concrete substrate. Typically, anchoring is provided with the use of transverse FRP wraps or stirrups located near the ends of an FRP sheet or strip.

8. Temporary Protection. Temporary protection may be required during installation and until the resins have cured to eliminate the chances of damage to the FRP system. Damage could occur as a result of any one of the following: rain, vandalism, dust, adverse temperatures, or excessive sunlight. No shoring shall be removed until the FRP system has been fully cured. If damage does occur to the system before full cure, the engineer should be made aware of the situation and the system manufacturer should be consulted in an effort to resolve the issue.

9. Curing of Resins. Curing of resins should be performed in accordance with the manufacturer's recommendations. The cure process is time-temperature-dependent, and under normal ambient temperatures the complete cure can take several days. If instructed, elevated cure systems may be used in which the resin must be heated to a specific temperature for a specified period of time. Any field modification of resin chemistry is not permitted. If application calls for several plies to be placed in more than

one day, full cure and monitoring of installed plies should be performed before installation of subsequent plies. The FRP system shall be protected in accordance with Section 1002.4(d)9 while curing.

10. Protective Coating or Finishing. All coatings should be applied in accordance with the manufacturer's recommendations. Coatings must be compatible with the FRP system. The FRP surface should be clean and dry before applying the coating. Cleaning with solvents is prohibited unless approved by the FRP manufacturer, due to the deleterious effects that solvents can have on the polymer resins. The owner should be consulted regarding the final appearance of the coatings. Normally, it is desired to match the color and texture of the adjacent concrete. The effectiveness of the coatings should be ensured through periodical inspections and maintenance.

(e) Inspection for QA/QC.

1. General. Quality assurance is attained through a set of inspections and applicable tests to document the acceptability of the installation. A requirement to provide a QA plan for installation and curing of all FRP materials should be included in the project specifications. The entities involved with inspections and testing will depend on the project size and complexity. In a complicated or large project it is likely that the inspections and tests will be performed by an outside consultant acting on behalf of the owner for QA. With minor projects, the owner itself may perform inspections and tests for QA. On site inspections and tests shall be performed in the presence of the contractor and the engineer.

Quality control shall be maintained by the contractor, possibly incorporating the use of its own inspector. The QC program should be detailed in the project specifications and cover all aspects of the strengthening project. The project size and complexity will also influence the degree of QC and the extent of testing, inspection, and record keeping.

2. Daily Inspection. Inspections should be held to high standards and should be performed regularly. Throughout the FRP system installation process, daily inspections should be conducted that include the following:

- Date and time;
- Ambient temperature, relative humidity, and any weather observations;
- Concrete surface temperature;
- Surface dryness;
- Method of surface preparation and resulting CSP;
- Surface cleanliness;
- Fiber laminate batch number and approximate location in the structure;

- Any cracks not injected with epoxy;
- Batch numbers, mixing times and ratios, and mixed resin appearance for putties, primers, saturants, adhesives, and coatings mixed on that day;
- Progression of resin curing;
- Installation procedures;
- Any pull-off test results including bond strength, mode of failure, and location;
- Tests and results of any field samples;
- Size and location of any delaminations or voids; and
- Overall advancement work in progress.

Copies of inspection records should be submitted to the owner or engineer. Witness panels shall also be submitted. The contractor should maintain sample cups of resin and records on the placement of each batch.

3. Acceptance. Acceptance or rejection should be based on compliance or noncompliance with design drawings and specifications. Evaluation for acceptance should include any material properties, placement tolerances, delaminations present, resin curing, and adhesion to substrate. Important aspects of placement of the FRP system include fiber orientation, cured thickness, ply alignment, fiber sheet dimensions, corner radii, and lap splice lengths. Once the FRP system has been installed, witness panels and pull-off tests should be used for evaluation and acceptance. If necessary, load testing may be used to verify strengthening of members.

4. Materials. Before starting the project, the manufacturer's certifications for all delivered FRP components shall be inspected to ensure compliance with contract documents. The number and types of samples to be tested will be indentified within the contract documents. If deemed necessary due to unseen project complexity, additional material testing may be conducted. Any material that does not comply must be rejected unless it receives approval from the engineer in special situations. Inspection of FRP materials may include, but are not limited to, tests for tensile strength, infrared spectrum analysis, gel time, pot life, glass transition temperature (T_g), and adhesive shear strength that are in accordance with ASTM standards, such as ASTM D3039. While tests for pot life and curing hardness are usually performed on site, most tests will be conducted on samples sent to a laboratory. The testing location and preceding curing location if applicable shall be specified within the QC test plan.

Special care should be taken in preparing any witness panels for the evaluation process. When specified, witness panels may be used to determine the tensile strength

and corresponding modulus, hardness, T_g, and strength of any lap splices of the installed FRP system. Witness panels provide this information within reasonable accuracy as they are prepared and cured under the same conditions as the actual FRP strengthening system. After match curing, panels should be transported to the laboratory for testing. Elastic modulus and strength of FRP materials may be established in accordance with ACI 440.3R (Test Method L.2) and with reference to the material specifications. If fabrication of flat witness panels on site is not possible, the test plan may incorporate panels that are to be provided by the system manufacturer.

The level of cure shall be determined by testing sample cups of mixed resin that have been prepared in accordance with the sampling plan.

5. Fiber Orientation. Fiber orientation shall be inspected by visual inspection for wet lay-up and precured systems. In wet lay-up systems, care should be taken to determine if any kinks and waviness are present after the application. Conformance with contract documents is important and any misalignment of more than 5 degrees (approximately 1 in/ft [80mm/m]) should be reported to the engineer. If removal and repair is deemed necessary, it shall be performed in accordance with Section 1002.4(f)5.

6. Delaminations. Inspection for delaminations shall start as a visual inspection that should be performed after a minimum of 24 hours of cure time. Acoustic sounding (hammer sounding), ultrasonics, and thermography can be used to detect delaminations if deemed necessary after the visual inspection. Delaminations and air voids can occur between multiple plies or between the fiber sheets and the concrete substrate. When evaluating delaminations and other inconsistencies, size, location, and quantity with relation to the total area of installation should be considered. Acceptance guidelines for wet lay-up systems as recommended by ACI are as follows:

- Delaminations less than 2 in^2 each (1300 mm^2) are permissible as long as the delaminated area is less than 5% of the total laminate area and there are no more than 10 such delaminations per 10 ft^2 (1 m^2);

- Delaminations greater than 25 in^2 (16,000 mm^2) can affect the performance of the installed FRP and should be repaired by selectively cutting away the affected sheet and apply an overlapping patch sheet with the equivalent number of plies; and

- Delaminations less than 25 in^2 (16,000 mm^2) may be repaired by resin injection or ply replacement, depending on the size, number, and locations of the delaminations.

Completion of any repairs should be followed by another inspection to determine if the repair was adequate. In the case of precured FRP systems, inspection and repair of delaminations should be performed under the engineer's guidance.

7. Cure of Resins. Relative cure of resin in FRP systems shall be examined by visual inspection, in which resin tackiness and hardness of surface or cup samples are

noted, or by laboratory testing of witness panels or cup samples. In either case, ASTM D3418 shall be followed. The resin manufacturer should be consulted for determining the quality of cure acceptable. The manufacturer should recommend the method of evaluating adhesive hardness for precured systems. If the cure of any resin is found to be unacceptable, the applicable area will be outlined and repaired in accordance with Section 1002.4(f)5.

8. Adhesion. Tensile adhesion testing shall be performed using methods as specified in ACI 503R or ASTM D4541. ACI 440.3R, Test Method L.1 may be followed as well. Tensile adhesion testing should be performed at least 24 hours after initial cure and before applying the protective coating. Various test locations should be specified in the contract documents, defined by the engineer, or recommended by the contractor and approved by the engineer. Tension adhesion strengths should be recorded. Failure should take place within the concrete substrate and only after exceeding a stress of 200 psi (1.4 MPa). Test locations that fail to meet this criterion, such as failure between plies or failure between FRP and concrete, should be reported to the engineer for evaluation and acceptance. NSM systems can not be tested for adhesion strength in the same manner. For NSM systems, sample cores may be extracted to visually confirm the consolidation of resin adhesive around the FRP bars or strips. These cores must be taken at the ends of the bars or strips so as to not cause discontinuity within the strengthening system.

All test locations shall be repaired in accordance with Section 1002.4(f)4. If defective work is indicated as a result of tensile adhesion testing results, repair should follow as recommended in Section 1002.4(f)5.

9. Cured Thickness. The cured laminate thickness or number of plies may be visually ascertained by taking small core samples of ½ in diameter. Samples resulting from adhesion testing may be used, when adequate, to verify laminate thickness or number of plies. The sampling frequency shall be specified in contract documents or recommended by the engineer. Cured thickness samples shall never be taken from splice areas or high stress areas. If the samples do not present the proper number of plies, or if they present a cured thickness that is 1/32 in (0.8 mm) less than that which is specified, the area shall be marked as unacceptable and repairs shall follow Section 1002.4(f)5. However, if the samples are acceptable for cured thickness, repairs to extracted sampling regions may be performed in accordance with Section 1002.4(f)4.

10. Additional Testing. In addition to inspection methods detailed in Sections 1002.4(e)1-(e)10, further testing may be performed if specified in contract documents. In-situ conventional load testing on the retrofitted structure and tensile testing of witness panels may be used. In-situ load testing of the structure can provide an overall evaluation of the effectiveness of the repair system and load rating of the structure. Tensile testing of witness panels, in accordance with ASTM D3039, can be used to measure strength, elastic modulus, and ultimate strain. If the average tensile strength and the lowest tensile strength are below 5% and 10% respectively, than those values specified in the contract documents, the system shall be deemed unacceptable.

(f) Post Inspection Repairs.

1. General. This section presents acceptable methods of repair for the types of defects identified in the inspection process. The adequacy of any repair procedure will depend on the type, size, and extent of the defect. For conditions or defects not presented within these specifications, repair procedures shall be proposed by the contractor and approved by the engineer before proceeding. The following sections detail repair methods for protective coatings, epoxy injection, minor defects, and major defects.

2. Protective Coating. Defects in protective coatings can cause long-term degradation of the FRP system as a result of localized moisture ingress. These defects consist of small cracks, blisters, and peeling. Any detected defects on the protective coating shall warrant further visual inspection to determine if the defect extends into the FRP system itself. If the defect does extend into the FRP system, repairs shall follow Sections 1002.4(f)3-(f)5.

Cracks are often nonstructural and are likely due to excessive coating thickness, shrinkage during cure, or FRP surface preparation. If small areas with cracks are found, the area shall be gently sanded and a new coating reapplied after application of any appropriate primer recommended by the manufacturer. In general, engineering judgment shall be used in determining an adequate area of coverage for the new coating, but as a minimum, the new coating shall extend 1 in. (25 mm) beyond the damage perimeter.

Blisters are often caused as a result of moisture entrapment. In any case, moisture content of the substrate should be below 0.05% before the application of any new coating. This will ensure that no further damage is caused after applying the new coating. If blistering is seen, the area up to 12 in. (305 mm) within the surrounding location shall be gently scraped clean. Recoating without complete removal of the existing defective coating is unacceptable. Once the old coat is removed, the area should be wiped clean and dried thoroughly. If required by the manufacturer, a primer shall be applied before applying the protective coating.

Excessive peeling indicates that the original coating may have been applied incorrectly as a result of inadequate surface preparation of the FRP system. If excessive peeling is identified, the entire coating should be scraped off and the surface shall be lightly sanded, wiped clean, and thoroughly dried prior to applying a new coating in accordance with the manufacturer's recommendations.

3. Epoxy Injection. Small defects can often times be adequately repaired by epoxy injection. Types and sizes of defects that can be corrected with epoxy injection are presented in this section. Voids or surface discontinuities less than ¼ in. (6.4 mm) in diameter shall be considered negligible and require no repair work, unless they occur next to edges or occur in more than five locations within an area of 10 ft^2 (0.9 m^2), in which case, repairs shall be performed in accordance with Section 1002.4(f)4. Defects having sizes between ¼ and 1 ¼ in. (6.4 and 32 mm) in diameter can be repaired using low-pressure epoxy injection unless the defect extends through the complete thickness of the laminate. It is possible for delamination to increase as a result of epoxy injection. If any delamination increase is detected, the repair procedure should be halted and repair shall be continued with methods of Section 1002.4(f)4.

4. Minor Defects. Defects with diameters between 1 ¼ and 6 in. (32 and 152 mm) and an occurrence of less than five per any unit surface area of 10 ft (3 m) length or width can be considered minor defects. These minor defects can include cracking, abrasion, blemishes, chips, and cuts. Repair of these defects shall start with removal of the defect area up to at least 1 in. (25 mm) beyond the perimeter of the defect. After removal, the area should be wiped clean and dried thoroughly. FRP of the same type as the original laminate shall be used to patch the area. The patch shall be of sufficient size to extend at least 1 in. (25 mm) beyond the area removed. If deemed more suitable, repair may be performed with the procedures of Section 1002.4(f)5.

5. Large Defects. Defects with diameters greater than 6 in. (152 mm) can be considered large defects. Large defects normally represent significant debonding between layers, insufficient adhesion to the concrete substrate, or large amounts of moisture entrapment. They may be in the form of peeling and debonding of large areas that are not localized and can lead to full replacement of the FRP system. Large defects should be carefully marked and cut out to at least 1 in. (25 mm) beyond all sides of the defect area. Cutting shall be continued until reaching a depth that exceeds the defect area. In some cases, the entire thickness of the multi-ply system may need to be removed. After removal and before patching, the area should be properly prepared. For these large defects, application of the patching FRP system shall follow the same procedures as the initial FRP application. As an extra step with large defects, an additional layer extending a minimum of 6 in. (152 mm) on all sides of the cut area shall be applied as an outer patch. Once these steps have been performed and the system has cured, the protective coating should be applied over the entire area.

REFERENCES

AASHTO, "Manual for Condition Evaluation of Bridges," 2nd Edition, pp 49-72, 1994.

AASHTO, "Standard Specifications for Highway Bridges," 16th Edition, 760 pp., 1996.

ACI Committee 440. Guide for the Design and Construction of Externally Bonded FRP Systems for Strengthening Concrete Structures. Farmington Hills, MI: American Concrete Institute, 2002.

ACI 318-08 (2008), Building Code Requirements for Structural Concrete and Commentary (318R-08), American Concrete Institute, Farmington Hills, MI.

ACI Concrete Repair Manual

Brayack, Daniel A. Technical and Economic Effectiveness for Repair with FRP of Concrete T-Beam Bridges: Case Study for PennDOT-District 3. Thesis. West Virginia Univ., 2006. Morgantown, WV: West Virginia University, 2006.

Davalos, Julio F., Karl E. Barth, Indrajit Ray, Chunfu Lin, and Daniel A. Brayack. District 3-0 Investigation of Fiber-Wrap Technology for Bridge Repair and Rehabilitation (Phase-I). Morgantown, WV: West Virginia University, 2006.

Davalos, Julio F., Karl E. Barth, Indrajit Ray, Chunfu Lin, William C. Sasher, and George Parish. District 3-0 Investigation of Fiber-Wrap Technology for Bridge Repair and Rehabilitation (Phase-2). Morgantown, WV: West Virginia University, 2007.

Davalos, Julio F., Karl E. Barth, Indrajit Ray, Chunfu Lin, Adam L. Justice, and Matt D. Anderson. District 3-0 Investigation of Fiber-Wrap Technology for Bridge Repair and Rehabilitation (Phase-3). Morgantown, WV: West Virginia University, 2008.

Guide for Selection and Specifying Materials for Repair of Concrete Surface: Guideline NO. 03733. International Concrete Repair Institute. Des Plaines, IL: International Concrete Repair Institute, 2006.

Mirmiran, Amir, Mohsen Shahawy, Antonio Nanni, and Vistasp Karbhari. Bonded Repair and Retrofit of Concrete Structures Using FRP Composites: Recommended Construction Specifications and Process Control Manual. National Cooperative Highway Research Board. Washington, D.C.: Transportation Research Board, 2004.

Parish, George C. CFRP Repair of Concrete Beams Aged by Accelerated Corrosion. Thesis. West Virginia Univ., 2008. Morgantown, WV: West Virginia University, 2008

Surface Preparation Guidelines for Repair of Deteriorated Concrete Resulting from Reinforcing Steel Oxidation: Guideline NO. 03730. International Concrete Repair Institute. Des Plaines, IL: International Concrete Repair Institute, 2006.

University of Missouri-Rolla. Preservation of Missouri Transportation Infrastructures; Validation of FRP Composite Technology Through Field Testing; Strengthening of Bridge P-0962 Vol. II: Materials & Construction. Rolla, MO: University of Missouri-Rolla, 2004.

Appendix E

Testing and Long-term Monitoring Guidelines

Guidelines for Bridge Testing and Long-Term Inspections and Monitoring of Repair and Rehabilitation Work

1. Bridge Testing

1.1 General

Bridge load testing, when applicable, should be performed before FRP strengthening and after FRP strengthening. In this manner, the characteristics of the retrofit can be directly investigated through comparison. Load testing can also be performed at specified time intervals, such as once a year, after the repair has been completed as a means of long-term monitoring as specified in Section 2.3. The type of truck and corresponding axel loads used before and after repair should be as identical as possible. Static loading and dynamic loading should be performed. Currently, the recommended data to be collected include, but are not limited to, deflection, strain, and dynamic characteristics such as natural frequency.

1.2 Static Loading

Static load cases should be developed to place the maximum load possible on particular beams. Loads on exterior beams should be maximized by placing trucks as close as AASHTO standards will allow to the parapet of the bridge. Once the trucks have been moved into the desired position, adequate time should be allowed for the braking effects of the trucks to negate and the deflection to level off. It is recommended that the centriod of load for each loading case used be placed over the quarter, half, and three quarter points of the span and data be taken for each location.

1.2.1 Deflection Measurement

Deflection measurements can be used to check for any changes in stiffness that may be obtained as a result of the retrofit. An increase in stiffness, indicated by a decrease in deflection measurements, should lead to the conclusion that strain is being developed within the FRP strips and hence, the FRP system is taking on load as intended.

LVDTs (Linear Variable Differential Transducers) can be placed at key points along the span to measure deflections. It is recommended that LVDTs be placed at quarter points along the span of each primary member of the bridge. At minimum, deflection measurements should be made at mid-span.

LVDTs should be securely mounted so that no movement of the instrumentation is possible. The possibility of magnetic interference with near metallic objects should be eliminated as well.

The specifications of the chosen LVDT should be adequate to measure the expected response of the bridge components under observation. Specifically, an adequate range and sensitivity of the LVDT should be known. Concrete T-Beam bridges of moderately short spans can have very small deflections. Therefore, using an LVDT with high sensitivity is important so that very small changes in deflection can be measured. In

general, an adequate range and sensitivity for the selection of an LVDT can be ±0.5 inches and 0.001 inches respectively.

It is imperative that the chosen LVDTs be accompanied by accurate calibration data. If required under manufacturer's recommendations, LVDTs should be recalibrated before any testing is performed.

1.2.2 Strain Measurement

Strain measurements may be achieved using foil strain gages or any new type of strain measuring equipment that has become available. Strain gages can be attached to many different bridge components. Gages can be mounted to reinforcing steel, exterior concrete surfaces, interior concrete (embedded gages), and mounted to FRP strips.

Gages can be mounted to existing reinforcing steel for the un-repaired bridge load testing by simply chipping away the concrete in selected locations and applying the gage in accordance with the manufacturer's recommendations. The removal of defective concrete during the repair process can create the opportunity to again mount strain gages at the same steel locations. In this manner, the strain can be measured in the reinforcing steel before and after repair. Changes in strain levels in reinforcing steel during pre-repair load testing and post-repair load testing can indicate that the flexural FRP strips are actually taking on load as intended.

Mounting gages to the concrete surface should be performed to determine the strain distribution throughout the depth of the section and to locate the neutral axis. This can be successfully performed by placing gages at quarter points along the depth of beam webs. Placing gages to concrete surfaces can be a very time consuming process due to surface irregularities inherent to most concrete finishing work. When in the repair process, it may be warranted to mount strain gages to concrete surfaces before the application of FRP. Once the FRP has been applied, another gage may be placed at the same location on the FRP. The strain measurements obtained from gages in the same locations on the concrete surface and FRP surface can be used to determine if potential slip exists between the concrete and FRP strip. It is imperative that all strain gages be mounted in exact accordance with the manufacture's specification so that proper performance of the instrument can be expected. Protective coatings and guards should also be used in accordance with the manufacturer's recommendations to protect against any adverse environmental conditions.

Gages used for measuring internal concrete strain can be used at selected locations and placed after defective concrete removal and before restoration of the cross-section. Embedded concrete gage readings can be used to validate data obtained from exterior strain readings and reinforcing steel strain readings.

1.3 Dynamic Loading

Dynamic loading can be achieved by providing forced excitation to the bridge so that vibration frequencies and damping effects can be measured. The recommended method of excitation is to drive a weighted dump truck over the bridge at speeds of 30-50 mph and slam on the brakes once the truck reaches the center of the bridge. Once the

truck has crossed the bridge completely, the structure should be subject to free vibration in which the natural frequency and damping effects can be recorded.

1.3.1 Measuring Dynamic Response

Dynamic characteristics such as the frequency of a structure can be directly related to the stiffness and geometry. Any changes in these properties that may result due to the FRP strengthening system can be determined from dynamic testing. The dynamic response from testing may be measured with accelerometers mounted to primary components of the bridge. Accelerometers should be mounted following the manufacturer's guidance. Special mounting techniques may need to be developed for attaching accelerometers to concrete beams due to the deteriorated condition of many beams. Whatever the technique used, it is important that the instrument be mounted firmly to the member and therefore have zero movement in relation to the member, assuring a solid base for accurate data collection.

1.5 Data Acquisition Setup

All instrumentation placed on the bridge shall be connected to proper data acquisitioning systems. The acquisition system shall be capable of measuring the required or desired data collection rate. It is recommended that deflection and strain data be collected at 10 scans/second while acceleration data be collected at 10,000 scans/second. Successful tests have been performed with Vishay System 6000 data acquisition systems and Strain Smart software. Battery backups should be used in case problems are encountered with the primary power supply. If desired, it is possible to make the data acquisition system along with selected instrumentation a permanent fixture at the bridge site to aid in long-term monitoring as described in Section 2.3.

2. Long-Term Monitoring

2.1 General

Long-term monitoring of concrete bridges rehabilitated with externally bonded FRP strips should be achieved through periodic nondestructive testing and bridge load testing procedures. It is recommended that visual inspection be performed yearly, aided by other testing procedures as required, as specified in Section 2.1.1.

2.2 Nondestructive Inspection and Testing

Nondestructive inspection (NDI) and testing (NDT) should be used to detect defects such as resin starvation, resin richness, fiber misalignment, discoloration, and delaminations. NDI and NDT techniques for structures strengthened with FRP have not been very widely researched. Therefore, most guidance for long-term monitoring and inspection for concrete structures strengthened with FRP is general in nature and can be enhanced with ingenuity as desired. NDI and NDT techniques may include visual

inspection, audio or tap testing, ultrasonics, thermography, and selective bond pull-off testing.

2.2.1 Visual Inspection

Currently, visual inspection should be considered the most economical and reliable NDI method. If flaws are found through visual inspection, the area should be adequately marked and subjected to closer visual inspection and forms of nondestructive testing such as ultrasonics and thermography to further classify the defect and type of repair that may be needed. The use of flashlights, magnifying glasses, or borescoped may be employed if deemed necessary.

2.2.2 Audio Testing

Audio testing or tap testing may be incorporated into the visual inspection process. This method of testing is not very favorable due to its highly subjective and time consuming nature. Tap testing should only be performed by skilled and experienced inspection personnel (ACI, 2007). It should be performed by tapping the subject area with a lightweight hammer while listening to the audible response. Making use of the audible range (10 to 20 Hz), a clear and sharp ringing sound is indicative of a well-bonded solid structure, while a dull sound may be a sign of damage such as delaminations.

2.2.3 Ultrasonics

Ultrasonic inspection can be used to detect internal delaminations or inconsistencies that may not be visible with the human eye or tap testing. Ultrasonic testing is performed by introducing a high-frequency sound wave into the structure at some specified angle to the surface (normal, parallel, inclined). Many different angles should be used during testing since flaws may not be noticeable in a particular direction. Defects are located as a result of ultrasonic waves striking an object and transmitting part of the energy back to the surface while the rest of the energy is transmitted through (ACI, 2007). A receiving transducer picks up the diminished sonic energy and displays it on a screen. In this manner, the defected areas can be located by comparison with flawless areas. Impact echo testers have been specially modified and successfully used to detect artificially created delaminations (Maerz et al. 2007).

2.2.4 Thermography

Long-term inspection is a vital component of the health monitoring of FRP repair and rehabilitation projects. In addition to the most commonly used techniques such as visual inspection for visible patches or discoloration and tap testing to locate debonding and delamination areas at FRP/concrete beam or slab interface. For long-term monitoring, more advanced methods such as infrared thermography (IRT) can be used in the field to detect delaminations, air-filled and water-filled debonds at the interface, by measuring the differences of thermal conductivity, specific heat of defective and defect-

free zones, and produce real-time images that can be interpreted effectively to evaluate the integrity of the FRP bond. IRT can effectively locate the size and extent of the delamination or debond. With the IRT method, a heat source is used to elevate the surface temperature of the testing area. Areas that are defect free will conduct heat more efficiently than areas with underlying defects. The quantity of heat that is either absorbed or reflected back to the surface can indicate defects within the FRP/concrete interface. Types of defects that can affect the thermal properties can include cracks, damage from impact, ingression of water, and debonding (ACI, 2007). IRT can be most effectively used to detect defects near the surface.

Although in the past IRT has been used successfully for field monitoring, this technique needs experienced technicians and equipment with specialized knowledge to successfully conduct the testing in the field and interpret the results. Tap testing and selective pull-off testing may be conducted to confirm the debond areas.

2.2.5 Pull-Off Strength Testing

The epoxy bond between the FRP and the concrete is critical for the long-term performance of the FRP system. As pull-off testing can be considered destructive if performed to a load carrying member such as a primary beam, possible degradation of the bond shall be tested by incorporating areas of low structural importance for periodic bond testing. It is recommended that FRP sheets be bonded to areas on bridge abutments in the same manner as they are applied to the load carrying components so that these bonded sheets can be tested and conclusions can be made concerning the durability of the FRP/substrate bond. These bonded test areas may also be subjected to intentional delaminations via forced air or water. Therefore, with delamination locations known, the accuracy of nondestructive testing equipment may be validated prior to use on primary members (Maerz et al. 2007).

Pull-off strength testing may also be performed on test specimens cast at the bridge during the concrete restoration process and then layered with the FRP during the normal application process. These specimens can be kept at the site and therefore exposed to the same environmental conditions. When NDI is performed to the rehabilitated bridge, pull-off bond strength testing may be conducted on the test specimens.

2.3 Periodic Load Testing

Periodic load testing can be used as an effective means of monitoring the long-term health of a rehabilitated bridge. Periodic load tests should be performed in the same manner as load testing just prior to and just after repairing the structure. In this way, periodic load tests can be compared to load tests conducted on the newly repaired bridge and any discrepancies can be noted while evaluating the changes in structural characteristics.

If it is specified that periodic load testing is to be conducted, strain gages as detailed in Section 1.2.2 may be permanently attached to the structure so that reapplication may not be necessary.

REFERENCES

ACI 440R-07 (2007). Report on Fiber-Reinforced Polymer (FRP) Reinforced for Concrete Structures. American Concrete Institute.

ACI Concrete Repair Manual

Casas, Joan R. "Monitoring and Reliability Management of Deteriorating Concrete Bridges." Maintaining the Safety of Deteriorating Civil Infrastructures; Proceedings of the 2nd International Workshop on Life-Cycle Cost Analysis and Design. (2001): Pages 127-141.

Davalos, Julio F., Karl E. Barth, Indrajit Ray, Chunfu Lin, Adam L. Justice, and Matt D. Anderson. District 3-0 Investigation of Fiber-Wrap Technology for Bridge Repair and Rehabilitation (Phase-3). Morgantown, WV: West Virginia University, 2008.

Hag-Elsafi, Osman, Sreenivas Alampalli, and Jonathan Kunin. "Application of FRP Laminates for Strengthening of a Reinforced-Concrete T-Beam Bridge Structure." Composite Structures. (2001): Pages 454-466. Elsevier Science Ltd. <www.elsevier.com/locate.compstruct>

Maerz, N., G. Galecki, and A. Nanni. "Experimental Non-Destructive Testing of FRP Materials, Installation, and Performance, Dallas County Bridge, Missouri, USA." Rolla, MO: University of Missouri-Rolla.

Reay, Jaron T., et al. "Long Term Durability of Carbon FRP Composites Applied to RC Bridges: State Street Bridge on Interstate 80." Journal of Bridge Engineering. ASCE. March/April (2006): Pages 205-216.

Rizzo, Andrea, Nestore Galati, and Antonio Nanni. Design and In-Situ Load Testing of Bridge No. 1330005 Route 3560 – Phelps County, MO. Rolla, MO: University of Missouri-Rolla, 2005.

Sasher, William C. Testing, Assessment and FRP Strengthening of Concrete T-Beam Bridges in Pennsylvania. Thesis. West Virginia Univ., 2008. Morgantown, WV: West Virginia University, 2008